Mechanistic studies of Rab GTPase membrane targeting and cycling in cells

Dissertation

zur Erlangung des akademischen Grades eines

Doktors der Naturwissenschaften

(Dr. rer. nat.)

eingereicht an

der Fakultät für Chemie und Chemische Biologie

an der Technischen Universität Dortmund

vorgelegt von

M. Sc. **Fu Li**

Aus Kaifeng, China

Dortmund, 2017

Declaration/Erklärung

Die vorliegende Arbeit wurde in der Zeit von November 2011 bis Oktober 2016 am Max-Plank-Institut für Molekulare Physiologie Dortmund unter der Anleitung von Dr.Yaowen Wu durchgeführt.

Hiermit versichere ich an Eides statt, dass ich die vorliegende Arbeit selbstständing und nur mit den angegebenen Hilfsmitteln angefertigt habe.

The work described in this Dissertation was performed from November 2011 to October 2016 at the Max Plank Institute of Molecular Physiology Dortmund under the guidance of Dr. Yaowen Wu.

I hereby declare that I performed the work independently and did not use any other but the indicated aids.

1. Gutachter: Prof. Dr. Roger Goody

2. Gutachter: Prof. Dr. Philippe Bastiaens

Contents

Zusammenfassung

Rab GTPasen spielen eine Schlüsselrolle in der Steuerung des vesikulären Transportes. Rab Proteine (>60 bekannt im Menschen) lokalisieren in spezifischen intrazellulären Membranen um dort diverse Membrantransportprozesse zu regulieren. Der GTPase-Zyklus wird durch Guaninnukleotidaustauschfaktoren (GEFs) und GTPase-aktivierende Proteine (GAPs) katalysiert. Im Zuge dieses Zyklus, wechselt Rab zwischen einer aktiven, GTP-gebundenen und einer inaktiven, GDP-gebundenen inaktiven Form. GTP-gebundenes Rab rekrutiert dabei Effektorproteine zu spezifischen Zellkompartimenten. GDP-*Dissoziationsinhibitor* (GDI) extrahiert GDP-gebundenes Rab aus Membranen indem es lösliche Komplexe bildet und so Rab ins Zytosol überführt. Es wird vermutete, dass *GDI displacement factors* (GDF) die gezielte Membranlokalisierung vermitteln indem sie die Dissoziation des Rab-GDI Komplexes an der Zielmembran katalysieren. Der genaue Mechanismus der gezielten Rab Membranlokalisierung bleibt jedoch unklar.

In dieser Arbeit wurde der Mechanismus der Rab Membranlokalisierung untersucht. Im Speziellen wurde die Rolle der hypervariablen C-terminale Domäne (HVD) und die Faktoren, die zur Regulation der Rab35 Lokalisation beitragen, analysiert.
Hierzu wurde die HVD mit einem artifiziellen Polyethylenglykol-Linker ausgetauscht. Die PEGylierten Rab-Proteine wurden weiterhin prenyliert, was die einzigartige Fähigkeit der Rab Prenylierungsmaschinerie, vielfältige C-terminale Sequenzen prozessieren zu können, hervorhebt.

Durch die Untersuchung von semisynthetischem PEGyliertem Rab1, Rab5, Rab7 und Rab35, konnten wir die Rolle der HVD in der Rab Membranlokalisation ermitteln. Für Rab1 und Rab5 scheint die HVD lediglich eine Funktion als Bindeglied zwischen der GTPase-Domäne und der Membran zu erfüllen. Die N-terminalen Reste der HVD von Rab7 vermitteln die Lokalisierung zur Membran später Endosomen und Lysosomen durch ihre Interaktion mit dem Rab7-Effektor *Rab-interacting lysosomal protein*. Das C-terminale polybasische Cluster (PBC) der Rab35 HVD ist essentiell für die Lokalisierung des Proteins zur Plasmamembran (PM). Der Grund für diese Abhängigkeit sind vermutlich die elektrostatischen Wechselwirkungen mit den negativ geladenen Lipiden der PM.

Um die Mechanismen der Membranlokalisierung von Rab35 zu ergründen, untersuchten wir den dynamische Fluss von Rab35 in Zellen durch *Fluorescence Localization after Photoactivation* (FLAP) und *Fluorescence Recovery after*

Photobleaching (FRAP)-Experimente. Es konnte festgestellt werden, dass Rab35 zwischen der PM und dem Golgi zirkuliert. Der Transport von Rab35 vom Golgi zur PM erfolgt schnell, vermutlich vermittelt durch GDI, wohingegen der Transport von der PM zum Golgi durch den endozytotischen Membranverkehr erfolgt. Dies deutet darauf hin, dass die Golgi-Membran als Zwischenstopp des Rab35 Zyklus fungiert. PRA1, ein GDF, ist essentiell für den endozytotischen Membranverkehr und daher auch für den räumlichen Rab35-Zyklus. Weiterhin sind sowohl DENND1A, ein Rab35 GEF, und OCRL1, ein Rab35 Effektorprotein, wesentlich für die spezifische Lokalisation von Rab35 und den Transfer zwischen PM und Golgi.

Unserer Ergebnisse deuten darauf hin, dass die gezielte Rab Membranlokalisierung einem komplexen Mechanismus unterliegt, der in unterschiedlichem Maße von GEFs, GAPs, GDIs, GDFs, Effektoren und den Interaktionen des C-Terminus sowie möglicherweise weiteren Interaktionspartnern, wie zum Beispiel Phosphatidylinositolphosphaten, bestimmt wird.

Abstract

Rab GTPases are the key regulators of vesicular transport. Rab proteins (>60 identified in humans) localize at distinct intracellular membranes to regulate diverse membrane trafficking events in the cell. The Rab GTPase cycle is catalyzed by guanine nucleotide exchange factors (GEFs) and GTPase activating proteins (GAPs), converting Rab between its GTP-bound active form and its GDP-bound inactive form.

The GTP-bound Rabs recruit effectors to the membranes of specific cellular compartments. GDP-dissociation inhibitors (GDIs) extract GDP-bound Rabs from membranes and form soluble complexes to maintain Rabs in the cytosol. GDI displacement factors (GDFs) are proposed to catalyze the dissociation of the Rab-GDI complexes at the destination for proper delivery to the target membrane. However, the mechanism of Rab membrane targeting remains poorly understood. In this thesis, we investigated the mechanism of Rab membrane targeting, the role of the Rab C-terminal hypervariable domain (HVD) and the factors involved in regulation of Rab35 cycling.

To this end, we substituted the HVD with an unnatural polyethylenglycol (PEG) linker to elucidate the function of the HVD. The PEGylated Rab proteins undergo normal prenylation, underlining the unique ability of the Rab prenylation machinery to process the diverse C-terminal sequences of the Rab family. By studying the behavior of semisynthetic PEGylated Rab1, Rab5, Rab7, and Rab35 proteins, we were able to resolve the role of the HVD of Rabs in membrane targeting.

The HVD of Rab1 and Rab5 is dispensable for membrane targeting and appears to function simply as a linker between the GTPase domain and the membrane. The N-terminal residues of the Rab7 HVD are important for late endosomal/lysosomal localization due to their involvement in interaction with the Rab7 effector Rab interacting lysosomal protein. The C-terminal polybasic cluster (PBC) of the Rab35 HVD is essential for plasma membrane (PM) targeting, presumably because of the electrostatic interaction with the negatively charged lipids on the PM.

To investigate the membrane targeting mechanism of Rab35, we examined its spatial cycling in live cells using fluorescence localization after photoactivation (FLAP) and fluorescence recovery after photobleaching (FRAP) techniques. We found that Rab35 cycles between the PM and the Golgi. The trafficking of Rab35 from Golgi to PM is a fast process, probably mediated by GDI, while Rab35 traffics from the PM to the Golgi via the

endocytic pathway, indicating that the Golgi may serve as an intermediate stop of Rab35 cycling. The PRA1 (GDF) plays an important role in the endocytic pathway, and is essential for Rab35 cycling. Both DENND1A (Rab35 GEF) and OCRL1 (Rab35 effector) are crucial for Rab35 cycling and membrane targeting.

Altogether, Rab membrane targeting is dictated by a complex mechanism involving GEFs, GAPs, GDIs, GDFs, effectors, the C-terminal interaction with membranes to varying extents, and possibly other binding partners like phosphatidylinositol phosphates.

Abbreviations

°C	degree Celsius
Å	Angstrom (1 Å = 10^{-10} m)
AA	Amino acid
ATCC	American type culture collection
BFP	Blue fluorescent protein
BSA	Bovine serum albumin
CBD	Chitin-binding domain
CBR	C-terminus binding region
CCV	clatrin coated vesicle
CCP	clatrin coated pit
CIM	CBR binding motif
COPI und II	coat protein complex I and II
COS7	CV-1 origin, SV-40, clonal isolate
C-terminal	Carboxy-terminal
Da	Dalton
DMEM	Dulbecco's modified eagle medium
DNA	deoxyribonucleic acid
DPBS	Dulbecco’s phosphate buffered saline
DrrA/SidM	defect in Rab recruitment/subtrate of Icm/Dot M
DTE	1,4-Dithioerythritol
EDTA	Ethylenediaminetetraacetic acid
EE	Early endosome
EEA1	early-endosomal autoantigen1
EGFP	Enhanced green fluorescent protein
EPL	Expressed protein ligation
ER	Endoplasmic Reticulum
ESI-MS	Electronspray ionization mass spectrometry
FBS	Fetal bovine serum
FITC	Fluorescein 5(6)-isothiocyanate
FLIP	Fluorescence Loss In Photobleaching
FRAP	Fluorescence recovery after photoactivation

FRET	Fluorescence resonance energy transfer
FTase	Farnesyltransferase
GAP	GTPase activating protein
GDF	GDI displacement factor
GDI	GDP dissociation inhibitor
GDP	Guaninediphosphate
GEF	Guaninenucleotide exchange factor
GF	Gel filtration
GFP	Green fluorescent protein
GG	Geranylgeranyl
GGPP	Geranylgeranylpyrophosphate
GGTase	Geranylgeranyltransferase
GTP	Guaninetriphosphate
GTPase	GTP-binding protein
HEPES	4-(2-Hydroxyethyl)piperazine-1-ethanesulfonic acid
HOPS	Homotypic fusion and vacuole protein sorting
Hsp	Heat shock protein
Icmt	Isoprenylcysteine carboxyl methyltransferase
IP	immunoprecipitation
IPTG	Isopropyl-β-D-thiogalactoside
ITC	Isothermal titration calorimetry
L	liter
LAMP1&2	lysosomal-associated membrane protein 1& 2
LB	lysogeny broth
LC-MS	Liquid chromatography-mass spectrometry
LE	Late endosome
MALDI-TOF-MS	Matrix assisted laser desorption/ionization-time of flight mass spectrometry
MCF-7	Michigan cancer foundation-7
MCS	Multiple cloning site
MDCK	Madin-darby canine kidney cells
MESNA	2-Mercaptoethanesulfonic acid
min	minute(s)
MPR	Mannose-6-phosphate receptor

NBD	7-Nitrobenz-2-oxa-1,3-diazol-4-yl
NBD-FPP	NBD-farnesyl pyrophosphate
NCL	Native chemical ligation
NEAA	non-essential amino acids
NGF	Nerve growth factor
NMR	Nuclear magnetic resonance spectroscopy
NSF	*N*-ethyl-maleimide sensitive fusion protein
NTA	Nitrilotriacetic acid
OCRL1	Inositol polyphosphate 5-phosphatase OCRL-1
OD_{600}	Optical density at 600 nm
PAGE	polyacrylamide gel electrophoresis
PCC	Pearson's correlation coefficients
PCR	Polymerase chain reaction
PEG	Polyethylenglycol
PLAP	Fluorescence Loss After Photoactivation
PM	Plasma membrane
PMSF	Phenylmethylsulfonyl fluoride
POI	protein of interest
PRA1/Yip3	Prenylated Rab Acceptor/Ypt interacting protein 3
PtdIns(3,4,5)P_3	Phosphatidylinositol 3,4,5-trisphosphate
PtdIns(4,5)P_2	Phosphatidylinositol 4,5-bisphosphate
PtdInsP_4	Phosphatidylinositol 4-phosphate
Rab	Ras-like (protein) from Rat brain
Rabex-5	Rabaptin-5-associated exchange factor for Rab5
RabF	Rab-Family
Rab-SF	Rab-Subfamily
Ras	Rat adeno sarcoma
RBP	Rab binding platform
RBP	Rab binding platform
RE	recycling endosome
REP	Rab escort protein
REP	Rab Escort Protein
RNAi	RNA interference

ROI	region of interest
RPE	retinal pigment epithelium
RRF	Rab recyling factor
RT	Room temperature
ScrRNA	Scrambled RNA
SDS	Sodium dodecyl sulfate
shRNA	Short hairpin RNA
siRNA	short interfering RNA
SNAP	Soluble NSF attachment protein
SNARE	Soluble NSF attachment protein receptor
SNX	sorting nexin
TEMED	*N,N,N′,N′*-Tetramethylethylenediamin
TEV	Tobacco Etch Virus
TGN	trans-Golgi network
TLC	Thin layer chromatography
TRAPPI&II	transport protein particle I & II
Tris	Tris(hydroxymethyl)-aminomethan
TTD	(4,7,10)-Trioxa-1,13-tridecanediamine
U	Unit
WT	Wild type
Yip	Ypt-interacting protein
Ypt	Yeast protein transport
µl	microliter

1 Introduction

Overview

The plasma membrane (PM), a lipid bilayer-based biological membrane, separates interior contents of a cell from its environment. The inner membranes of a cell constitute various organelles such like endoplasmic reticulum (ER), Golgi apparatus, endosomes, lysosomes and mitochondria in eukaryotic cells. Within these distinctly separated organelles, many kinds of chemical reactions happen all the time. All above organelles including vesicles which mediate transport among them to form a continuous membrane group which called the endomembrane system. Such membrane system is the key for the formation of morphologically and functionally distinguishable features, like vesicular coats, tubules, and signaling platforms. In the endomembrane system, most proteins and lipids could be carried to their destination correctly via vesicular transport. The specificity of proteins and lipids transport is based on the selective packaging of the intended cargoes, moving to the destination membranes along the microtubules or other cytoskeletons, and finally fusion of the vesicle with the appropriate target compartment. Many players including small GTPase Rabs, ARF, phosphoinositides, tethers, and Soluble NSF Attachment protein REceptors (SNAREs) are involved in these critical processes.

In the past forty years, a central question in this field is how the organelles in a cell remain distinct despite the constant flux of membrane and protein trafficking all the time. In this thesis, I will discuss how Rab GTPases play their roles during membrane trafficking with a particular focus on the mechanisms of Rab GTPase membrane targeting and cycling in cells.

1.1 Rab GTPase

1.1.1 Rab GTPases and their discoveries

Ras superfamily contains five major kinds of small GTPases including Ras, Rho, Ran, Rab and Arf (Colicelli, 2004). The GTPase proteins of each subfamily have similar structures, sequences and functions. However, different family proteins play multiple and divergent roles. The Ras family members mainly regulate signaling transduction, gene expression, cell proliferation and differentiation. The Rho family members mainly regulate cytoskeletal organization but also have an effect on gene expression. The Sar/Arf

family control vesicle budding whereas the Ran family regulate nuclear transport as well as microtubule organization during mitosis (Goitre et al., 2013). Rab (Ras-related in brain) GTPase family is the biggest member of the Ras superfamily and is the key proteins to control the vesicles trafficking. Ras superfamily proteins are versatile and are key regulators of virtually all fundamental cellular processes. Therefore, it is not surprising that their dysfunction leads to the pathogenesis of serious human diseases, including cancer, neurodegeneration and other developmental syndromes (Wennerberg et al., 2005).

Rabs are monomeric GTPases with small sizes around 25 KDa and the regulation of their functions dependents on association or dissociation of GTP. These so-called small 'G' proteins act as molecular switches inside cells. Their activities are regulated by factors to bind and hydrolyze guanosine triphosphate (GTP) to guanosine diphosphate (GDP). When they are bound to GTP or GDP, they are active ('on') or inactive ('off'), respectively. Rab GTPases play roles in all steps of membrane trafficking including budding, formation, motility, tethering, docking and fusion of vesicles (Segev, 2001; Zerial and McBride, 2001; Stenmark, 2009).

The first identified functional Rab GTPase was Sec4 in *Saccharomyces cerevisiae*. The story started before 1980 when Schekman and colleagues found some yeasts are blocked in secretion and become dense than normal cells due to the accumulation of dense secretory vesicles and other membranes. Hence, they discovered 23(sec1-sec23) secretion mutants in yeast and Sec4 mutation that lead to the accumulation of TGN-derived vesicles that are destined for the plasma membrane.

Before the identification of SEC4, YPT1 gene (Rab1 homology in mammalian cells) was also discovered using genetic analysis methods that had high homology to Ras (Gallwitz et al., 1983). Comparison of SEC4, YPT1 and Ras protein sequences showed that SEC4 is rather close to YPT1 than to Ras. The Ras-like protein Sec4 and YPT1 performed a diverse set of functions indicating that they are essential for yeast growth (Schmitt et al., 1986). However, they couldn't rescue the Ras1/Ras2 double deletion (Goud et al., 1988). The overexpression of SEC4 could suppress the phenotypes of many of the late acting SEC mutants (Salminen et al., 1987).

Hence, Segev and colleagues found that the YPT1 conditional-lethal mutant cause membranes and vesicles to accumulate within the yeast, which prevent complete

glycosylation of invertase, and decrease its secretion (Segev et al., 1988). Ypt1 protein was then shown to regulate secretion at the Golgi apparatus (Bacon et al., 1989).Through the studies of SEC4 and YPT1, a novel family of GTPases were discovered which controlled membrane dynamics in cells. The first Rab GTPase in mammalian cells was identified during the process of searching for the Ras superfamily members by screening rat cDNA library with oligonucleotide probes (Touchot et al., 1987). They identified four genes which encoding proteins homologous to the yeast YPT proteins; these genes were named Rab (Ras-like GTPase from rat brain)-1,-2,-3,-4. Later studies demonstrated these genes also have homology to the yeast SEC4 protein (Zahouri et al., 1989). Soon after the mouse Rab1 was found which could replace the Ypt1 in yeast and perform full functions. This indicated that secretion as the other membrane trafficking events are controlled by an evolutionarily conserved Rab GTPases system (Haubruck et al., 1989). These findings led to people to ask if Rab GTPases dominate membrane transport in secretion (Bourne, 1988). In consistent with this idea, a large family of highly conserved Rab GTPases contained in exocytic and endocytic compartments were discovered, each with a specific subcellular localization (Chavrier et al., 1990). These findings initiated that the mechanisms of Rab in regulating membrane protein transport.

Since the first homolog of Rab, Sec4 (Rab8 homolog in human) being found 30 years before, people have identified approximately 70 types of Rab GTpases in human, 29 types in C.elegans, 29 types in Drosophila melanogaster, 57 types in Arabidopsis Thaliana and 13 types in yeasts (Pereira-Leal et al., 2001; Colicelli,2004; Yoshimura et al., 2010).

1.1.2 The GTP-GDP cycle of Rab GTPase

Rab GTPases work as the key regulators of intracellular membrane trafficking which are controlled by the cycling between GTP-bound active and GDP-bound inactive forms to carry out their functions.

As depicted in Figure 1.1, the exchange of GDP to GTP is catalyzed by GEFs while GAPs stimulate a Rab's intrinsic rate of GTP hydrolysis, thus inactivating the Rabs by converting bound GTP to GDP. Therefore, Rab GTPase can be switched on and off. GDIs extract GDP-Rabs from membranes and form soluble complexes to maintain Rabs in the inactive state (Bobs et al., 2007; Stenmark, 2009).

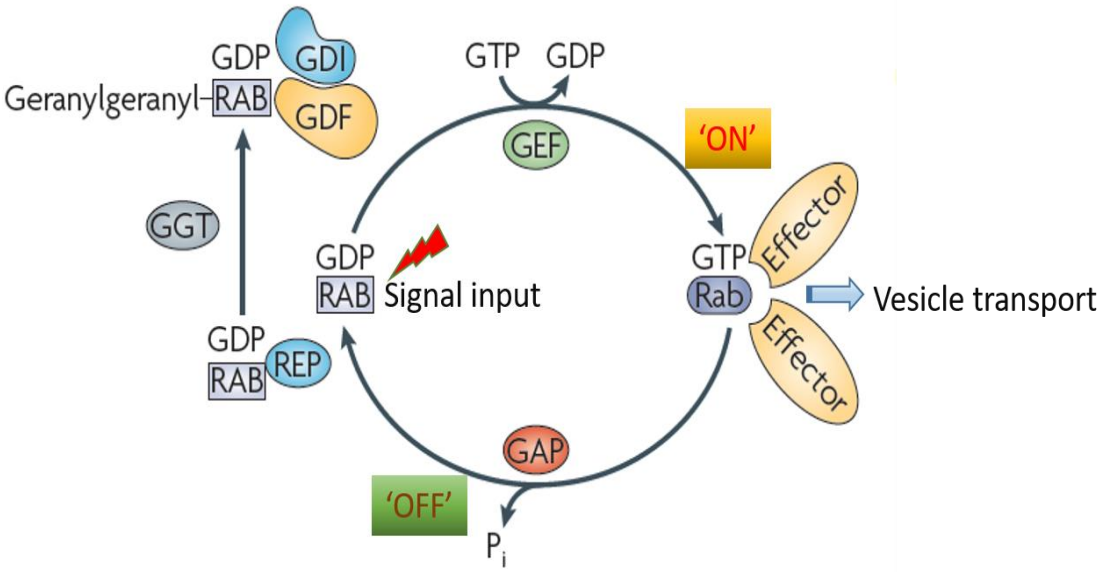

Figure 1-1. Rab GTPase GDP-GTP cycle and its circuitry. REP, Rab escort protein; GDI, Guanosine nucleotide dissociation inhibitors; GDF, GDI displacement factor; GEF, Guanine nucleotide exchange effector; GAP, GTPase-activating protein; GDP, guanosine diphosphate; GTP, Guanosine triphosphate. (Adapted from: Stenmark, 2009)

The newly synthesized Rab GTPase, in the GDP-bound form, is presented by Rab escort protein (REP) to Rab geranylgeranyl transferase (Rab GGTase). The Rab GGTase transfers one or (usually) two geranylgeranyl groups to the cysteine(s) at the C-terminus of Rab protein, which is known as prenylation. With the one or two hydrophobic geranylgeranyl groups, Rab GTPases can reversibly associate with membranes to regulate vesicular trafficking. Exchange of GDP for GTP is facilitated by guanine nucleotide exchange factors (GEFs), which recognize specific residues in the Rab switch regions and increase the dissociation rate of GDP by several orders of magnitude (Vetter and Wittinghofer, 2001; Delprato et al., 2004). Considering the high concentration of GTP (about 1 mM, GTP/GDP=10:1) in cytosol, GTP binds to Rabs as GDP is released from Rab GTPases. Once activated, GTP-bound form Rab GTPases have the ability to interact with effectors such as sorting adaptors, tethering factors, kinases, phosphatases and motors, which are defined as those proteins binding tightly only to the 'ON'-state (Eathiraj, et al.,2005).

Once the Rabs complete their functions, hydrolysis of the their bound GTP and convert into GDP-bound form 'OFF'-state occurring, which are catalyzed by GTPase

activating-proteins (GAPs) to accelerate the intrinsic GTPase activity of the Rab GTPases. About 40 different yeast and human Rab GAPs with restricted specificities have been identified, most of which contain TBC (Tre2/Bub2/Cdc16) domain (Albert and Gallwitz, 1999; Albert et al., 1999; Hass et al., 2007). The catalytic TBC domain crystal structures of GAP-Rab complexes showed that the Rab GAP requires two conserved Arg and Gln 'finger' residues that accelerate the catalytic activity of the Rab GTPases. On the contrary, Ras GAP needs only one conserved argine finger (Ahmadian, et al., 1997; Pan, et al., 2006). The inactivated GDP-bound Rab is extracted by guanosine nucleotide dissociation inhibitor (GDI) from membrane and then complete this round of GTPase cycle. Indeed, to help the extraction of Rab from the high affinity Rab-GDI complex, membrane-localized GDI displacement factor (GDF) has been postulated that might function to disrupt the high affinity Rab–GDP–GDI complexes and to promote the release of Rabs (Sivars, et al., 2003).

1.1.3 Regulation of Rab GTPase by GEFs, GAPs, REPs, GDIs, effectors

In the inactive (GDP-bound) conformation, accessory factors facilitate the targeting of Rab GTPases to intracellular compartments (Sivars et al., 2003; Rak et al., 2003). After nucleotide exchange to the active (GTP-bound) conformation, Rab GTPases interact with functionally diverse effectors including lipid kinases, motor proteins and tethering complexes.

All the functions of small GTPases are dependent on their structural conformation and changing during variant interaction with GEF, GAP, GDI and other effectors. The small GTPases-GEFs (-GDIs, -GAPs, -effectors) complexes structures give the clues of their functions. Like other small GTPases, Rab GTPases have similar structure information that consists of a six-stranded β sheets which flanked by five α helices. The GTP-binding domain consists five (G1-G5) loops which are responsible for the GDP/GTP and Mg^{2+} binding and GTP hydrolysis (Valencia et al., 1991; Bourne et al., 1991).These G1-G5 domains contain the guanine nucleotide binding site which is comprised of conserved motifs that recognize the guanine base (G4, N/TKxD motif) and α-, β-phosphate and the magnesium ion (G1, P-loop with Gx4GKS/T sequences), and the association of G3 motif [Dx2G (Q/H/T)] with Mg^{2+} and the γ-phosphate of GTP (Wennerberg et al., 2005).

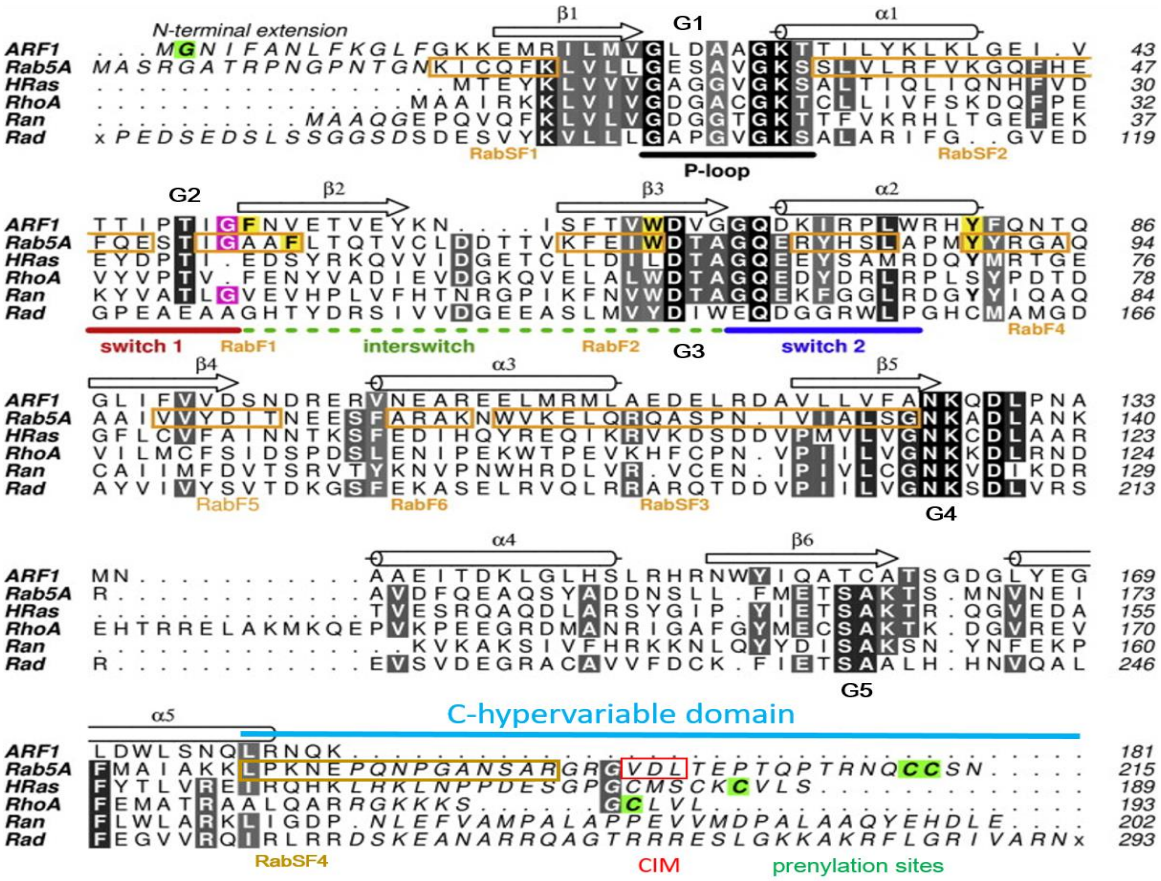

Figure 1-2. Structure-based sequence alignment of representative small GTPases.
The P loop is black, switch 1 is deep red, the interswitch is green, G-domain is black and switch 2 is blue. The glycine insertion in Arf, Rab, and Ran is highlighted in pink. The three residues that comprise the aromatic triad in Arfs and Rabs are highlighted in yellow. Residues that are modified by lipid enzymes to enable membrane attachment are highlighted in green. RabSF and RabF motifs are framed in orange. The c-terminal hypervariable domain is marked in shallow blue. The prenylation sites of cysteine are green. (Adapted from Khan AR and Ménétrey J, 2013)

In Ras GTPase family, there are two switch elements, termed Switch I and Switch II. The two switch regions sense the status of the bound nucleotide and are involved in the hydrolysis of GTP. However, the forms of nucleotide binding to the switch 1 and 2 are different among small GTPases. In Ras, Rab, and Rho GTPases, the switch 1 interacts with the guanine base and/or the sugar of both GDP and GTP. In the GTP-bound form, switch I and II are bound to the γ-phosphate via the invariant Threonine (G2 motif) and Glycine (G3 motif) residues. GTP hydrolysis causes the loss of the γ-phosphate and allows the two switch regions to relax into the GDP-bound conformations. However, Arf, Arf-like and Ran proteins demonstrate a large conformation change when GDP-bound is exchange to GTP-bound (Vetter and Wittinghofer, 2001). Aside from the G1-G5 motifs,

Pereira-Leal and Seabra identified five Rabs sequences, F1–F5 (F1, F3, and F4 are in Switch domains, Figure 1-2). These motifs are conserved and are distinct from other Ras superfamily members. The differences of these motifs were also considered as the classification criteria of the Rab family. In addition, four conserved (RabSF1-RabSF4) regions of Rab subfamily were identified and proposed to be effector-interaction motifs (Pereira-Leal and Seabra, 2000). Interestingly, RabSF4 is located in the C-terminal hypervariable domain, a region characterized by its sequence divergence.

In total, there are three Rab subfamily-conserved elements not in switch regions, which define the Rab family, distinguish with the other Ras family members. More and more crystal structures of Rabs and their effectors support the Rab classification model. The Rab3a and its effector Rabphilin showed that effector must recognize switch domain determinant and interact preferentially with the RabSF1, 3 and 4 motifs (Ostermeier and Brunger, 1999). Another example is Rab7 with its effector RILP (Rab-interacting lysosomal protein) which show that the RabSF1 and RabSF4 (hypervariable domain) are important for their recognition and interaction (Wu et al., 2005).

In general, the release of GDP from GTPase is very slow but can be accelerated by GEFs to yield effective activation in cells. The exchange reaction is initiated from a low-affinity GTPase-GDP:GEF complex. Then, the complex is converted into a high-affinity GTPase:GEF complex after the release of GDP. The loading of GTP to GTPase induces the dissociation of GEF interaction and produce the active GTP-bound form of GTPase. The first two crystal structures of nucleotide-free GTPases/GEFs were Ras/SOS complex and Arf1-Gea2 complex (Boriack-Sjodin et al., 1998; Mossessova et al., 1998; Snyder et al., 2002), giving us general pictures of how GEFs work with GTPases. Firstly, GEF is localized close to the GTPase switch I motif because of the steric hindrance by the GDP binding. Thus GEFs contact with the switch II of the GTPase extensively. GEFs contact with switch I/II formation is important to stabilize the unstable nucleotide-free GTPase and to avoid from unfolding. GEFs facilitate the dissociation of GDP by different means for examples Ras-SOS, Cdc42-Dock9 or Arf1-Gea2. Dock9, one Cdc42 GEF, approach a hydrophobic residue close to the $Mg2^{2+}$-binding site which lowers its GDP affinity. The Arf1 GEF of Gea2 inserts an acidic residue into the phosphate-binding site that contributes repulsive electrostatic interactions to expel the bound nucleotide. By combining the above two means, SOS remodel Ras switch II motif leading to a

conserved alanine to put methyl group near the Mg^{2+}-binding site, thus forming a similar hydrophobic repulsion to expel the GDP binding.

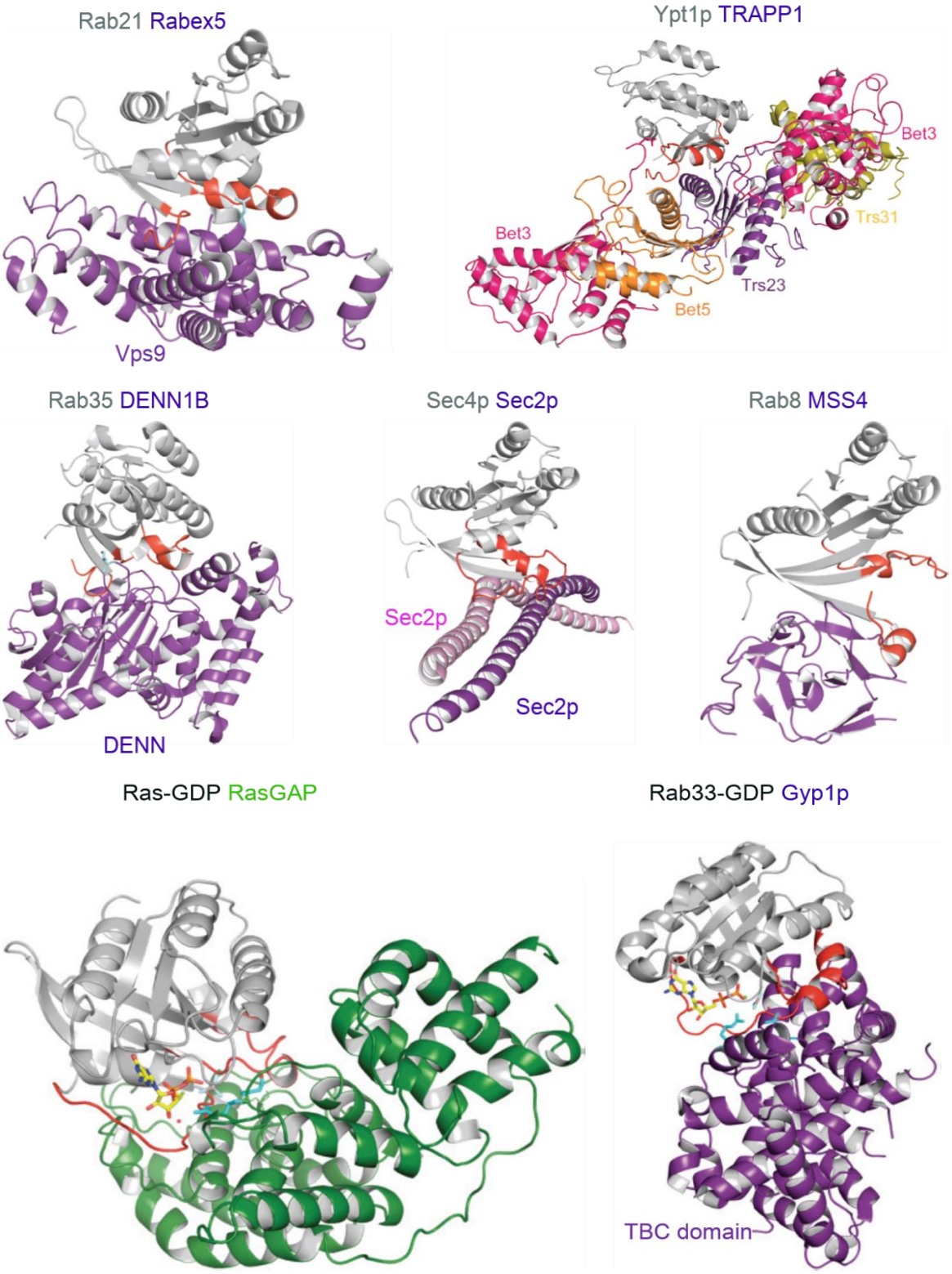

Figure 1-3. Representative structures of Rab:GEF, Rab:GAP complexes. Small GTPases in *gray* with their switch regions are shown in *red*. Rab21: Rabex-5 complex (PDB code: 2OT3); Ypt1: TRAPP complex

(PDB code: 3CUE); Rab35: DENN1B (PDB code: 3TW8); Sec4p: Sec2P complex (PDB code: 2OCY); Rab8: MSS4 (PDB code: 1FU5). Ras: GAP complex (PDB code: 1WQ1); Rab33: Gyp1p complex (PDB code: 2G77) (From Cherfils and Zeghouf, 2013).

After the GDP is released from GTPase:GEF complex, the nature of GTP loading to the nucleotide-free complex was discovered by the structural dynamics of the GTPase and the GEF. Several domains are contained in these processes, for examples, Sec7-domain containing Arf/GEF (Renault et al., 2003), a Prone family RhoGEF (Thomas et al., 2007), a DOCK family RhoGEF (Yang et al., 2009), and a Vps9 family RabGEF (Uejima et al., 2010).

Rab GTPases GEFs can be subdivided into at least four types for their various functional domains, probably because of the large members of different Rab subfamilies (Hutagalung and Novick, 2011; Cherfils and Zeghouf, 2013). The GEF subfamilies contain conserved catalytic domains DENN (Rab35 GEF) and Vps9 (Rab21/22 GEF) motif with the surrounding of other domains (Figure 1-3, Delprato et al., 2004; Wu et al., 2011). However, Sec2 (Sec4 GEF) and the TRAPP (Ypt1/Rab1 GEF) complex are the unique subfamily which work as dimeric and pseudo-dimeric complexes, respectively (Burton et al., 1993; Cai et al., 2007). Moreover, MSS4 in mammals, weakly stimulates nucleotide exchange in a range of secretory Rab proteins (Nuoffer et al., 1997; Wixler et al., 2011). However, biochemical studies and structure of nucleotide free Rab8 with MSS4 indicate that MSS4 family members are just chaperones for nucleotide-free Rabs but not actual GEFs (Itzen et al., 2006).

Although the mechanisms have not been fully understood, it has been known that GEF proteins containing VPS motif and DENN motif can activate a group of even overlapping Rab GTPases (Marat et al,. 2011; Carney et al,. 2006). TRAPP and Sec2/Rabin8 are not like DENN domain containing GEF proteins; they have very specific substrates, Ypt1/Rab1, Ypt31/32/Rab11 and Sec4/Rab8, in yeast and mammalian cells respectively (Thomas and Fromme, 2016; Barrowman et al., 2010; Hutagalung and Novick, 2011).

Once carried out their vesicle transport, GTPases dissociate from the membrane and prepare for the next round cycle. GAPs accelerate the slow intrinsic GTPase activity to exchange GTP-bound form to GDP-bound form. Similar with GTPase GEFs, the GAPs are subfamilies specific which are verified by the structural information (Calmels et al.,

1998). To date, most GAPs share a common conserved TBC (Tre-2/Cdc16/Bub2) domain (Strom et al., 1993; Du et al., 1998; Albert et al, 1999; Vollmer et al., 1999; Eitzen et al., 2000). The first discovered TBC domain GAP, GYP6 (GAP for Ypt6) was found in yeast (Strom et al., 1993). Although more GAPs containing TBC domain were found later, the GAPs number is still much less than the number of Rabs (Fukuda, 2011). This phenomenon may be explained that one TBC-containing GAP is able to inactivate multiple Rab GTPases (Frasa et al., 2012). The structure of Rab33-GDP: Gyp1 complex demonstrates that the classical arginine finger (Arg343) and the glutamine finger (Gln378) on the TBC domain of Gyp1 was faced with the switch II glutamine (Gln 92) of Rab33. Both fingers from GAP protein contribute to stabilize the β-phosphate of GTP so that γ-phsphate of GTP easily hydrolyze and dissociate from Rab (Figure 1-3) (Pan et al., 2006; Rak et al., 2000). Indeed, some TBC domains lack of conserved glutamine or arginine finger also perform as RabGAPs (Frasa et al., 2012).

Aside from GEF and GAP, two other proteins, GDI (GDP-dissociation inhibitor) and REP (Rab escort protein) are also crucial for the function of Rabs. The structures of Rab-GDI and Rab-REP show how these regulators associate with Rab proteins that mediate membrane insertion. Although REP is similar to GDI and both of them are members of the GDI superfamily, they have diverse functions in the Rab GTPase cycles. REP associate with RabGGT to facilitate the addition of geranylgeranyl lipid moieties to the C-termini of Rabs, and then interact with either prenylated or unprenylated Rabs. However, GDI only tightly binds to the inactive Rab with its prenyl groups and thus to extract prenylated Rabs from members (Pylypenko et al., 2006; Wu et al., 2007). The structural of GDIs shows that they are highly conserved from yeast to human cells (Figure 1-4A). Both RabREP and RabGDI contain a two-site interface with Rab GTPases where one domain recognizes the GDP-bound Rab RabF regions and the other domain interacts with Rabs geranylgeranylated C-terminus (An et al., 2003; Rak et al., 2003; Rak et al., 2004; Pylypenko et al., 2006). In addition, domain I also can interact with the binding motif (CBR interacting motif, CIM) in the Rab hypervariable region.

The structures of the complexes between RabGGTase and REP-1, as well as between Rab7 and REP-1 provided detailed biophysical information of REP1 and RabGGTase working mechanisms (Pylypenko et al., 2003; Rak et al., 2004). Although the structure of the catalytic ternary complex has not been solved, it was computationally

modelled and biochemically validated by using structural information from the binary complexes (Figure 1-4 C) (Wu et al., 2009). REP1 binds with high affinity to both unprenylated Rab7 (K_d =0.22 nM) and even higher affinity with monoprenylated Rab7 (K_d=0.061 nM).

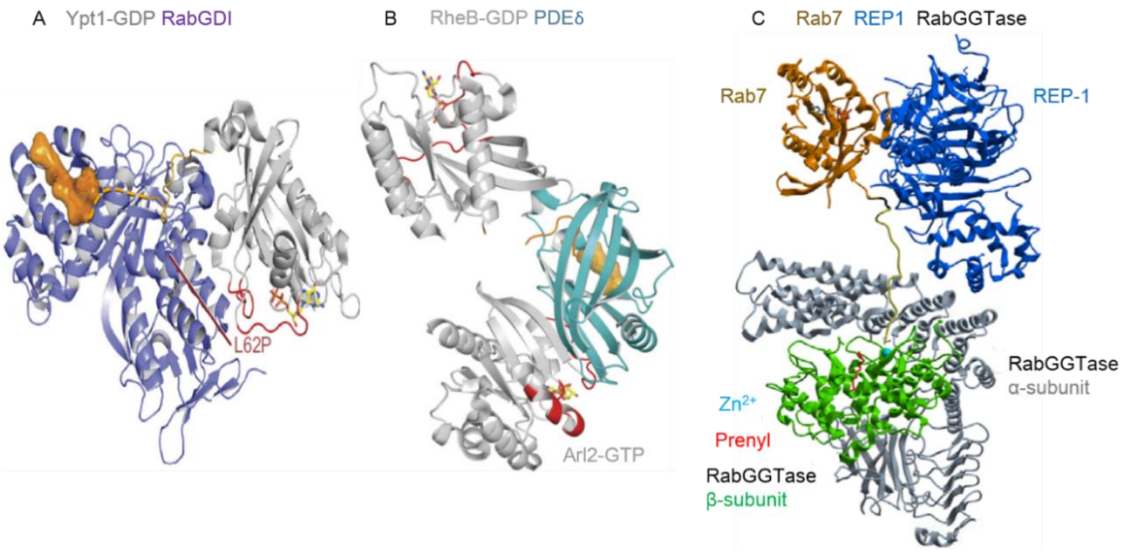

Figure 1-4. Structures of RabGDI, RasGDI and RabREP. (A)The Ypt1: RabGDI(PDB code: 2BCG) complex between doubly geranylgeranylated Ypt1-GDP in gray, switch regions in red, C-terminal extension in yellow with disordered regions in broken line, geranylgeranyl lipids in orange surface and RabGDI in blue is shown. The location of the missense LP mutation found in X-linked mental retardation is indicated. (B)The complex between PDEδ and farnesylated RheB-GDP(PDB code: 3T5G) in gray, with switch regions in red, C-terminal extension in red with disordered regions in broken line, farnesyl lipid in orange surface, and PDEδ in cyan. The β-sandwich of PDEδ is shown with the same orientation as the β-sandwich of RhoGDI. The complex between PDEδ and Arl2-GTP (PDB code: 1KSH), the candidate GDF for PDEδ, is overlaid. (This picture from Cherfils and Zeghouf, 2013) (C) Rab-GDP, REP-1 and GGTase-II form a ternary complex (This picture from Wu et al., 2009). Prenyl groups are transferred in two consecutive reactions from GGPP to Rab. Structure of the complex GGTase-II (α and β subunits are colored gray and green, respectively), REP-1 (blue) and Rab7 (orange) based on structures of prenylated Rab7: REP complex (PDB code, 1VG0) and REP-1: RabGGTase (PDB code, 1LTX). The farnesyl group is show in stick representation in red, and Zn2+ as a turquoise ball in cyan.

Unlike REP1, GDI binds poorly to unprenylated Rab but with high affinity to mono- or diprenylated Rab7. Combination of the structural and biochemical analysis suggests that the second prenyl group may bind to the outside part of the pocket in REP and even displace the first one to reduce its affinity. Although detailed structures showed the interaction between prenylated Rabs with GDI or REP, is the mechanism still needs to be

addressed that why GDI extracts Rab from the membranes with such high affinity. There is a theory to explain how GDI removes a membrane bound Rab through masking its hydrophobic prenyl tails from the aqueous environment (Wu et al., 2007). It was proposed that the opposite reaction would require additional factors to efficiently break the stable Rab-GDI interaction, such as a GDF or the molecular chaperone Hsp90 (Lee et al., 2009; Goody et al., 2005; Ignatev et al., 2008 Chen and Balch, 2006). An integral membrane protein Yip3/PRA1 was found as GDI-displacement factor (GDF), and it has been shown to catalyze the dissociation of GDI from Rab9/Rab5 (Dirac-Svejstrup et al., 1997, Sivars et al., 2003). However, it is unclear that how GDFs play roles in these processes. It is difficult to get the structure of the Rab:GDI:GDF complex, probably due to the low solubility of Yip3/PRA1.

A GDI-like solubilizing factor is PDEδ, which was considered as a GDI because it can displace prenylated Rab13-GDP from the membrane (Marzesco et., 1998). Subsequently, PDEδ was found to accelerate the dissociation of Ras family GTPase from membrane and therefore it was classified as Ras GDI (Nancy et al., 2002). The structure of PDEδ is similar to the β-sandwich lipid-binding domain of RhoGDIs (Hanzal-Bayer et al., 2002; Nancy et al., 2002). The complex structure of farnesylated RheB (a member of Ras family) with PDEδ shows that PDEδ uses its two β-sheets to accommodate the farnesyl lipid of RheB, similar with that RhoGDI holds the geranylgeranyl lipid of Rho protein (Figure 1-4B) (Ismail et al., 2011; Fansa et al., 2015). However, PDEδ does not carry an additional GTPase-binding domain, and it recognizes RheB only by its farnesylated C-terminus.

1.1.4 The prenylation of Rab GTPase

Except the 160-170 amino acids length core motif of Rab GTPase, the C-terminal extension or C-terminal hypervariable domain (HVD) is also important for its functions (Figure 1-2, Chavrier et al., 1991; Stenmark et al., 1994). The small GTPase Rab proteins are post-translationally modified by geranylgeranyl-transferase II (RabGGTase) which adds the geranylgeranyl moiety (ies) to one or (in most cases) two cysteines at the C-terminus which secures the attachment of their active form to membrane (Casey et al., 1996). The structures of Rab GTPases prenyl tails show these proteins have cysteine-linked geranylgeranyl groups which come from soluble 20-carbon geranylgeranyl

pyrophosphate (GGPP) (Farnsworth et al., 1990; Glomset et al., 1990; Swanson and Hohl, 2006).

RabGGTases prefer transfer the 20 carbon geranylgeranyl moieties to the C-terminal of Rabs with CXC, CC, CCX, CCXX and CCXXX sequences, and some cases are mono cysteine Rabs with CXXX such like Rab8 and Rab13 (Khosravifar et al., 1991; Kinsella et al., 1992). In addition, Rab GTPases ending in CXC undergo carboxymethylation by Isoprenylcysteine Carboxyl Methyltransferase (ICMT). The Methyl esterification neutralizes the negative charge of the prenylcysteine and thereby increases membrane affinity (Smeland et al., 1994; Dai et al., 1998).

RabGGTase contains α and β subunit which form heterodimer structures that has delegated substrate recognition to Rab escort protein (REP) (Armstrong et al., 1993; Zhang et al., 2000; Nguyen et al., 2010). REP interacts with the newly synthesized unprenylated GDP-bound form of Rab protein (Alexandrov et al., 1998; Seabra, 1996b; Sanford et al., 1993) and mediates its recognition by RabGGTase (Pylypenko et al., 2003; Alexandrov et al., 1999; Anant et al., 1998). Upon Rab:REP:RabGGTase:GGPP complex being formed, consecutive double prenylation without dissociation of the mono-prenylated intermediate from GGTase-II (Thoma et al., 2001c). The mono-prenylated Rab still tightly associate with REP to secure the complete di-prenylation of Rab (Shen and Seabra, 1996). Complete the double prenylation, binding of the second GGPP molecule triggers the release of Rab from Rab:REP complex to possible membrane attachment (Thoma et al., 2001b). Hence, REP is released and prepared for another round of Rab prenylation.

All the prenyltransferases require only Zn^{2+} but FTPase and RabGGTase also need extra Mg^{2+} for their catalytic ability (Chen et al., 1993; Moomaw and Casey, 1992; Seabra et al., 1992). The combinations of biochemical and spectroscopic methods that utilize isoprenoid and protein-based fluorescent probes have illustrated the prenylation mechanisms. In addition, the structural information come from the computationally model of Rab7:RabGGTase:REP-1 (Figure 1-4 C) raises clues of prenylation of Rab GTPase by RabGTTase (Wu et al., 2009). This model revealed that Rab switch I and II motifs could interact with the Rab binding platform (RBP) of REP to facilitate their association. Moreover, the determinant element is the interaction between the unprenylated Rab and

the hydrophobic patch on the surface of REP, termed the C-terminal binding region (CBR), with the so called CBR binding motif (CIM) which localize the Rab C terminus (Rak et al., 2004; Wu et al., 2009). The CIM of most Rabs contains two large hydrophobic residues surrounding a more polar residue. The catalytic ternary complex model reveals that the RBP of REP first recognizes the Rab GTPase and thus assembles Rab GTPase together, leading to a low- to intermediate-affinity complex (Nguyen et al., 2010). With the association of CBR and CIM, the affinity of this complex is further increased by an order of magnitude, which leads to the Rab C-terminus pointing to the REP-associated RabGGTase.

The Rab C-terminus cysteines bind to the active site of RabGGTase through a series of weak interactions in a step by step fashion. The weak interactions secure the protein substrate specificity does not need to be encoded in the prenylatable C terminus, facilitating the unspecific reorganization between GTPases and REP. This sequential complex assembly with progressively weaker and smaller binding interfaces, and enables cysteine residue(s) close to the C terminus to be prenylated by RabGGTase. This working style also secures the multiple prenylation events on a single substrate being fulfilled completely.

After double prenylation of the cysteines, new GGPP will be loaded to the REP1 making prenylated Rab being released from Rab:REP complex. The newly prenylated Rabs will be delivered to some membranes and insert into the lipid bilayer with hydrophobic isoprenoids tail(s) (Alexandrov et al., 1994). To date, only two REP proteins, REP1 and REP2, are found in mammalian cells, while only one Mrs6p is found in yeast (Cremers et al., 1994; Fujimura et al., 1994). The prenylation of Rab is crucial for its cycle in cells and will induce diseases by causing the absence or mutations of REP protein. A disease termed choroideremia is characterized by progressive atrophy of the choroid, retinal pigment epithelium (RPE) and retina that lead to eventual blindness (Seabra et al., 1993). Later analysis of tissue samples from patients with this disease revealed that the unprenylated Rab27a lacks its normal function and accumulates in retinal due to the mutation of REP-1. Intriguingly, the REP-2 can’t compensate the REP1 mutation and does not prenylate Rab27a in vivo (Cremers et al., 1994; Seabra et al., 1995). The accumulation of non-functional Rab27a proteins induces a massive apoptosis of retinal cells, which leads to a progressive degeneration of the retina.

1.1.5 The functions of Rab GTPases in vesicular traffic

Rab proteins are the key regulators in vesicular traffic via interacting with various effector proteins in respective pathways. The newly synthesized proteins and lipids are transported to their destination via exotic pathway. Moreover, cells absorb nutrients, molecules outside of plasma member and receptors on the cell surface are dependent on endocytosis machinery. Both above pathways require various coated vesicles to transport different contents in cells. At least three kinds of coated vesicles involved in the selective cargo transport (Juan and Benjamin, 2004). Three kinds of coated vesicles, coat protein complex-I (COPI) (Presley et al., 2002), coat protein complex-II (COPII) and clatrin (Fotin et al., 2004a; Fotin et al., 2004b), are required for intracellular membrane trafficking, corresponding to retrograde, anterograde(exotic pathway) and endocytic pathways, respectively. The vesicular traffic contains several connective steps including cargo selection, coated-vesicle formation, uncoating, directed vesicular movement, target membrane recognition, and fusion. (Figure 1-5). During each step, a unique set of Rab interacting proteins/effectors are required.

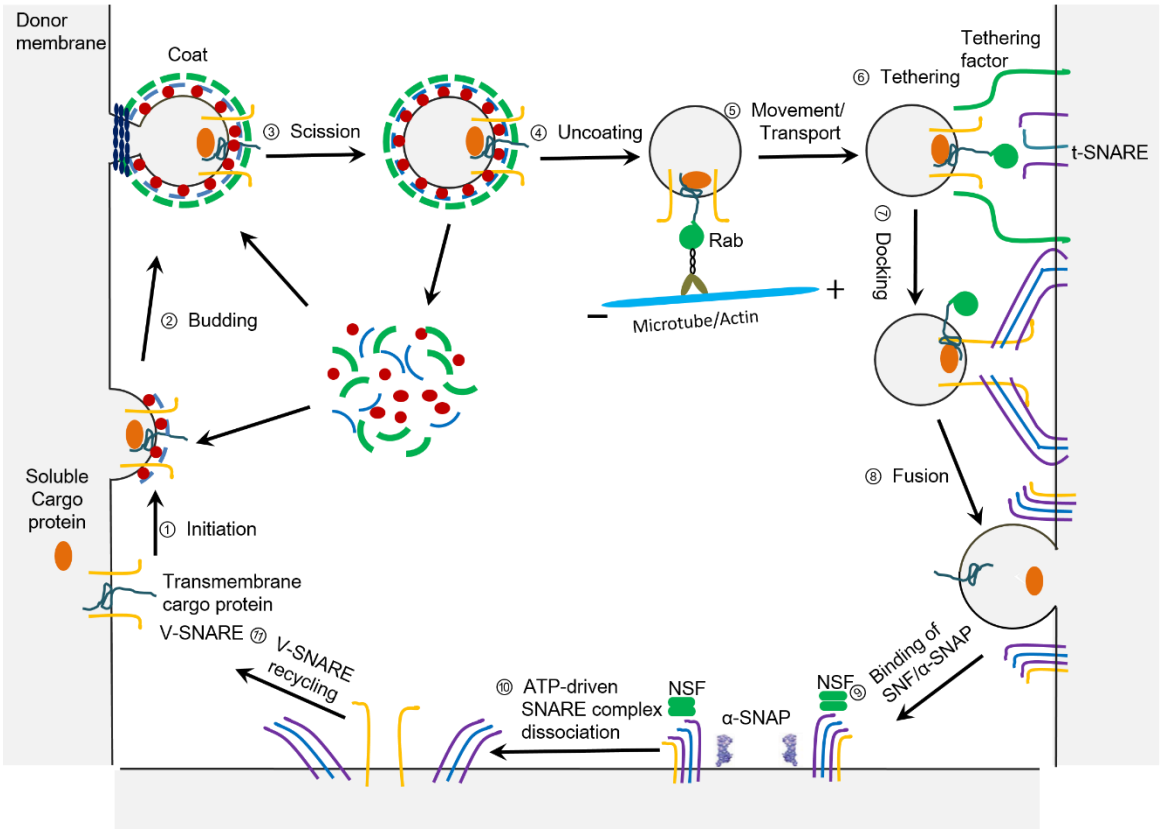

Figure 1-5. Steps of vesicles budding and fusion. (1) Initiation of coat assembly. The membrane-proximal coat components (blue) are recruited to the donor compartment by binding to a membrane-associated

GTPase (red) and/or to a specific phosphoinositide. Transmembrane cargo proteins and SNAREs begin to gather at the assembling coat. (2) Budding. The membrane-distal coat components (green) are added and polymerize into a mesh-like structure. Cargo becomes concentrated and membrane curvature increases. (3) Scission. The neck between the vesicle and the donor compartment is severed either by direct action of the coat or by accessory proteins such like dynamin. (4) Uncoating. The vesicle loses its coat due to various events including inactivation of the small GTPase, phosphoinositide hydrolysis, and the action of uncoating enzymes. Cytosolic coat proteins are then recycled for additional rounds of vesicle budding. (5) Movement or transport. GTP-Rab proteins directly or via effectors recruit motor proteins to drive the movement of vesicles along microtubules and actin filaments. (6, 7) Tethering, the vesicles are transported to the target compartment. GTP-Rab proteins mediate recruitment of effectors, tethering factors, SNAREs, facilitating tethering, docking and fusion of vesicles at the target membrane. The v- and t-SNAREs assemble into a four-helix bundle. (8) This "*trans*-SNARE complex" promotes fusion of the vesicle and acceptor lipid bilayers. Cargo is transferred to the acceptor compartment. (9, 10) A cis-SNARE complex in the fused membrane α-SNAP binds to this complex and recruits NSF, which hydrolyzes ATP to dissociate the complex. (11)The SNAREs are recycled to the donor membrane for next round cycle.

Effectors are defined as proteins that preferentially interact with their respective GTP-bound form of Rabs. One notable exception is protrudin, which interact preferentially with the GDP-bound form of Rab11 (Shirane and Nakayama, 2006).

In the COPII controlled anterograde process, the newly synthesized lipids and proteins at ER are transported to their destination at the endosomes, plasma membrane or outside of a cell (Gurkan et al., 2006). To balance the proteins and lipids within ER and Golgi, COPI mediated retrograde pathway sends back those lost proteins and lipids from Golgi to ER (Lippincott-Schwartz and Liu, 2006). The endocytic pathway is responsible for nutrients uptake and internalization of various signal carriers, is carried out by clathrin coat vesicle though some non-clatrin coats that works in this process (Edeling et al., 2006).

The cargo selection and vesicle formation might be initiated at plasma membrane, ER, Golgi and endosome and the vesicles bud from these donor membranes (Figure 1-5, step1). The small GTPases Arf and Sar are the main participants in COPI and COPII formation, respectively (Memon 2004; Barlowe et al., 1994). The active GTP-Sar1 recruits the Sec23:Sec24 to form the membrane-proximal layer, while Sec13:Sec31 forms the second membrane-distal layer, step by step. During COPI Coat assembly, GTP-Arf, simultaneously recruits the mem-cytobrane-proximal βγδζ, and the membrane-distalαβ'ε sub-complexes (Hara-Kuge et al., 1994) at the same time which is different from the

stepwise assembly of COPII by Sar1. Both Arf and Sar are also controlled by their GEFs and GAPs in assembling and disassembling of COP coats. The clathrin coats are more complicated than COPI and COPII. During the clathrin coats formation, Arf and/or specific phosphoinositides such as PtdIns(4)P or PtdIns(4,5)P_2 recruit a variety of adaptor AP-1,-2,-3 heterotetrameric complexes and the monomeric GGA, Hrs, Epsin1 and ARH proteins from cytosol to membrane (Bonifacino and Lippincott-Schwartz, 2003; Wang et al., 2003; Bonifacino and Traub, 2003).

Apparently several Rabs are also involved in the coat budding process. For example Rab9 directs the vesicle transport from the late endosome to trans-Golgi network (TGN). GTP-bound Rab9 recruits its effector TIP47 that interacts with the mannose-6-phosphate receptors (M6PRs) and transfer M6PRs from endosome to TGN. The interaction between Rab9 and TIP47 enhances the affinity of TIP47 with M6PRs and induces the richness of M6PRs in vesicles (Diaz and Pfeffer, 1998; Carroll et al., 2001; Aivazian et al., 2006). Another well studied case is the cargo selection of retromer complex. Retromer functions in conjunction with numerous associated proteins, including select members of the sorting nexin (SNX) family (Seaman et al., 1998; Bonifacino and Hurley., 2008). The retromer contains sorting nexins (SNXs) dimer which associated with the Vps26-Vps29-Vps35 trimer (Horazdovsky et al., 1997; Seaman et al., 1998). The SNXs are composed of a PX domain that interacts with phosphoinositides, and a Bar domain which facilitates membrane curvature formation (Carlton et al., 2005; Frost et al., 2008). GTP-bound Rab5 and GTP-bound Rab7 interact with the Vps26-Vps29-Vps35 in a sequential manner (Rojas et al., 2008).The Vps26-Vps29-Vps35 interacts with Rab5 indirectly and is dependent on Rab5's effector, phosphatidylinositol 3-kinase. As an effector of Rab7, Vps26-Vps29-Vps35 can be recruited by Rab7 directly (Rojas et al., 2008). Furthermore, Rab9 may play either a similar or complementary role in this process (Carroll et al., 2001; Dong et al., 2013).

Some other GTPases have been involved in vesicles budding and fission (Figure 1-5, step2). For example, at the beginning step of endocytosis, the scission and release of clatrin coated vesicles (CCVs) are driven by dynamin, a vesicle invaginates. Around the neck of the vesicle, dynamin forms a spiral circle which extends lengthwise and constricts through GTP hydrolysis. Hence the vesicle neck breaks and results in the pinching off of the vesicle from the parent membrane (Praefcke and McMahon, 2004). Recently

identified Rab35 forms a tripartite complex with MICAL-L1 and ACAP2 to serve as a scaffold for recruitment of EHD1 to endosomal recycling tubules (Kobayashi and Fukuda 2013; Kouranti et al. 2006). EHD1 is one member of Dynamin-like EHD family and plays role in the process of the tubule scission.

To fuse the vesicle with acceptor membranes, it crucial to release the coats from vesicles, a process that termed uncoating (Figure 1-5, step4). In addition to promote coats formation, Rabs may also play a role in uncoating. For example, Ypt1/Rab1 has been proposed to be involved in the ER-to-Golgi traffic pathway. It presumably recruits factors that facilitate uncoating of COPII vesicles in the preparation for fusion (Jedd et al.1995; Lian et al., 1994; Moyer et al., 2001; Pind et al., 1994). Rab5 regulates the early endocytic pathway and is found on clathrin-coated vesicles (CCVs). Firstly, the assemble clathrin adaptor AP-2 complex recruit clathrin to newly formed endocytic vesicles. Meanwhile the AP-2 complex also bind another cargo such like transferrin receptor for internalization, or clathrin triskelions to facilitate coat formation (Benmerah and Lamaze, 2007; Owen et al., 2004; Sorkin 2004). The reorganization of clahrin by AP-2 is dependent on the phosphorylation of its μ2 subunit (Jackson et al., 2003). The μ2 kinase can be recruited by Rab5 to AP-2 to phosphorylate μ2 subunit. With the action of the Rab5 GAP GAPVD1, μ2 kinase was released from AP-2 to prevent it from phosphorylating the μ2. PtdIns(4,5)P_2 is also a significant component for recruiting AP-2 during clathrin-mediated endocytosis (Höning et al., 2005; Zoncu. et al., 2007). Modulation of PtdIns(4,5)P_2 levels by Rab5 may occur through recruitment of effectors such as PtdIns(3)P kinases or PtdIns phosphatases (Christoforidis et al., 1999, Shin et al., 2005).

Rab proteins are critical for vesicle movement often using motor proteins (kinesins/dyneins and myosins) along actin- or microtubule-based cytoskeletal structures (Figure 1-5, step5). There are several well studied examples of such Rabs and their effectors in this process. To balance the receptors contents on plasma membranes, the recycle transport are needed for sending back various receptors from cytosol. Rab11 interacts with myosin Vb (Myo5b) through its effector, Rab11 family interacting protein 2 (Rab11-FIP2), to regulate plasma membrane recycling (Hales et al., 2002). The transport of melanin-containing melanosomes to the plasma membrane is regulated by Rab27a which interacts with its effector melanophilin/Slac2-a that binds to the actin

motor myosin Va (Myo5a) in melanocytes (Bahadoran et al., 2001; Hume et al., 2001; Matesic et al., 2001; Stromet al., 2002; Wu et al., 2001; Wu et al., 2002). Mutation in any one member of the Myo5a, Rab27a, and melanophilin tripartite complex leads to the rare autosomal recessive disorder Griscelli syndrome (GS), the mouse mutants *dilute*, *leaden*, and *ashen* (Myo5a, Rab27a, and melanophilin, respectively) (Van et al., 2009). These patients display various symptoms ranging from hypopigmentation (GS3, melanophilin mutation) and immunological defects (GS2, Rab27a mutations) to neurological impairments (GS1, MyoVa mutations). In yeast, Ypt31p/Ypt32p facilitates the recruitment of the Myosin V type motor Myo2p directly from Golgi to exocytic vesicles, whereas the downstream GTPase Sec4p binds directly to Myo2p to coordinate the transport of exocytic vesicles along the actin (Jin et al., 2011; Lipatova et al., 2008).

Aside from the above vesicle transports which are driven by actin, another major membrane traffic pathway relies on microtubules in animal cells. Microtubules provide high-speed, long-range transport, while actins usually facilitate slower and short-range local transport events (Jordens et al., 2005). Rabs have been proposed to interact with microtubule-based motors to regulate these pathways, either interacting with kinesins (plus-end directed motors) or the dynein (minus-end directed motors) family. Dynein and dynactin form a complex, which stimulate processive motility of vesicles along microtubules (McGrail et al., 1995; Vaughan and Vallee, 1995). Rab6 localizes to the Golgi and has been shown to be involved in exocytic traffic to the plasma membrane by recruiting Rabkinesin-6 (kinesin family member 20A) directly to facilitate intra-Golgi transport (White et al., 1999; Utskarpen et al., 2006; Echard et al., 1998; Martinez et al., 1994). Rab6 also indirectly regulates microtubule motors through the effector proteins Bicaudal D1/D2 that link Rab6-containing vesicles to the dynein-dynactin motor complex, and it also links kinesin for exocytosis (Grigoriev et al., 2007; Hill et al., 2000; Matanis et al., 2002; Young et al., 2005). Another well studied case is Rab7, which coordinates the trafficking of late endosome and the lysosome or centrosome. Rab7 interacts with its effector Rab-interacting lysosomal protein (RILP) to recruit the dynein-dynactin motor complex to transport along microtubule (Johansson et al., 2007; Jordens et al., 2001). Several intracellular pathogens manipulate Rab7-effector's interaction for their growth or replication after invasion host cells. The *Salmonella* secretes effector protein SifA can hijack Rab7 that prevents the interaction between RILP and Rab7 to facilitate growth of

the membrane-bound compartment in which the bacterium can replicate (Guignot et al., 2004; Harrison et al., 2004). *Heliobacter pylori* secrets the VacA cytotoxin and causes the formation of large vacuoles. These vacuoles contain bacteria and their surfaces are highly enriched in Rab7 that can recruit RILP to direct endosmal traffic (Li et al., 2004; Terebiznik et al., 2006).

Once the vesicle is closed to the acceptor membrane, it is critical to ensure the fidelity of transport. A machinery termed tethering/docking has been addressed clearly (Chia and Gleeson, 2014; Cai et al., 2007) (Figure 1-5, step6 and 7). The tethering factors are classified into two types: One is long coiled-coil tethers and the other is multiprotein complexes (Sztul and Lupashin, 2006). Both kinds of tethers are Rab effectors which mean that Rab proteins also play roles in the tethering process. Rab effector tethering factors include Uso1p/p115, the COG complex, Vac1/EEA1, the GARP complex, the HOPS complex, and the CORVET complex. Coiled-coil tethers such as Golgins family include p115/Uso1, giantin, GM 130, Golgin97, Golgin185, Golgin210 and so on, which localize at the Golgi complex or closed to the endosomes (Short B et al., 2005). Uso1/p115 was defined as an essential factor in ER to Golgi transport in yeast (Sapperstein et al., 1995). GM130 and GRASP65 are Golgi peripheral membrane proteins that play a key role in Golgi stacking and vesicle tethering (Puthenveedu et al., 2006; Diao et al., 2008). Both GM130 and GRASP65 have been identified as effector of Rab1 (Barr et al., 1998; Moyer et al., 2001). Rab1 recruits GM130-GRASP65 complex and interacts with p115 is thought to tether ER-derived COPII vesicles to the Golgi (Sztul and Lupashin, 2006).

Multiprotein complexes such as TRAPPs were proposed to participate in the tethering processes. The TRAPPI (7 subunits) and TRAPPII (10 subunits) complexes are multisubunit tethers that regulate traffic in ER-to-Golgi, intra Golgi, and endosome-to-late Golgi traffic, respectively (Cai et al., 2005; Cai et al., 2007; Sacher et al., 1998). Unlike the above tethers, the TRAPP complexes do not work as Rab1/Ypt1 effector but act as GEFs for Rab1 which active the GTP-bound form for interacting with effectors to coordinate membrane traffic (Barrowman et al., 2010). The TRAPPI subunit Bet3 that binds to the COPII subunit Sec23 (Cai et al., 2007; Yu et al., 2006) and Bet3 also has genetic interactions with Bet1, Sed5, Sec22, and all SNARE proteins that function in ER-to-Golgi traffic (Rossi et al., 1995; Sacher et al., 1998). Mammalian mBet3 can form the

homotypic tethering of COPII-coated vesicles from vesiculotubular clusters, an intermediate compartment between the ER and Golgi (Yu et al., 2006). The active Rab1/Ypt1 recruits effectors such as Uso1/p115 and giantin, tether these intermediate vesicles to the Golgi. In addition, TRAPP may interact with the COPI coat and exhibits its function in regulating intra-Golgi and endosome-to- late Golgi traffic (Yamasaki et al., 2009).

The final step of vesicular transport is fusion with the acceptor membrane. Rothman and coworkers used Nethylmaleimide-sensitive factor (NSF)/α-Nethylmaleimide-sensitive factor attachment protein(α-SNAP) as an affinity bait to fractionate a brain lysate, and identified a set of three membrane-associated 'SNAP Receptors,' or SNAREs (Söllner et al., 1993). SNAREs control membrane fusion in all kinds of trafficking steps of the secretory pathway (Jahn and Scheller, 2006; Hong, 2005). Most SNAREs are C-terminally anchored transmembrane proteins, with their functional N-terminal domains facing toward the cytosol. Each type of transporting vesicle carries a specific 'vesicle associat (v)-SNARE' that binds to a cognate 'target associate (t)-SNARE' on the target membrane (Rothman, 1994). Both v-SNARE and t-SNAREs contain a heptad repeat 'SNARE motif' that can participate in coiled-coil formation (Bock et al., 2001). Structural and biochemical studies showed that the SNARE complex generated by the pairing of a cognate v- and t-SNARE is a very stable four-helix bundle, with one α helix contributed by the monomeric v-SNARE and the other three α helices contributed by the oligomeric t-SNARE (Fasshauer et al. 1997, Sutton et al. 1998). v-SNAREs and t-SNAREs are also termed R-SNAREs and Q-SNAREs for at the characteristic position within the SNARE motif, the v-SNAREs and t-SNAREs contain an Argine (R) and an Glutamine (Q), respectively (Fasshauer et al., 1998.). The structural analysis shows that SNARE complex composes v- and t-SNAREs pair in a parallel fashion (Hanson et al., 1997, Lin and Scheller, 1997, Sutton et al., 1998). Therefore, the concept of trans-SNARE complex means that v- and t-SNAREs are from separate membranes, while cis-SNARE complex means v- and t-SNAREs are in the same membrane. A trans-SNARE complex persists throughout the fusion reaction to become a cis-SNARE complex in the fused membrane (Figure 1-5, step8). Hence α-SNAP binds along the edge of the SNARE complex (Rice and Brunger, 1999) and recruits NSF (Figure 1-5, step9). ATP hydrolysis by NSF untwists the four-helix bundle and dissociates the cis-SNARE complex (Figure 1-

5, step10) (Mayer et al., 1996; May et al., 1999; Yu et al., 1999). Thus, the v-SNAREs and t-SNAREs are recycled for another round of complex formation (Figure 1-5, step11).

Rabs regulate fusion process by interacting directly with SNARE proteins or SNARE related proteins, such as SM or Lgl proteins, which can regulate SNARE function. For example, Rab5 is found on early endosomes and plays a critical role in endocytic pathway through the function of its numerous effectors. Rab5 effectors, EEA1 and rabenosyn-5, interact with the SNARE proteins, Syntaxin13, Syntaxin6 and the SM protein VPS45, respectively (Nielsen et al., 2000; Simonsen et al., 1999). This interaction is required to drive homotypic early endosome fusion (McBride et al., 1999).

Another example is the Rab7 effector, the Vici Syndrome protein EPG5, determines the fusion specificity of autophagosomes with late endosomes/lysosomes (Wang et al., 2016). Firstly, Rab7 and the late endosomal/lysosomal R-SNARE VAMP7/8 recruit EPG5 to the late endosomes/lysosomes. In parallel, EPG5 is also recruited to LC3/LGG-1 (mammalian and *C. elegans* Atg8 homolog, respectively) and to assembled STX17-SNAP29 Qabc SNARE complexes on autophagosomes. Therefore, EPG5 can stabilize and facilitate the assembly of STX17-SNAP29-VAMP7/8 *trans*-SNARE complexes. Moreover, EPG5 promotes STX17-SNAP29-VAMP7-mediated fusion of reconstituted proteoliposomes. The depletion of SNAP25 can partially rescue the autophagy defect caused by EPG5 knockdown (Wang et al., 2016).

In summary, by combining the regulation from above various factors, a clear map of Rab GTPase vesicular transport and recycling turned out. Newly synthesized Rab proteins are captured by Rab escort protein (REP) at the ER exit sites. REP acts as a molecular chaperone of unprenylated Rab to make it soluble in cytosol. Then REP presents Rab proteins to heterodimeric RabGGTase for being modified with (usually) two geranylgeranyl moieties. Afterwards, the prenylated Rab proteins are delivered by REP to their target membranes. The released REP recycles backs to cytosol to support additional rounds of Rab prenylation. Prenylated Rab proteins associate with the membrane where GEFs facilitate Rab-GDP exchange to Rab-GTP.GTP bound Rab proteins are active and can bind to various effectors that are involved in vesicle budding and cargo selection. GTP-Rab proteins directly, or via effectors, recruit motor proteins to drive the movement of vesicles along microtubules or actin filaments. Once the vesicles are close to the target

compartment, GTP-Rab proteins recruit effectors, tethering factors, SNAREs, facilitatete thering, docking and fusion of vesicles at the target membrane. After completing the vesicle transport, Rab GTPases undergoes hydrolysis of its bound GTP with the help of GAPs. Related effectors are released from the inactive Rab-GDP and participate in a new round of transport. GDIs extract Rab-GDP proteins from membranes and solubilize them in cytosol. For the cycled Rab GTPases, GDI delivers them to the donor membrane similar to REP. GDF may facilitates the release the prenylated Rab proteins from GDI on endosome vesicles and perform GDP-GTP exchange by GEFs.

1.1.6 The localization of Rab GTPase in cells

Rab proteins constitute the largest branch of the Ras GTPase superfamily. To date, about 70 members in mammalian cells and 13 members in yeast have been found with various functions and distinct localizations (Klopper et al. 2012; Steinet al. 2012). The much larger number of Rabs in mammals meets the requirements of the higher complexity of transport events in higher eukaryotes.

The factors controlling each step of vesicular transport are coordinated in time and space. The molecular features and functional properties of Rabs that fit with such a spatiotemporal coordination (Zerial and McBride 2001; Pfeffer 2013b; Barr 2013). Rab GTPase localization is highly compartmentalized and organelles often have a unique complement of Rab proteins (Figure 1-6) (Galvezet al. 2012; Hutagalung and Novick 2011; Stenmark 2009). In addition, Rab GTPases can shuttle between the cytosol and the membrane in either an inactive GDP-bound or active GTP-bound conformation.

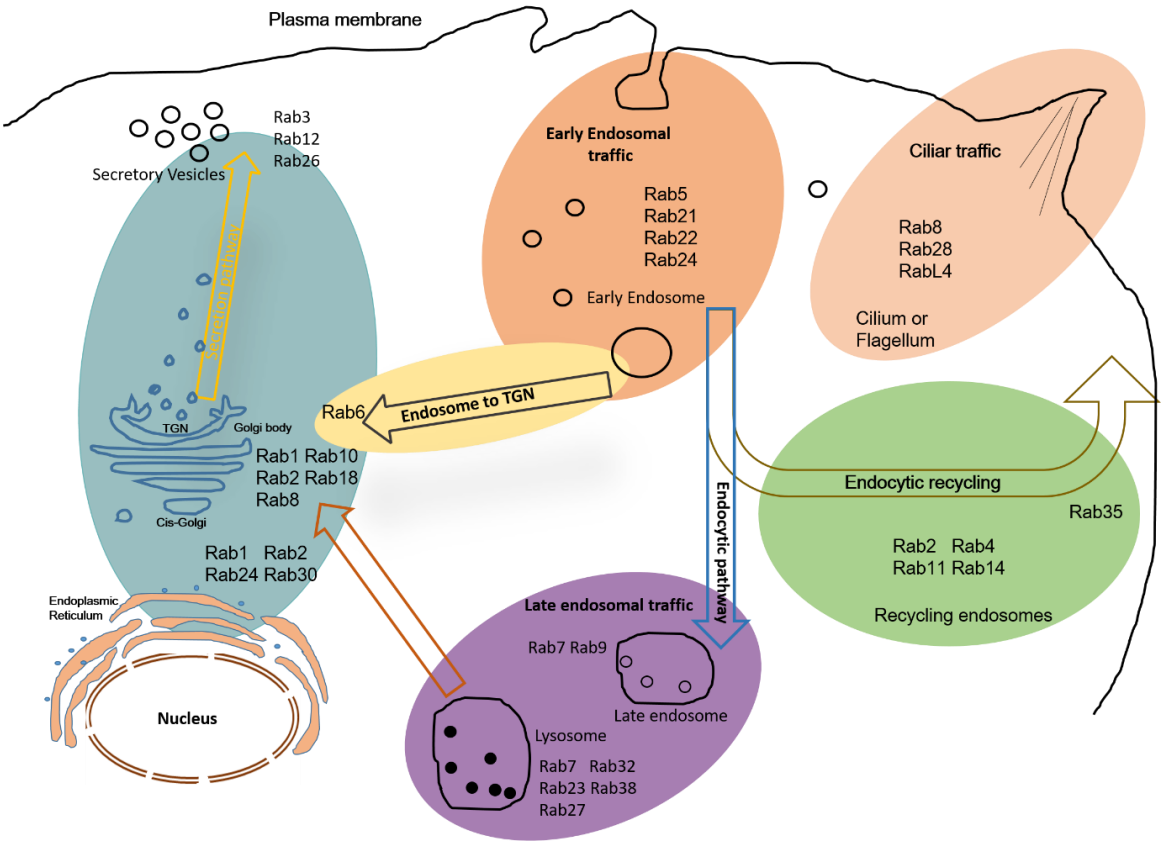

Figure 1-6. The localizations and functional groups of Rabs in mammalian cell.

A typical cell shows the intracellular localization and associated vesicle transport pathway(s) of several groups Rab GTPases. The secretion group including Rab1, Rab2, Rab24 and Rab30 regulate ER-Golgi parts and Rab1, Rab2, Rab8, Rab10 and Rab18 are contained in intra-Golgi traffic and regulate biosynthetic traffic from the trans-Golgi network (TGN) to the plasma membrane. While several secretory vesicles and granules use Rab3, Rab12 and Rab26 regulate post-Golgi vesicle transport, secretory vesicles, finally release molecular to the outside of cell environment. This group is highlighted in *cyan*. Rab2 is also involved in recycling group which including other Rab proteins Ra4, Rab11, Rab14 and Rab35. The recycling group is highlighted in shallow *green*. Rab6 regulates intra-Golgi traffic which is highlighted in *yellow*. There are numerous Rabs associated with endosomal traffic, and the most active site of localization is the early endosome. Most early endocytic steps rely on Rab5, which mediates fusion of endocytic vesicles to form the early endosome and the other Rabs including Rab21, Rab22, and Rab24. This early endosomal traffic is highlighted in *orange*. Traffic can be directed towards the lysosome for degradation, which relies on action of several Rabs including Rab7, Rab9, and Rab23 are involved in late endosomal and lysosomal trafficking. In this group, Rab27 is well-studied in the melanosome transport that also relies on Rabs 32 and 38. This group is highlighted in *purple*. In addition, Rab24 and Rab33 mediate formation of the preautophagosomal structure that engulfs cellular components to form the autophagosome that is subsequently targeted to the lysosome/vacuole. Rab21 and Rab25 regulate transport of integrin to control cell adhesion and cytokinesis. Rab13 directs traffic to and regulates formation of tight junctions in polarized epithelial cells.

Rab GTPases are one of the main coordinators of membrane domain formation and

dynamics. The first reported example is Rab5 which localizes on early endosome (Chavrier et al., 1990), and later more cases showed that different Rabs localize at distinct organelles or compartments (Zerial and McBride, 2001). Furthermore, a large amount of evidences show that Rabs work as the organelles and compartments identity marker (Marino and Heidi, 2001; Pfeffer, 2001; Barr, 2011). The works in Rab GTPases have revealed molecular features and functional properties that fit with such a spatiotemporal coordination (Zerial and McBride 2001; Pfeffer 2013b; Barr 2013). For example, Rab1 is present on the Golgi (including ERGIC); Rab6 on the Golgi; Rab5 on early endosomes and Rab7 on late endosomes (Zerial and McBride, 2001; Segev, 2001). More interestingly, Rab GTPases are now known to collect integral and peripheral membrane proteins to different organelles even on the same organelle with distinct domain (or scaffold), which is referred to as Rab domains (Sonnichsen et al., 2000). Well studied cases are early endosomes that compose separate domains enriched in Rab5 and Rab4 that are involved in endosome fusion and endocytic recycling, respectively. The recycling endosome contains domains that are enriched in Rab4 and Rab11, which are involved in vesicle trafficking from the early endosome and to the plasma membrane, respectively. Another example is Rab7 and Rab9 which localize at late endosomes (Barbero, et al., 2002).

1.1.7 Membrane targeting of Rab GTPase in cells

How Rabs associate their destination membrane or organelles by effectors is discussed partially in above sections. More evidences indicate that regulators of Rab GTPases include effectors, REP, GDIs, GDF, and GEFs which may contribute to their membrane targeting.

A best case is Rab5 and its effectors. Biochemical and cellular studies show that it is a key regulator of early endocytic trafficking (Zeigerer et al. 2012). Rab5 has a unique complexity of regulators and provides important insights into the membrane compartmentalization /targeting (Christoforidis et al. 1999a). Indeed, several of these effector molecules act indirectly but cooperatively with other components of the transport machinery. For example, the localized synthesis of phosphatidylinositol 3-phosphate (PtdIns(3)P) by PtdIns(3)P kinases is regulated by Rab5. A positive feedback loop of Rab5 recruitment and activation ensure the localized enrichment of Rab5 (Horiuchi et al. 1997; Stenmark et al. 1995). Rab5 interact with PtdIns(3)P kinases to regulate the

generation of PtdIns(3)P (Christoforidis et al. 1999b; Murray et al. 2002). The Rab5/PtdIns(3)P effectors oligomerize complexes that stabilize the Rab5 membrane domain (McBride et al. 1999). Dynamics of these oligomers need free energy from the form of GTP (Rab5) and ATP (through NSF). However, the molecular details of various proteins contribute to the formation of the oligomers is to be addressed. These proteins function sequentially or concomitantly with the recruitment by Rab5 membrane domain where these activities can be amplified.

Along recruiting specific effectors to restricted membrane microdomains, the GTPases might also confer membrane identity by controlling the local levels of phosphatases (PtdInsPs). For example, OCRL1/INPP5F, the inositol polyphosphate 5-phosphatase, is an effector of multiple Rabs including Rab1, Rab5, Rab6, Rab8 and Rab35 (Noora et al., 2006; Dambournet et al., 2011).

RabGGTaseII transfer geranylgeranyl moieties to one or (in most cases) two cysteine residues of Rab C-terminal end with the help of REP. This secures Rab for being able to associate with membranes and fulfilling their proper functions. For the newly synthesized Rabs, REP works as chaperon to solubilize prenylated Rab in cytosol and delivers it to the targeted membrane. The prenylated Rabs insert into the membrane via their one, or most cases two, hydrophobic geranylgeranyl moieties into the lipid bilayer (Shahinian and Silvius, 1995). However, it still unclear that if other factors are also involved in the delivery of prenylated Rab GTPase by REP. Some evidences indicate the attachment ability of two moieties is stronger than one (Gomes et al., 2003) and may induce unsuccessful membrane targeting/attachment. However, an exception is Rab1 with CAAX terminal (Rab1-CLLL), which can be delivered to the ER/Golgi membrane and functions well (Overmeyer et al., 2001). Several Rabs with CAAX box tail such as Rab8 (-CVLL), Rab13 (-CSLG) and Rab18 (-CSVL), can complete their membrane targeting and perform their various functions with only one prenylated cysteine (Huber et al.1993; Joberty et al., 1993). These CAAX box ends of Rabs are prenylated by RabGGTase but not FTase nor GGTaseI which are responsible for the prenylation of Ras, Rho, Rac with CAAx box C-terminal end.

The inactive Rab-GDP will be extracted by GDIs from membrane and becomes soluble in the cytosol. GDIs carry the prenylated Rab-GDP to deliver to a target

membrane. However, it is still unclear that how GDI and Rab-GDP complex associate with its destination membrane. A hypothesis was proposed that there is one factor which would catalyze the dissociation of Rab from GDI. Considering the tight affinity between Rab and GDI (KD=4.5nM) (Wu et al., 2010), an assistance is required to release Rab from its GDI. Pffefer and colleagues used screening methods and identified a protein PRA1/Yip3 which works as GDI displacement factor (GDF) (Dirac-Svejstrup et al., 1997). Prenylated Rab acceptor-1 (PRA1) and Ypt-interacting protein III (Yip3) feature four transmembrane domains, with their N and C termini facing toward the cytosol while the remaining bulky parts of their sequences being membrane embedded (Calero et al.,2002; Lin et al., 2001) . PRA1/Yip3 localizes at Golgi and endosomes (Martincic et al., 1997; Bucci et al., 1999) where it interacts with prenylated Rab proteins (Sivars et al., 2003; Abdul-Ghani et al., 2001). Meanwhile, PRA1/Yip3 also weakly interacts with GDI (Hutt et al., 2000).

Rab9-GDI complex can be dissociated by Yip3/PRA1 at pico-molar level, which is indicted by the rate of 35S-GTPγS binding. Intriguingly, Yip3/PRA1 is not a common GDF which only works for endosomal Rab proteins, such as Rab5, Rab7 and Rab9. Mammalian Yip family contains 16 members in human and 14 members in mice. The Yip1 can recruit Ypt1 on ER-Golgi Yip1 in vivo (Barrowman et al., 2003). The working model of Yip3/PRA1 indicates several possible factors that preferably interact with Rab5, Rab7 and Rab9 in vitro and in vivo.

Another explanation of membrane targeting mechanism is GEFs mediated Rabs localization. GEFs have the ability to exchange Rab GDP-bound to Rab GTP-bound and displace GDIs by lowering the affinity between Rabs and GDIs. Upon GTP binding, Rab proteins undergo a conformational change. This protects them from being removed by Rab GDI and allows for Rab effector protein binding. The first case of GEF displacing GDI via GDP-GTP exchange is the identity of DrrA/Sidm. *Legionella pneumophila*'s DrrA/Sidm, a virulence effector which plays a key role in hijacking the host vesicular trafficking by recruiting Rab1 to the cytosolic face of the Legionella-containing vacuole (LCVs). DrrA/Sidm acts as a GDP-GTP exchange factor (GEF) for the small GTPase Rab1 (Rab1A, Rab1B), thereby converting Rab1 to an active GTP-bound state, leading to the incorporation of Rab1 into LCVs (Schoebel et al., 2009; Wu et al., 2010; Murata et al., 2006; Machner and Isberg, 2006). Interestingly, the Rab1 can even be recruited to plasma

membrane with the ectopic expression of DrrA/Sidm at PM (Murata et al., 2006). A similar case is the Rab3GEF which is necessary for recruiting Rab27 to melanosomes (Tarafder et al., 2011).

A general function of GEFs is to provide the thermodynamic driving force for Rab membrane targeting via nucleotide exchange (Wu et al., 2010). Therefore GEFs might be sufficient to mediate specific targeting of Rabs to membranes. However, in order to ensure that this mechanism works, GEFs need to be localized to particular membranes. This hypothesis was proved by a more recent evidences that Rabex-5 (Rab5GEF), and Rabin8 (Rab8GEF) display the minimal targeting machinery for recruiting Rabs from the cytosol to the correct membranes (Blümer et al., 2013). GEFs are indeed recruited to or activated at cellular membranes on demand by factors acting upstream, such as Rab cascades or feedbacks (Rivera-Molina and Novick, 2009; Mizuno-Yamasaki et al., 2010; Poteryaev et al., 2010), and/or dependence on changes in membrane phosphoinositide composition (Shin et al.,2005 ; Christoforidis et al., 1999).

Rabs contain a conserved GTPase domain and a structurally flexible C-terminal amino acid sequence of variable length (~25- 40 amino acids), termed C-terminal hypervariable domain (HVD or HVR) that bearing the one or two prenylated cysteine residues at the very end. In contrast to the conservation of GTPase domain, the C-terminal sequence is very divergent in sequence among Rab proteins. Zerial and colleagues designed a series of chimeric Rabs such like Rab5 with Rab7's HVR, Rab2 with Rab5's HVR or Rab7's HVR. These chimera target Rabs to the corresponding Rab's HVR membranes. Compared to the divergence sequences of hypervariable sequence of each Rab/Rab family, a hypothesis was proposed that these domains contain the targeting information to associate a specific membrane compartment. More recent work has shown similar results for GTPase domain/hypervariable sequence Rab9/Rab5 and Rab9/Rab1 chimaeras (Aivazian et al., 2006). All above cases showed that C-terminal hypervariable domain mediate membrane targeting via its interaction with Rabs eggectors. On the contrary, the presence of poly basic regions in the Rab35 and KRas C-terminus contributes to the localization on negatively charged membranes (Heo et al., 2006). However, subsequent works by Seabra and colleagues strongly suggest that multiple regions

contribute to the correct Rab membrane targeting (Ali et al., 2004). They swapped the C-terminal hypervariable domains of Rab1A, Rab2A, Rab5A, Rab7A and Rab27A, causing these Rabs to localized to correct compartmental membranes. These evidences indicate that the Rabs membrane targeting is determined by conserved GTPase domain but not the C-terminal hypervariable domain (Ali et al., 2004; Tarafder et al., 2011). Therefore the model that the C-terminal hypervariable domain determines Rabs membrane association might not be universal. Thus, the function of the Rab HVD and a complete model for Rab membrane targeting remain to be established.

In summary, the mechanisms of Rab membrane targeting via its prenylation tail(s), its regulators are including GEF, GDF, and effectors. However, the mechanisms of membrane targeting are quite complicated which need to be further elucidated.

1.1.8 Rab cascades and feed-back

As membrane flows from one organelle to another in a cell, it must transit through a connective membrane units or Rab defined compartments. Rab acting as compartment organizer is regulated by different factors including GEF, GDI, GAP, and effectors. Therefore, a question is turned out that how the Rabs which localize at different compartments membrane are active and inactive from one to another. To solve this problem, a model of Rab cascade is proposed which address the compartment transitions from an upstream Rab to a downstream Rab by recruiting effectors which work as the GAP and the GEF for the upstream and downstream Rabs, respectively (Markgraf et al., 2007; Rivera-Molina and Novick, 2009; Pfeffer, 2012; Novick , 2016).

For example, a cascade involved Ypt31/32(Rab11 homolog) and Sec4 (Rab8 homolog) play a role during membrane transit from late Golgi to plasma membrane via secretary pathway (Benli et al., 1996; Goud et al., 1988; Jedd et al., 1997; Salminen et al., 1987).

GTP-bound form Ypt31/32 recruits Sec2, the GEF of Sec4, which activates Sec4 that is associated with secretory vesicles. The loading of Sec4 into secretory vesicles secures their delivery and fusion with the plasma membrane (Ortiz et al., 2002). In this cascade, Sec4 can be involved in the correct pathway by association with secretory vesicles which is dependent on its direct upstream Rab. Moreover, Sec2 also interacts

with Sec15, an effector of Sec4, as a supplement to help recruit Sec4 on secretory vesicles (Guo et al., 1999; Medkova et al., 2006; Salminen and Novick, 1989).

To date, the best well studied of Rab GEF cascade is the transition from early endosome to late endosome which is directed by Rab5 and Rab7 (Rink et al., 2005; Poteryaev et al., 2010). Endocytic cargo is initiated from Rab5-containing early endosome that can undergo maturation to become Rab7-containing late endosome for being targeted to lysosomes (Rink et al., 2005). The HOPS complex contains one of its subunits, the Vps39 protein which is a GEF for Rab7. Herein, Rab7 also serves as an effector of Rab5 (Cabrera et al., 2009; Rieder and Emr, 1997). In the meanwhile, the HOPS complex is also an effector of Rab7 (Seals et al., 2000). Therefore, Rab5-mediated recruitment of the HOPS complex in turn promotes the association of Rab7 with this membrane and then initiates the maturation towards the lysosome/vacuole. This process of Rab conversion appears to proceed in several steps. Firstly, the active GTP-Rab5 associates with early endosomes. Secondly, the association of Rab5 membranes progressively forms larger endosomal compartments via homotypic fusion that moves from the cell periphery towards the cell center along microtubules. Thirdly, a transient overlap Rab5 with Rab7 occurs, which is mediated by the HOPS complex. Finally, Rab5 compartments convert to Rab7 compartments which are destined for the lysosome/vacuole. These results indicate a maturation model where every transport compartment gains the necessary factors to move forward while losing those that defines the upstream compartments (Rink et al., 2005). Another support for the maturation model comes from the studies of the Golgi in *S.cerevisiae.* Both studies show that specific Golgi cisternae transitions from early Golgi to late Golgi through the secretory pathway (Losev et al., 2006; Matsuura-Tokita et al., 2006).

The divalent effectors of Rab also can affect Rab conversion and target traffic appropriately from a compartment that serves multiple pathways. In the early endocytic pathway, another Rab5 effector, rabenosyn-5, has a binding site and is an effector of Rab4 that is involved in targeting proteins to the Rab11-positive recycling endosome. Functional study with the over expression of rabenosyn-5 in cells showed that the overlap of Rab5 and Rab4 is prolonged (De Renzis et al., 2002).

The GEF cascade mechanism explains how a downstream Rab can be recruited to a membrane domain that is initially carries an upstream Rab. GAPs play key roles in this process to avoid an extended period of overlap of Rab domains within a compartment; it is also important to inactivate the upstream Rab once the downstream Rab has been recruited and activated. For example, RabGAP-5(the GAP for Rab5) works in regulating endosomal traffic; abnormal expression of RabGAP-5 in HeLa cells blocked trafficking of substrates from early endosomes to the lysosome (Haas et al., 2005).

In short, the discoveries of Rab cascade indicates the nature of energy saving and high efficiency work model in cells.

1.1.9 Rabs related diseases

1.1.9.1 Rab and cancer

Rab proteins work together with their cognate effectors, coordinate the dynamics of trafficking pathway and determine the cargo proteins' destination in cells. Aberrant Rab GTPases functions by mutations or post-translational modifications will disrupt the regulatory network of vesicle trafficking, which have implications in tumorigenesis, Parkinson's disease, Huntington's disease and bacteria induced diseases via hijack Rab and Rab regulators.

Many Rab GTPases have been proposed to be involved in the progression of multiple cancer types. Membrane traffic plays a significant role in cancer biology, primarily in the loss of cell polarity and in the metastatic transformation of tumor cells (Mosesson et al., 2008). More evidences showed that a group of Rabs including Rab1, Rab2A, Rab3, Rab4, Rab8, Rab11, Rab21, Rab23, Rab25, Rab27B, Rab35, Rab37 and Rab38 promote tumor cell migration and invasion, and consequently exhibit their effects on tumorigenesis and metastasis by interruption of intracellular signal transduction (Yoon et al., 2005; Caswell et al.,2007; Bravo-Cordero et al., 2007; Yang et al.,2016; Luo et al., 2015; Yang et al 2009; Tang et al.,2009; Hou et al., 2008; Cheng et al.,2004; Wheeler et al., 2015). One of well characterized example Rab involved in cancer is Rab25, which regulates apical endocytosis and transcytosis in epithelial cells (Casanova et al., 1999; Wang et al., 2000). High expression level of Rab25 has been frequently found in poor prognosis in breast and ovarian cancer patients due to amplification of the Rab25 gene.

High expression level of Rab25 also promotes anti-apoptotic phosphoinositide 3-kinase (PI3K)-Akt pathway and inhibits pro-apoptotic molecules expression such as BAK, and thereby increasing aggressiveness of cancer cells (Cheng et al., 2004). Later studies showed that Rab25 can interact with β1-integrin subunit and promote invasiveness of tumor cells into a three-dimensional extracellular environment (Caswell et al., 2007). Interestingly, Rab25 only facilitates tumor progression but does not initiate tumorigenesis. Norman and co-workers found that Rab25 can maintain a pool of α5β1-integrin heterodimers at the tip of the invasive pseudopod which facilitates efficient integrin recycling and secures a stable association of the pseudopod within the extracellular environment (Caswell et al., 2007). Similarly, Rab11 has been found to enhance cancer cell invasion in breast cancer where it mediates α6β4 integrin trafficking (Yoon et al., 2005). The oncogenic gene Rab1 was found to be over-expressed in some poor survival cancer types (Bao et al., 2014; Thomas et al., 2014; Xu et al., 2015). Mechanistically, over expressed Rab1A stimulates mTORC1 signalling and facilitates oncogenic growth under amino acids stimulation, and therefore increases the invasion in colorectal cancer (Thomas et al., 2014; Xu et al., 2015).

More recently, Rab35 gene has been identified to be an oncogene through two gain-of function mutations in tumor cells. Constitutively active Rab35 mediates internalization of platelet-derived growth factor receptor α (PDGFRα) to LAMP2-positive endosomal membrane, where it drives the activation of oncogenic PI3K/Akt signaling (Wheeler et al., 2015). This suggests that the cooperation between Rab-mediated vesicle dynamics and oncogenic signaling leads to tumor progression.

1.1.9.2 Rab and neurological diseases

Recent discoveries showed that Rabs are related to several prevalent neurological diseases. Some Rab proteins including Rab3, Rab11 and Rab23 are involved in synaptic function, neurite outgrowth and nervous system developmental processes (Jenkinset al., 2007). Membrane trafficking may perturb neurons via their unique polarized structure and function.

Ferrer and colleagues got the first evidence that Rab is connect with Parkinson's disease (PD) in mouse (Dalfó et al., 2004). PD is the most prevalent neurological disease which is characterized by disordered movement due to loss of

dopaminergic nerve cells in the substantial nigra (Forno, 1996). The missense point mutations of α-synuclein protein cause an autosomally dominant inherited form of PD (Gasser, 2009). Lewy bodies are considered as the hallmark of PD that contains α-Synuclein (α-syn) protein aggregates in neurons (Spillantini et al., 1998; Spillantini and Goedert, 2000). Rab3a, Rab5, and Rab8 have been found that they can interact with point mutation of A30P α-syn protein that could induce PD. However, the wild type α-syn couldn't be recruited by above Rabs. In addition, high copies of the α-syn gene can also lead to PD (Ibáñez et al., 2004; Singleton et al., 2003). Furthermore, Rab1 has been found to be involved in the process of α-syn proteins transport. The overexpression of α-syn proteins disrupts ER-to-Golgi transport, which can be rescued by overexpression of Ypt1/Rab1 (Cooper et al., 2006). Moreover, over expression of Rab1 can reduce α-synuclein-induced toxicity in PD animal models and mammalian dopaminergic cells. Subsequent data indicates that α-syn proteins may also affect Rab3 and Rab8 membrane traffic pathways (Gitler et al., 2008). Above results may have given us a clue of PD therapy via regulation of Rab GTPase expression level in brain.

Huntington's disease (HD), which was known as Huntington's chorea, is an inherited or genetic disorder due to a trinucleotide repeat of huntingtin (htt) gene in the central nervous system (Goedert et al., 1998). Huntington's disease usually develops in both men and women adulthood and can cause a very wide range of symptoms. The htt gene mutation produces an N-terminal polyglutamine repeat with the length of the expansion, and finally forms the polyQ repeat (Gil and Rego, 2008). The polyQ repeat associates with membranes and plays a role in membrane trafficking though its unclear way that how it produces a disease status (DiFiglia et al., 1995; Velier et al., 1998). Htt can interact with two effectors of Rab8 optineurin protein and FIP-2 at the Golgi (Faber, et al., 1998; Hattula and Peränen, 2000; Sahlender et al., 2005). Mutant of htt disrupts clathrin-mediated traffic from post Golgi to lysosomes (Del Toro et al., 2009). The mutation prevents Rab8 to recruit optineurin at the Golgi and leads to the reduction of AP-1 and clathrin-dependent targeting of lysosomes. In addition, Rab8 recruits and maintains htt proteins at the Golgi via the interaction with FIP-2, and the association of optineurin with myosin VI (Myo6), respectively (Sahlender et al., 2005). Besides its interaction with Rab8, Htt may also inhibit the catalytic ability of nucleotide exchange of a GEF for Rab11 (Li et al., 2008; Li et al., 2009). Overexpression of Rab11S25N (dominant-

negative mutant, DN) in normal adult brains induces neurodegeneration that is similar to the HD mutant mouse model. The possibility of this phenotype is Rab11DN mutant which delays the recycling of transferrin to the plasma membrane from recycling endosomes (Li et al., 2009). It is still unclear that how the interplay between Rab8 and Rab11 target proteins to the plasma membrane for localizing both of them to the recycling endosome (RE) (Ang et al., 2003; Ang et al.,2004; Ullrich et al., 1996). More Rabs were observed to be involved in pathophysiology of Huntington disease. Gunawardena and co-workers found Htt influences the motility of various Rabs containing vesicles, including Rab2, Rab3, Rab7 and Rab19, and Rab-mediated functions in the neurons of fruit fly larvae (White II et al., 2015).

1.1.9.3 Rab and pathogenic microorganism induced diseases

After long term of natural evolution, microorganisms got the ability of manipulating different Rabs, escape from the host cell degradation, and obtain nutrients and building blocks to multiply. The majority of intracellular pathogens hijack Rabs involved in the endocytic pathway, while the causative agent of Legionnaire's disease uses a bifunctional protein to capture Rab1. *Legionella pneumophila* protein SidM/DrrA was first characterized as both a GDF and a GEF for Rab1, cause the pneumonia which is known as Legionnaire's disease (Machner M et al., 2006; Machner, et al., 2007; Murata et al., 2006). The crystal structure of SidM/DrrA and Rab1 complex illustrated that the GDF activity is mediated by the region of SidM/DrrA that mediates GEF activity on Rab1. The high affinity of SidM/DrrA for GDP-bound Rab1 may account for its GDF activity (Suh et al., 2010). The N-terminal domain of SidM/DrrA mediates adenosine monophosphorylation (AMPylation) of Rab1 at switch II region, and Rab1-GTP is the preferred substrate for SidM/DrrA-mediated AMPylation (Muller et al., 2010). In mammalian cells, the AMPylation activity of SidM/DrrA causes cytotoxicity and the release of Rab1 from the host effector protein MICAL-3 but not the bacterially encoded effector LidA (Müller et al., 2010). *Legionella* hijacks Rab1 through manipulating the SidM/DrrA and forms vacuolar-like compartment which is destined for Golgi complex.

Some most recent cases include that intracellular uropathogenic E.*Coli* (UPEC) leads to infections in urinary tract and Rab35 facilitates UPEC survival within

vacuoles in bladder epithelial cells (Dikshit et al., 2015). Indeed, UPEC enhances the expression of both Rab35 and TfR, and recruits these proteins to UPEC-containing vacuoles, thereby enhancing iron delivery into the vacuole. Moreover, Rab35 helps UPEC to escape lysosomal degradation, which further promotes intracellular survival of UPEC. The compartment occupied by UPEC reassembles that of Anaplasma phagocytophilum and also recruits Rab35, which perhaps to promote iron delivery to the bacteria at the same time (Huang et al., 2010).

1.2 Small GTPase Rab35

In recent ten years, Rab35 became one of the most studied Rabs since it was identified as an important player in endocytic recycling and cytokinesis. Increasing evidences shown that it is involved in multiple cellular processes, including endosomal trafficking, exosome release, phagocytosis, cell migration, immunological synapse formation, neurite outgrowth, and even tumorigenesis.

1.2.1 The discovery of Rab35 and its localization in cells

Flier and coworkers first cloned gene of H-ray, the primary name of Rab35, from human skeletal muscle and found that it is ubiquitously expressed in various tissues (Zhu et al., 1994). Later the Rab35 gene was called Rab1c for its high sequence similarity to Rab1a and Rab1b. Systematic sequencing revealed that Rab35 is conserved in all animal metazoans and seems to even predate the rise of metazoans (Klopper et al., 2012). Rab1a/1b and Rab35 have strong homology in the GTPase domain and switch regions, but they clearly differ in the last C-terminal 30 amino acids, which is called C-terminal hypervariable domain (HVD). Therefore, Rab1a/1b and Rab35 have distinct membrane localizations as well as different cellular functions. Rab1a/1b regulates ER-to-Golgi vesicular traffic and therefore they localize to the endoplasmic reticulum (ER) and Golgi (Stenmark, 2009). However, Rab35 localizes to both endosomes and the plasma membrane. The evolutionarily conserved C-terminal polybasic domain distinguishes Rab35 from other Rab proteins. Recent evidences have confirmed that the plasma membrane localization of GTP-bound Rab35 is dependent on its polybasic region in HVD that direct binds to the negatively charged phosphoinositides PtdIns(4,5)P_2 and PtdIns(3,4,5)P_3 (Heo et al., 2006; Gavriljuk et al., 2013; Li et al., 2014).

1.2.2 The Rab35 GEFs, GAPs

The roles of Rab35 protein are dependent on its GTP-GDP cycle wherein that active GTP-bound forms recruit their downstream effectors in various biological processes. Several Rab35 GEFs such as DENND1A/B/C, Folliculin and GAPs, for example EPI64A/B/C, have been identified (Chaineau et al., 2013).

1.2.2.1 Rab35 GEFs: DENN1 family and Folliculin

All the known Rab35 GEFs contain DENN (differentially expressed in normal and neoplastic cells) domain which is an evolutionarily conserved motif that exits all eukaryotes from yeast to human (Marat et al., 2011; Zhang et al., 2012). The DENN domain was first identified as a Rab-binding module in the Rab6/Rab11 interacting protein Rab6ip1 (Janoueix-Lerosey et al., 1995; Miserey-Lenkei et al., 2007). More data showed that all DENN domain proteins have GEF activity with all members of any given family targeting one or two Rabs (Yoshimura et al., 2010). The first evidence of DENN1 working as GEF of Rab35 was found in C.elegnas (Sato et al., 2008). RME4 (DENND1A homology in C. *elegans*) catalyzes the GDP-GTP exchange of REM5 (Rab35 homology in C. *elegans*) to regulate receptor-mediated endocytosis of yolk proteins. RME4 interacts specifically with GDP-bound RME. It was identified that Rab35 plays a fundamental and conserved role after cargo internalization. In mammal cells, all three members of DENND1A family including DENND1A/connecdenn 1, DENND1B/connecdenn 2 and DENND1C/connecdenn 3 showed GEF ability for Rab35 in different pathways (Marat et al., 2010, Allaire et al., 2010). The structure of DENND1B:Rab35 complex revealed that DENND1B composes an N-terminal lobe and a C-terminal lobe (See Figure 1-4) (Wu et al., 2011). The C-terminal lobe has a core β-sheet flanked by α-helices which interacts with the switch I and II of Rab35 that surround the nucleotide-binding pocket. Once binding to the DENN domain, switch I changes its conformation and lowers the affinity of Rab35 for GDP, facilitating GDP dissociation and allowing GTP to bind.

DENND1A was shown as a major GEF for Rab35 in the endocytic pathway (Marat et al., 2011). Disrupting DENND1A function impairs trafficking through endosomes which is similar with Rab35 depletion, showing that it is a real Rab35 GEF with function. Before the identification of DENND1A as Rab35 GEF, DENND1A was found to interact directly with clathrin, clathrin adaptor AP-2, intersectin, endophilin A1 and NECAP to

form clathrin-coated vesicle (CCV) components (Allaire et al., 2006; Ritter et al., 2007). In addition, in vitro experiment also showed that DENND1A and Rab35 are required for the CCVs formation (Allaire et al., 2010; Kulasekaran et al., 2015). More recently, Echard and coworkers using TIRF-microscopy revealed that DENND1A is loaded onto CCVs just after the scission of CCPs from the plasma membrane and a few seconds before Rab35 loading on (Cauvin et al., 2016). However, the mechanism of how DENND1A is loaded into CCV still needs to be addressed. DENND1A is a ubiquitously expressed protein but is particular expressed at high levels in neurons and enriched in presynaptic nerve terminals. The fact that knock down of DENND1A impairs synaptic vesicle endocytosis in cultured hippocampal neurons may indicates the functions of Rab35 in synapse formation (Allaire et al., 2006).

DENND1B is widely expressed and its DENN domain shares high identity with that of DENND1A (Marat et al., 2010). On CCVs, DENND1B has a strong GEF activity for Rab35 via peptide motifs in its C-terminal region to interact directly with clathrin heavy chain and AP-2. Depletion of DENND1B induces enlargement and perturbs the localization of early endosomes (Marat and McPherson, 2010), which similar to knock down of DENND1A or Rab35 (Allaire et al., 2010), indicating a role for DENND1B in the regulation of Rab35 activity at early endosomes. Moreover, Knock down of DENND1B induces the blocking of megalin transport that from early endosomes to recycling endosomes and finally back to cell surface. Meanwhile, this fast recycling pathway of megalin is dependent on Rab35 indicating the role of DENND1B as a GEF for Rab35 (Shah et al., 2013).

Similar with DENND1A/B, DENND1C is found in many tissue types and also functions as a GEF for Rab35, though with much lower enzymatic activity (Marat and McPherson, 2010; Yoshimura et al., 2010). The C-terminal region of DENND1C contains a unique actin interacting motif which is not present in DENND1A/B proteins. DENND1C mediates this motif to interact with actin and a pool of the protein co-localizes with actin filaments, targeting Rab35 to actin and to control actin dynamics (Marat et al., 2012; Shim et al., 2010).

Folliculin is a renal tumor suppressor and most loss-of-function mutations cause benign skin tumors and renal-cell carcinoma (Nickerson et al., 2002). The crystal

structure of Folliculin reveals a strong structural similarity to the DENN domain of DENND1B and therefore folliculin may functions as a GEF for Rab35 (Nookala et al., 2012). Depletion of folliculin leads to a reduction of E-cadherin and a decrease in adherens junctions, indicating that it regulates the formation of adherens junctions (Nookala et al., 2012). Folliculin is also localized at the midbody of mitotic cells and loss of folliculin induces more multi-nucleated cells, suggesting that it is necessary for cytokinesis (Nahorski et al., 2012). Interestingly, Rab35 is essential for the termination step of cytokinesis and the knock down of Rab35 increases the number of multi-nucleated cells. This may be a reflection of the role of folliculin in regulating Rab35 via catalyzes its GDP-GTP exchange (Kouranti et al., 2006; Chesneau et al., 2012). However, more data are needed to demonstrate whether folliculin is a functional Rab35 GEF or not in cells.

1.2.2.2 Rab35 GAPs

To date, there are five TBC domain proteins that have been identified as GAPs for Rab35, including TBC1D10A-C/EPI64A-C, TBC1D13 and TBC1D14. TBC1D10C was first identified as a GAP for Rab35 that regulates receptor recycling and immunological synapse formation in T cells (Patino-Lopez et al., 2008). Subsequently, all TBC1D10 family members including TBC1D10A, B and C were demonstrated to show GAP abilities for Rab35 and regulate exosomes release pathway that is mediated by multivesicular bodies (MVBs) (Hsu et al., 2010). Overexpression of TBC1D10B inhibits the formation of recycling carriers from endosomes and prevents Rab35 in mediating cytokinesis (Kouranti et al., 2006; Chesneau et al., 2012).

In adipocytes, Rab35 regulates the process of the glucose transport which is carried out by the glucose transporter GLUT4 under the insulin stimulation. Overexpression of the Rab35 GAP TBC1D13 prevents the translocation of GLUT4 upon insulin stimulation, and reduces Rab35 activation in cells (Egami et al., 2011). In addition, TBC1D13 showed specific GAP ability for Rab35 *in vitro* and constitutively active mutant Rab35 Q67L can rescue the defects that are induced by TBC1D13 overexpression (Davey et al., 2012).

In *Drosophila* neuronal system, the mutants of one TBC domain-bearing protein skywalker (TBC1D24 homology) lead to enhanced synaptic transmission and constitutively active Rab35, indicating that skywalker works as Rab35 GAP

(Uytterhoeven et al., 2011). Moreover, skywalker shows GAP activity toward Rab35 in vitro. Loss-of-function of skywalker mutation increases the Rab35 dependence on synaptic vesicles transport and finally boosts neurotransmission. On the contrary, the overexpression of dominant negative Rab35 exhibits fewer functional synaptic vesicles, which is similar to the phenotypes in hippocampal neurons following knock down of the Rab35 GEF DENND1A (Allaire et al., 2006). However, it is still unknown that if TBC1D24 works as Rab35 GAP only in neurons or in ubiquitous systems.

1.2.3 The effectors of Rab35 and its functions

GEFs and GAPs control the Rab35 GDP-GTP cycles and Rab35 GTP bound form and plays roles via the interaction with its various effectors in different pathways.

1.2.3.1 Rab35 and cytokinesis

Rab35 was proposed to play crucial roles in the cytokinesis via recruiting its effector OCRL1, an inositol polyphosphate 5-phosphatase, which converts PtdIns(4,5)P_2 to PtdIns(4)P to dismiss the F-actin at the Intercellular bridge and thus completes a successful abscission. The working model of Rab35 for cytokinesis is described in Figure 1-7. In consist with above mentioned discoveries, the deletion of Rab35 in *Drosophila* S2 cell or mammalian cells induces cytokinesis defects and the formation of binucleated cells (Echard et al., 2004; Dambournet et al., 2011). In addition, Rab35 is also involved in the formation and maintenance of microtubule-based meiotic spindles in mice oocytes, an earlier step of cell division (Wang et al., 2016). Depletion of Rab35 in oocytes impairs normal spindle formation and decreases polar body extrusion.

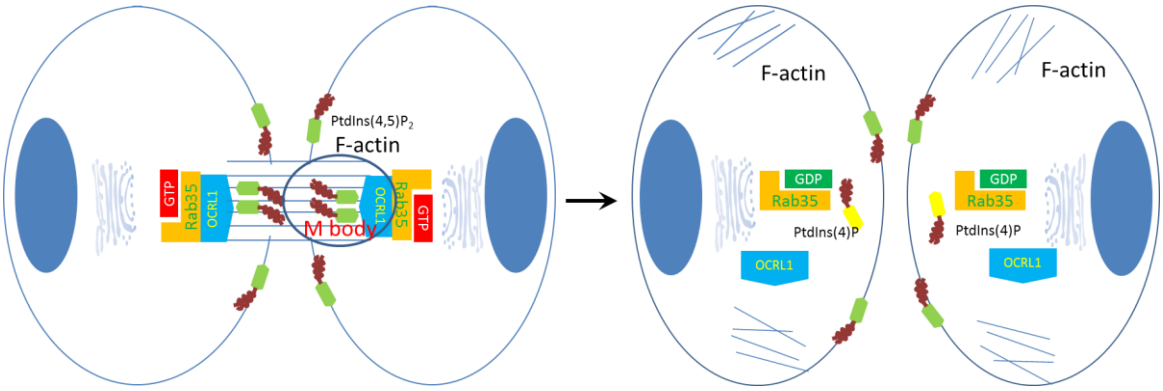

Figure 1-7. Working model of Rab35 in cytokinesis.

1.2.3.2 Rab35 and endocytic recycling

Another important function of Rab35 is to promote endocytic recycling. Deletion of Rab35 induces cytokinesis failure but also with the presence of large intracellular vacuoles in cells that indicates a trafficking block. Later investigations found that Rab35 controls a fast endocytic recycling pathway from endosomes to the plasma membrane (Kouranti et al., 2006). Subsequently, it was found thatthe dominant-negative mutant Rab35S22N or deletion of Rab35 led to an accumulation of endocytic carriers such as transferrin (Tf) and Tf receptor (TfR) at some compartment membrane of intracellular vacuoles (Patino-Lopez et al., 2008). Consequent evidences show that the deletion of Rab35 induces TfR recycling defects in cells (Dikshit et al., 2015). More evidences show the Rab35-dependent endocytic recycling back to the plasma membrane. For example, Rab35 controls the trafficking of major histocompatibility complex class-II (MHC-II)-peptides in HeLa-CIITA cells (Walseng et al., 2008), MHC-I in COS-7 cells and HeLa cells (Allaire et al., 2010; Allaire et al., 2013), T-cell receptor (TCR) in Jurkat T cells (Patino-Lopez et al., 2008), Megalin in L2 rat yolk sac cells when autosomal recessive hypercholesterolemia (ARH) is depleted (Shah et al.,2013), GLUT4 in adipocytes (Davey et al., 2013), M- and N-Cadherin in C2C12 and COS-7 cells (Charrasse et al., 2013) and β1-integrin in COS-7 and HeLa cells (Argenzio et al., 2014, Allaire et al., 2013). More important, Rab35 also transports internalized toxin Shiga and CI-mannose-6-phosphate receptors (CI-M6PR) from the endosomes to the trans-Golgi network (TGN) (Fuchs et al., 2007; Cauvin et al., 2016).

Rab35 proteins work with its effectors MICAL-L1 and centaurin β2/ACAP2, an ARF6 GAP in the process of transporting ARF6 positive recycling endosomes (Rahajeng et al., 2012; Kanno et al., 2010).

Aside from the functions in cytokinesis, OCRL1 also participate in the trafficking from endosomes to the TGN (Choudhury et al., 2005, Vicinanza et al., 2011). Rab35 recruits OCRL1 to facilitate the hydrolysis of PtdIns(4,5)P_2 and further decreases the density of F-actin. The depletion of either Rab35 or OCRL1 leads to accumulation of PtdIns(4,5)P_2- and F-actin-binding proteins on enlarged peripheral endosomes, and delays trafficking of internalized M6PR to the TGN. Meanwhile, Rab35 depletion also impair the transport of N- and M- cadherin via transferrin-, clathrin- and AP2-positive

endosomes which increase the ability of cell migration (Charrasse et al., 2013).

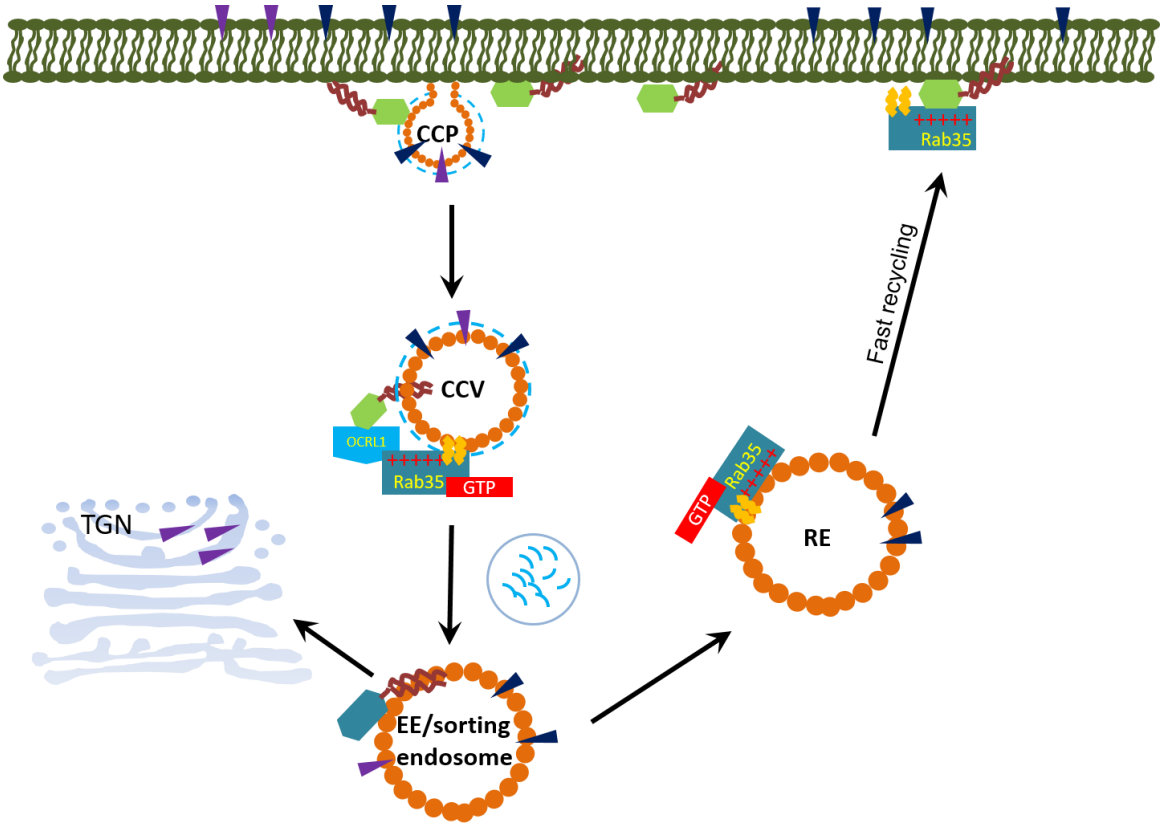

Figure 1-8. Model of Rab35 endocytic recycling. CCP, clathrin coat pit; CCV, clathrin coat vesicle; EE: early endosome; RE, recycling endosme

Latest evidences showed that Rab35 functions with OCRL1 to promote PtdIns(4,5)P_2 hydrolysis on newborn endosomes, thus leading to the uncoating of clathrin and subsequent trafficking and sorting steps from early endosomes (Cauvin et al., 2016)

1.2.3.3 Rab35 and neurite outgrowth

Presley's lab and, especially Fukuda's lab, performed a lot of wonderful and meticulous works to address how Rab35 controls the neurite outgrowth in response to NGF stimulation in PC12 cells (Chevallier et al., 2009; Kobayashi and Fukuda, 2012; Kobayashi and Fukuda, 2013; Kobayashi et al., 2014; Etoh and Fukuda, 2015).

Neurite outgrowth is the first step in the processes of neuronal differentiation and regeneration and leads to synaptic polarization and plasticity. After treatment of nerve growth factor (NGF), Rab35 accumulates on ARF6-positive perinuclear recycling endosomes and recruits both MICAL-L1 and ACAP2 in PC12 cells (Kobayashi and Fukuda, 2012; Rahajeng et al., 2012). Thus MICAL-L1 and ACAP2 recruit EHD1, a

protein inducing membrane fission due to its similarities to dynamin (Kobayashi and Fukuda, 2013; Kobayashi et al., 2014; Giridharan et al., 2013). MICAL-L1 interacts directly with EHD1 while ACAP2 recruits EHD1 indirectly through inactivation of ARF6 and thereby maintaining the scaffold factor for EHD1, PtdIns4P (Kobayashi and Fukuda, 2013). Finally, Rab35 positive endosomes are translocated to the neurite tips and facilitate neurite outgrowth (Kobayashi et al., 2014). Previous findings provided similar cases that Rab35 is required for EHD1 recruitment on recycling endosomes (Allaire et al., 2010). Rab35-Q67L (constitutive active mutant) promotes neurite outgrowth in PC12 cells and in N1E-115 cells (Langemeyer et al., 2014). Interestingly, ARF6-T27N (constitutively active mutant) inhibits neurite outgrowth and endocytic recycling (Grant and Donaldson., 2009; Kobayashi and Fukuda, 2012; Radhakrishna et al., 1997; Dutta and Donaldson, 2015). It is consistent with the evidences that Rab35 and ARF6 are antagonistic by recruiting effector as the other's GAP (Miyamoto et al., 2014).

During the neurite outgrowth, Rab35-GTP inhibits ARF6 activity by recruiting its effector ACAP2 which works as Arf6 GAP. Meanwhile, ARF6-GTP also inhibits Rab35 activation by recruiting its effector EPI64A-C (TBC1D10A-C) as GAP for Rab35 (Hanono et al., 2006). Indeed, ARF6-GTP could interact with EPI64A-C which constitutes a family of functional GAPs for Rab35 (Patino-Lopez et al., 2008; Chesneau et al., 2012; Fuchs et al., 2007; Hsu et al., 2010). More data of overexpression of ARF6 Q67L,EPI64, or Rab35 S22N all lead to the formation of PtdIns(4,5)P_2-rich vacuoles that block endocytic cargo recycling and inhibit cytokinesis (Patino-Lopez et al., 2008; Chesneau et al., 2012). Interestingly, ARF6 recruits EPI64B and thus preventing the activation of Rab35 on clathrin-coated pits (CCP) but not on CCVs (Chesneau et al., 2012, Montagnac et al., 2011; Cauvin et al., 2016). The precise spatial and temporal inactivation and activation of Rab35 by its GAP EPI64B and its GEF DENND1A lead to the production of new born clathrin-coated endosome from plasma membrane.

The crosstalk between Rab35 and Arf-6 ensures the precision of CCPs scission. ARF6 interacts with a PtdIns(4)P 5-kinase and maintains PtdIns(4,5)P_2 production level and hence is essential for recruiting key CCP proteins. Once CCPs scission complete, Rab35 recruits OCRL1 in order to hydrolyze PtdIns(4,5)P_2 and promotes clathrin uncoating (Cauvin et al., 2016). In conclusion, the balance between Rab35 and Arf6 is predicted that it is either Rab35-GTP/ARF6-GDP, or Rab35-GDP/ARF6-GTP at a

membrane, which could be important to control local phosphoinositide levels and F-actin dynamics.

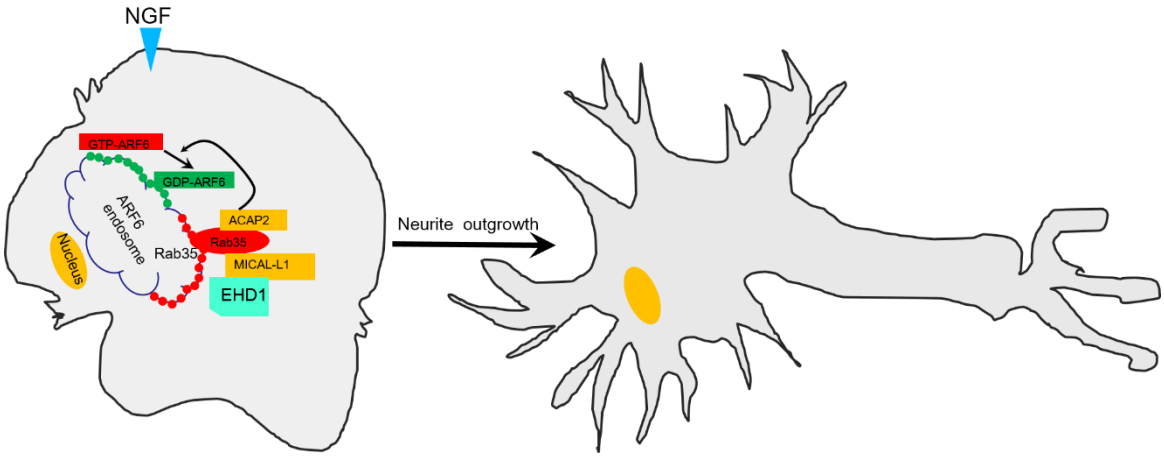

Figure 1-9. Functional model of Rab35 in a successful neurite outgrowth.

Altogether, there have been clear evidences that Rab35 always works in the presence of proteins which are related to phosphatidylinositol metabolism, such as Arf6 and OCRL1. These data give us a strong clue that Rab35 may associate with negatively charged phosphoinositide PtdIns(4)P, PtdIns(4,5)P_2 and PtdIns(3,4,5)P_3 via polybasic HVD domain during its regulation of neurite outgrowth and endocytic recycling.

1.2.3.4 Rab35 and Drosophila bristles development

Besides its functions at cellular level, Rab35 also also play roles in Drosophila development. For example, Drosophila bristles are mechanosensory organs found on the cuticle and their shape and growth depends on actin bundles. Rab35 was identified in a screen for Rab GTPases that influence bristle formation and the GTPase regulates bristle development by recruiting fascin (Zhang et al., 2009). The direct binding of Fascin to GTP-bound form of Rab35, i.e. the activated form of Rab35, specifically by DENND1C/connecdenn 3, is necessary to recruit fascin to actin (Marat et al., 2012). Fascin is an actin-crosslinking protein that assembles F-actin filaments into tightly packed parallel bundles. It contains two actin-binding sites, one on each of its N- and C-termini that facilitate bundling of adjacent actin filaments (Adams, 2004). Fascin has been linked to many biological functions requiring actin regulation. Fascin also contributes to the formation of actin structures in mammalian cells including filopodia, lamellipodia and dendritic spines (Jayo and Parsons, 2010). Rab35 induces actin-rich protrusions in PC12

cells and regulates lamellipodia and filopodia formation in Drosophila (Shim et al., 2010; Chevallier et al., 2009). It is thus possible that many of fascin's functions lie to the downstream of Rab35.

1.2.3.5 Rab35 and diseases

Rab35 was presumed associated with tumorigenesis for depletion of Rab35 decreased cell adhesion and increased cell migration, which is often observed in cancer cells (Allaire et al., 2013).

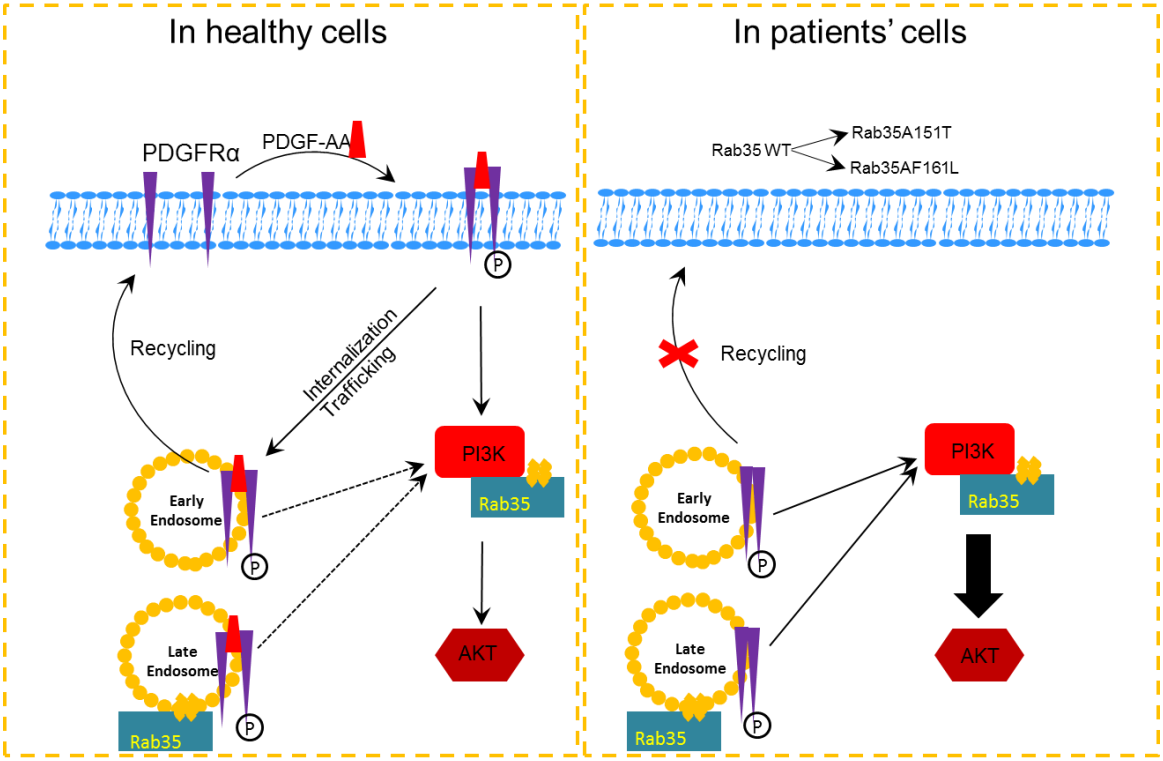

Figure 1-10. The model of Rab35 works as an oncogene.

Studies from Sabatini lab and Sawyers lab provided direct evidences that Rab35 link to cancer through its regulatory roles in the phosphatidylinositol-3-kinase (PI3K)/ AKT signaling pathway (Wheeler et al., 2015). Rab35 knock down suppresses phosphorylation-induced AKT activation in different cell types, whereas expression of Rab35Q67L mutant induces constitutive AKT signaling. Expression of active Rab35 is sufficient to drive PDGFR-α into Lamp2-positive endosomes even without ligands and lead to AKT phosphorylation. Interestingly, AKT-dependent phosphorylation enhances the ability of DENND1A GEF for Rab35 and promotes Rab35 activation in a positive feedback fashion (Kulasekaran et al., 2015). The most important thing is that two somatic

Rab35 mutations were found to constitutively activate PI3K/AKT signaling in cancer patients. Both of two mutations lead to the expression of GTP-locked Rab35, suppressing apoptosis and promoting cellular transformation in HeLa cells. Altogether, Rab35 is a pivotal protein which plays roles in several biological processes including cell migration, phagocytosis, immune synapse and exosome release.

1.3 Lowe syndrome and OCRL1

Lowe syndrome patients suffer primarily from congenital cataracts, neonatal hypotonia, intellectual disability (with distinct behaviors) and renal proximal tubule dysfunction (Fanconi syndrome). Lowe syndrome is estimated to be prevalent in the general population of approximately 1 in 500,000. The mutation of OCRL1 (Oculocerebrorenal syndrome of Lowe) gene which localizes at Xq26.1, causes Lowe syndrome, an x-linked disorder (Charnas and Gahl, 1991).

OCRL1 is the major 5-phosphatase which converts PtdIns(4,5)P_2 to PtdIns(4)P by hydrolyzing the 5-phosphate (Suchy et al., 1995; Zhang et al., 1995). Cell extracts from fibroblasts cultured from Lowe syndrome patients universally exhibit a markedly reduced ability to dephosphorylate PtdIns(4,5)P_2 (Su et al.,1999; Lin et al., 1997). In addition, OCRL1 appears to be the major PtdIns(4,5)P_2-hydrolyzing enzyme in human kidney proximal tubule cells, and kidney cells derived from Lowe syndrome patients have roughly double the normal cellular contingent of PtdIns(4,5)P_2 (Zhang et al., 1998). Thus, the OCRL1 phenotype correlates well with the loss of phosphatase activity.

Lowe syndrome patients almost universally have renal Fanconi syndromes, including acidosis, amino aciduria, phosphaturia, and proteinuria (Charnas and Gahl, 1991). The defect in protein reabsorption has been suggested to be resulted from improper function or trafficking of the cell surface receptor megalin (Lowe, 2005; Norden et al., 2002). Megalin, a member of the LDL receptor family, is a 600-kDa transmembrane protein that recycles at the apical domain of polarized epithelial cells (Christensen and Birn, 2002). Megalin binds to numerous protein ligands that dissociate from the receptor after internalization and are targeted to lysosomes for degradation. In patients with Fanconi syndrome, ligand handling is somehow compromised, resulting in excess secretion of filtered proteins into the urine. However, OCRL1 does not directly modulate endocytosis or postendocytic membrane traffic and that the renal manifestations observed

in Lowe syndrome patients are the downstream consequences of the loss of OCRL1 function (Cui et al., 2010). Almost all affected males have some degree of intellectual disability; 10%-25% function in the low-normal or borderline range, approximately 25% in the mild-to-moderate range, and 50%-65% in the severe-to-profound range of intellectual disability. However, the reason of mental retardation among these patients is still unclear.

The localization of OCRL1 is primarily at the *trans*-Golgi network (TGN) and is also associated with a subset of endosomes , plasma membrane and clathrin-coated pits, suggesting a potential function of this enzyme in membrane traffic through these compartments (Choudhury et al., 2005; Choudhury et al., 2009; Erdmann et al., 2007; Ungewickell et al., 2004; Dressman et al., 2000). This broad distribution is mediated by its many interactions (Figure 2-8B). OCRL1 interacts with clathrin, AP-2 (clathrin adaptor), 16 Rab GTPases, and the endocytic proteins APPL1 (adapter protein containing PH domain, PTB domain and leucine zipper motif 1) or Ses1/2 (sesquipedalian 1 and 2) via competitive manner. The broad intracellular distribution of OCRL1 indicates that the physiological importance of phosphoinositides in endocytic trafficking (Ben El Kadhi et al, 2011; Vicinanza et al., 2011; Erdmann et al., 2007), actin polymerization(Suchy et al., 2002) establishment of cell polarity (Grieve et al., 2011) and cytokinesis (Dambournet et al., 2011). Lack of OCRL1 leads to an accumulation of intracellular PtdIns(4,5)P_2 and/or PtdIns(3,4,5)P_3, and therefore some pathological phenotypes are considered as the consequence of these changes (Zhang et al.,1998)

1.3.1 The OCRL1 domains

The OCRL1 domain structure comprises an N-terminal PH (pleckstrin homology) domain, a 5-phosphatase domain, an ASH (ASPM–SPD2–Hydin) domain and a C-terminus RhoGAP (Rho GTPase activating) domain (Figure 2-8A) (Pirruccello and Camilli, 2012). A loop in the PH domain contains an unusual clathrin box which mediates the interaction of OCRL1 with clathrin heavy chain (Mao et al., 2009; Lafer, 2002). The second clathrin box is presented in RhoGAP domain enhances the OCRL1 binding to clathrin (Erdmann et al., 2007; Ungewickell et al., 2004). OCRL1 is directed to late-stage endocytic clathrin-coated pits, and to endosomal/Golgi coats via these two clathrin-binding motifs and one clathrin adaptors binding motif which exits between PH and

inositol 5-phosphatase domains (Ungewickell et al., 2004; Choudhury et al., 2009). The inositol 5-phosphatase domain is the core motif to hydrolyze PtdIns(4,5)P_2, forming PtdIns(4)P. The membranes targeting of OCRL1 is crucially dependent on the ASH domain interactions with GTP-bound Rab proteins (Hyvola et al., 2006). OCRL1 interacts with at least 16 different Rabs, for examples, Rab5 (endosomes), Rab6 (Golgi and endosomes) and Rab35 (fast recycling route), by functional and colocalization studies (Dambournet et al., 2011; Hyvola et al., 2006). However, the structure of OCRL1-Rab8a complex reveals the interaction between Rab8 and OCRL1 via the Rab interaction surface on the ASH domain and C-terminal catalytic domain helix of OCRL1 (Hou et al., 2011). This unusual binding mode of OCRL1 for a Rab is different from the typical model that Rab effectors recognize a hydrophobic triad in the GTP-bound Rab protein, which incorporates residues from its switch and interswitch regions. The F668 is contained in the Rab-binding interface of OCRL1, an IgG-like β-strand structure of the ASH domain. Both F668A and F668V mutants impair the OCRL1 interaction with Rab8a due to the lower hydrophobicity of alanine compared with phenylalanine (Hou et al., 2011).

The RhoGAP domain of OCRL1 interacts with Rac and GTP-bund form of Cdc42, both of which belong to the Rho GTPases family (Erdmann et al., 2007; Faucherre et al., 2003). The interaction with Rac may due to the localization of OCRL1 at membrane ruffles (Faucherre et al., 2005). In addition, OCRL1 also interacts with two regulators of 5-kinases Arf1 and Arf6, and a mutation in the RhoGAP domain will disrupt their interactions and leads to Lowe syndrome (Lichter-Konecki, 2006). Three endocytic proteins APPL1 (adaptor protein, phosphotyrosine interacting with PH domain and leucine zipper 1), Ses1 and Ses2 interact with the RhoGAP domain of OCRL1 via their F&H motif, which contains a 12-13-amino-acid sequence forming an amphipathic helix that recognizes an evolutionarily conserved surface on the RhoGAP domain of OCRL1 (Erdmann et al., 2007; Swan et al., 2010; Pirruccello et al., 2011). APPL1 is an adaptor protein with multiple functional domains including the BAR (Bin1/amphiphysin/rvs167) domain, PH domain and PBT (phosphotyrosine binding) domain. APPL1 interacts with Rab5 via BAR domain and binds receptors (for example growth factor receptors) through its PTB domain (Miaczynska et al., 2004; Mao et al., 2006; Lin 2006). APPL1 and its homologous protein APPL2 (without F&H motif) form APPL heterodimer, which binds AKT (a PI(3,4,5)P3 effector) and associate dynamically with endosomal membranes.

Therefore, they are proposed to function in endosome-mediated signaling pathways linking the cell surface to the cell nucleus (Chial et al., 2008; Miaczynska et al., 2005).

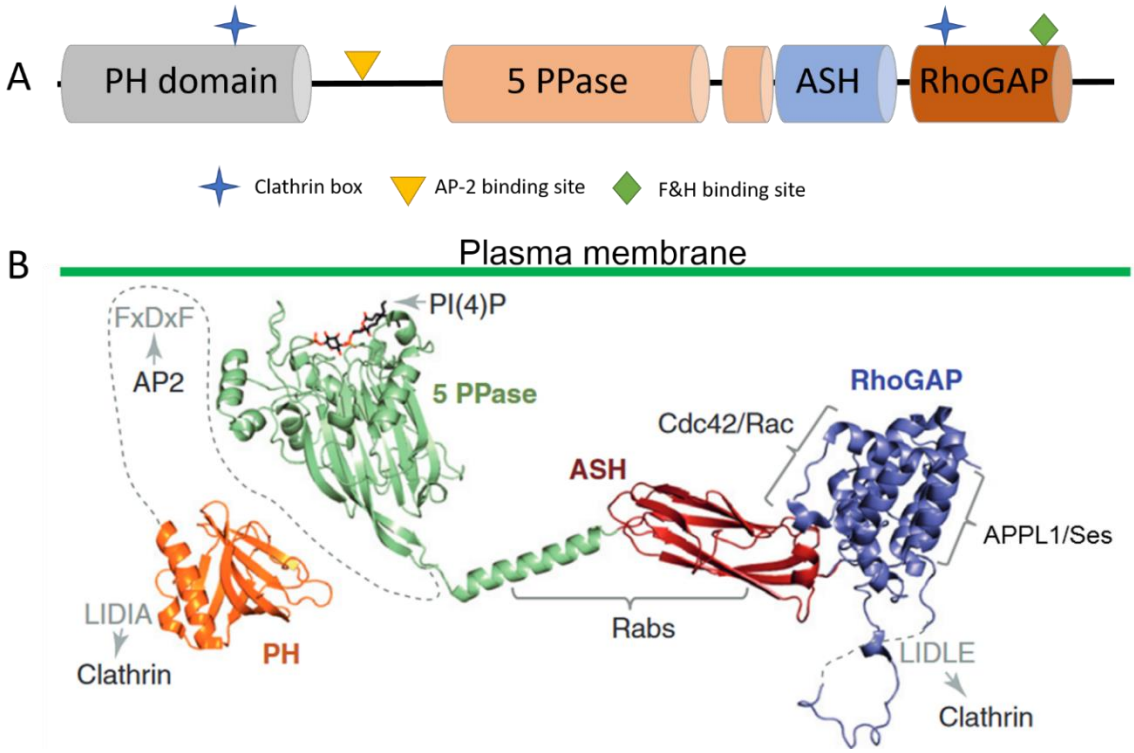

Figure 2-8. The functional domains strutures of OCRL1. (A) Scheme of OCRL1 protein domains. (B) Combinational structure of OCRL1 derived from individual structures of its domains (orange= PH domain, PDB code: 2KIE; green=5-phosphatase domain, PDB code: 3MTC; red = ASH domain, PDB code: 3QIS; and blue =RhoGAP domain, PDB code: 2QV2). (Adapted from Pirruccello and Camilli, 2012). PH, pleckstrin homology; ASH, ASPM–SPD2–Hydin domain; RhoGAP, Rho GTPase activating domain.

OCRL1 may also play a role in phagocytosis due to the interaction with APPL1 and APLL2 heterodimer to dephosphorylate PtdIns(3,4,5)P_3 (Bohdanowicz et al., 2012). As endosomes mature and acquire PtdIns(3)P, APPL proteins will be displaced by Ses1 and Ses2 oligomers from the F&H binding surface (Swan et al., 2010). Both Ses1 and Ses2 proteins contain a PH domain which induces their oligomerization and a C-terminal F&H motif that mediates the interaction with OCRL1 (Swan et al., 2010; Noakes et al., 2011). Interestingly, OCRL1 associates with endocytic vesicles at both the APPL and Ses stage possibly via its Rab-dependent interactions. Moreover, phosphorylation of APPL1 on two serine residues in the F&H domain forces the OCRL1 dissociation (Erdmann et al., 2007). Therefore, the localization of OCRL1 on the endosomal membrane induces lipid turnover with sorting events which is possibly controlled by this precise regulation.

1.3.2 OCRL1 mutations and Lowe syndrome

Complete or partial deletion, frameshift and nonsense mutations of OCRL1 gene cause OCRL1 losing its interactions, misfolding, or catalytic inactivity and result in Lowe syndrome. Non-sense and frameshift mutations in PH domain were found in Dent disease but rarely in Lowe syndrome patients (Hichri et al., 2010). Case studies showed that the amount of missense mutations found in Lowe syndrome patients affect conserved residues in 5-phosphatases, directly affecting OCRL1 proteins either folding, substrate binding or catalytic activity (Tsujishita et al., 2001; Hichri et al., 2011). The majority of mutations in the hydrophobic core of OCRL1 and several missense mutations clustered around the active site lead to Lowe syndromes, indicating that the catalytic activity of OCRL1 is crucial for diseases.

The missense mutations in ASH–RhoGAP motif induce the destabilization of OCRL1 protein, which is evidenced by these mutations containing patient cell lines express low quantity of OCRL1 protein (Hichri et al., 2010). In addition, overexpression of OCRL1 missense mutants leads to their cytosolic localization in cells (McCrea et al., 2008). The mutations in the F&H binding surface on the RhoGAP domain of OCRL1 disrupt the integrations with Rho and Rab GTPases which also lead to the Lowe syndrome in human (Pirruccello et al., 2011).

Altogether, the mutations through the whole OCRL1 970 amid acids including missense, frameshift, or nonsense were found in Lowe syndrome patients. However, how the importance of OCRL1 interactions in its physiological function still needs to be elucidated.

2 Materials and methods

2.1 Materials

2.1.1 Biochemistry

Chemicals	Supplier
Acetic acid	Merck
Acetonitrile	JT Baker
Acetone	JT Baker
Acrylamid/Bisacrylamide (37.5:1, 30 % w/v)	Applichem
Ammonium sulfate	Applichem
Ammonium persulfate (APS)	Merck
Ampicillin (Amp)	Serva
Bradford reagent	Bio-Rad
Bromphenol blue	Serva
Bovine serum albumine (BSA)	Sigma
Chloroform	JT Baker
Complete Mini EDTA-free protease inhibitor tablets	Roche
Coomassie Brilliant Blue G250+R250	Serva
Deoxycholic acid sodium salt (DCS)	Serva
Dimethylsulfoxide(DMSO)	Sigma
Disodium hydrogenphosphate	Roth
Dithioerythitol (DTE)	Gerber
Disodium hydrogen phosphate (Na2HPO4)	Merk
Dithiothreitol (DTT)	Gerbu
Ethylenediaminetetraacetic adic (EDTA)	Gerbu
Ethanethiol	Sigma
Ethanol	JT Baker
Ethidium bromide	Sigma
Gernylgernyl pyrophosphate (GGPP)	Sigma
Glycerol	Gerbu
Glycine	Roth
Guanosine diphophate (GDP)	Pharma Waldhof
4-(2-Hydroxyethyl)piperazine-1-ethanesulfonic acid (HEPES)	Roth
Hydrochloric acid	JT Baker
Imidazol	Gerbu
Isopropyl-β-D-thiogalactopyranoside (IPTG)	Gaiberg
Kanamycin	Boehringer
NBD FPP	By Kui Hong Tan
Magnesium chloride	Merk
Methanol	Applichem
β-Mercaptoethanol	Serva
Nocodazole	Sigma
phenylmethylsulfonylfluoride (PMSF)	Sigma
Phosphatase Inhibitor Cocktail 1	Sima

Potassium dihydrogenphosphate	Roth
Potassium hydroxide	JT Baker
2-Propanol	JT Baker
Sodium chloride(NaCl)	Sigma
Sodium dodecylsulphate (SDS)	Roth
Sodium dihydrogenphosphate(NaH_2PO_3)	JT Baker
Sodium hydroxide(NaOH)	JT Baker
Sodium 2-mercaptoehanesulfonate (MESNA)	Sigma
N,*N*,*N'*,*N'*-tetramethylethylendiamin (TEMED)	Roth
Trihydroxymethylaminomethane (TRIS)	Roth
Tris-HCl	JT Baker
Triton X-100	Serva
Tween 20	SERVA
Urea	JT Baker
UltraPure Agarose	Invitrogen

2.1.2 Molecular biology

Materials	**Supplier**
100 mM dNTP mix	Invitrogen
Anti-HA	Abcam
Anti-OCRL	Thermofisher
Anti-PRA1	Abcam
Anti-RILP	Sigma-Aldrich
Anti-β-Actin	Sigma-Aldrich
BigDye	Applied Biosystems
Calf Intestinal Phosphatase	NEB
DNA ladder	Fermentas
DpnI	Fermentas
DyeEx 2.0 Spin Kit	QIAGEN
Dynabeads Protein A	Invetrogen
FastDigest Age I	Fermentas
FastDigest BamHI	Fermentas
FastDigest EcoRI	Fermentas
FastDigest HindIII	Fermentas
FastDigest NdeI	Fermentas
FastDigest SapI	Fermentas
FastDigest SpeI	Fermentas
FastDigest XhoI	Fermentas
Gel Extraction kit	QIAGEN
GelPilot loading dye, 5x	QIAGEN
Low molecular weight marker	Amersham Biosciences
PCR Purification kit	QIAGEN
Phusion master mix	FINNZYMES
Prestain Protein marker	NEB
Rapid T4 ligase	Fermentas
Red mix	VWR
Spin Midiprep kit	QIAGEN
Spin Miniprep kit	QIAGEN
T4 DNA Ligase	Fermentas

2.1.3 Cell biology

Materials	Supplier
[32P] orthophosphate	PerkinElmer
Alexa Fluor® 594 goat anti-rabbit IgG	Thermo
DMEM without phosphates	Invitrogen
DMEM/F12 medium	Sigma
DPBS	Sigma
Dulbecco's Modified Eagle's Medium (DMEM)	Sigma
Fetal bovine serum (FBS)	Invitrogen
Fugene® 6 transfection reagent	Roche
L-Glutamine	Invitrogen
Lipofectamine 2000	Invitrogen
Lipofectamine 3000	Invitrogen
NEAA	Invitrogen
Penicillin/streptomycin	Invitrogen
Sodium pyruvate	Invitrogen
Trypsin/EDTA	Sigma

2.1.4 Other materials

Materials	Supplier
Amicon Ultra-4,15 (10K, 30K) Concentrator	Milipore
BioSep-SEC-2000 gel filtration	Phenomenex
Chitin beads	NEB
Electroporation cuvettes	Bio-Rad
Eppendorf tube (0.5 mL, 1.5 mL, 2.0 mL)	Eppendorf
Falcon Tube (50 mL, 15 mL)	Stradat
Glutathione Sepharose	GE Healthcare
HiTrap Ni-NTA column	Pharmacia
NAP-5 desalting column	Amersham
Nitrocellulose membrane	GE
Nitrocellulose paper	Schleicher&Schuell
Quartz cuvette (1cm)	Hellma Optik
Superdex 75/200 Gel filtration	Pharmacia Biotech
Whatman FP 30/0.2, 0.4 μm cellulose filter	Schleicher&Schuell
X-film	Fuji
ZapCap filter	Nalgene

2.1.5 Instruments

Instruments	supplier
1.0 mm 10-well combs	BioRad
1.0 mm 15-well combs	BioRad
1.0 mm cassettes for western blots	Invitrogen
Argon Laser LGK 7872 ML05 (458/488/514 nm)	Lasos

Äkta prime system with REC112 recorder	Pharmacia Biotech
Biorad PE 9700 thermocycler	Applied Biosystems
Centrifuge 5415R	Eppendorf
Centrifuge 5810R	Eppendorf
Centrifuge Allegra X-22R	Beckman Coulter
Centrifuge Avanti J20-XP	Beckman Coulter
Centrifuge Optima L-70K Ultracentrifuge	Beckman Coulter
Electroporation device *E. coli* Pulser	Bio-Rad
Eppendorf Micromanipulators 5171	Eppendorf
Eppendorf Transinjector 5246	Eppendorf
FLA-5000 (Fluorescence image reader)	Fujifilm
Fluoroskan Ascent Fl type 374	Thermo BioAnalysis
Gel Imaging Station	BioRad
Incubator Shaker Series I26	New Brunswick
Isothermal titration calorimeter	MicroCal
Leica TCS SP2	Leica Microsystems
Leica TCS SP5	Leica Microsystems
MALDI-TOF-MS	Applied Biosystem
Microfluidizer	Microfluidics
PCR-Cycler	Eppendorf
SDS-PAGE Mini-Protean II system	Bio-Rad
Shaker	Infors
Thermomixer 5436 (1.5 mL)	Eppendorf
Thermomixer 5436 (2 mL)	Eppendorf
UV/Visible Spectrometer DU 640	Beckman Coulter

2.1.6 Buffers and growth medium

LB medium

5 g/L	yeast extract
10 g/L	Tryptone
10 g/L	NaCl

Antibiotics

125 mg/L Ampicillin
34 mg/L Chloramphenicol
125 mg/L Ampicillin

SDS-PAGE stacking gel buffer (4X)

0.5 M	Tris-HCl, pH 6.8
0.4 % (w/v)	SDS

SDS-PAGE loading buffer (2x)

62.3 mM	Tris-HCl, pH 6.8
2 % (w/v)	2 % (w/v)
10 % (v/v)	glycerol
5 % (v/v)	β-Mercaptoethanol
0.001 % (w/v)	bromophenol blue

Distaining solution

10 % (v/v)	acetic acid

LB agar plates

15 g/L	Bacto agar
50 mg/L	Ampicillin

SDS-PAGE running buffer(10x)

0.25 M	HCl
2 M	Glycine
1%(W/V)	SDS

SDS-PAGE resolving gel buffer(4X)

1.5 M	Tris-HCl, pH 8.8
0.4 % (w/v)	SDS

Coomassie staining solution

10 % (v/v)	
40 % (v/v)	
0.1 % (w/v)	Coomassie Brilliant Blue R250

TAE buffer (1x)

40 mM	Tris acetate, pH 8.5

2 mM	EDTA
20 mM	Glacial acetic acid

PBS (10x)

80 g/L	NaCl
2 g/L	KCl
14.4 g/L	$Na_2HPO_4 \cdot 2\ H_2O$
2.4 g/L	KH_2PO_4

DNA loading buffer (5x)

30 %(w/v)	Sucrose
20 % (v/v)	glycerol
0.2 % (w/v)	orange G

Bug buffer

50 mM	NaH_2PO_4, pH 8.0
0.3 M	NaCl

Buffer A

50 mM	NaH_2PO_4, pH 8.0
0.3 M	NaCl
2 mM	β-mercaptoethanol

Buffer B

50 mM	NaH_2PO_4, pH 8.0
0.3 M	NaCl
2 mM	β-mercaptoethanol
0.5 M	Imidazole

Breaking Buffer

25 mM	NaH_2PO_4, pH 7.5
0.5 M	NaCl
2 mM	$MgCl_2$
10 μM	GDP

4% PFA

4 g paraformaldehyde	1x PBS (pH 7.4)

RIPA lysis buffer

50mM	Tris pH 7.5
150 mM	NaCl
1 mM	EGTA
1 mM	EDTA
1% (W/V)	IGEPAL
0.25% (W/V)	Na deoxycholate
2.5 mM	Na pyrophosphate
1 mM	*β*-glycerophosphate
0.1 mM	PMSF

Transfer buffer

25 mM	Tris-base
192 mM	glycine
20 %	methanol

Frozen medium

10%	DMSO
20%	FBS
70%	DMEM

TBS buffer(10x) (pH 7.6)

0.2M	Tris base
1.5M	NaCl

Annealing Buffer

100mM	K-acetate
30mM	HEPES-KOH pH 7.4
2mM	Mg-acetate

2.2 Methods

2.2.1 Molecular biology methods

2.2.1.1 Plasmids, bacterial strains and cell lines in this study

Plasmids

Plasmid Name	Insert	Resistance marker
DENND1A-mCherry	DENND1A	Kanamycin
Dynamin2-K44A-mCherry	Dynamin2-K44A	Kanamycin
Dynamin2-mCherry	Dynamin2	Kanamycin
paGFP-Rab35a-PBC-1M	Rab35a-PBC-1M	Kanamycin
paGFP-Rab35a-PBC-2M	Rab35a-PBC-2M	Kanamycin
paGFP-Rab35a-PBC-3M	Rab35a-PBC-3M	Kanamycin
paGFP-Rab35a-PBC-4M	Rab35a-PBC-4M	Kanamycin
paGFP-Rab35a-PBC-5M	Rab35a-PBC-5M	Kanamycin
paGFP-Rab5a	Rab5a	Kanamycin
paGFP-Rab7a	Rab7a	Kanamycin
pEGFP- RILP	RILP	Kanamycin
pEGFP-Rab11a	Rab11a	Kanamycin
pEGFP-Rab35a	Rab35a	Kanamycin
pEGFP-Rab35a-C201A	Rab35a-C201A	Kanamycin
pEGFP-Rab35a-PBC-1M	Rab35a-PBC-1M	Kanamycin
pEGFP-Rab35a-PBC-2M	Rab35a-PBC-2M	Kanamycin
pEGFP-Rab35a-PBC-3M	Rab35a-PBC-3M	Kanamycin
pEGFP-Rab35a-PBC-4M	Rab35a-PBC-4M	Kanamycin
pEGFP-Rab35a-PBC-5M	Rab35a-PBC-5M	Kanamycin
pEGFP-Rab35a-PBC-5M-C201A	Rab35a-PBC-5M-C201A	Kanamycin
pEGFP-Rab35aQ67L-PBC-5M	Rab35aQ67L-PBC-5M	Kanamycin
pEGFP-Rab35a-S150A	Rab35a-S150A	Kanamycin
pEGFP-Rab35a-S22N	Rab35a-S22N	Kanamycin
pEGFP-Rab35aS22N-PBC-5M	Rab35aS22N-PBC-5M	Kanamycin
pEGFP-Rab35a-S67L	Rab35a-S67L	Kanamycin
pEGFP-Rab5aD35Q79L-CSC	Rab5aD35Q79L-CSC	Kanamycin
pEGFP-Rab5aS34N	Rab5aS34N	Kanamycin
pEGFP-Rab5aS79L	Rab5aS79L	Kanamycin
pEGFP-Rab7a	Rab7a	Kanamycin
pEGFP-Rab7a-D24CC	Rab7a-D24CC	Kanamycin
pEGFP-Rab7a-D24CSC	Rab7a-D24CC	Kanamycin
pEGFP-Rab7a-D27CC	Rab7a-D27CC	Kanamycin
pEGFP-Rab7a-D27CSC	Rab7a-D27CC	Kanamycin
pEGFP-Rab7a-D34CC	Rab7a-D3CC	Kanamycin
pEGFP-Rab7a-D34CSC	Rab7a-D3CC	Kanamycin
pEGFP-Rab7a-V180A	Rab7a-V180A	Kanamycin

pEGFP-Rab8a	Rab8a	Kanamycin
pEGFP-RILP	RILP	Kanamycin
pHA-Rab35	Rab35	Kanamycin
pHA-Rab7	Rab7	Kanamycin
pHA-Rab7Q67L	Rab7Q67L	Kanamycin
pHA-Rab7Δ24	Rab7Δ24Q67L	Kanamycin
pHA-Rab7Δ24Q67L	Rab7Δ24Q67L	Kanamycin
pHA-Rab7Δ27	Rab7Δ27	Kanamycin
pHA-Rab7Δ27Q67L	Rab7Δ27Q67L	Kanamycin
pHA-Rab7Δ34	Rab7Δ34	Kanamycin
pHA-Rab7Δ34Q67L	Rab7Δ34Q67L	Kanamycin
PLL3.7-shRNA-OCRL-3	shRNA-OCRL-3	Ampicillin
PLL3.7-shRNA-OCRL-4	shRNA-OCRL-4	Ampicillin
PLL3.7-shRNA-PRA1	shRNA-PRA1	Ampicillin
PLL3.7-shRNA-Rab35-1	shRNA-Rab35-1	Ampicillin
PLL3.7-shRNA-Rab35-3	shRNA-Rab35-3	Ampicillin
PLL3.7-shRNA-Rab35-4	shRNA-Rab35-4	Ampicillin
PLL3.7-shRNA-RILP-1	shRNA-RILP1	Ampicillin
pMAL-MBP-RILP	RILP	Ampicillin
pmCherry-Rab35a	Rab35a	Kanamycin
pmCherry-RILP	RILP	Kanamycin
pRFP-C-RS DENND1A	shRNA-DENND1A	Ampicillin
pTWIN1-EGFP- Rab1Δ34-GGS	EGFP- Rab1Δ34-GGS	Ampicillin
pTWIN1-EGFP- Rab35Δ11	Rab35Δ11	Kanamycin
pTWIN1-EGFP- Rab7Δ34-GGS	EGFP- Rab7Δ35-GGS	Ampicillin
pTWIN1-EGFP-Rab1Δ13	EGFP-Rab1Δ13	Ampicillin
pTWIN1-EGFP-Rab5-GGS-Δ35	EGFP-Rab5-GGS-Δ35	Ampicillin
pTWIN1-EGFP-Rab5Q79L-GGS-Δ35	EGFP-Rab5Q79L-GGS-Δ35	Ampicillin
pTWIN1-EGFP-Rab5-Q79L-Δ14	EGFP-Rab5-Q79L-Δ14	Ampicillin
pTWIN1-EGFP-Rab5-Δ14	EGFP-Rab5-Δ14	Ampicillin
pTWIN1-EGFP-Rab7Δ15	EGFP-Rab7Δ15	Ampicillin
pTWIN1-EGFP-Rab8Δ11	Rab8Δ11	Kanamycin
pTWIN1-EGFP-Rab8Δ16	Rab8Δ16	Kanamycin
pTWIN1-Rab7Δ34	Rab7Δ34	Kanamycin

Empty pTWIN vector was obtained from New England Biolabs (Beverly, MA, USA).Empty pEGFP and pmCherry vectors from Clontech Laboratories.

Bacterial strains

Bacterial strains	**Genotypes**
XL1 Blue (Stratagene)	*recA1, endA1, gyrA96,* thi-1, *hsdR17*, *supE44*, *relA1*, *lac* [F´, *proAB*, *lacIq*ZΔM15, *Tn10* (Tetr)]
BL21(DE3)(Stratagene)	F-, *ompT*, lon, *hsd*S (rB-, mB-), *dcm*, *gal*, λ(DE3)
Top10(Thermo Fisher)	F– *mcr*A Δ(*mrr-hsd*RMS-*mcr*BC) Φ80*lac*ZΔM15 Δ*lac*X74 *rec*A1 *ara*D139 Δ(*ara leu*) 7697 *gal*U *gal*K *rps*L (StrR) *end*A1 *nup*G

BL21(DE3) Codon Plus RIL (Stratagene)	F-, *ompT*, lon, *hsd*S (rB-, mB-), *dcm*, *gal*, λ(DE3), endA, Hte [argU ileY leuW CamR]
DH5α(Thermo Fisher)	F– Φ80*lac*ZΔM15 Δ(*lac*ZYA-*arg*F) U169 *rec*A1 *end*A1 *hsd*R17 (rK–, mK+) *pho*A *sup*E44 λ– *thi*-1 *gyr*A96 *rel*A1

Mammalian Cell lines

Cell Line	Origin	Supplier
COS-7	African green monkey kidney fibroblast	ATCC
HeLa	Human cervical adenocarcinoma	ATCC
MDCK	Madin-darby canine kidney cells	ATCC
SH-SY5Y	Human neuroblastoma cell	ATCC

2.2.1.2 Preparation of competent cells

1 L of LB medium was inoculated with 10 mL of an overnight-grown culture of the desired *E.coli* strain. The culture was incubated at 37°C, 220rpm on a shaker, until the OD600 reached about 0.5 (ca. 4 h). The culture was cooled on ice for 20 min, transferred to sterile centrifugation vessels and centrifuged for 10 min at 4°C at 2000 g. The supernatant was discarded.

Electro-competent cells

The bacterial cell pellet was gently resuspended in 5 mL of ice-cold sterile GYT

(0.125% (w/v) yeast extract, 0.25% (w/v) tryptone, 10% (v/v) glycerol) and centrifuged twice as described above. Cell pellet were resuspended in 1 mL GYT, dispensed in 50 µl aliquots, shock frozen in liquid nitrogen and stored at -80°C.

Chemical-competent cells

The pellet was gently resuspended in 20 mL of ice-cold sterile 100 mM CaCl2 solution and incubated on ice for 30 min. The cells were centrifuged at 2000 g for 5 min at 4°C and were resuspended in 1 - 5 mL of TFBII buffer (10 mM MOPS, pH 7.0, 75 mM $CaCl_2$, 10 mM NaCl, 15 % glycerol). Aliquots of 100 µl were shock frozen in liquid nitrogen and stored frozen at -80°C.

2.2.1.3 Preparative PCR

The appropriate 5'- and 3'-primers were designed and synthesized by Eurofins Genomics. The PCR reaction mixture was prepared in steps shown in in a PCR tube. The mixture was incubated in Biorad PE 9700 thermocycler (Applied Biosystems) using PCR program as below.

High fidelity PCR for sub-cloning

Step	Content	Volume (µL)
1	Forward primer(con.10µM)	2
2	Revers primer(con.10µM)	2
3	Template DNA(10~50ng)	1
4	Phusion master mix	25
5	ddH_2O	20
Total		50

PCR program

Step	Temp(°C)	Time
1	98	30 s
2: 36 cycles	98	8 s
3: 36 cycles	50~65	20 s
4: 36 cycles	72	15 s-30 s/kb
5	72	7 min
6	8	Hold

2.2.1.4 Purification of PCR products by agarose gel electrophoresis

Depending on the size of the DNA fragment, the agarose concentration was between 0.8 and 2 % (w/v).

1. Dissolve the required amount of agarose by heating in TAE buffer.
2. Add Red safe to a final concentration of 0.5 µg/mL
3. Pour the solution into the gel casting equipment and allowed to polymerize.
4. Mix the samples with 5X DNA loading buffer and load into the wells. A 1 kb DNA ladder (Fermentas) was used as a molecular weight standard.
5. Run the gels horizontally at 10 V/cm immersed in TAE-buffer until fragment separation was complete.

6. Excise the bands of interest and extract the DNA from the gel using a gel extraction kit from Qiagen according to the instructions of the manufacturer.We also used PCR kit to retake the PCR product (Qiagen DNA or Omiga clean up kit).

2.2.1.5 Construction of vectors

Restriction enzyme digestion

Both vector and purified PCR product were digested by the appropriate restriction enzymes. Digestions of DNA fragments were performed as recommended by the manufacturer at 37°C for 3 h. The reaction was stopped by addition of DNA loading buffer. Fragments produced by restriction enzyme digestion were purified using agarose gel electrophoresis. An example is shown below.

Step	Contents	Vector volume (µL)	PCR product Volume (µL)
1	Buffer(10x)	3	4
2	DNA	2 (total 1µg)	30
3	BamHI	1(20U/µl)	1
4	XhoI	1 (20U/µl)	1
5	ddH_2O	23	4
Total		30	40

Dephosphorylation of 5'-Phosphorylated DNA fragments

An essential step during cloning and before the ligation of two DNA fragments is the dephosphorylation of 5'-end of destination vector to prevent its self-ligation. Self-ligation of cut vector will prevent fragment insertion and produce empty vectors. For dephosphorylation, 0.5 U/µg DNA of alkaline phosphatase (calf intestinal phosphatase CIP) is added directly on the restriction mix and reaction tubes are incubated for 1 h at 37°C. Stop the reaction for 15min at 70°C.

Ligation

For ligation 1-10 *f*mol of linear plasmid DNA was mixed with a 3 fold molar excess of insert fragment. Ligation was performed in ligation buffer in a volume of 20 µl, using 5 units of T4 DNA ligase for 1 h at 22°C (Rapid ligation, for short DNA fragment) or 1 units of T4 DNA ligase for 12~14 h at 16°C (long DNA fragment). An example is shown below.

Step	Contents	Volume(μL)
1	Linear vector	3
2	Insert	8
3	Rapid ligation buffer 5x or Ligation buffer 10x	4 or 2
4	Rapid T4 ligase 5 U/μL or T4 ligase 1 U/μL	1
5	ddH_2O	4 or 6
Total		20

2.2.1.6 Chemical transformation

1. Add the ligation mixture containing approximately 1 ng of the desired plasmid DNA to 50~100 μL chemical competent cells. The mixture was incubated on ice for 25~ 30 min without shaking.
2. Heat the cells at 42°C for 45 s and immediately cooled on ice for 2 min.
3. Spread on LB plate directly (Ampicillin resistance) or add 600 μL of LB medium into the cells EP tube.
4. Incubate at 37°C for 50 min for Kanamycin resistance on a shaker.
5. Spread 100 μL cells on agar plates supplemented with the corresponding antibiotics.
6. Invert plates and incubate overnight (12-16 h) at 37°C.

2.2.1.7 Colony PCR screen

1. Pick a single bacterial colony growing on LB agar plate with the corresponding antibiotics using a sterile yellow tip.
2. Inoculate the colony into 4 mL of LB medium with the corresponding antibiotics.
3. After 3 hours growth, withdraw 1 μL culture in a PCR test tube using sterile tips.
4. Perform PCR as shown below.

Cloning PCR for vector identification

Step	Content	Volume (μL)
1	Forward primer(con.10μM)	1
2	Revers primer(con.10μM)	1
3	LB medium mixture of cell	1
4	Red mix	10
5	ddH_2O	7
Total		20

PCR program

Step	Temp(°C)	Time
1	94	4min
2: 36 cycles	94	45 s
3: 36 cycles	50~65	45 s
4: 36 cycles	72	1 min/kb
5	72	10 min
6	8	Hold

5. Analyze the PCR products by agarose gel electrophoresis. The one showing a band of PCR product at the expected molecular weight suggests a successful cloning.

Agarose concentration in % (w/v) Size of DNA fragments

2.5	<100bp
2.0	0.1 - 1.0 kb
1.8	0.2 – 2.0 kb
1.5	0.3 – 3.0 kb
1.2	0.5 – 5.0 kb
1.0	0.5 – 7.0 kb
0.8	0.8 – 12.0 kb
0.5	30.0 kb

2.2.1.8 Preparation of plasmid DNA

Plasmid DNA was prepared using the plasmid mini-prep kit (Qiagen) as follows:

1. Pick a single bacterial colony to seed 4 mL of LB medium containing the appropriate antibiotics.
2. Grow the culture overnight (12~14 h) at 37°C，220rpm on shaker.
3. Harvest cells by centrifugation (16,000 g, 1 min). Discard the supernatant.
4. Resuspend the cell pellet in 250 μL Solution I with RNase A by vortex.
5. Add 250 μL Solution II and mix gently until the solution becomes clear.
6. Add 350 μL Solution III into clear lysate and mix gently to precipitate chromosomal DNA, lipids, and proteins.
7. Remove the precipitates by centrifugation (14000rpm, 10 min).

8. Load the supernatant on a silica spin column. Centrifuge the column for 1 min at 14,000 rpm.

9. Wash the column with 500 µL HB buffer, 700 µL wash buffer (with ethanol) twice by centrifugation (14,000 rpm, 1 min).

10. Centrifuge the column for 1.5 min at 14,000 rpm to get rid of ethanol.

11. Elute the plasmid DNA with 70 µL EB buffer by centrifugation (14,000 rpm, 1.5 min).

2.2.1.9 DNA sequencing

For DNA sequencing, the cloned plasmid was subjected to PCR using the BigDyeDesoxy terminator cycle sequencing kit. The sequencing reactions were prepared and PCR program was set as shown below.

Sequencing PCR

Step	Content	Volume (µL)
1	Bigdye	2
2	5x Sequencing buffer	2
3	primer(con.10µM)	1
4	Plasmid(200~500ng/µL)	1
5	ddH_2O	4
Total		10

PCR program

Step	Temp(°C)	Time
1	94	4min
2: 25 cycles	94	20 s
3: 25 cycles	50	30 s
4: 25 cycles	60	2.5 min
5	8	hold

Ethanol precipitation

1. Dilute the PCR product with 10 µL H2O.

2. Add 2 µL 3M sodium acetate (pH 5.5) to the sample tube.

3. Add 2 µL 0.1M EDTA to the sample tube.

4. Add 50µL 100% ethanol to precipitate DNA and incubate for 15 min at room temperature.

5. Centrifuge the sample at 14,000 rpm for 20 min at room temperature. Remove the supernatant.

6. Wash the precipitate once with 200 µL 70 % ethanol. Centrifuge the sample at 14000 rpm for 15 min at room temperature.

7. Dry the sample under vacuum.
8. The sample was analyzed by the in house sequencing facility.

2.2.1.10 Transformation by electroporation

1. Add ca. 1 ng of plasmid DNA in a volume of 0.5 µL to 50 µL electro-competent cell suspension in a chilled electroporation cuvette (0.2 µm path length).
2. Tap the cuvette to exclude air bubbles.
3. Apply a high voltage pulse using an *E.coli* Pulser from Biorad (conditions: 25 µF, 200 Ω, 1800V).
4. Immediately add 600 µL of LB medium to the cuvette after pulsing.
5. Grow the culture at 37°C, 220 rpm for 50 min on a shaker.
6. Spread 100 µL cell suspensions on agar plates containing the appropriate antibiotics.
7. Invert plates and incubate overnight (12-16 h) at 37°C.

2.2.1.11 Short hairpin (shRNA) construct generation

The principle of shRNA construct design is shown in Figure 2-1. Firstly, we need search for target sequences located throughout the mRNA. The consensus sequence should correspond to: AAGN18TT. A 5' guanine is required due to the constraints of the U6 promoter. Normally we test 4 targets for each gene of interest.

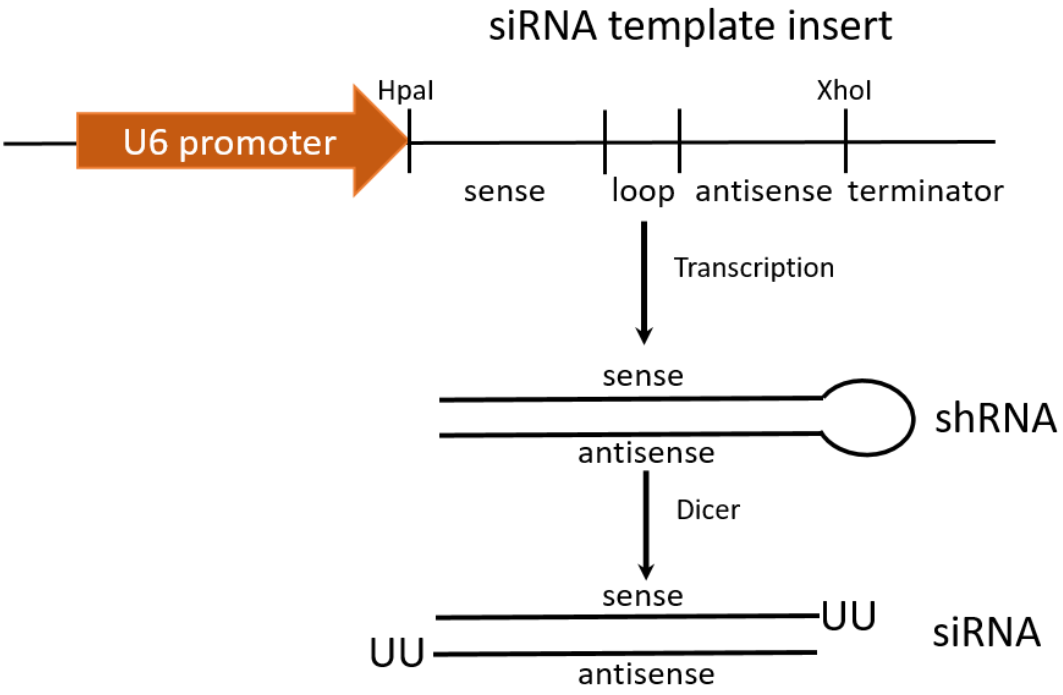

Figure 2-1. The principle of shRNA constructs design.

1. Oligo Design: A multiple cloning site immediately following the U6 promoter. An HpaI site leaves a blunt end prior to the –1 position in the promoter. The oligo design must incorporate a 5' T in order to reconstitute the –1 nucleotide of U6. An XhoI site cuts downstream of the U6 start site.
2. Oligo format: Sense oligo, 5'T-(GN18)-(TTCAAGAGA)-(81NC)-TTTTTTC; antisense oligo, compliment of sense but with additional nucleotides at 5' end to generate XhoI overhang. The loop sequence (TTCAAGAGA) is based upon previous report (Rummelkamp et al., 2002). Order oligos through Eurofins with 5' phosphates and PAGE purified.
3. Annealing oligos by below steps

Step	Contents	Volume (μL)
1	Sense oligo(100pmol/μL)	1
2	Antisense oligo(100pmol/μL)	1
3	Annealing Buffer	48
	Total	50

4. Annealing by PCR program below

Step	Temperature(°C)	Time (min)
1	95	4
2	70	10
3	4 (decrease temperature slowly:0.1°C/min)	180
4	4	10

5. Digest PLL 3.7 vector 1 μg with XhoI and HpaI for 3h at 37°C then treats with CIP for 1h at 37°C.
6. Ligate linearized product and annealed oligos at 60fmol of each component in a final concentration of 10μL.
7. Transformat the ligation product into XL1 competent cells.
8. Spread the transformation product on LB plate with Ampicillin antibiotic.
9. Invert plates and incubate overnight (12-16 h) at 37°C.

2.2.2 Protein expression, purification and modification methods

2.2.2.1 Expression and purification of GFPRab1, 5, 7, 35-thioester proteins

Expression of GFP-Rab5a(Q79L)Δ14 in E. coli

1. Transform plasmid pTWIN-His-EGFP-Rab5(Q79L)Δ14 into BL21(DE3) cells and select on a LB agar plate containing 100 mg/L Carbenicillin (similar function as Ampicillin).
2. The second day, pick a single colony from the agar plate using a sterile yellow tip and inoculate it into 100 mL of LB-medium containing 125 mg/L ampicillin.
3. Incubate at 37°C at 170 rpm on a rotatory shaker overnight.
4. Inoculate this pre-culture into 5 L of LB-medium containing 125 mg/L ampicillin.
5. Grow cells in five 5 L flasks at 37°C on a shaker (170 rpm) until the absorbance at 600 nm (OD_{600}) reached 0.5-0.7 (ca. 4 h). Take a sample of 40µL from the cell suspension; mix it with 20 µL 4×SDS sample buffer, boile at 99°C for 5 min as a control for step 9.
6. Put the flasks in the cold room to reduce the temperature of the culture to 20°C.
7. For induction of the protein expression, add IPTG to the culture to a final concentration of 0.2 mM.
8. Incubate at 20°C on a shaker (170 rpm) overnight (18 h).
9. Before harvesting cells, take a sample of 30 µL from the cell suspension, mix it with 15 µL 4×SDS sample buffer, boile at 99°C for 5 min and run a denaturing SDS-PAGE to estimate the protein expression level.
10. Harvest cells by centrifugation in the centrifuge Avanti J20-XP (Beckman Coulter) at 6000 rpm, 4°C for 15 min.
11. Discard the supernatant carefully and wash the cells with PBS by centrifugation in the centrifuge Eppendorf 5804 (Eppendorf) at 5000 rpm, 4°C for 10 min. The weight of the cells about 35g.

Here the cells can be frozen in liquid nitrogen and stored in -80°C.

Lysis of E. coli cells

12. Resuspend the cell pellet in 25 mL ice-cold Breaking Buffer (30 mM NaH_2PO_4, pH 7.5, 0.3 M NaCl, 1 mM $MgCl_2$) freshly supplemented with 1 mM PMSF, 10 µM GDP.

Note: The PMSF and GDP should be added freshly. Don't add any reducing substances.

13. Pass the cell suspensions through the chilled pressure chamber of Microfluidizer 3 times at 40,000 psi.

14. Add new portion of PMSF to 0.5 mM and TritonX-100 to 1% (v/v). Note: The TritonX-100 should be added after breaking the cells.

15. Centrifuge the cell lysate in the ultracentrifuge Optima L-70K (Beckman Coulter) at 35,000 rpm, 4°C for 30 min.

16. Filter the supernatant through a 0.2 μm ZapCap filter (Nalgene).

Purification of EGFP-Rab5a(Q79L)Δ14 α-thioester

17. Load the filtrate with a flow rate of 2 mL/min on a 5 mL Hi-Trap Ni-NTA column that has been equilibrated with the Buffer A (50 mM NaH_2PO_4, pH 8.0, 0.3 M NaCl, 2 mM β-mercaptoethanol).

18. Wash the column with Buffer A with a flow rate of 5 mL/min until the absorbance reached the baseline.

19. Wash the column with 2% Buffer B (50 mM NaH_2PO_4, pH 8.0, 0.3 M NaCl, 2 mM β-mercaptoethanol, 0.5 M imidazole) with a flow rate of 5 mL/min until the absorbance reached the baseline.

20. Elute the column with a gradient of 2-100% Buffer B with a flow rate of 5 mL/min for 250 mL. Collect 5 mL/fraction.

21. Run SDS-PAGE and identify the fractions of interest.

22. Wash the column with 2 mM NaN3.

23. Collect the fractions of interest and dialyze the sample against buffer for (25 mM Tris-HCl, pH 8.0, 100 mM NaCl, 4 mM sodium citrate, 2 mM β-mercaptoethanol).

24. Concentrate the protein to 5ml and Run gel filtration on the Superdex-75 column using buffer (25mM NaH_2PO_4, pH7.5, 30 mM NaCl, 1 mM $MgCl_2$, 20 μM GDP). Note: Prepare fresh solution, filter the buffer through a 0.2 μm membrane filter (Whatman) and degas on a vacuum-membrane pump (ILM/VAC GmbH) by stirring for 0.5 h at room temperature (23°C).

25. Concentrate the protein and add sodium 2-mercaptoehanesulfonate (MESNA) powder into the protein and a concentration of 0.5 M. Incubate overnight on a rotating wheel at 23°C.

26. Run SDS-PAGE and test the EGFP-Rab5a(Q79L)Δ14 α-thioester efficiency.

27. Concentrate the sample to at least 10 mg/mL, separate them in aliquots and froze them flashily in liquid nitrogen. Store the protein in -80°C.

2.2.2.2 Universal C-terminal protein labeling with oxyamine ligation

1. Dilute EGFP-Rab5a(Q79L)Δ14 α-thioester solution with 5-fold volume of Buffer A . Note: the MESNA concentration is not lower 50mM but not higher than 100mM.

2. Load EGFP-Rab5a (Q79L)Δ14 α-thioester onto a Ni-NTA column equilibrated with Buffer A containing 100 mM MESNA. Collect flow-through.

3. Wash column with 2-5% Buffer B containing 100 mM MESNA. Collect and pool flow-through and concentrate protein.

4. Run a gel filtration on a Superdex 60 column using Elution Buffer (30 mM NaH_2PO_4, pH 7.5, 50 mM NaCl, 100 mM MESNA). Note: Prepare fresh solution, filter buffer through a 0.2 µm filter and degas for 30 min at room temperature.

5. Identify and collect fractions of interest by SDS-PAGE. Concentrate protein and snap-freeze in liquid nitrogen. Store protein at -80 °C.

6. Incubate 200 µl protein-thioester (5-25 mg/mL) with 100 µl bis(oxyamine) (1 M stock solution in reaction buffer, final 333 mM) in Reaction Buffer (30 mM NaH_2PO4, pH 7.5, 50 mM NaCl) on ice overnight. The reaction product EGFP-Rab5a(Q79L)Δ14-ONH_2 is monitored by ESI-MS.

7. Dialyze protein twice against 1 L Dialysis Buffer (30 mM NaH_2PO_4 pH 7.5, 50 mM NaCl, 2 mM DTE) at 4 °C.

8. Incubate 50 µM EGFP-Rab5a(Q79L)Δ14-ONH2 with 0.5 mM Keto-PEG1 for 20 h or overnight on ice in the presence of 100 mM Aniline in Incubation Buffer (30 mM NaH_2PO_4, pH 7.0, 50 mM NaCl, 2 mM DTE).

9. Remove unreacted small molecules by passing the reaction mixture over a NAP-5 desalting column pre-equilibrated with 30 mM sodium phosphate (pH 7.5, 50 mM NaCl, 1 mM $MgCl_2$, 10 µM GDP, and 5 mM DTE).

10. Add MESNA powder to final concentration 500 mM into the protein solution and incubate on ice for 2 h.

11. The reaction is monitored by ESI-MS check the two StBu groups were totally removed.

12. Perform gel filtration to purify the ligated protein in prenylation buffer (50 mM HEPES, pH 7.2, 50 mM NaCl, 5 mM DTE, 2 mM $MgCl_2$, 10 μM GDP).
13. Concentrate the protein fractions to about 1-5 mg/mL for further prenylation and microinjection studies.

2.2.2.3 *In vitro* prenylation

4 μM PEGylated Rab or wild type or mutants, 6 μM REP, 6 μM RabGGTase were incubated in prenylation buffer (50 mM HEPES, pH 7.2, 50 mM NaCl, 5 mM DTE, 2 mM $MgCl_2$, 10 μM GDP) at 25 °C, and 50 μM NBD-FPP was added to initiate the reaction. At defined time intervals, 10 μl samples were withdrawn and quenched by addition of 10 μl of 2 × SDS-PAGE sample buffer. For an end-point assay, 6 μM PEGylated Rab or wild type proteins, 10 μM REP, and 6 μM RabGGTase were mixed with 40 μM NBD-FPP in prenylation buffer and incubated for 1.5 h at 25 °C, followed by quenching with 2 × SDSPAGE sample buffer. The samples were boiled at 95 °C for 3 min and were loaded onto 15% SDS-PAGE. The fluorescence bands corresponding to the NBD-farnesylated protein were visualized in the gel using a Fluorescent Image Reader FLA-5000 (Fuji, excitation laser: 473 nm, cut-off filter: 510 nm) followed by staining with Coomassie Blue and scanning. The fluorescence intensities of the bands were quantitatively analyzed using AIDA densitometry software. The traces were fitted to a single exponential equation.

2.2.3 Analytical methods

2.2.3.1 SDS-PAGE

Preparation of SDS-Polyacrylamide Gel Electrophoresis (PAGE) gels

1. Pour the solution into a Biorad Multi-casting apparatus (9 gels). Add 70% ethanol on the top of the resolving gel. Incubate at room temperature until the resolving gel was polymerized (ca. 30 min).
2. Remove the ethanol and add the stacking gel solution prepared as below. Insert combs immediately.

3. Incubate at room temperature until the stacking gel was polymerized (ca. 20 min). The gels can be stored in 4°C in a wet paper packet which is contained in a closed plastic bag.

Sequence	1	2	3	4	5	6
Type of gel (%)	Acrylamide/ bisacrylamide (29:1, 30 %)	Mili-Q H2O	Seperating gel buffer (4X)	Stacking gel buffer (4X)	10 % APS	TEMED
Resolving gel (60 mL)						
10 %	20 ml	25ml	15ml	-	300 µl	30 µl
15%	30 ml	15ml	15ml	-	300 µl	30 µl
Stacking gel (30 mL)						
5 %	5 mL	17.5 mL	-	7.5 mL	240 µl	30 µl

SDS-Gel electrophoresis

4. Prepare protein samples by adding an half amount of SDS-PAGE sample buffer (4x) and heat them for 5 min at 99°C.
5. Run gels electrophoresis at 100V until the bromphenol blue front entered the buffer solution.
6. Visualize fluorescent proteins by exposing the unstained SDS-PAGE gel to UV light or fluorescent image reader.
7. Stain the proteins by heating the gels in the Coomassie staining solution in a microwave. Incubate on a shaker at room temperature for 10 min.
8. Distain the protein by heating the gels in the distaining solution in a microwave. Incubate on a shaker at room temperature.

2.2.3.2 MALDI-TOF-mass spectrometry

Matrix Assisted Laser Desorbtion Ionization - Time Of Flight (MALDI-TOF) spectra were recorded on a Voyager-DE Pro Biospectrometry workstation from Applied Biosystems (Weiterstadt, Germany). Protein samples were desalted using small GF spin columns (DyeEx 2.0 Spin Kit, Qiagen) and mixed with an equal volume of matrice (saturated sinapinic acid solution in 0.3 % TFA/acetonitrile (2:1 v/v)). The mixture was quickly spotted on a MALDI sample plate, air-dried. Spectra were measured with the following instrument settings: acceleration voltage = 25 kV, grid voltage = 93 %, extraction delay time = 750 ns and guide wire = 0.3 %. The laser intensity was manually adjusted during the measurements in order to obtain optimal signal to noise ratios. Calibrations were carried out using a protein mixture of defined molecular mass (Sigma).

Spectra recording and data evaluation was performed using the supplied Voyager software package. The accuracy of the method for proteins within the molecular weight range of 20-30 kDa is ca. ± 20 Da.

Electronspray ionization mass spectrometry (ESI-MS)

Liquid Chromatography-Electrospray Ionization-Mass Spectrometry (LC-ESIMS) analysis was performed on an Agilent 1100 series chromatography system (Hewlett Packard) equipped with an LCQ ESI mass spectrometer (Finnigan) using Jupiter C4 columns (5 μm, 15 x 0.46 cm, 300 Å pore-size) from Phenomenex (Aschaffenburg) for proteins and 125/21 NUCLEODUR 5 μm C18 columns for peptides. For LC separation a gradient of buffer B (0.1 % formic acid in acetonitrile) in buffer A (0.1 % formic acid in water) with a constant flow-rate of 1 mL/min was applied. Mass spectra data evaluation and deconvolution was performed using the Xcalibur software package. The accuracy of the method for proteins within the molecular weight range of 20 kDa is ca. ± 1-2 Da and 70 kDa is ca. ± 15 Da.

2.2.4 Microcsopy

Laser Scanning Confocal Microscopy (LSCM)

Confocal images of live and fixed cells were obtained with Leica SP2 and Leica SP5 confocal laser-scanning microscope. TagBFP and pa-GFP was excited with 405 nm, EGFP and mCitrine with the 488 line of a multiline Argon laser. mCherry and dsRed was excited with the 561 nm line of a DPSS laser. Excitation light was focused into the sample by a 60x/1.2 NA oil objective or a 40x/0.9 NA air objective using either the DM405/488/561/633 or the DM458/515 dichroic mirror.

Detection of fluorescence was done by an acousto-optic tunable filter (AOTF) and SIM scanner. Blue fluorescence (Alexa 405 or TagBFP) was detected in a channel with bandwidth 425-478 nm and through a SDM490 emission beam splitter. Green and Citrine FPs were collected between 498-551 nm and through a SDM 510 emission beam splitter or SDM 560 if sequential imaging with the 561 nm laser was used. mCherry fluorescence was detected by collecting photons within the range of 575-675 nm. Live cell imaging was performed in an incubation chamber adjusted to 37°C, while fixed cells experiments were performed at RT (~ 25°C). The process of LSCM is shown in Figure 2-2 as below.

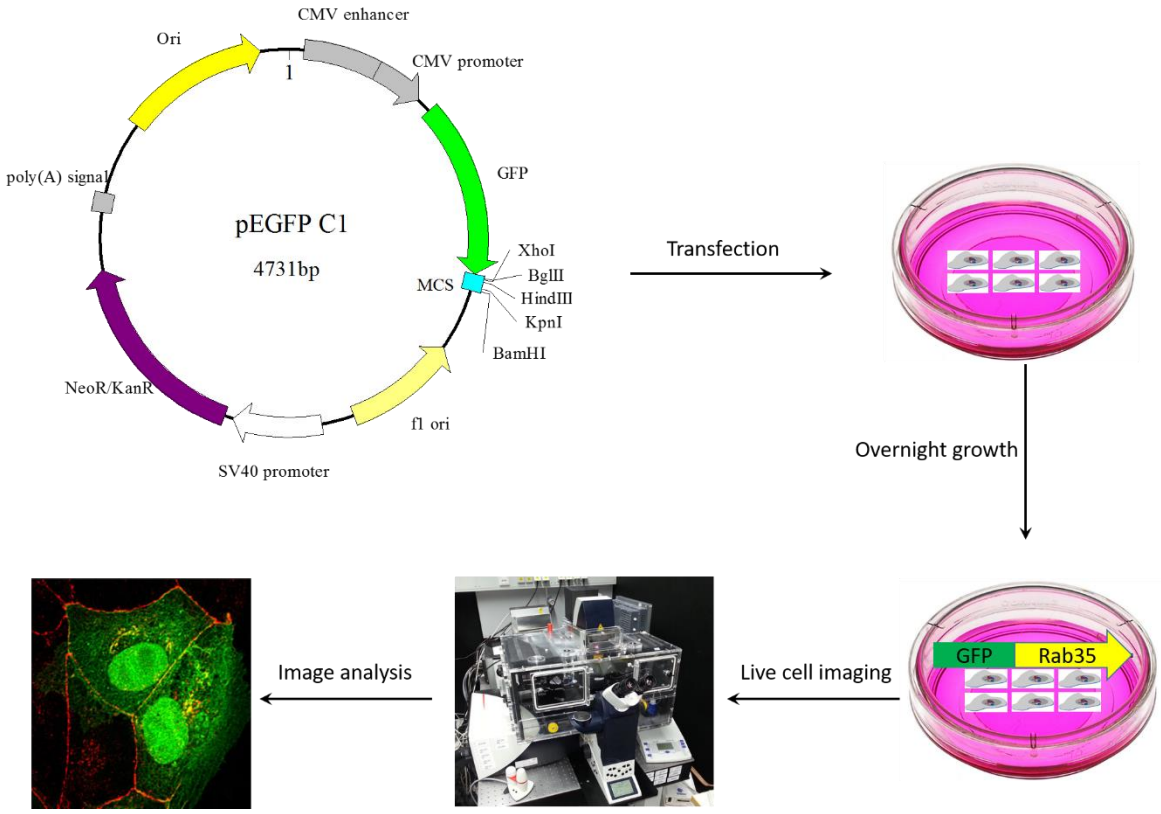

Figure 2-2. The process of Laser Scanning Confocal Microscopy (LSCM).

Fluorescence Loss After Photoactivation (FLAP)

FLAP experiments were carried out at 37°C on a Leica SP5 confocal microscope in imaging medium. Transiently transfected 15- 24 hrs post-transfection, cells were allowed to equilibrate in the incubation chamber on the microscope and imaged with laser setting adjusted to minimize photobleaching (typically 488 and 561 lasers used at 10%). The fluorescence was collected via a 63x/1.4 NA oil objective, with a custom routine that followed through the three stps of FRAP/FLAP analysis: (1) Pre-bleach imaging (2 images with 488 and 561 lasers only). (2) Bleaching/Photoactivation (2 times with the 405 laser only at 80%) in a pre-defined region of interest (ROI). (3) Post-bleach imaging (150 frames at 10 sec interval using the 488 and 561 lasers only). After standard image processing, mean intensities of photoactivatable PA-GFPRab35, PA-GFPRab5, PA-GFPRab7 in the photoactivated ROI yielded fluorescence loss curves, which were normalized to mKate2-Giantin to account for changes in the structure and intensity in the ROI resulting from the dynamic nature of live cells. Another ROI processed and normalized in the same manner was chosen at the cell periphery to investigate vesicular transport form the recycling endosome to the plasma membrane. For measuring half time

of plasma membrane gain or recycling endosome loss of Rab35, Rab5, Rab7 fluorescence in the selected ROIs, normalized fluorescence decay cures were averaged and average curve was then fitted to a single exponential function in Igor Pro. $I = I_0 + A \exp(-t/\tau)$ Where (I) is the intensity, (A) exponential constant, (t) is time; (τ) is the exponential time-constant.

2.2.5 Mammalian Cell Culture and related works

2.2.5.1 Subculture of Mammalian Cells

Cells were maintained in Dulbecco's Modified Eagle's Medium (DMEM) supplemented with 10% fetal bovine serum (FBS), 1% L-glutamine and 1% nonessential amino acids (NEAA) and 1% *sodium* pyruvate grown at 37°C in a 90% humidified incubator with 5% CO_2. For starving, phenolred free Earle's Balanced Salt Solution (EBSS) was used.
Exponentially growing cells become confluent and reach a density where all available substrate of the culture dish is occupied. When this happens, cell growth is usually inhibited by contact inhibition and cells need to be subcultured to new dishes with much less density to allow for further cell growth. When cultured cells reached 80-90% confluency, cells were washed once with PBS, covered with 1 ml trypsin (10cm petra dish) for 4 min at 37°C (MDCK cells required longer time ~ 12 min). Detached cells were washed with 3 ml complete growth media to inactivate any remaining trypsin and cell suspension transferred to a falcon tube and pipetted gently up and down to separate cells to a single cell suspension. If cell number and/or viability were to be determined, 10 μL of cell suspension in a total of 3ml media were used in Cell counter (BioRad) cell viability analyzer and the desired number of cells required for seeding into different cell culture dishes was calculated. For maintenance of cells lines, cells were subcultured at a ratio of 1:10 into new culture dishes.

2.2.5.2 DNA transfection

For confocal microscopy, 2.0×105 cells were cultured on 35 mm glass bottom dishes (MatTek, Ashland, MA) for 20 hours prior to transfection. Transient plasmid expression was achieved by overnight transfection with X-treme GENE HP DNA transfection reagent (06366244001, Roche). For nocodazole treatment, cells were treated with 20 μM nocodazole for 1.5 h followed by confocal fluorescence microscopy.

2.2.5.3 siRNA transfection

siRNAs were transfected into Hela cells in 35mm MaTTeK dish with lipofectamine 2000 (Invitrogen) based on its protocol.

1. Add a cell suspension containing 4 x 105 cells in 2ml of growth medium with serum but without antibiotics.
2. Dilute 3 µg of siRNA into 100 µl of Opti-MEM.
3. Dilute 3 µl of Lipofectamine™ 2000 into 100 µl Opti-MEM Medium and incubate for 5 min at room temperature. Note: Once the Lipofectamine™ 2000 is diluted, combine it with the siRNA within 30 min. Long time incubation may result in decreased activity. This dilution can be prepared in bulk for multiple wells.
4. Combine the diluted siRNA from step 2 with the diluted Lipofectamine™ 2000 from step 3. Incubate at room temperature for 20 min to allow DNA-Lipofectamine™2000 complexes to form.
5. Add the DNA-Lipofectamine™ 2000 complexes from step 4 (200 µl) directly to each well containing cells and mix gently by rocking the plate back and forth.
6. Change with fresh medium after incubation for 4 h at 37°C in a CO_2 incubator.
7. The lipofectimin™ 2000 usage can be calculated as below ratio.

Culture Vessel	96-well	48-well	24-well	12-well	6-well	35-mm	60-mm	100-mm
Surface Area (cm^2)	0.3	0.7	2	4	10	10	20	60

2.2.5.4 Stable cell line generation

In order to establish stable cell lines that constitutively express GFP-tagged proteins or small-hairpin RNAs. We used the protocol is described as below.

1. Designed and construct your interested gene vectors such as mCherry/GFP-tagged or shRNA plasmids. The above vector encodes kanamycin for selection in bacteria and neomycin (G418) for selection in mammalian cells. For shRNA knock-down construct, we choose pLL3.7 vector from Addgene #11795 as backbone, which encodes ampicillin for selection in bacteria and puromycin for selection in mammalian cells.

2. Prepare low-passage cells (not higher 20 passages).
3. Transfect the mCherry/GFP-tagged or shRNA constructs into HeLa or MDCK cells. 3μg of plasmid DNA and 4.5μL Xtreme GENE HP DNA transfection reagent in 300μL OptiMEM per 6x105 HeLa cells in to 100mm dishes.
4. The following day, replace the standard media with media containing 600μg/mL G418 or 1μg/mL puromycin for shRNA knockdown cells.
5. Carefully change the media in the dish every one or two days, taking care not to pipette directly onto the cells.
6. Over time (2-3 weeks) this will select the cells that have stably recombinant with the GFP plasmid or shRNA into their genomic DNA.
7. Using sterile yellow tips to pick up the single colony of cells with 10X objective lens under microscope, and culture the cells in 6-well-plate.
8. When the wells are confluent, rinse with PBS and trypsinize with trypsin-EDTA. Split into one well of a 6-well plate (for passaging) and one well of your choice for imaging or western blot in order to screen the colonies and decide which are worth keeping and which should be discarded.
9. Using 300μg/mL G418 or 0.5μg/mL puromycin to maintenance the identified cells.
10. Freeze the cells as passage 1 and further passage from the 6-well plate.

2.2.5.5 Western Blotting

Western blotting is one of immuno-blotting which can detect proteins that were separated electrophoretically are transferred to a nitrocellulose or PVDF membrane to enable immunological protein detection with antibodies.

Firstly loading the interest protein into SDS-gel and run electrophoresis. After electrophoresis blots were assembled in semidry bot modules or wet transferring according to the manufacturer's manual. Nitrocellulose membranes were activated for 5 min in methanol, and then left to equilibrate in 1 x transfer buffer together with the gel and two pieces of (Whatmann) filter paper. The blot sandwich was assembled in the following sequence from bottom-up: filter paper, NC membrane, gel and the second filter paper. For a mini-gel semidry transfer was done at 40V for 20 min or wet transferring at 100V for 40min. Following transfer, NC membrane was transferred to incubation box for the remaining binding sites of the membrane blocked with 5% milk or BSA for 1 hour on a shaker at RT. Membranes were then incubated with primary antibodies diluted in 1 ml 3%

milk 1x TBST solution. NC membrane was sealed in a plastic bag after discarding air bubbles and incubated overnight at 4 °C. Next day, blots were transferred again to incubation boxes, washed 3 times, 5 min each with 0.1% TBST. Blots were then incubated with the appropriate secondary antibodies diluted in 10 ml TBS for 1 hour at room temperature. Finally, blots were washed 5 times, 5 min each with 0.1% TBST solution and detected with HRP X-film system.

2.2.5.6 Immunoprecipitation (pull down)

HeLa cells were transfected with HA-Rab7(Q67L), HA-Rab7(Q67L)Δ24-CSC, HA-Rab7(Q67L)Δ27-CSC, or HA-Rab7(Q67L)Δ34-CSC. After 24 hours, the cells were lysed by adding 100µl IP buffer (50 mM Tris, pH7.5, 15mM EDTA, 100mM NaCl, 0.1% TX-100, 1 mM DTT, protease inhibitor cocktail). 30 µl amylose beads were washed with 5 ml binding buffer (50mM HEPES, pH7.5, 30mM NaCl, 0.2mM β-ME) and were subsequently incubated with 60 µl (10mg/ml) recombinant MBP-RILP or MBP proteins for 1 hour with mild shaking. The beads were washed again with 5 ml binding buffer and 5 ml PBS. The beads were blocked with 10% BSA for 1 hour on ice and were rinsed with PBS. MBP-RILP or MBP beads were incubated with HA-Rab7Q67L, HA-Rab7Q67LΔ24-CSC, HARab7Q67LΔ27- CSC, or HA-Rab7Q67LΔ34-CSC cell lysates for 3 h on ice with mild shaking. The beads were washed using cold washing buffer (20mM Tris, pH7.9, 100mM NaCl, 0.1% NP40) for three times. The bound proteins were eluted from the beads using 20 µl hot denaturing SDS-sample buffer (with 6M urea). The samples were subject to 15% SDS-PAGE and western-blotting. The process of pull down assay is desribled in Figure 2-3.

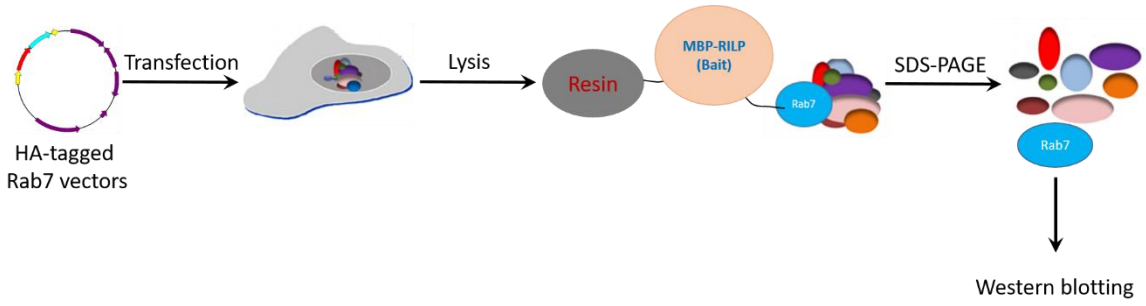

Figure 2-3. The process of pull down assay.

2.2.5.7 Cell fixation and immunofluorescence (IF)

Cells were fixed with 4% paraformaldehyde in PBS for 30 min at RT, rinsed three times (3X) with TBS and permeabilized with 0.5% Triton-X100 for 30 min at room temperature. For saponin extraction, 0.5% saponin was added into the medium at this step. After blocking with 5% FBS/0.1M Glycine/PBS for 1h, cells were incubated with anti-RILP (Sigma-Aldrich) antibody (1µg/ml) in 5% FBS/PBS for 1h, and subsequently treated with the secondary antibody (Alexa Fluor® 594 goat anti-rabbit IgG(H+L)) at a 1/500 dilution for 1h.

2.2.5.8 Microinjection of PEGylated Rab proteins

For each experiment, about 50 HeLa cells were injected with the purified PEGylated Rab proteins at concentrations of 5-7 mg/ml in prenylation buffer (50 mM HEPES, pH 7.2, 50 mM NaCl, 5 mM DTE, 2 mM $MgCl_2$). The microinjection was performed with Eppendorf Transinjector 5246 and Eppendorf micromanipulators 5171.

2.2.5.9 Determination of the GTP/GDP ratio

The analysis was performed essentially as described before (Colombo et al., 1998). HeLa cells were transfected with HA-Rab7, HA-Rab7Δ24-CSC, HARab7Δ27-CSC, or HA-Rab7Δ34-CSC (and the corresponding Q67L mutants). After 16 h, the cells were washed with PBS for 3 times and were changed to the phosphate-free Dulbecco's modified Eagles medium containing 0.5mCi/ml [^{32}P] orthophosphate (PerkinElmer Life Sciences). After 4 h incubation, the cells were washed 3 times with cold PBS and then lysed in lysis buffer (50mM HEPES, pH 7.4, 1% Triton X-100, 100 mM NaCl, 5 mM $MgCl_2$,mM PMSF, 0.1 mM GTP, 1 mM ATP and 10mM Na-phosphate). Nuclei and debris were removed by centrifugation at 15 000 g for 2 min, and the supernatant was subjected to immunoprecipitation with 1µl Anti-HA tag antibody (Abcam) on 20µl Dynabeads protein ASepharose CL-4B (Invitrogen) for 10 min at room temperature. The beads were then washed three times with wash buffer (50 mM HEPES, pH 7.4, 500 mM NaCl, 5 mM $MgCl_2$, 1% TritonX-100) and then three times with PBS containing 0.02% Tween-20. The bound nucleotides were then eluted in 20µl elution buffer (2 mM EDTA, 2 mM DTT, 0.2% SDS, 5 mM GDP and 5 mM GTP) for 10 min at 70°C. A volume of 5 µl of the samples were spotted onto 0.1 mm PEI -cellulose TLC plates (Merck) which were

developed for 40 min in developing buffer (1.2M ammonium formate, 0.8M HCl). The plates were dried and placed in autoradiography cassettes containing intensifying screens. For visualization of the [^{32}P]-labeled GTP and GDP, Fuji films were exposed at -80°C for 4 days. The processes of GTP/GDP ratio is described in Figure 2-4.

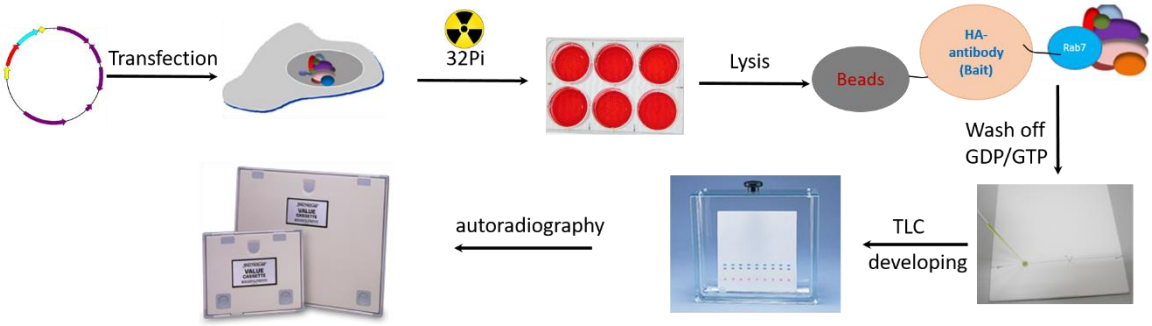

Figure 2-4. The principle of GTP/GDP ratio assay.

3 Aims of this work

As the key regulator of vesicular transport, Rab has to be localized at correct and specific membrane where it plays function properly. However, we still don't know what determine the spatial cycling and localization of Rabs. This work has used a combination of chemical biology, biochemistry, cell biology and biophysical methods to address the mechanism of Rab membrane targeting.

To further understand the significance of the C-terminal hypervariable domain (HVD) in Rab membrane targeting and prenylation, new methods are needed to manipulate the structure of Rab C terminus. In this work, we semisynthesized a series of Rab probes, where the C-terminal hypervariable region and prenylatable cysteine residues are replaced by PEG linkers and thiols, respectively. In order to further understand the mechanism of Rab prenylation, we want to know whether there is nothing required for Rab C-terminal sequence and to what extent the Rab prenylation machinery could tolerate the replacement in the Rab C-terminal sequence. We also use chemical-biological tools to probe whether the HVD of Rabs contains a general targeting signal for Rab localization. By combining this semisynthetic strategy with cell imaging, we aim to elucidate the role of the HVD, GEFs, GAPs and effectors in the subcellular Rab targeting.

To determine the cycling of Rab35 and to reveal its dynamics in the cell, we employ fluorescence localization after photoactivation (FLAP) and fluorescence recovery after photobleaching (FRAP) techniques to reach our aims. In this work, we knock down PRA1, a potential GDF of Rab35, to exame its function in the cycling of Rab35. Moreover, we aim to find out the detailed function of Rab35 GEF DENND1A for Rab35 membrane targeting. An effector of Rab35, OCRL1 is also considered a factor to affect the Rab35 membrane targeting.

Taken together, this study aim to discovery the contributions of the different regulators including GEFs, GDIs, GAPs, GDF, effectors and PtdInsPs for Rab membrane targeting and trafficking in cell.

4 Results and discussion

4.1 The role of the hypervariable C-terminal domain in Rab GTPases membrane targeting

Intracellular membrane trafficking requires correct and specific localization of Rab GTPases. The hypervariable C-terminal domain (HVD) of Rabs is posttranslationally modified by isoprenyl moieties that enable membrane association. A model asserting HVD directed targeting has been contested in previous studies, but the role of the Rab HVD and the mechanism of Rab membrane targeting remain elusive (Chavrier et al., 1991). In addition, the geranylgeranyl moieties(C-20 isoprenyl) are attached onto one or two (most cases) cysteines at their C terminal end by Rab geranylgeranyl transferase (RabGGTase). To fulfill the function of prenylation, RabGGTase along with REP, Rab forms of a ternary catalytic Rab:REP:RabGGTase complex (Pylypenko et al., 2003; Rak et al., 2004; Wu et al., 2009). Structural and biochemical analysis showed that key bindings of the ternary complex involve the GTPase domain and the C-terminal interacting motif (CIM) of Rab with REP and RabGGTase with REP (Guo et al., 2008; Wu et al., 2009). However, it remains elusive how the single Rab prenylation machinery can process the whole Rab family with diverse C termini.

To elucidate the function of the HVD, we will substitute this region with an unnatural polyethylenglycol (PEG) linker by using oxime ligation. In this section, we will discuss the HVD functions in Rab prenylation and membrane targeting. Through localization studies and functional analyses of semisynthetic PEGylated Rab1, Rab5, Rab7, and Rab35 proteins, we demonstrate that the role of the HVD of Rabs in membrane targeting is more complex than previously understood. Our findings suggest that Rab membrane targeting is dictated by a complex mechanism involving GEFs, GAPs, effectors, and C-terminal interaction with membranes to varying extents, and possibly other binding partners.

4.1.1 Construction of PEGylated Rab Proteins

In this study, we chose small GTPase Rab7 as the model protein to test the functions of Rab HVD in prenylation and membrane targeting. Firstly, we substitute the peptide which downstream of the essential CIM motif by a PEG linker (synthesized by Long Yi).

According to previous report, the length of the linker is critical for Rab prenylation (Wu et al., 2009) that we generate a C-terminal-length wild type like PEGylated Rab7 protein conjugate. We constructed pTWIN-Rab7 vectors which contain gene sequences of truncated the amino acid residues after the CIM motif of Rab7 protein. pTWIN vectors are designed for protein purification or for the isolation of proteins with an N-terminal cysteine and/or a C-terminal thioester (Evans et al., 1999). Expression of the fusion proteins is under the control of the T7 promotor/Lac operator and is regulated by IPTG due to the presence of a Lac repressor gene (see the protocol in appendices). The cloning and expression strategies are shown in figure 4-1-1.

pTWIN-Rab7Δ15-intein fusion vector is transformed into BL21 (DE3) *E.Coli* cells to express the target truncated Rab7 protein. As shown in figure 4-1-1, the expressed Rab-intein-CBD fusion protein was purified from crude cell lysate using chitin agarose. Rab7Δ15-thioester protein was generated by intein-mediated protein splicing using 0.5M MESNA (2-mercaptoethanesulfonate) as the thiol reagent. Subsequently, Rab7Δ15-thioester was treated with bis(oxyamine) at pH 7.5 on ice for 4 h to achieve oxyamine-modified protein, Rab7Δ15-ONH2, which is competent for oxime ligation with a chemical linker containing a ketone moiety (Figure 4-1-2A) .

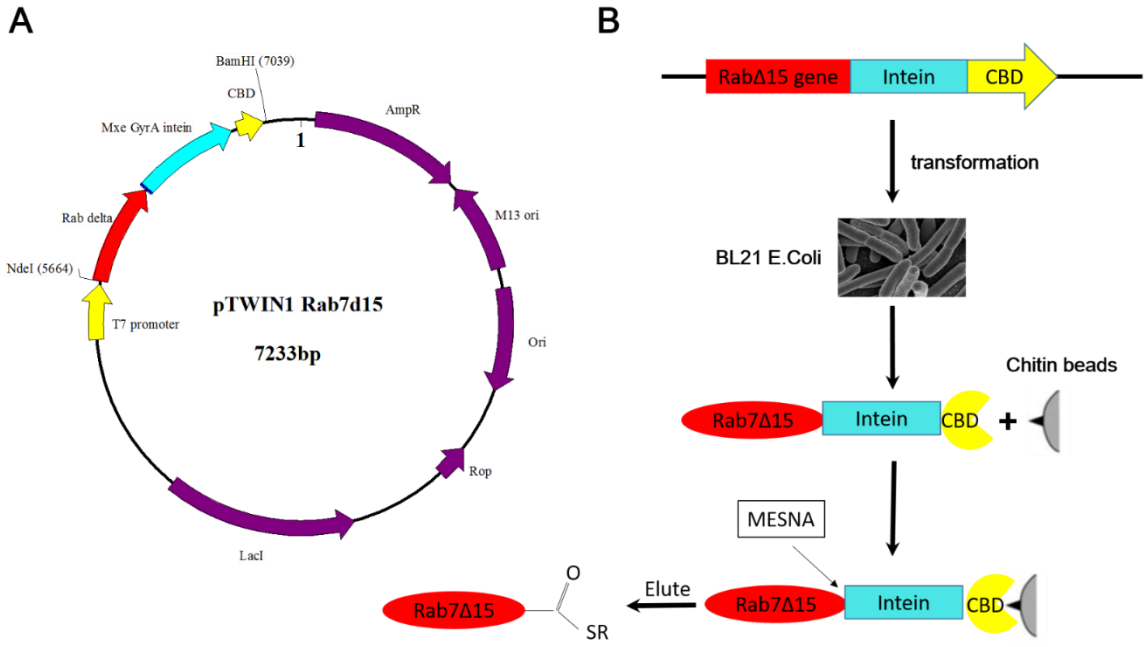

Figure 4-1-1. Production of Rab7 thioesters using IMPACT™ system.

(A) The construct map of Rab7d15-intein fusion gene. (B) The route of Rab7d15-thioester production.

MESNA: Sodium 2-mercaptoethanesulfonate; CBD: chitin binding domain.

Figure 4-1-2 shows a chemical PEG linker (PEG1) that containing a ketone group

for oxime ligation and two prenylatable cysteines. The PEG-1 linker contains two cysteines protected with StBu groups, which can be removed by the treatment with reducing reagents after protein ligation. The final product Rab7-PEG-1 was obtained after incubation of PEG1-linker with Rab7Δ15-ONH2 on ice overnight. We confirmed the reaction results by SDS-PAGE and ESI-MASS data (Figure 4-1-2 and table 4-1-1).

Furthermore, we asked whether the prenylation reaction is affected by a single cysteine containing at the Rab C-terminal end. We designed and synthesized a chemical linker PEG-2 that contains a $(PEG)_8$ linker with a ketone group for protein ligation and only one prenylatable thiol linked by disulfide bond, which can be readily cleaved by using 5 mM DTE during protein ligation. With the similar chemical reaction processes like Rab7-PEG-CC, we got the Rab7-PEG-SH and monitored by LC-MS (Figure 4-1-2 C and D).

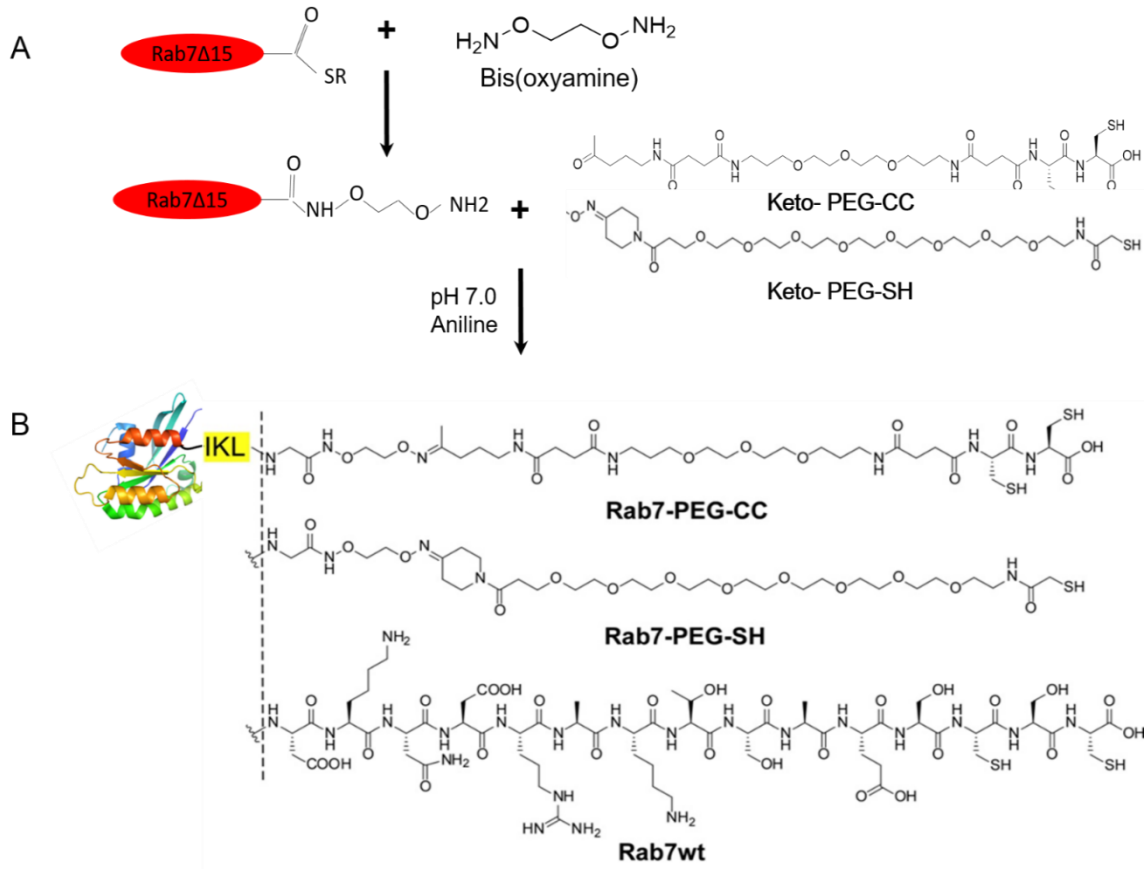

Figure 4-1-2. Routines of Rab7-PEG-CC and Rab7-PEG-SH production.
(A) Production of the Rab7d15-ONH2. (B) Production of Rab7-PEG-CC and Rab7-PEG-SH which are different with wild type Rab7 at the C-terminal end.

We have known the C-terminal hypervariable domain (HVD) of about 40 amino acids shows high level of sequence divergence among Rab family members. To

investigate the role of HVD, a long PEGylated chemical linker PEG-3 was synthesized (by Yi Long) to replace the whole HVD of 34 amino acids in Rab7 (Figure 4-1-3A). As the CIM motif is necessary for the Rab:REP interaction, it was kept in the linker. Figure 4-1-3B shows the Rab7 C-terminal sequence that was replaced by the PEG3 fragment. The CIM (IKL) was replaced by VKL.

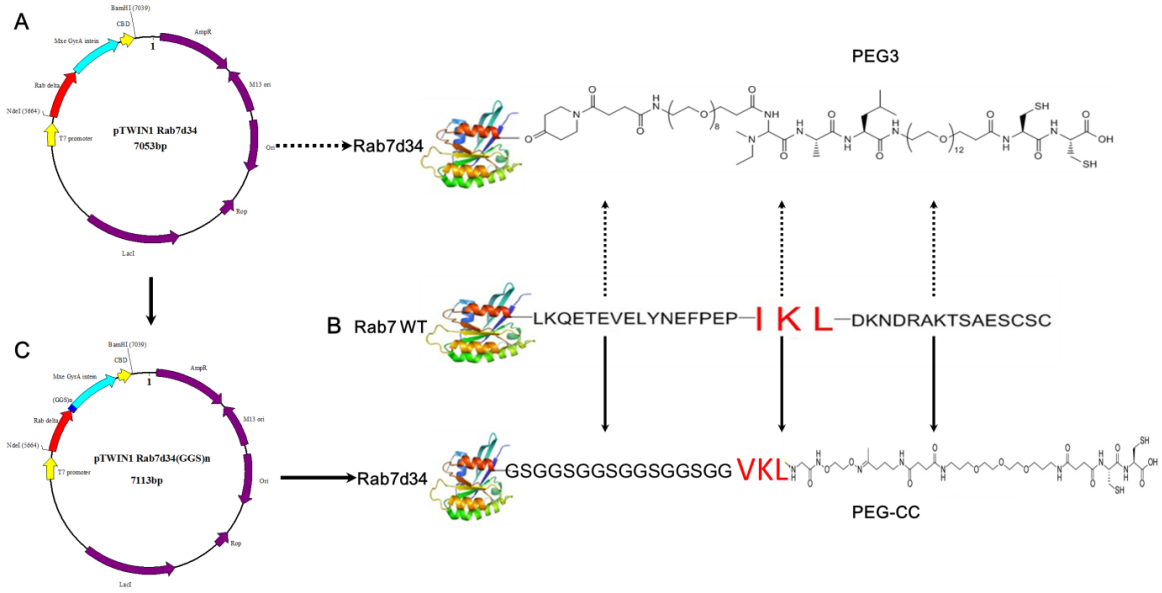

Figure 4-1-3. The replacement strategy of the Rab7 HVD sequence.

(A)The construct without the HVD of Rab7d34 and it is ligated with PEG3 linker. (B) A modified strategy to get the Rab7-(GGS)n-PEG-CC. The amino acid sequence before the CIM domain is replaced by GGS repeats.

However, the oxime ligation between Rab7Δ34-ONH_2 and PEG3 cannot be achieved based on the establishment ligation conditions. We then sought to use a non-specific sequence linker GGS repeats ($(GGS)_n$) (Pedersen, et al., 1998) to replace the C-terminal hypervariable region before the CIM. As shown in Figure 4-1-3C, a $(GGS)_n$-VKL-PEG1-CC was used to replace the C-terminal 34 amino acids of Rab7. The successful semisynthesis of the protein conjugate Rab7Δ34-(GGS)n-VKL-PEG1-CC is indicated by LC-MS and SDS-PAGE.

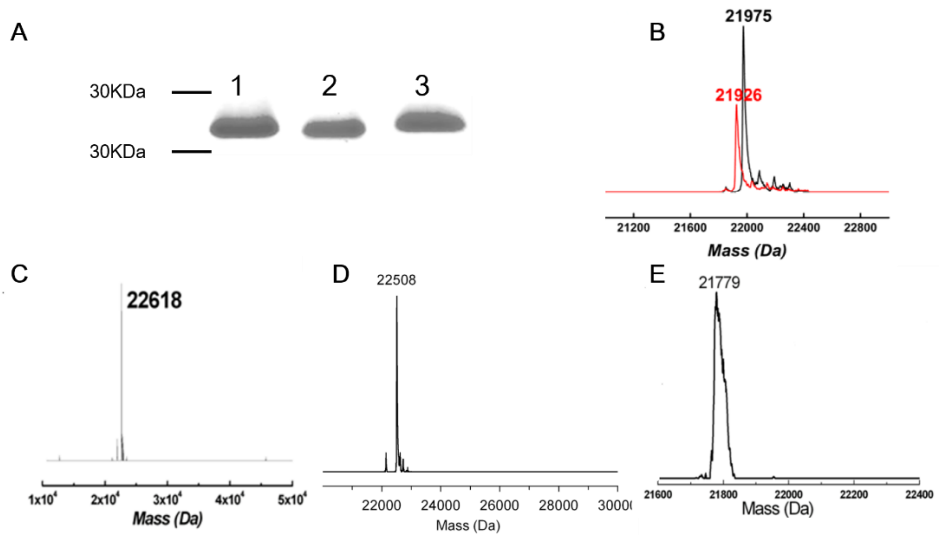

Figure 4-1-4. The modifications of Ra7Δ15-PEG-CC. (A) SDS-PAGE analysis of Rab7Δ15- thioester (lane 1), Rab7Δ15-ONH2 (lane 2) and Rab7-PEG-CC (lane 3). (B) ESI-MS spectra of Rab7Δ15-thioester (red) and its reaction product with bis(oxyamine), Rab7Δ15-ONH2 (black). (C) ESI-MS spectrum of the oxime ligation product Rab7Δ15-PEG-CC(M_{cal} = 22613 Da). (D) ESI-MS spectrum of the oxime ligation product Rab7Δ15-PEG-SH (*M*cal=22504Da). (E) ESI-MS spectrum of the oxime ligation product Rab7Δ15-(GGS)n-PEG-CC(Mcal=21772Da).(These data from Long Yi).

4.1.2 PEGylated Rab proteins undergo prenylation in vitro

Based on EPL method, we have successfully got the PEGylated Rab proteins including Rab7-PEG-CC, Rab7-PEG-SH and Rab7-$(GGS)_n$-PEG-CC. These PEGylated Rab7 proteins were firstly tested by prenylation assay using NBD-FPP. NBD-FPP is a fluorescent analog of the lipid substrate GGPP, with an NBD group coupling to a C-15 farnesyl moiety, mimicking the length of a C-20 native lipid substrate (Wu et al., 2006). As shown in Figure4-1-4, Rab7-PEG-CC displays nearly identical prenylation efficiency to that of the wild type Rab7 protein. The prenylation kinetics at room temperature further supported that Rab7-PEG-CC can be prenylated as efficient as that of wide-type Rab7. Next, we further examined whether intact cysteine residues are indispensable for prenylation. Interestingly, Rab7-PEG-SH undergoes prenylation with an observed rate that is ca. 2-fold higher than that of wild-type protein (Figure 4-1-5B). These findings indicate that Rabs do not require specific sequences in the HVD for prenylation, except for the CIM and an SH group as an isoprenyl acceptor. Rab7Δ34-GGS-PEG-CC displayed a little faster prenylation efficiency than that of the wild type Rab7. To confirm the native posttranslational modification, prenylation of PEGylated Rab7 proteins were performed using GGPP as the substrate. Prenylation of Rab7-PEG-CC using GGPP also

led to the doubly geranylgeranylated protein as shown by ESI-MS. The thiol group in Rab7-PEG-SH can be prenylated as efficient as cysteines at the Rab C-terminus, indicating flexibility within RabGGTase prenylation machinery. Prenylation of Rab7Δ34-$(GGS)_n$-VKL-PEG1-CC using GGPP led to the double-geranylgeranylated protein as indicated by ESI-MS result (Figure 4.14C,D and E). These results demonstrate that the whole HVD of the Rab, except for the CIM, does not encode the prenylation specificity. The amino acids downstream of the CIM can be replaced by a nonpeptidic PEG linker containing cysteines or thiol groups without perturbing Rab prenylation in vitro.

In vitro prenylation analysis of the PEGylated Rab proteins probes provides insights into the mechanism of Rab protein prenylation. This study together with previous reports suggests that the specificity of the Rab prenylation machinery is conferred by three binding interfaces, involving the GTPase domain, the CIM, REP, and RabGGTase (Pylypenko et al., 2003; Pak et al., 2004). The HVD of Rabs, with the exception of the CIM, does not contribute specificity to the assembly of the ternary protein complex. Once the ternary protein complex is established, the Rab C terminus is concentrated within the microenvironment of the complex, thus enhancing the probability of C-terminal cysteines reaching the active site of RabGGTase. As a consequence, the protein substrate specificity of RabGGTase does not need to be encoded in the Rab C terminus, in contrast to that of CaaX protein prenyltransferases.

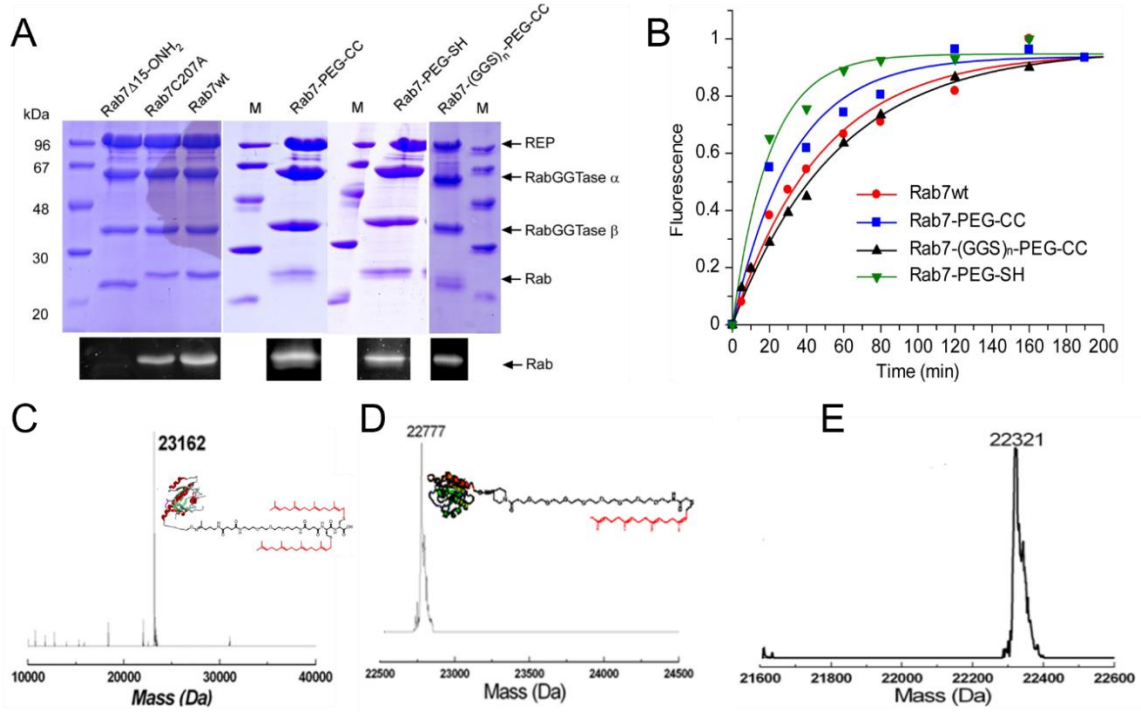

Figure 4-1-5. *In vitro* prenylation of PEGylated Rab proteins.

(A) Incorporation of fluorescent isoprenoid (NBD-farnesyl) into Rab7 protein and conjugates. The reaction mixtures were resolved by SDS-PAGE (upper panel: coomassie blue staining; lower panel: fluorescent laser scan of NBD). (B) Reaction kinetics of prenylation from the SDS/PAGE assay using the fluorescent analog of GGPP, NBD-FPP. The solid lines show single exponential fits for Rab7 wild type (kobs = 0.021/min), Rab7-PEG-CC (kobs = 0.031/min), Rab7-(GGS)n-PEG-CC (kobs = 0.018/min), and Rab7-PEG-SH (kobs = 0.050/min).(C) ESI-MS spectra of the Rab7-PEG-CC after prenylation with GGPP (M_{cal} = 22780 Da). (D) ESI-MS spectra of the Rab7-PEG-SH after prenylation with GGPP (M_{cal}=22780 Da). (E) ESI-MS spectra of the Rab7-$(GGS)_n$-PEG-CC after prenylation with GGPP(M_{cal}=22316). Reaction condition: 6 µM PEGylated Rab7, 10 µM REP, and 6 µM RabGGTase were mixed with 100 µM GGPP in prenylation buffer and incubated for 1 h at 37 °C.

The model is consistent with the fact that RabGGTase has essentially no sequence preference for the context of the prenylatable cysteines, and the C-terminal sequences occurring in Rab GTPases include CC, CXC, CCX, CCXX, CCXXX, and CXXX. Hence, any cysteine- or thiol-containing fragment that can be properly presented to the active site of RabGGTase is able to undergo prenylation. This property allows RabGGTase to process all members of the family of more than 60 Rab proteins with hypervariable C-terminal sequences, a feature that is uncommon in protein-modifying enzymes. This unique property of the Rab prenylation machinery also enables it to process Rab proteins with unnatural C-terminal moieties.

4.1.3 GFP-tagged PEGlytated Rab proteins for studying membrane targeting

4.1.3.1 Preparation of PEGylated Rab Proteins

To gain insights into the role of the Rab C terminus in membrane targeting, we use GFP (green fluorescent protein) tag as a fluorescent indicator, which does not interfere with Rab localization and function (Ali et al., 2004). We cloned the truncated Rab1, Rab5, Rab7 genes into the modified pTWIN-eGFP vectors with 10xHis tag at the C-terminal of sequence. The fusion proteins were purified by Ni-NTA chromatography. We prepared PEGylated EGFP-Rab1, EGFPRab5, EGFP-Rab7, and EGFP-Rab35 proteins by ligating Keto-PEG-CC to the truncated EGFP-Rab and EGFP-Rab-(GGS)n proteins, as done for the PEGylated Rab7 conjugates. All of semi-synthetic proteins were characterized by LC-MS spectra (Table 4-1), SDS-PAGE and in vitro prenylation assay.

Table 4-1. LCMS results of Rab protein probes used in this study. (Calculated mass)

Protein (P)	P-COSR	P-ONH2	P-PEG1	P-PEG1-CC	P-PEG1-C(GG)C(GG)	P-PEG2-SH	P-PEG2-S(GG)
Rab7Δ15	21974 (21972)	21926 (21922)	22792 (22789)	22617 (22613)	23162 (23157)	22508 (22500)	22777 (22772)
GFP-Rab1 Δ13	49732 (49752)	49683 (49702)	50553 (50569)	50378 (50381)	50923 (50937)	50271 (50280)	50540 (50538)
GFP-Rab5 Δ14	50001 (50019)	49954 (49969)	n.d	n.d	n.d	50545 (50547)	50814 (50809)
GFP-Rab5-Q79L-Δ14	49988 (49989)	49943 (49945)	50798 (50821)	50623 (50621)	51168 (51216)	50520 (50522)	50789 (50790)
GFP-Rab7 Δ15	50889 (50905)	50836 (50855)	51707 (51722)	51532 (51536)	52077 (52096)	51459 (51433)	51818 (51816)
GFP-Rab8 Δ13	49659 (49652)	49602 (49602)				50168 (50180)	50437 (50435)
GFP-Rab35 Δ11	50527 (50542)	50481 (50492)	51346 (51359)	51170 (51183)	51175 (51163)		
Rab7Δ34-(GGS)n-GG	21135 (21131)	21086 (21081)	21954 (21948)	21779 (21772)	22321 (22316)		
GFP-Rab1Δ31-GGS)n-GG	49122 (49134)	49078 (49084)	49938 (49951)	49775 (49975)	50320 (50319)		
GFP-Rab5Δ35-Q79L-(GGS)n-GG	49186 (49191)	49150 (49140)	50007 (50007)	49834 (49839)	50379 (50384)		
GFP-Rab7Δ34-(GGS)n-GG	49025 (49037)	48977 (48987)	49841 (49855)	49678 (49673)	50223 (50224)		

n.d stands for not done.

4.1.3.2 Prenylation of PEGylated GFP-Rab Proteins in vitro

These protein conjugates were subjected to in vitro prenylation. As shown in Figure 4-1-6,

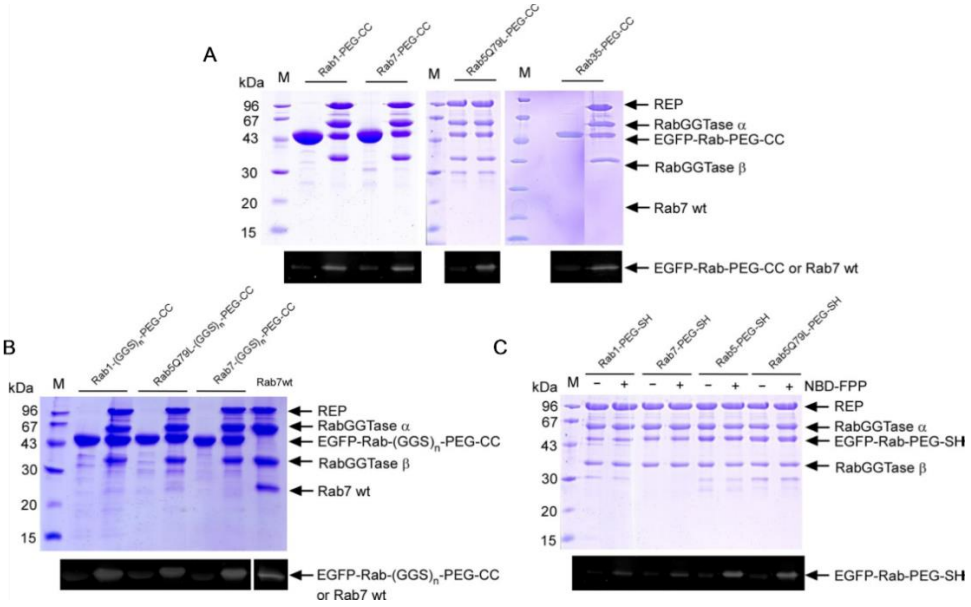

Figure 4-1-6. In vitro prenylation of PEGylated GFP-Rab proteins.

Prenylation reaction through incorporation of NBD-FPP to Rab proteins was resolved by SDS-PAGE (upper: Coomassie blue staining; lower: fluorescent scan for NBD fluorescence). M, molecular marker. (A) Prenylation of GFP-Rab-PEG-CC proteins. Left lanes of Rab1, Rab7 and Rab35 indicate EGFP-Rab-PEG-CC proteins alone as negative controls, while the left lane of Rab5Q79L indicates a mixture of prenylation

enzymes with GFP-Rab5Q79L-PEG-CC in the absence of NBD-FPP. Right lanes indicate prenylation reaction. Wide type Rab7 was used as a positive control for prenylation reaction. (B) Prenylation of GFP-Rab-(GGS)n-PEGCC proteins. Left lanes of Rab1, Rab5Q79L and Rab7 indate GFP-Rab-(GGS)n-PEG-CC proteins alone as negative controls. Right lanes indication prenylation reaction. Wide type Rab7 was used as a positive control for prenylation reaction. (C) Prenylation of GFP-Rab- PEG-SH proteins in the presence of and the absence of lipid substrate NBD-FPP.

all PEGylated Rab proteins undergo prenylation in vitro. Furthermore, we also performed the prenylation with GGPP, the natural substrates of RabGGTase. The prenylation results were monitored by ESI-MS which is shown in Figure 4-1-7. These results imply that Rab probes were efficiently prenylated *in vitro*, and again indicate that the RabGGTase machinery is indeed very flexible for protein prenylation.

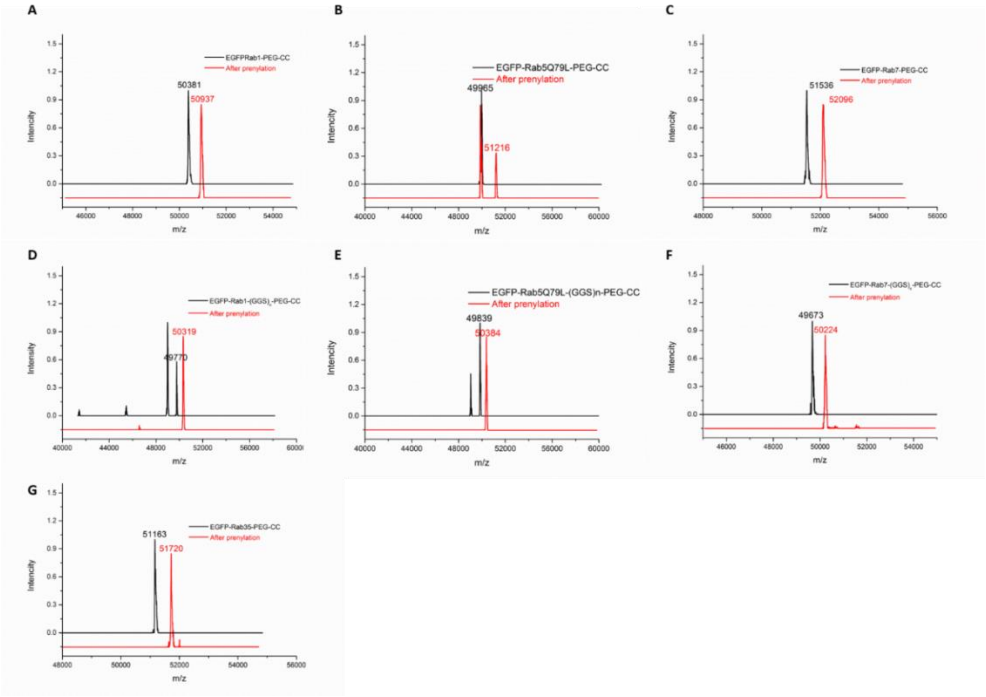

Figure 4-1-7. In vitro prenylation of PEGylated GFP-Rab proteins. ESI-MS spectra of the Rab1-PEG-CC (A), Rab5Q79L-PEG-CC (B), Rab7-PEG-CC (C), Rab1-(GGS)nPEG-CC (D), Rab5Q79L-(GGS)n-PEG-CC (E), Rab7-(GGS)nPEG-CC (F), and Rab35-PEG (G) before and after prenylation with GGPP. Reaction condition: 6 μM PEGylated Rab7, 10 μM REP, and 6 μM RabGGTase were mixed with 100 μM GGPP in prenylation buffer and incubated for 1 h at 37 °C.

4.1.3.3 The C-terminal sequence downstream from the CIM in HVD is not crucial for Rab 1/5/7 membrane targeting

I have summarized current models of membrane targeting in section 2.1.7. However, the function of HVD in membrane targeting is still not clear. Here, we use PEGylated Rab1, Rab5, Rab7, and Rab35 as probes to investigate this classical but still not yet resolved question.

Firstly, we microinjected the GFP-tagged PEGylated Rab proteins into cells without expressing respective mCherry-Rab wild types as a control. After one night incubation after microinjection, the localization of Rab protein conjugates was confirmed by confocal microscopy. We checked the membrane targeting of GFP-Rab1-PEG-CC, GFP-Rab5-Q79L-PEG-CC and GFP-Rab7-PEG-CC proteins. The results showed that the PEGylated Rab proteins with a dicysteine motif such as Rab1-PEG-CC, Rab7-PEG-CC and Rab35-PEG-CC localize to intracellular structures suggesting that PEGylated Rab proteins are prenylated in the cells (Figure 4-1-8).

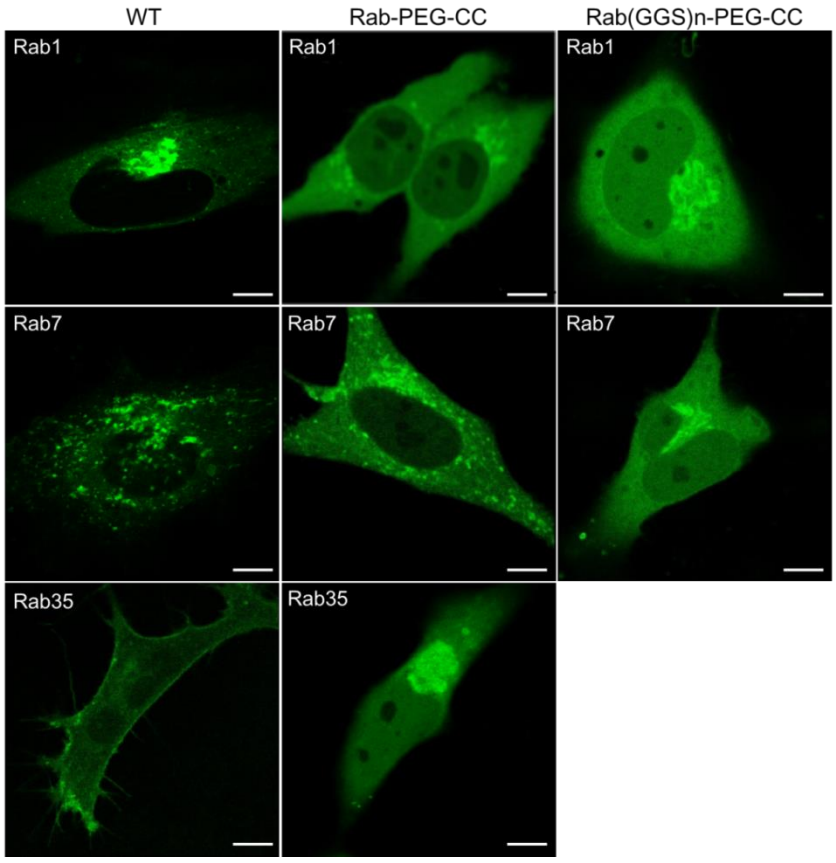

Figure 4-1-8. Subcellular localization of EGFP-Rab1, 7, 35-PEG-CC and EGFP-Rab-(GGS)n-PEG-CC proteins in non-transfected HeLa cells. Scale bar, 10 μm.

To investigate the localizations of these PEGylated Rab proteins in cells, we microinjected them into HeLa or MDCK cells expressing Cherry-Rab wild-type

proteins as a marker for their subcellular localizations. We foundthat both Rab1-PEG-CC and Rab7-PEG-CC colocalize with the wild-type Rab1 and Rab7 on the Golgi apparatus and late endosomes/lysosomes, respectively (Figure 4-1-9 A and C). To demonstrate that the PEGylated Rab proteins are functional, we prepared Rab5Q79L mutants that are deficient in GTPase activity and therefore are constitutively in the active GTP-bound state. Constitutively active Rab5 promotes the formation of enlarged endosomes, in line with its function in homotypic endosome fusion (Stenmark et al., 1994). Likewise, microinjection of Rab5Q79L-PEG-CC into the cell leads to the formation of enlarged vesicles (Figure 4-1-9 D).

Moreover, Rab5Q79L-PEG-CC colocalized with the Rab5Q79L mutant on the enlarged early endosomes when it was introduced into cells expressing Cherry-Rab5Q79L (Figure 4-1-9 B). These results suggest that PEGylated Rab1-PEG-CC, Rab5-PEG-CC and Rab7-PEG-CC proteins are correctly targeted and functional, indicating the downstream sequence behind of CIM in hypervariable domain is not essential for their membrane targeting and function, in these Rab proteins.

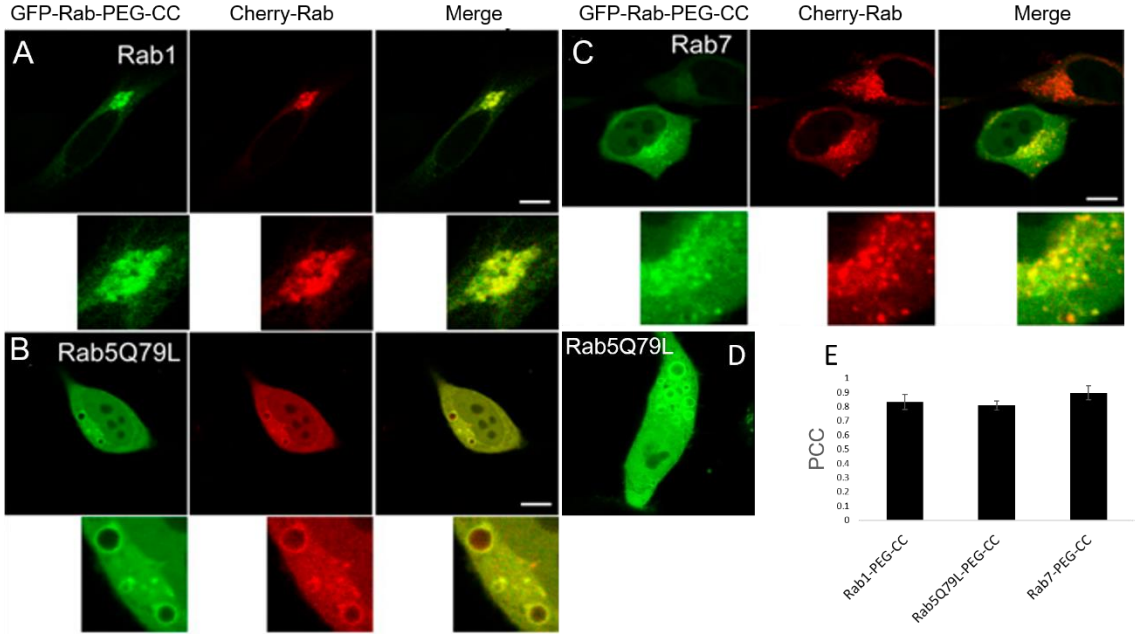

Figure 4-1-9. Subcellular localization of GFP-Rab-PEG-CC.

(A) GFP-Rab1-PEG-CCcolocalize with mCherry-Rab1 wild-type protein at the Golgi apparatus. (B) GFP-Rab5Q79L-PEG-CC colocalize with mCherry-Rab5Q79L on enlarged endosomes. (C) GFP-Rab7-PEG-CC colocalize with mCherry-Rab7 wild-type protein. (D) GFP-Rab5Q79L-PEG-CC induces formation of enlarged vesicles. (E) Pearson's colocalization coefficient (PCC) analysis of chimeric Rab proteins with wild-type Rab proteins. Scale bar, 10μm.

4.1.3.4 Membrane targeting of Rab GTPases is determined by the double cystein prenylation motif

Next, we further examined whether the prenylation of single cysteine residues are indispensable for membrane targeting. A set of GFP-Rab1-PEG-SH, GFP-Rab5-PEG-SH and GFP-Rab7-PEG-SH proteins was conjugated with two cysteines being replaced by a single thiol group was subjected to membrane targeting studies. Like Rab-7-PEG-SH, all the GFP-Rab-PEG-SH undergoes prenylationin vitro with the substrates NBD-FPP and GGPP, respectively (Figure 4-1-6 C and Table 4.1).

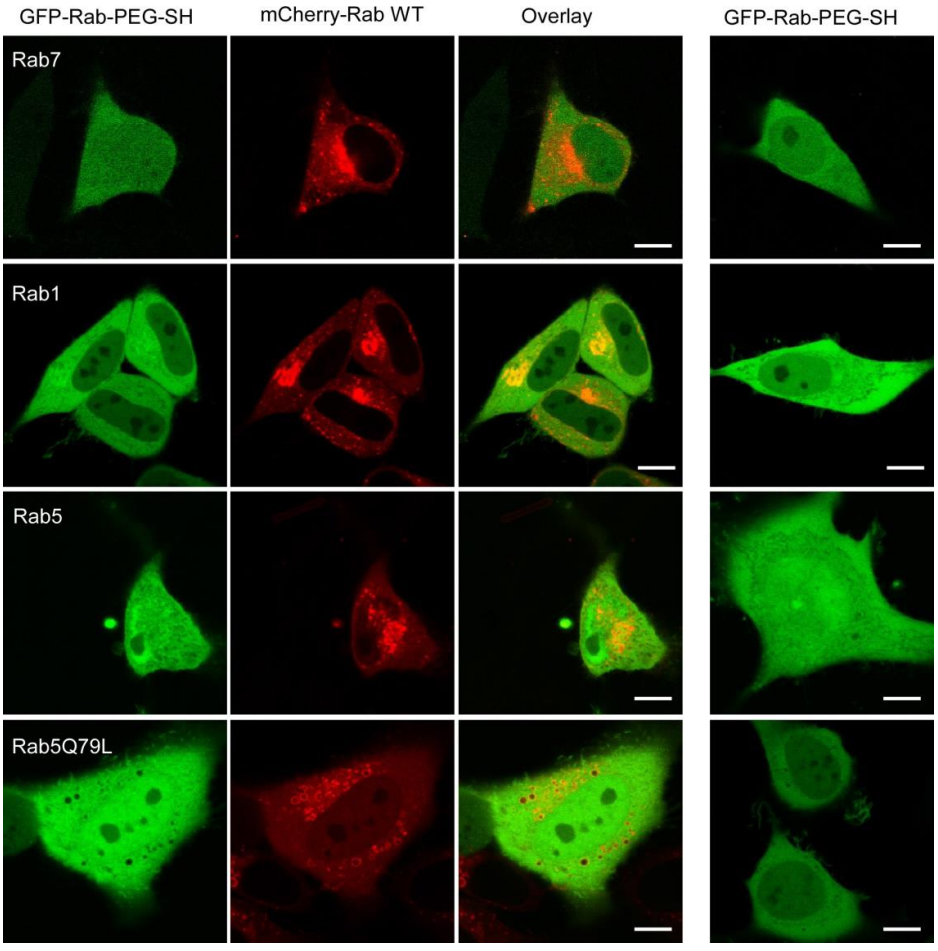

Figure 4-1-10. Subcellular localization of GFP-Rab-PEG-SH proteins in HeLa cells expressing mCherry-Rab wild type proteins (left panel) and in non-transfected HeLa cells (right panel). Scale bar, 10 μm.

GFP-Rab1-PEG-SH, GFP-Rab5-PEG-SH and GFP-Rab7-PEG-SH proteins were microinjected into HeLa cells with or without expressing respective mCherry-Rab wild type proteins. Interestingly, these Rab-PEG-SH proteins are largely cytosolic and not functional in the cell (Figure 4-1-10), although they can be prenylated in vitro as well as wide type Rab proteins (Figure 4-1-7C and Table 4.1). These results indicate that

digeranylgeranylation rather than the sequence of the prenylation motif is essential for the correct subcellular localization and function of Rab proteins, in keeping with a previous report on Rab5 membrane localization (Gomes et al., 2003). One exception that C-terminal prenylation is not required is Rab13, which associates with vesicles via protein-protein interactions in its GDP-bound form (Ioannou et al., 2016).

At the same time, we also constructed vectors which express single cysteine Rab-C protein via site mutation method. Rab-C is largely cytosolic, similar to that of Rab-PEG-SH proteins in cells, albeit Rab1-C still localizes on the Golgi body partially. These results indicate that the prenylation of single cysteine residue is not sufficient for correct membrane targeting in digeranylgeranylation Rabs which have double cysteines end such like -CC, -CXC, CCX, -CCXX, -CCXXX.

4.1.3.5 The localization of Rab-$(GGS)_n$-PEG-CC proteins in cells

Since the C-terminal sequence downstream from the CIM is not essential for membrane targeting of Rab1, 5, 7 proteins in cells, we asked if the amino acid sequence before CIM is crucial for membrane association. To answer this question, we microinjected the Rab-$(GGS)_n$-PEG-CC proteins into HeLa cells expressing mCherry-tagged wide-type Rab protein.

As depicted in Figure 4-1-11, both Rab1-$(GGS)_n$-PEG-CC and Rab5Q79L-$(GGS)_n$-PEG-CC colocalize with the wild-type Rab1 and Rab5Q79L on the Golgi apparatus and enlarged early endosomes, respectively. These results showed that the replacement of the whole HVD of Rab1 and Rab5 does not interfere with the correct membrane targeting and function of Rab proteins in cells. Together with the data shown in section 4.1.3.2, we can conclude that the HVDs of Rab1 and Rab5 are not essential for their membrane targeting and function.

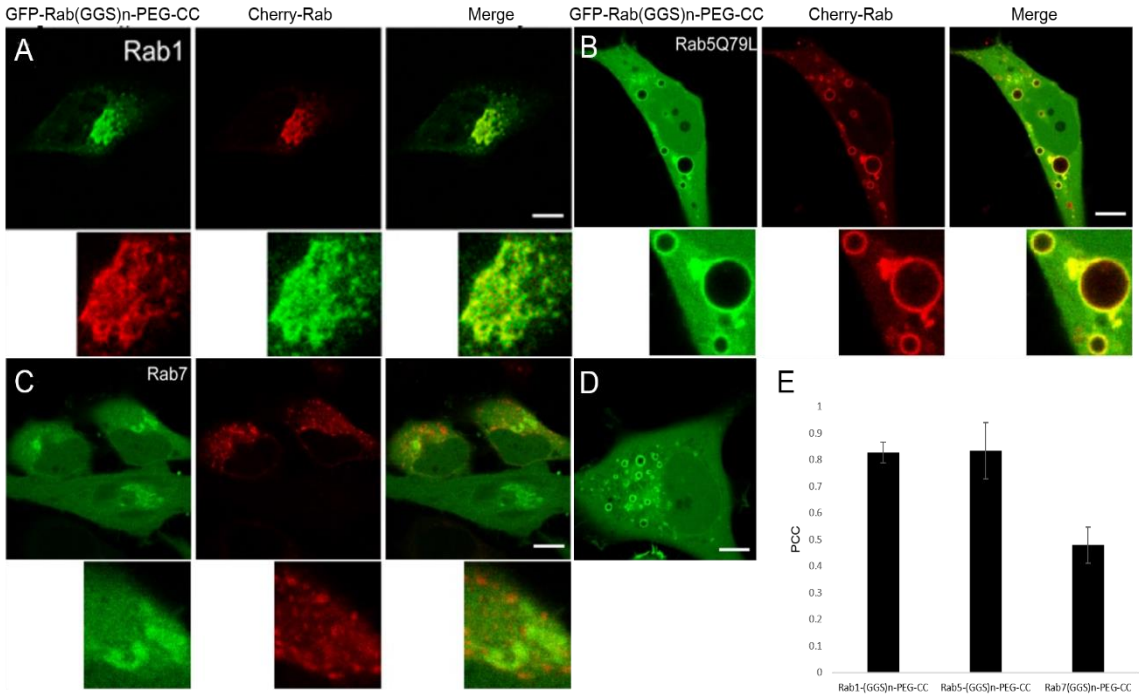

Figure 4-1-11. Subcellular localization of GFP-Rab-$(GGS)_n$-PEG-CC proteins in Hela cells.(A) GFP-Rab1-$(GGS)_n$-PEG-CC colocalize with mCherry-Rab1 wild-type protein at the Golgi apparatus.(B) GFP-Rab5Q79L-$(GGS)_n$-PEG-CC colocalize with mCherry-Rab5Q79L on enlarged endosomes.(C) GFP-Rab7-$(GGS)_n$-PEG-CC does not colocalize with mCherry-Rab7 wild-type protein.(D) single microinjection of GFP-Rab5Q79L-$(GGS)_n$-PEG-CC induce formation of enlarged vesicles.(E) Pearson's colocalization coefficient analysis of chimeric Rab proteins with wild-type Rab1,5,7 proteins, respectively. Scale bars, 10 μm.

To examine the effects of carboxyl methylation on Rab protein localization, two kinds of prenylation motifs, CXC and CC were included. After prenylation, Rab proteins with C-terminal CXC undergo carboxyl methylation by isoprenylcysteine carboxy-methyltransferase (Icmt) at the ER membrane, whereas those having CC and CCXX sequences in their C termini are not carboxymethylated (Bergo et al., 2001; Li and Stahl, 1993; Smeland et al., 1994). To further confirm our ideas, we generate a set of constructs to substitute the hypervariable domain of Rab1 and Rab5 with a $(GGS)_n$-VKL-$(GGS)_n$-CC fragment, Rab1Δ31-$(GGS)_n$-CC, Rab5Δ35-$(GGS)_n$-CC and Rab5Q79LΔ35-$(GGS)_n$-CC for functional study. Rab1Δ31-$(GGS)_n$-CSC, and Rab5Δ35-$(GGS)_n$-CSC and Rab5Q79LΔ35-$(GGS)_n$-CSC constructs were also designed and generated. In these chimeric proteins, only the CIM and the prenylation motif were retained while the rest of the HVD was replaced with flexible GGS repeats. Analogous scenarios were observed in the cells expressing Rab1 and Rab5 chimeric proteins, correct membrane localization and induction of the enlarged early endosomes by Rab5Q79LΔ35-CSC or Rab5Q79LΔ35-CC

(Figure 4-1-12).

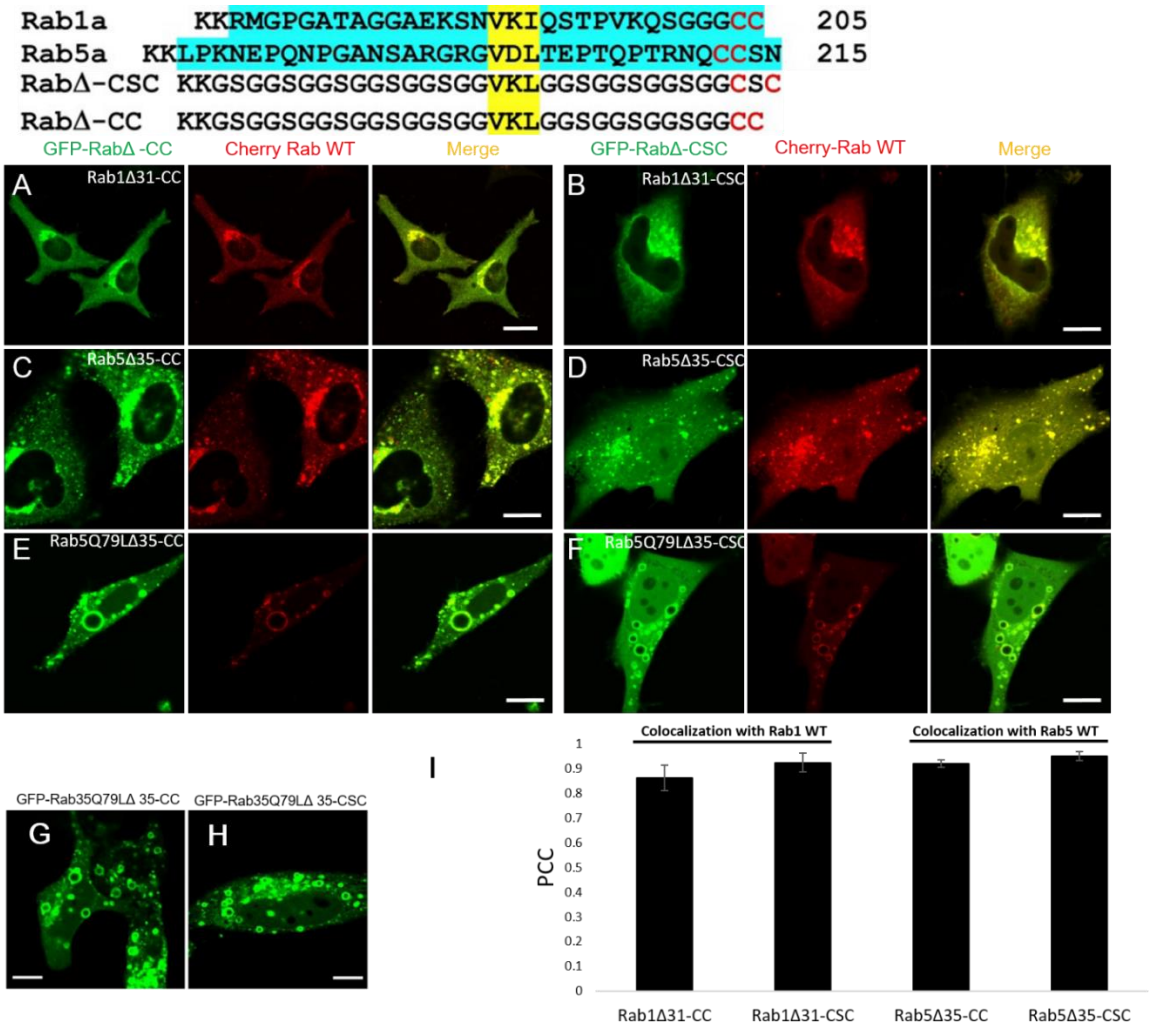

Figure 4-1-12. Subcellular localization of Rab proteins with C-terminal substitutesions. The HVD of Rab1, Rab5 is completely substituted with a $(GGS)_n$-VKL-$(GGS)_n$-CSC or $(GGS)_n$-VKL-$(GGS)_n$-CC fragment. The HVD is highlighted in cyan, the CIM motif is highlighted in yellow, and prenylatable cysteines are in red. (A, B) GFP-Rab1Δ31-CSC/CC proteins colocalize with mCherry-Rab1 wild type protein on the Golgi body. (C, D) GFPRab5Δ35- CSC/CC proteins colocalize with mCherry-Rab5 wild type protein on the early endosomes. (E, F) GFP-Rab5Q79LΔ35-CSC/CC proteins colocalize with mCherry-Rab5 on the enlarged endosomes. (G, H) Expression of EGFP-Rab5Q79Δ35-CSC/CC proteins induces formation of enlarged endosomes. (I) Pearson's colocalization coefficient analyses of the experiments were performed in (A-F). Measurements are performed in HeLa cells. Scale bar, 10 μm.

However, an interesting scenario is observed that the membrane localization of GFP-Rab7-$(GGS)_n$-PEG-CC with the substitution of the whole hypervariable domain is different from that of the wild-type Rab7 protein (Figure 4-1-13E). Furthermore, we found that Rab7-$(GGS)_n$-PEG-CC colocalizes with the Golgi marker, Giantin (Figure 4-1-

13F). In order to confirm these results, we also constructed the Rab7aΔ34-$(GGS)_n$-CSC and Rab7a34-$(GGS)_n$-CC conjugates to check their membrane targeting. Both Rab7aΔ34-$(GGS)_n$-CSC and Rab7a34-$(GGS)_n$-CC proteins do not localize to late endosome and lysosome but mistargeting to the Golgi apparatus, similar to Rab7-$(GGS)_n$-PEG-CC proteins.

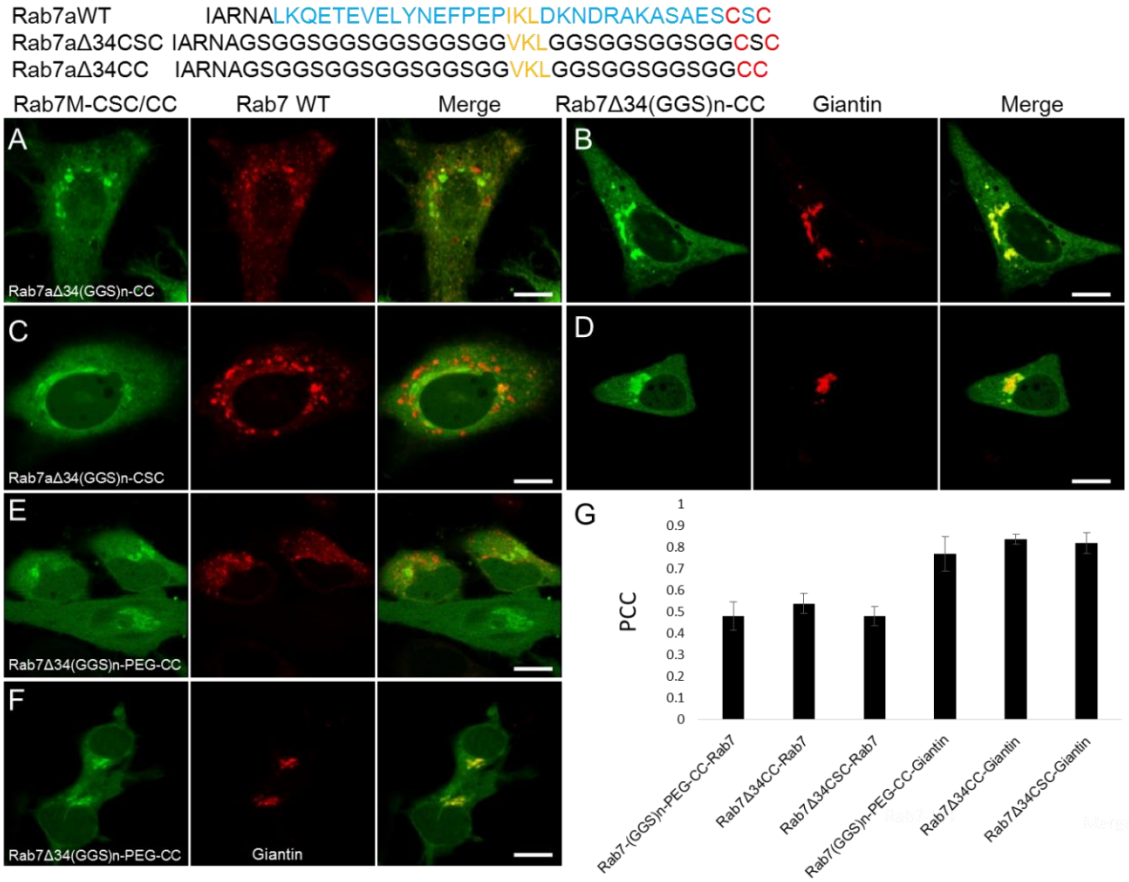

Figure 4-1-13. Subcellular localization of Rab proteins with C-terminal substitutesions and PEGylated Rab. The HVD of Rab7 is completely substituted with a $(GGS)_n$-VKL-$(GGS)_n$-CSC or $(GGS)_n$-VKL-$(GGS)_n$-CC fragment. The HVD is highlighted in cyan, the CIM motif is highlighted in orange, and prenylatable cysteines are in red. (A, C) GFP-Rab7Δ34-CSC/CC proteins are not colocalize with mCherry-Rab7 wild type protein on the late endosomes and lysosomes. (B, D) GFPRab7Δ35- CSC/CC proteins colocalize with Giantin on the Golgi body. (E, F) GFP-Rab7-$(GGS)_n$-PEG-CC does not colocalize with mCherry-Rab7 wild-type protein (E) but colocalizes with mKate2-Giantin at the Golgi apparatus (F). (G) Pearson's colocalization coefficient analysis of the experiments performed in (A-F). Measurements are performed in HeLa cells. Scale bar, 10 μm.

To confirm whether the localization of Rab7-$(GGS)_n$-PEG-CC and Rab7Δ34-$(GGS)_n$-CSC on the Golgi body, the cells were treated with 20μM nocodazole for 1hour. The nocodazole disrupts the microtubule network, leading to the formation of

Golgi fragments that are distributed throughout the cell (Lippincott-Schwartz, 1998). With the treatment of nocodaole, Rab7-$(GGS)_n$-PEG-CC was found to colocalize extensively with Giantin on the Golgi fragments (Figure 4-1-14). These results indicate that the HVD of Rab7 upstream from the CIM is essential for membrane targeting, and mutation in this region leads to the mistargeting to the Golgi apparatus.

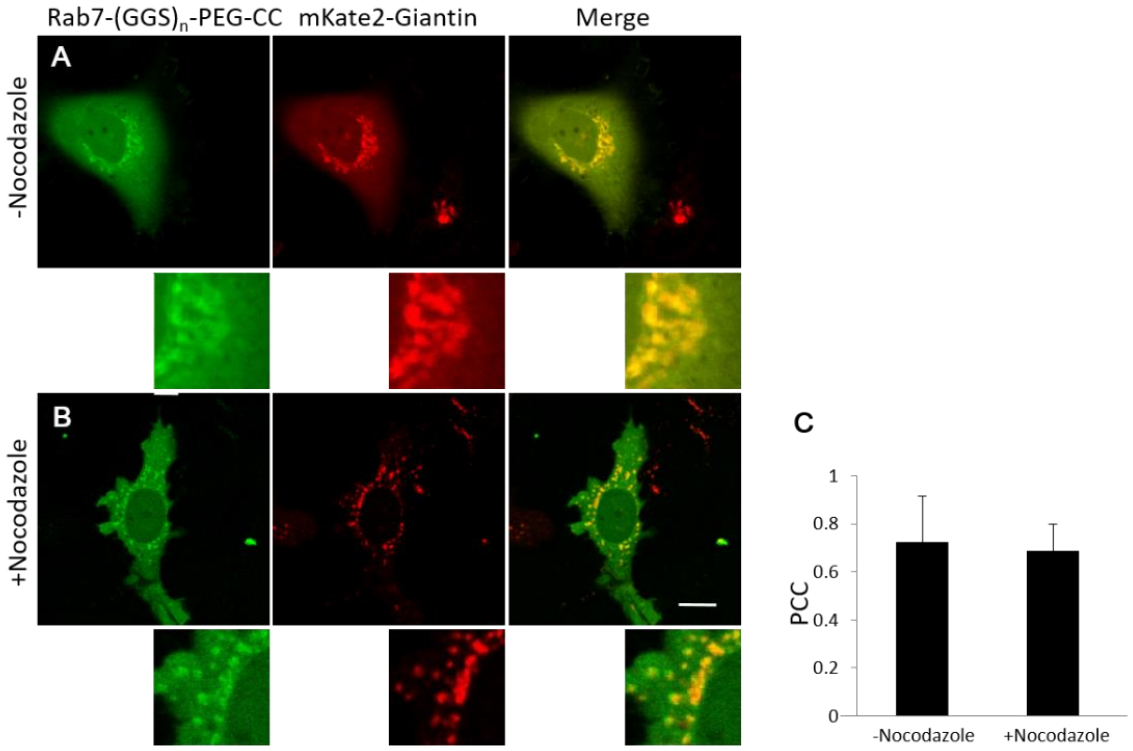

Figure 4-1-14. Localization of EGFP-Rab7-$(GGS)_n$-PEG at the Golgi apparatus. (A) EGFP-Rab7-$(GGS)_n$-PEG colocalize with mKate2-Giantin on the Golgi body. (B) EGFP-Rab7-$(GGS)_n$-PEG distributes on the disturbed Golgi structures in the presence of 20μM Nocodazole, (C) Pearsons colocalization coefficient analysis of the experiments performed in (A) and (B), respectively. Scale bar, 10 μm.

4.1.4 Mechanism of Rab protein membrane targeting

4.1.4.1 Binding to RILP is essential for Rab7 membrane targeting

We sought to find out what kind of factor plays a role in Rab7 membrane targeting to the late endosome and lysosome. To map the region that is essential for Rab7 targeting, we substituted the Rab7 HVD partially or completely with $(GGS)_n$-VKL-$(GGS)_n$-CSC or $(GGS)_n$-VKL-$(GGS)_n$-CC fragments and generate EGFP-Rab7Δ24-$(GGS)_n$-CSC/CC, EGFP-Rab7Δ27-$(GGS)_n$-CSC/CC and EGFP-Rab7Δ34-$(GGS)_n$-CSC/CC constructs. The chimeric Rab7 proteins were expressed in HeLa cells, and their subcellular localization

was examined. Rab7Δ24-CSC colocalizes with the wild-type protein Rab7, whereas partial colocalization and no significant colocalization but rather mislocalization to the Golgi apparatus were observed in Rab7Δ27-CSC and Rab7Δ34-CSC/CC proteins, respectively (Figure 4-1-15).

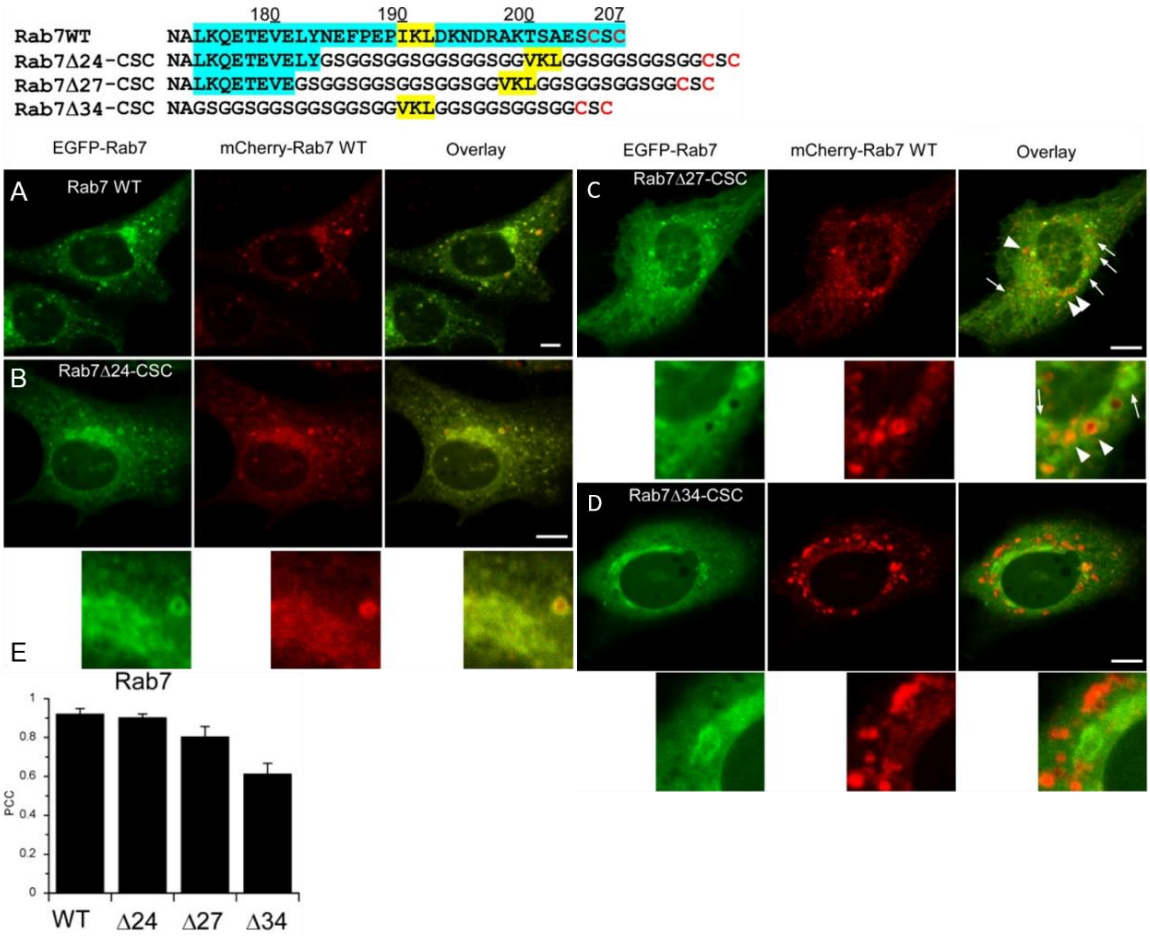

Figure 4-1-15. Colocalization of EGFP-Rab7Δ-CSC and wild type Cherry-Rab7 proteins. The HVD of Rab7 is partly or completely substituted. The HVD is highlighted in cyan, the CIM is highlighted in yellow, and prenylatable cysteines are in red. EGFPRab7 wild-type protein and EGFP-Rab7Δ-CSC proteins are co-expressed with mCherry-Rab7 (A–D) in HeLa cells. The arrowheads indicate Rab7 vesicles that do not contain Rab7Δ27-CSC, whereas the arrows indicate Rab7Δ27-CSC vesicles that do not contain Rab7. (E) Pearson's correlation coefficients (PCC) for colocalization with Rab7. Scale bars, 10 μm.

Above results suggest that residues (174–183) of the HVD are involved in Rab7 membrane targeting. These residues are known to be involved in binding to the Rab7 effector, Rab-interacting lysosomal protein (RILP). In particular, V180, L182, and Y183 are involved in hydrophobic interactions with RILP (Wu et al., 2005). Since we have known Rab7 interact with RILP via the upstream of CIM in HVD region, the colocalization of Cherry-RILP protein with Rab7, Rab7Δ24-$(GGS)_n$-CSC/CC,

Rab7Δ27-$(GGS)_n$-CSC/CC and Rab7Δ34-$(GGS)_n$-CSC/CC proteins were checked, respectively. Colocalization of RILP with Rab7 wild-type, Rab7Δ24-CSC, Rab7Δ27-CSC, and Rab7Δ34-CSC/CC proteins at the clustered late endosomes/lysosomes decreases sequentially (Figure 4-1-16).

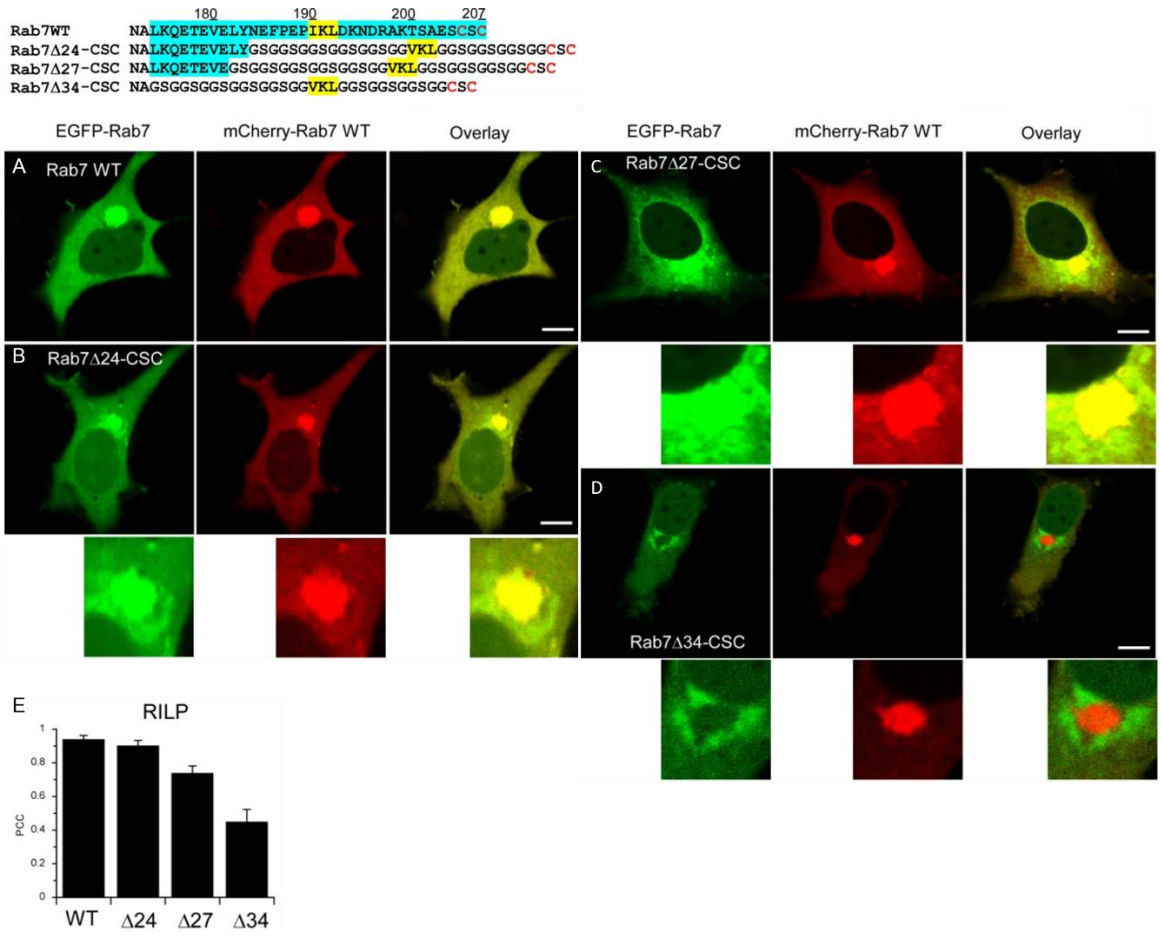

Figure 4-1-16.Colocalization of EGFP-Rab7Δ-CSC and mCherry-RILP proteins. The HVD of Rab7 is partly or completely substituted. The HVD is highlighted in cyan, the CIM is highlighted in yellow, and prenylatable cysteines are in red. EGFP-Rab7 wild-type protein and EGFP-Rab7Δ-CSC proteins are coexpressed with mCherry-RILP (A–D) in HeLa cells. (Scale bars: 10 μm.) Pearson's correlation coefficients (PCC) analysis for colocalization with RILP performed in experiment (E). Scale bars, 10 μm.

Next, we confirm the interaction between Rab7 and RILP in vitro. Firstly, we constructed pGATEV-GST-$RILP_{241-320}$ plasmid and purified GST tagged truncated $RILP_{241-320}$ protein. On the other hand, we also got purified MBP-Rab7 full length, MBP-Rab7Δ24, MBP-Rab7Δ27 and MBP-Rab7Δ34 protein. The assay of interaction between Rab7 proteins and RILP was performed with ITC. Unfortunately, the aggregation of coil-coiled $RILP_{241-320}$ during titration deteriorates the read-out. We then used pull down assay. RILP proteins were loaded on affinity matrix (Amylose Resin) to pull down Rab7

proteins from cell lysate. A HA-tag was conjugated with Rab7aQ67L Rab7aΔ24Q67L, Rab7aΔ27Q67L and Rab7aΔ34Q67L, respectively. At the same time, MBP protein was used as a negative control. The results showed that binding of Rab7 full-length, Rab7Δ24-CSC, Rab7Δ27-CSC, and Rab7Δ34-CSC to RILP declines sequentially (Figure 4-1-17), in line with the colocalization results of Rab7 with RILP in cells (Figure 4-1-16).

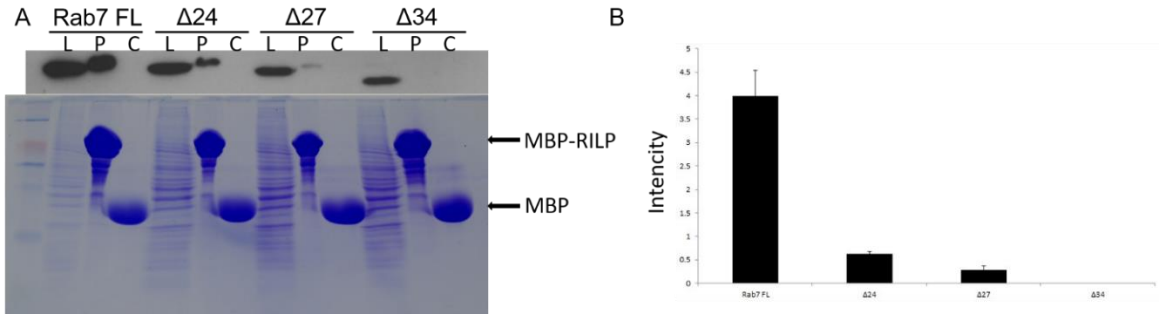

Figure 4-1-17. RILP pull down HA-Rab7. (A) Binding of Rab7Δ-CSC proteins with RILP. HeLa cells were transfected with full-length and truncated (C-terminally replaced) HARab7Q67L (constitutively active) proteins. Proteins were pulled down from cell lysate with MBP-RILP or MBP (control)-coated beads. Beads were subjected to SDS/PAGE and Western blotting with anti-HA antibody (Upper).The protein level of cell lysate, MBP-RILP and MBP on the beads was examined by Coomassie blue staining (Lower). C, control; L, cell lysate; P, pull down.(B) Quantitation of Rab7 proteins bound to RILP as shown in B. Measurements were performed in triplicate.

To exclude the possibility of C terminal truncation might affect the nucleotide exchange, we examined the GTP/GDP ratio of Rab7 and Rab7Q67L (GTPase deficient) proteins in HeLa cells. We checked nucleotides status and found that the truncated Rab7 chimera proteins undergo normal nucleotide exchange in the cell (Figure 4-1-18). Taken together, these results indicate that residues of Rab7 HVD, particularly amino acids 174–183, which are indispensable for the Rab7–RILP interaction, are also essential for correct targeting. Therefore, the interaction with RILP appears to be essential for Rab7 membrane targeting. Indeed, colocalization of RILP with Rab7 wild-type, Rab7Δ24- CSC, Rab7Δ27-CSC, and Rab7Δ34-CSC/CC proteins in the clustered late endosomes/lysosomes decreases sequentially (Figure. 4.1.15A-E), in line with the Rab7WT colocalization and the RILP pull-down results (Figure. 4-1-17B). These results also explained the idea that HVD may be involved in membrane targeting for Rab7 (Chavrier et al., 1991; Ali et al., 2004).

To further investigate the role of RILP in Rab7 membrane targeting, we knocked

down RILP in HeLa cells by siRNA. As negative control, a stable cell line expressing of scrambled shRNA was used. The level of RILP knock-down was determined by western blot using anti-RILP antibody. We got very nice knock down (KD) effect in cells (Figure 4-1-19H).

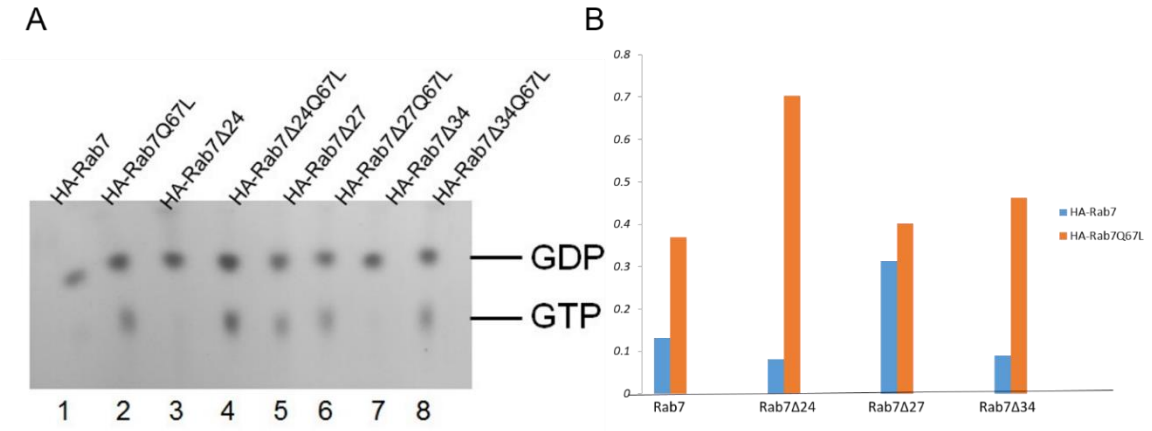

Figure 4-1-18. GTP: GDP ratio of Rab7 and mutants in cells. (A) Hela cells were transfected with HA-Rab7 wild type (Lane1), HA-Rab7Δ24-CSC (Lane3), HA-Rab7Δ27-CSC (Lane5), HA-Rab7Δ34-CSC (Lane7), and the corresponding GTPase-deficient Q67L mutants (Lane 2, 4, 6, 8). The bound nucleotides were determined by thin-layer chromatography (TLC). (B) Quantification of GTP/GDP ratio shown in (A).

We microinjected GFP-Rab7-PEG-CC and GFP-Rab7-$(GGS)_n$-PEG-CC proteins into both scrambled cells and RILP KD cells. After about 24 hours, these cells were fixed and performed immunofluorescence experiment to confirm the endogenous RILP knock down. As shown in the Figure 4-1-19, Rab7 wild type and Rab7-PEG-CC are largely cytosolic in RILP knock-down cells. The subcellular localization of these proteins is normal in scrambled cells (Figure 4-1-19 A, B, and C). In contrast, Rab7-$(GGS)_n$-PEG-CC and Rab7Δ34- CSC lack of RILP binding mistargeted on the Golgi apparatus. The membrane localizations are not affected by RILP knock-down (Figure 4-1-19 C, G and F). These results demonstrate that RILP plays an essential role in Rab7 membrane targeting. We also checked the puncta which stand for the membrane-associated level of Rab7 at endosomes. Knockdown of RILP significantly reduces the membrane binding of Rab7 (Figure 4-1-19 D and I). Therefore, RILP appears to be a targeting factor for Rab7 and determines the steady-state distribution of Rab7 on subcellular compartments.

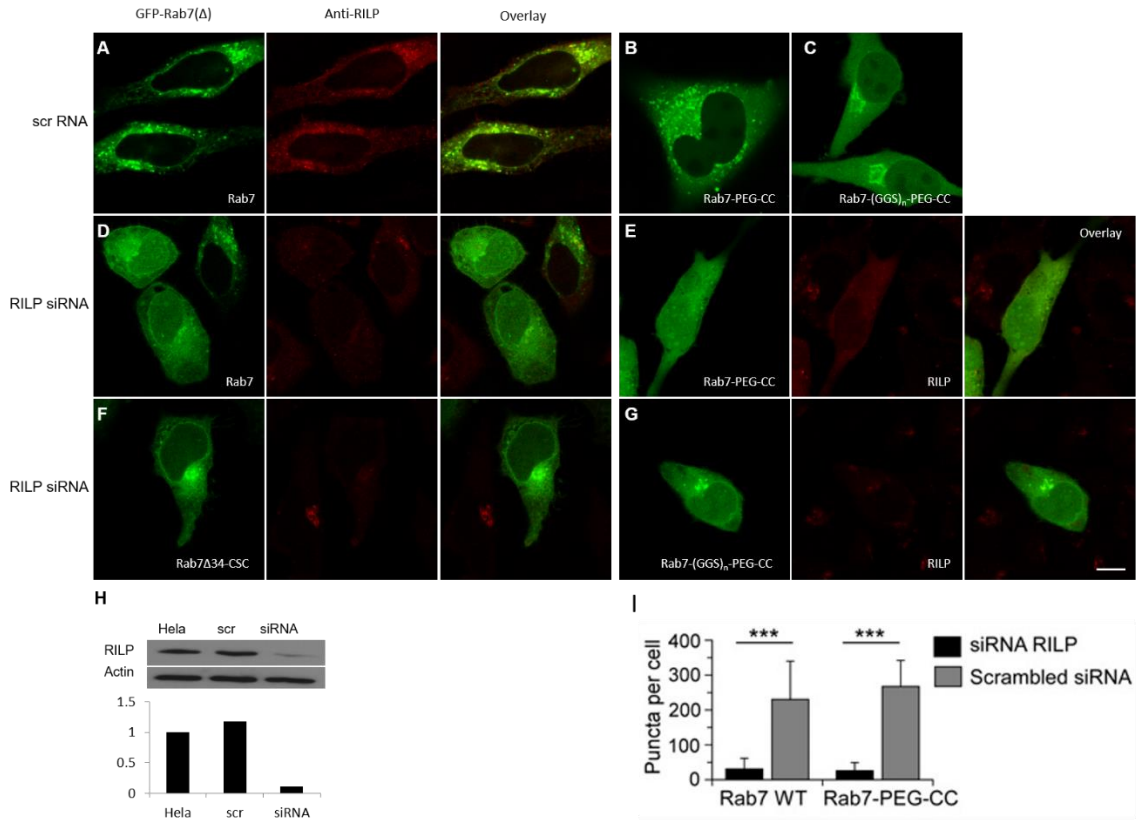

Figure 4-1-19. Effect of RILP RNAi on Rab7 localization. (A–C) Subcellular localization of EGFP-Rab7 WT (A), EGFP-Rab7-PEG-CC (B), and EGFP-Rab7-$(GGS)_n$-PEG-CC (C) in control siRNA cells. (D-G) Subcellular localization of EGFP-Rab7 WT (D), EGFP-Rab7-PEG-CC (E), EGFP-Rab7Δ34-CSC (F), and EGFP-Rab7-$(GGS)_n$-PEG-CC (G) in RILP siRNA cells. Endogens RILP was detected by immunofluorescence. (H) Knockdown of endogenous RILP in HeLa cells, detected by Western blot using anti-RILP antibody. Scrambled siRNA (scr) cells were used as a control. (I) Quantification of membrane localization of Rab7 WT and Rab7-PEG-CC in siRNA or control cells by counting Rab7-positive vesicles in the cell. ***P < 0.001. Scale bars, 10 μm.

4.1.4.2 The C-terminal polybasic cluster is important for Rab35 localization to the plasma membrane

For the Rab membrane targeting, a very distinct example is Rab35. Rab35 was initially called H-Ray and later Rab1C due to its high sequence similarity to Rab1A and Rab1B. However, although strong homology of Rab35 with Rab1A/B in the GTPase domain and switch regions, they clearly differ in the C terminal hypervariable domain. The distinct feature of Rab35 is its evolutionarily conserved polybasic C-terminal extremity. Interestingly, the plasma membrane localization of Rab35 is GTP-dependent and may involves this region through its direct binding to the PtdIns(4,5)P_2 and PtdIns(3,4,5)P_3 (Heo et al.,2006; Gavriljuk et al., 2013). To test whether down stream of CIM in HVD of

Rab35 is crucial for its membrane targeting, we generated Rab35-PEG-CC which C-terminal polybasic cluster substituted by the PEG linker.

GFP-Rab35-PEG-CC was microinjected into Hela cells with or without mCherry-Rab35 protein expression. The results showed that Rab35-PEG-CC does not localize on the plasma membrane (PM) but mislocalizes on the Golgi apparatus (Figure 4.1.19 A, B, C). Next, we examined the localization of Rab35 constructs with the HVD being replaced by $(GGS)_n$-VKL-$(GGS)_n$-CSC or $(GGS)_n$- VKL-$(GGS)_n$-CC fragment. Not surpringly, both proteins mistarget to the Golgi apparatus (Figure 4-1-20 D and E).

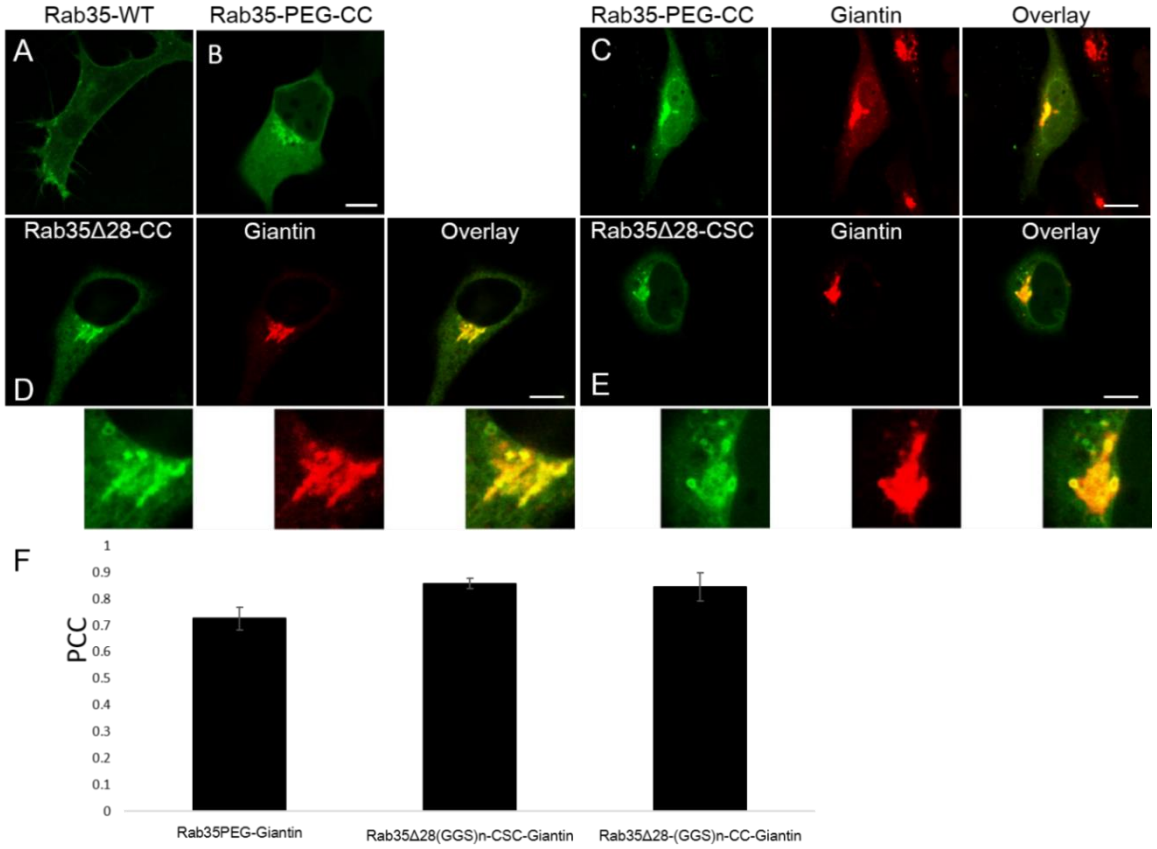

Figure 4-1-20. Subcellular localization of EGFP-Rab35-PEG-CC, Rab35-(GGS)n-CSC/CC. (A) The EGFP-Rab35 wild-type protein in Hela cells. (B) EGFP-Rab35-PEG-CC localizes in the perinuclear region but not the plasma membrane. (C) EGFP-Rab35-PEG-CC colocalizes with mKate2-Giantin at the Golgi apparatus. (D, E) EGFP-Rab35Δ28-CSC/CC proteins colocalize with mKate2-Giantin on the Golgi body. (F) Pearson's colocalization coefficient analysis of chimeric Rab proteins with Giantin. Scale bar, 10μm.

To confirm its Golgi localization, cells were also treated with 20μM nocodazole for 1.5 hours and Rab35-PEG-CC was found to colocalize extensively with Giantin on the fragmented Golgi structures in the nocodazole-treated cells (Figure 4-1-21B). These

results demonstrate that the polybasic region is essential for the PM targeting and/or PM membrane affinity, presumably because of interaction with negatively charged phosphatidylinositol phosphate lipids (Heo et al., 2006). It is not clear whether Rab35 initially targets to the Golgi apparatus and subsequently redistributes to the PM. This question will be addressed in section 4.2.

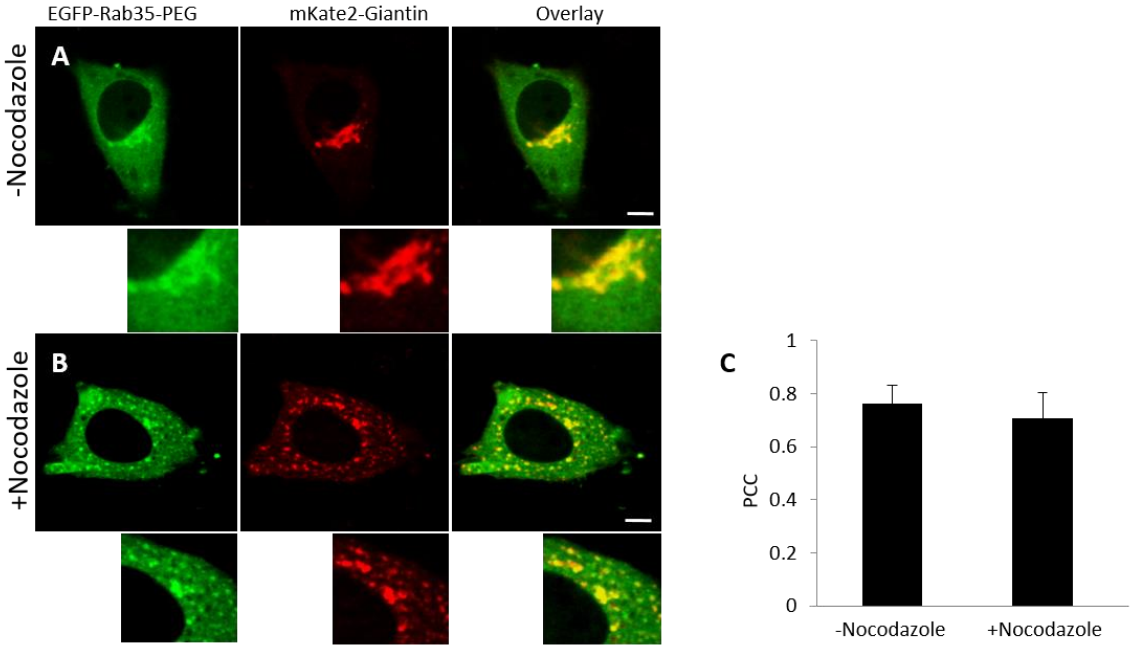

Figure 4-1-21. Localization of EGFP-Rab35-PEG-CC at the Golgi apparatus. (**A**) EGFP-Rab35-PEG-CC colocalize with mKate2-Giantin on the Golgi body. (**B**) With 20μM Nocodazole treatment, EGFP-Rab35-PEG-CC distributes on the disturbed Golgi structures. (**C**) Pearsons' colocalization coefficient analysis of the experiments performed in (**A**) and (**B**), respectively. Scale bar, 10 μm.

4.1.5 Conclusion and discussion

In the present study, we have combined synthetic chemistry, bioorthogonal chemistry, and protein engineering to introduce unnatural C-terminal fragments into Rab proteins. This method resolves inherent problems of the traditional HVD swapping approach in the analysis of Rab membrane targeting. Because the HVD may be only a partial determinant for membrane targeting in some Rabs, investigation of chimeric Rab proteins may lead to ambiguous results (Chavrier et al., 1991; Aivazian et al., 2006; Ali et al., 2004).

Analysis of subcellular localization and function of the PEGylated Rab proteins probes facilitates elucidation of Rab membrane targeting and the role of the hypervariable domain in this process. Our findings suggest that the HVDs of individual Rab proteins

play distinct roles in membrane targeting. In the case of Rab1 and Rab5, the HVD is not required for membrane targeting, probably because it is not involved in binding with potential targeting factors, including effectors and GEFs (Aivazian et al., 2006, Cai et al.,2008; Delprato and Lambright, 2007; Mishra et al., 2010). It serves rather as an anchoring chain that physically connects the functional GTPase domain with the membrane. The HVD can be substituted by a nonnative PEG linker of sufficient length. The digeranylgeranyl lipid anchor is important for membrane association, whereas the sequence of the prenylation motif is not essential for correct membrane targeting. However, natively monogeranylgeranylated Rabs (e.g., Rab8, Rab13, Rab18, Rab23, and Rab28) obviously do not require diprenylation for appropriate targeting to subcellular membranes. In contrast, some of the N-terminal residues of the Rab7 HVD are involved in binding with the Rab7 effector RILP, and the results presented here suggest that this interaction stabilizes Rab7 association with late endosomes/lysosomes. Because residues of the Rab7 HVD are one of the elements involved in the interaction with RILP (binding to the GTPase domain is also required), a Rab chimeric protein with the Rab7 HVD would bind to RILP less efficiently (Wu et al., 2005). In keeping with this result, replacing the hypervariable domain of Rab5 with that of Rab7 only led to partial is localization from early endosomes (Ali et al., 2004). Moreover, knockdown of RILP renders Rab7 largely cytosolic in cells. Therefore, RILP appears to be a targeting factor for Rab7 and determines the steady-state distribution of Rab7 on subcellular compartments. Evidence has been presented that the Rab9 effector TIP47 might interact with the Rab9 HVD, and this interaction has been implicated in Rab9 localization (Aivazian et al., 2006). The C-terminal polybasic cluster of Rab35 HVD appears to play a key role for PM targeting, probably due to the electrostatic interaction with negatively charged lipids on the PM. However, we cannot rule out the possibility that other unidentified.

Rab35 effectors that associate with the C terminus of Rab35 may play a role in enhancing its interaction with the PM. It is not clear how and why those Rabs lacking in affinity to effectors or lipids are mistargeted to the Golgi apparatus. There might be two hypotheses for the role of the Golgi membranes as the initial site for Rab attachment or as the default localization of mislocalized Rabs. In the former case, newly synthesized prenylated Rabs would be delivered to the Golgi membranes and be subsequently sorted

to the designated compartments. Loss of targeting elements would lead to accumulation of Rabs in the Golgi apparatus. In the latter case, Rabs would initially target to their subcellular compartments and be transported to the Golgi apparatus via GDI recycling and/or vesicular transport, because Rabs could not stably associate with their cognate membranes. However, the question then arises as to the origin of the specificity of Golgi localization. Further work is required to elaborate this question.

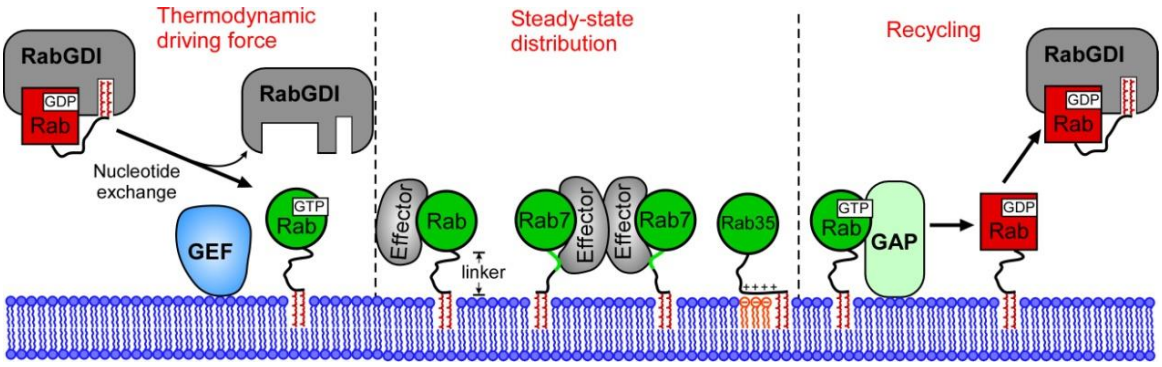

Figure 4-1-22. Model for Rab membrane targeting. Initial insertion of Rab proteins into membranes is driven by GEF-mediated nucleotide exchange. Binding of activated Rab proteins (GTP-bound) with effectors or other binding partners determines the steady-state distribution of Rab proteins on membranes. GAPs deactivate Rab proteins at specific sites and trigger the recycling of Rab proteins from membranes. The GTPase cycle controlled by GEFs and GAPs dictates the thermodynamic equilibrium of Rab membrane localization and defines the boundary of a Rab realm.

From the results presented here together with evidence from earlier studies, it appears that Rab membrane targeting is governed by complex mechanisms, with the involvement of Rab regulators and binding partners including GEFs, GAPs, and effectors. GEF-mediated nucleotide exchange provides the thermodynamic driving force for Rab membrane insertion, which is indispensable for the stable attachment of Rabs to membranes (Tarafder et al., 2011; Blümer, et al., 2013). GEFs and GAPs appear to regulate Rab localization, because the nucleotide-bound state defines Rab membrane association (Wu et al., 2010). Indeed, emerging evidence suggests that Rabs are relayed on the trafficking pathway through GEF and GAP cascades, which determine the boundary between Rab proteins (Kinchen and Ravichandran, 2010; Nordmann et al., 2010; Poteryaev et al., 2010; Rivera-Molina and Novick, 2009; Zhu et al.,2009). In such cascades, Rab A recruits the GEF that targets Rab B along the pathway to the membrane, and Rab A is subsequently inactivated by a GAP recruited through Rab B and as an effector of Rab B, hence, is detached from the membrane. As a consequence, conversion

of a Rab A to a Rab B membrane is achieved. Once Rab proteins are activated and stabilized on the membrane (GTP-bound), the steady-state Rab localization might be dictated by binding partners, including effectors and lipids (Figure 4-1-22).

Such a stabilization of Rabs on their cognate membranes by effectors appears to play an essential role in Rab membrane targeting, because depletion of effectors (RILP knockdown) or loss of binding to effectors (Rab HVD replacement) leads to mislocalization of Rab proteins. Some effectors associate with a specific membrane independently of Rabs (Houghton et al., 2009). For those effectors that are recruited to membranes in a Rab-dependent manner (Stenmark, 2009), there must be a synergy between Rabs and effectors in membrane localization. For example, Rabenosyn-5 has two distinct binding sites for Rab4 and Rab5, suggesting its coordinative role in Rab4 and Rab5 localization and function (Eathiraj et al., 2005). Based on the above observations, we propose a mechanistic model of the HVD roles for Rabs membrane targeting is shown as Figure 4-1-22.

4.2 Cycling of Rab35 between the Golgi apparatus and the plasma membrane

Correct intracelluar localization of Rab GTPases is essential for their functions in vesicular transport and signaling transduction. The mistargeting of Rabs may cause diseases, for example, when they are hijacked by pathogenic effectors. Rab35 plays various roles, including endosomal trafficking, exosome release, phagocytosis, cell migration, immunological synapse formation and neurite outgrowth (Klinkert and Echard, 2016). However, membrane targeting mechanism of Rab35 is still unclear.

In this study, we combine the biochemistry, microinjection, RNA interference, fluorescence recovery after photobleaching (FRAP), fluorescence localization after photobleaching (FLAP) and cell biological techniques to investigate the mechanism of Rab35 plasma membrane targeting. We reveal how GEF, effector and GDF of Rab35 work together to regulate the spatial cycling of Rab35. In addition, we show that the depletion of OCRL1 induces the disruption of the Rab35 plasma membrane localization, suggesting a link of Rab35 to the Lowe syndrome.

4.2.1 The polybasic region is essential for plasma membrane localization of Rab35

In section 4.1.2.2, we have shown that the polybasic cluster (PBC) is essential for the association of Rab35 with the plasma membrane, probably through binding to the negatively charged phosphoinositide PtdIns(4,5)P_2 and PtdIns(3,4,5)P_3 (Li et al., 2014; Heo et al., 2006).

To illuminate the function of the PBC, we sequentially mutate the positively charged amino acids (lysine and arginine) to glutamine (Q), leading to Rab35-PBC-1M to -5M constructs (Figure 4-2-1). We express these Rab35 mutant proteins in HeLa or Cos-7 cells and check their intracellular localization. Quantification of the enrichment of Rab35 wild type and its PBC mutants at the PM shows that with sequential increase in the number of mutation residues in the PBC region, Rab35 gradually reduces its PM-colocalization and mistargets to the perinuclear region (Figure 4-2-3A). The PM/cytosol ratio of PBC-2M drops down dramatically (Figure 4-2-3B). We, therefore, conclude that at least four

positively charged amino acids are required for the Rab35 PM localization. Additionally, although we speculate that the cluster of six glutamine residues (6Q) may affect the localization of Rab35, no obvious localization changes were found when they are substituted by $(GGS)_2$ repeat amino acids (Figure 4-2-1C, Rab35-6Q_M).

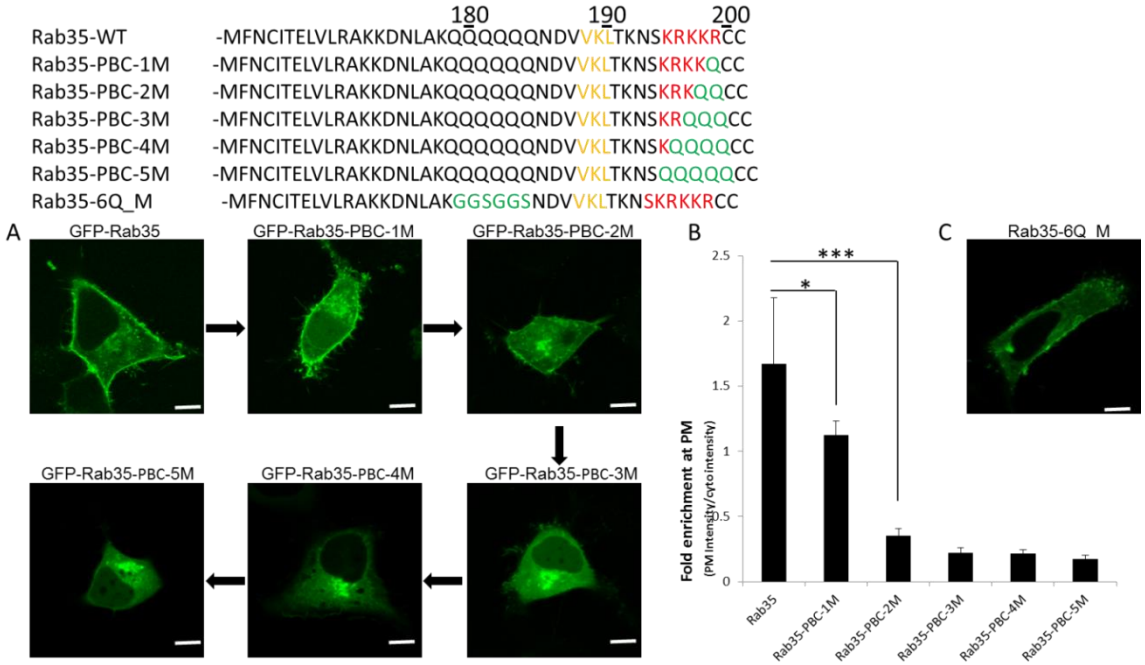

Figure 4-2-1. Subcellular localization of Rab35 and its PBC mutants. (A) The membrane targeting of Rab35 wild type, Rab35-PBC-1M, -2M,-3M,-4M and -5M. (B) The fold enrichment at PM of Rab35 wide type and its mutants. (C) The subcellular localization of Rab35-6Q_M. The polybasic region is highlighted in red, the CIM is highlighted in yellow, and the mutation sites are highlighted in green. *P < 0.05; ***P < 0.001. Scale bar, 10μm.

The association of Rab proteins with the membrane is generally mediated by hydrophobic interactions via the C-terminal geranylgeranyl moieties attached to one or two cysteines. To investigate the role of C-terminal prenylation motif in Rab35 localization, we generated Rab constructs with single C-terminal cystein including Rab1b-C, Rab5a-C, Rab5a-Q79L-C, Rab35-C and Rab35-5M-C (Figure 4-2-2). The results show that Rab1-C, Rab5-C and Rab5-Q79L-C are almost cytosolic or on ER rather than localized at their respective targeting membranes, in keeping with previous report (Gomes et al., 2003). However, natively monogeranylgeranylated Rabs (e.g., Rab8, Rab13, and Rab27) obviously do not require diprenylation for appropriate targeting to subcellular membranes. For these double cysteines Rab proteins, it is probably due to the weak binding force of a single geranylgeranyl with membrane, which is not sufficient to

ensure these Rab proteins' membrane localization. Surprisingly, considerable amount of Rab35-C molecules still localize at the plasma membrane, although some portion of Rab35-C protein is found in the cytosol. The Rab35-PBC-5M-C protein, by contrast, is largely cytosolic and loses its localization at perinuclear region.

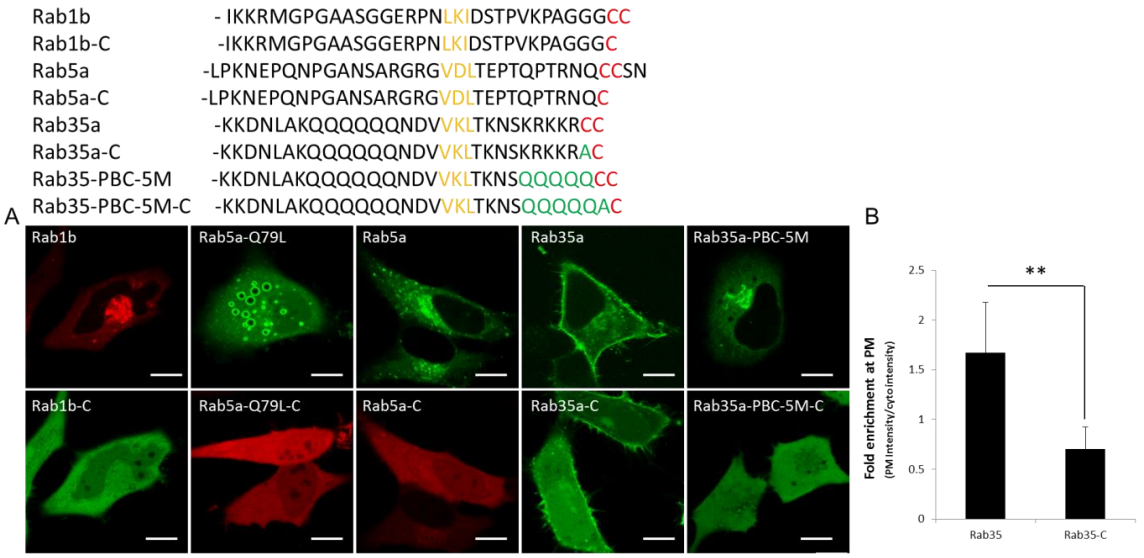

Figure 4-2-2. Subcellular localizations of Rab1b, 5a, 5aQ79L, 35a, 35a-PBC-5M wild type and Rab-C mutant. (A) The membrane localizations of Rab1b/-C, Rab5a/-C, Rab5aQ79L/-C, Rab35a/-C and Rab35a-PBC-5M/-C. (B) Quantification of GFP-Rab35a enrichment at the PM relative to cytosol GFP-Rab35 intensity under these conditions. The prenylated cysteine(s) is highlighted in *red*, the CIM is highlighted in *orange*, and the mutation sites are highlighted in *green*. **P < 0.01. Scale bar, 10μm.

These results indicate that the PBC of Rab35 is an essential element for PM localization. This cellular localization is not only limited in PM targeting. A very similar scenario is found in K-Ras4B protein, which also has a polybasic lysine-rich sequence at the C-terminus that leads to the PM enrichment (Hancock et al., 1990; Choy et al., 1999; Jang et al., 2015). Next, we investigate the membrane localization of the Rab35 PBC mutant proteins in cells. Rab35-PEG-CC, Rab35Δ28-$(GGS)_n$-CC and Rab35Δ28-$(GGS)_n$-CSC proteins have been shown to localize at the Golgi apparatus (Section 4.1.2.2). It seems that Rab35 mistargets to the Golgi when it is lack of the PBC domain. In contrast to the enrichment at the PM, the degrees of the localization at the Golgi apparatus of Rab35 PBC mutants increase gradually with the increase of PBC mutation number (Figure 4-2-3A). Therefore, Rab35 PBC domain is crucial for its proper membrane localization. Rab35 may cycle between the PM and the Golgi apparatus.

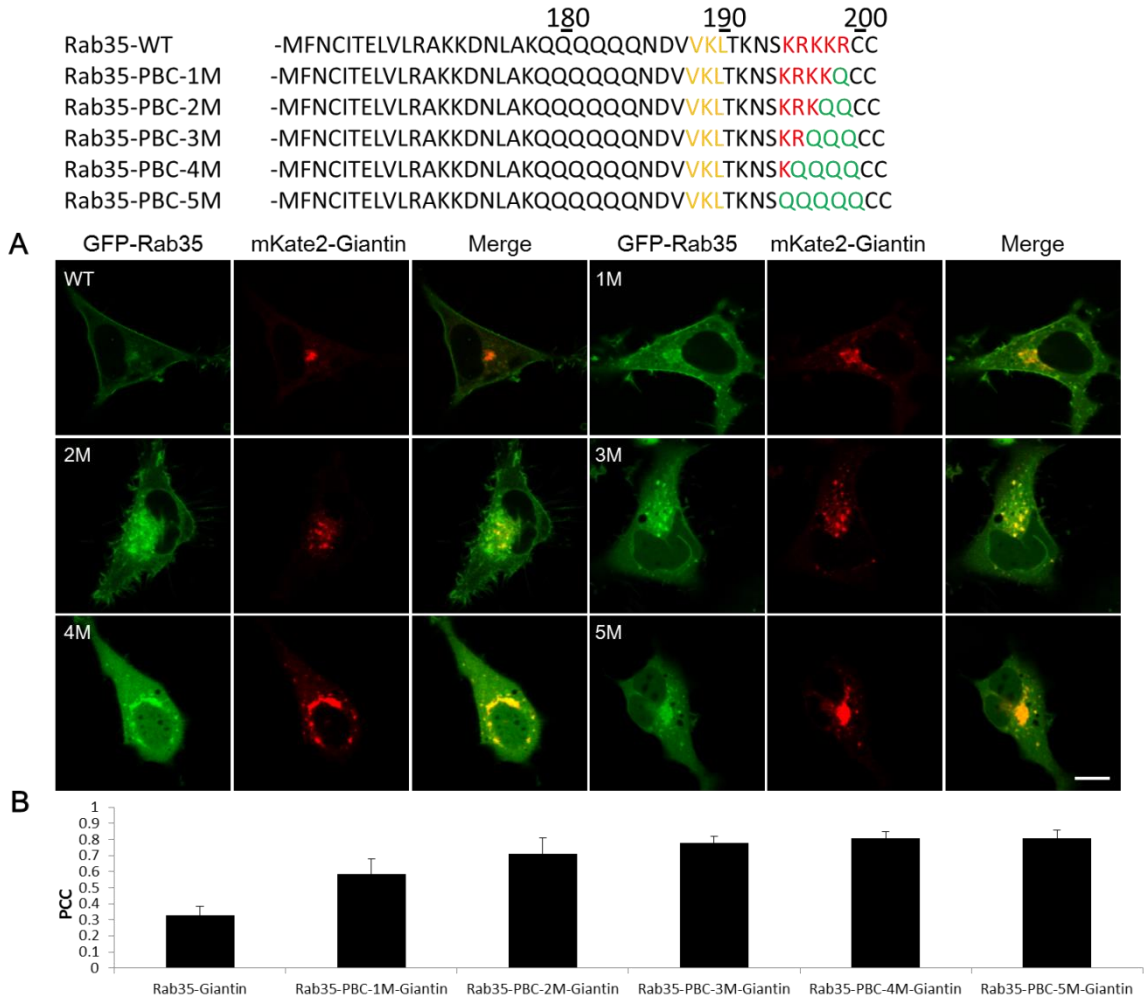

Figure 4-2-3. Subcellular localization of GFP-Rab35 wide type and PBC mutant proteins at the Golgi apparatus. (A) The membrane targeting of Rab35-WT,Rab35-PBC-1M, Rab35-PBC-2M, Rab35-PBC-3M, Rab35-PBC-4M and Rab35-PBC-5M, with more Rab35 PBC mutant mistargeting on Golgi apparatus. (B) Pearsons colocalization coefficient analysis of the experiments performed in (A). Scale bar, 10μm.

To confirm the Golgi localization of Rab35 PBC mutants, we treated the cells with 5μM nocodazole for 1 hour, and find that both Rab35-PBC-4M and Rab35-PBC-5M colocalize extensively with Giantin on the Golgi fragments (Figure 4-2-4).

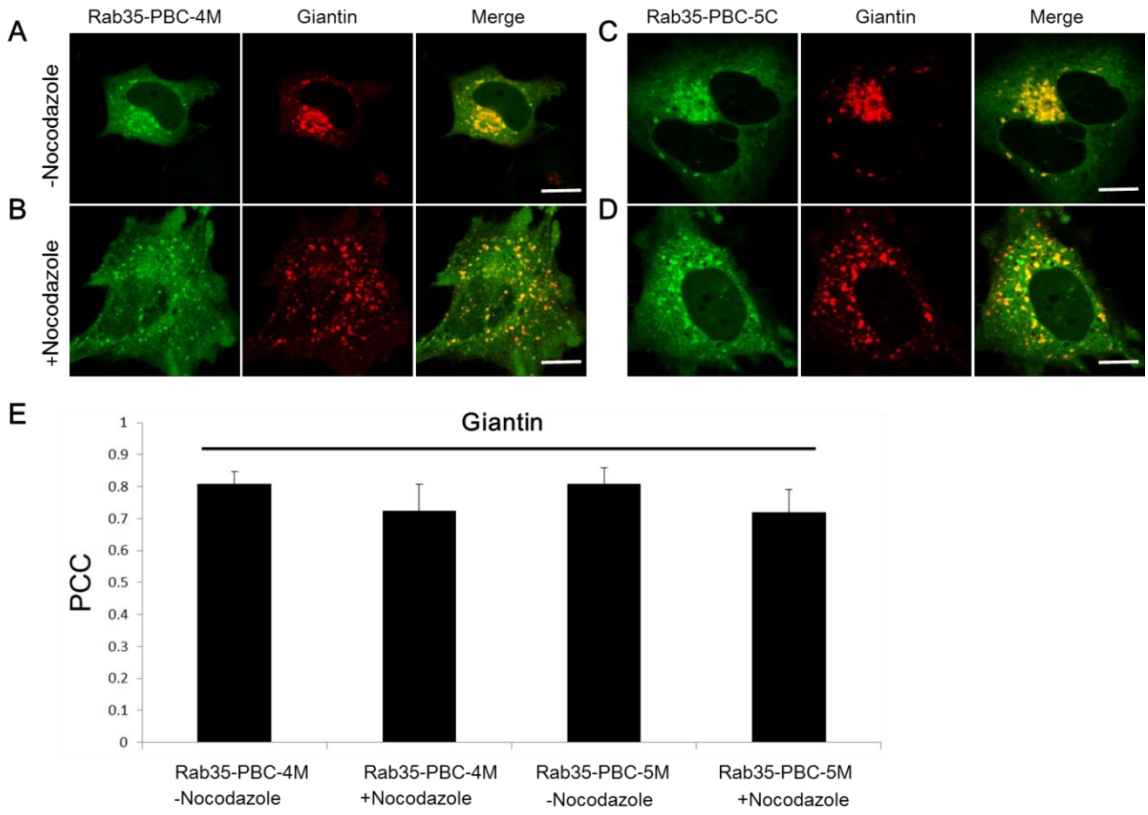

Figure 4-2-4. Colocalization of GFP-Rab35 PBC mutants with the Golgi marker Giantin in the presence of nocodazole. (A, B) GFP-Rab35-PBC-4M colocalizes with the Golgi marker Giantin with (B) or without nocodazole (A) treatment. (C, D) GFP-Rab35-PBC-5M colocalizes with the Golgi marker Giantin with (D) or without nocodazole (C) treatment. (E) Pearsons colocalization coefficient (PCC) analysis of the experiments performed in (A), (B), (C) and (D). Scale bar, 10μm.

4.2.2 Rab35 membrane targeting is not affected by Rab11

Previous studies have revealed that Rab35 is involved in fast recycling pathways, which send various receptors back to the PM from the cytosol or Golgi (Ilektra et al., 2006; Patino-Lopez et al, 2008; Barth and Julie, 2009). In addition, Rab11 is known to associate primarily with perinuclear recycling endosomes and regulates recycling of endocytosed cargos. The different localization profiles of Rab11 in diverse cell types have complicated the assessment of its precise function in intracellular membrane transport. In non-polarized cells Rab11 was found to be associated with both Golgi and recycling endosomes (Ullrich et al., 1996; Ren et al., 1998). In polarized and regulated secretory cells Rab11 localized to the Golgi as well as a variety of specialized membrane compartments (Urbe´et al., 1993; Deretic et al., 1996; Goldenring et al., 1996; Goldenring et al., 1997; Sheehan et al., 1996; Calhoun and Goldenring, 1997). More data have shown

that Rab11 regulates vesicular trafficking from the trans-Golgi network (TGN) and recycling endosomes to the plasma membrane (Chen et al., 1998; Prekeris, 2003; Takahashi et al., 2012; Andreas et al., 2010). To examine whether the trafficking of Rab35 is affected by Rab11 in recycling pathway, we examined the localization of Rab35 and Rab35-PBC-5M with the co-expression of Rab11 in HeLa cells, respectively. Figure 4-2-5 shows that Rab35 and PBC-5M mutant colocalize with Rab11 in the cells.

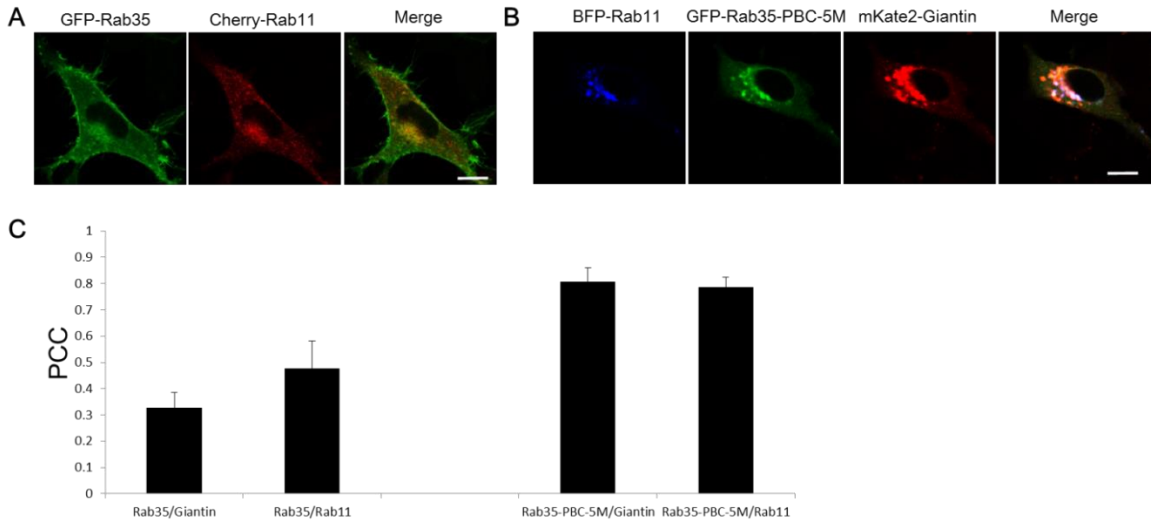

Figure 4-2-5. Colocalization of Rab35 wild type and its PBC mutant proteins with Giantin and Rab11. (A) Colocalization of Rab35 and Rab11 in Hela cells. (B) Colocalization of Rab11, Rab35-PBC-5M and Giantin. (C) Pearson's correlation coefficients (PCC) analysis of the experiments performed in experiments (A) and (B). Scale bar, 10μm.

Bastiaens and coworkers found Rab11 plays roles in trafficking of KRas-4B to the PM via the endocytic recycling (Malte et al., 2014). Interestingly, KRas-4B also contains a polybasic cluster at the C-terminal tail. We ask if the alterations of Rab11 function would perturb the membrane targeting of Rab35 in cells. The depletion of Rab11 was first performed by using RNA interference with Rab11 siRNA in HeLa cells. We examined the membrane association of Rab35 in Rab11 knock-down cells and found that the PM enrichment of Rab35 only slightly decreases compared to the control (Figure 4-2-6 B and A). In contrast to previous results that Rab11 regulates the localization of KRas-4B in cells (Figure 4-2-6G, Schmick et al., 2014), the PM targeting of Rab35 shows only a little change with the expression of Rab11, Rab11DN (the dominant negative form), or Rab11QL (dominant active form) conditions (Figure 4-2-6D, E, and F). These results indicate that Rab11-associated recycling endosomes are not involved in the recycling of

Rab35 to the PM in cells.

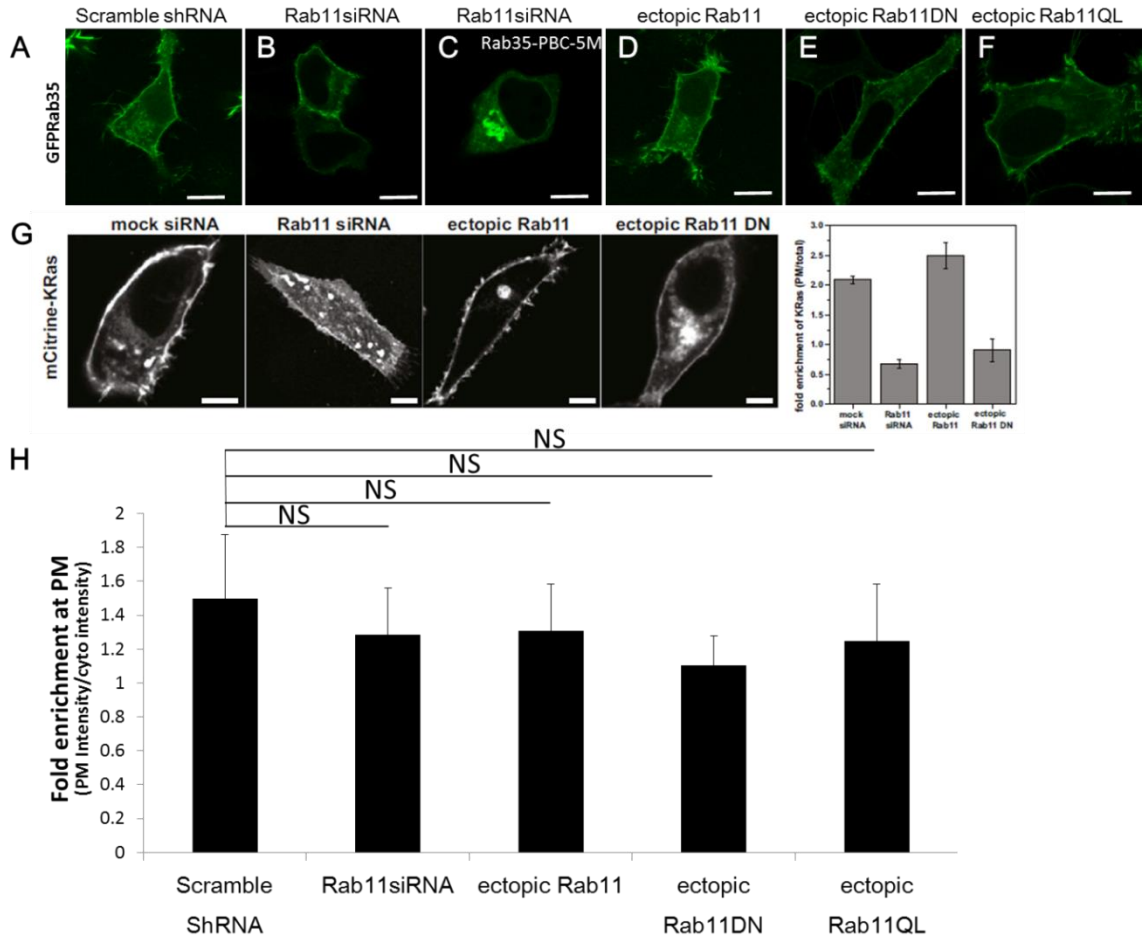

Figure 4-2-6. The effects of Rab11 knock down and mutations for the localization of Rab35. (A-F) The subcellular localization of GFP-Rab35 wide type (A) in the scrambled shRNA cells. The subcellular localization of GFP-Rab35 (B) and GFP-Rab35-PBC-5M (C) in Rab11 knock-down cells. The subcellular localization of GFP-Rab35 wide type in the co-expression of Rab11 wild type (D), Rab11DN (dominant negative, E) and Rab11QL (dominant active, F) cells. (G) The localization of mCitrine-KRas-4B is regulated by Rab11 protein (Schmick et al., 2014). (H) Quantification of GFP-Rab35 enrichment at the PM relative to the cytosolic GFP-Rab35 under these conditions (A-F). NS, not significant. Scale bar, 10μm.

4.2.3 Rab35 cycles between the Golgi apparatus and the plasma membrane

4.2.3.1 Rab35 trafficks from the Golgi apparatus to the PM via a non-vesicular pathway

The Golgi localization of Rab35 PBC mutants raises the question whether Rab35 cycles between the PM and the Golgi. The photoactivatable green fluorescence protein (paGFP) was employed to study the dynamics of Rab35 trafficking in HeLa and in Cos-7 cells.

Wild type GFP exists in two forms, which give rise to a major and a minor absorbance peak at 397nm and 475nm, respectively. Intense illumination at 400 nm shifts the population to the 475nm form, thereby increasing the absorbance of the minor peak. This photoconversion feature led to the development of photoactivatable green fluorescence protein (paGFP) (George et al., 2000). By selecting a form of GFP with a negligible 475nm peak, photoconversion will produce a much greater proportional increase in the absorbance at 475nm compared to the standard GFP and therefore increases contrast. paGFP exhibits very low green emission (max 517nm) with 488nm excitation, which can be increased to 100-fold by stimulation with 405nm light. This means that, paGFP activated by photo-irradiation will yield bright signals over a dark background. The advent of paGFP offers new possibilities to study biomolecules, such as pulse-chase labeling and single molecule localizations. We generated a panel of paGFP-Rab35 and its PBC mutant constructs for studying their dynamics by confocal microscopy.

We co-expressed paGFP-Rab35 and mKate2-Giantin as Golgi marker in HeLa cells. Photo-activation of paGFP-Rab35 at the Golgi region, which is indicated by mKate2-Giantin, led to transient observation of Rab35 accumulation at the Golgi, followed by rapid decrease of the fluorescence at the Golgi with the concurrent increase at the PM. Figure 4-2-7 shows the two processes of the FLAP measurments: (1) dissociation of Rab35 from the Golgi membrane; (2) association of Rab35 to the PM. The half times ($t_{1/2}$) of Golgi dissociation ($t_{1/2}$=19.4±5.7s) and PM association ($t_{1/2}$=28.9±14.9s) are similar, suggesting that Rab35 trafficks from the Golgi to the PM.

The trafficking of Rab35 from the Golgi to the PM may be a fast process. Sevral reports have defined the rapid/fast recycling from endosomes to the PM with half- times

of 50 seconds to 2 minutes, depending on the internalized lipid analogs. The half-time of a vesicular recycling is typically 4~5 minutes and up to 9~10 minutes in different cell lines (Hao and Maxfield, 2000). So we speculated that the trafficking of Rab35 from the Golgi to the PM may not undergo a vesicular transport process, which is cytoskeleton dependent.

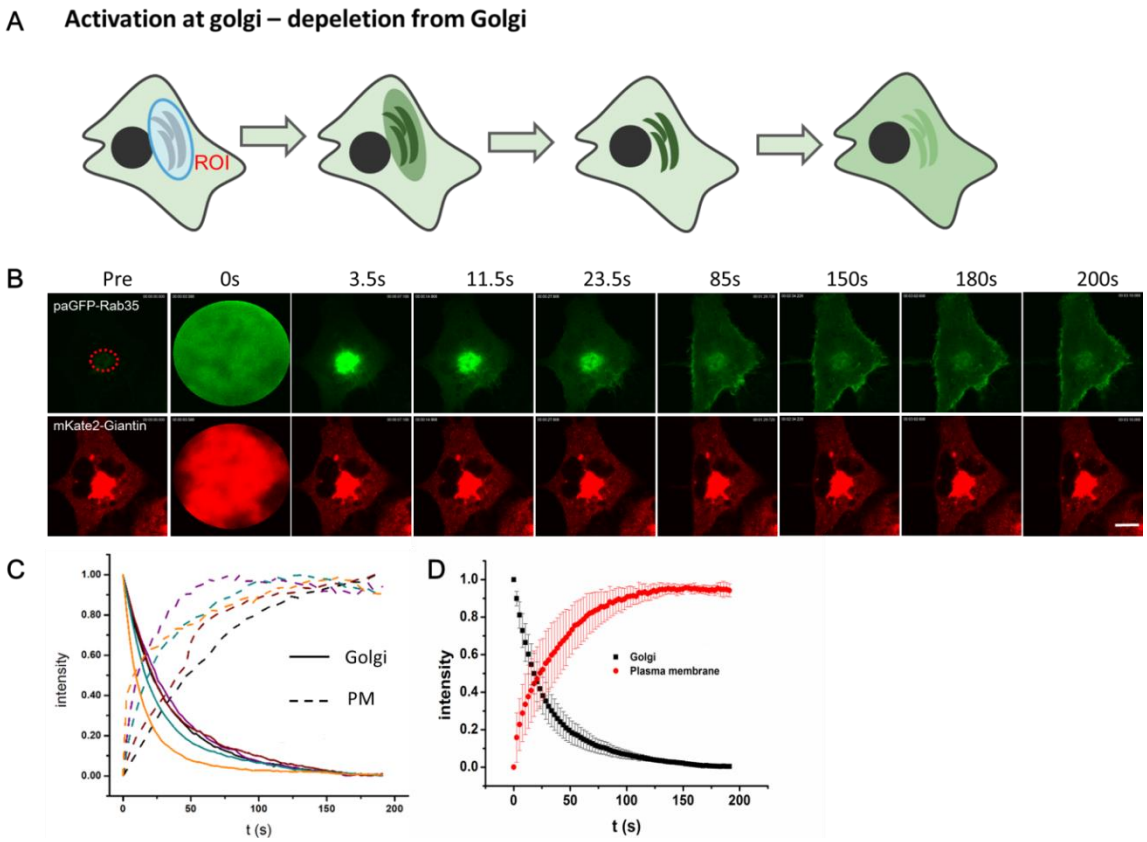

Figure 4-2-7. The trafficking of paGFP-Rab35 from the Golgi apparatus to the PM. (A) Scheme of the photoactivation process of a paGFP protein in a cell. (B) Representative time-lapse sequences of fluorescence distribution of paGFP-Rab35 photoactivated at the Golgi (upper row, the red circle is active site) and of mKate2-Giantin (lower row). (C, D) Quantification of Rab35 dissociation kinetics from the Golgi and association kinetics to the PM. Scale bar, 10μm.

To confirm our hypothesis, the cells were treated with 5μM nocodazole for 5 minutes to disrupt microtube and therefore vesicular transport. We obtained the $t_{1/2}$s of disassociation from the Golgi and association to the PM for 21.6±6.4 seconds and 19.4±9.1 seconds, respectively which are similar to the $t_{1/2}$s without nocodazole treatment (Figure 4-2-8C). Taken together, we conclude that Rab35 trafficks from the Golgi to the PM in a non-vesicullar transport pathway.

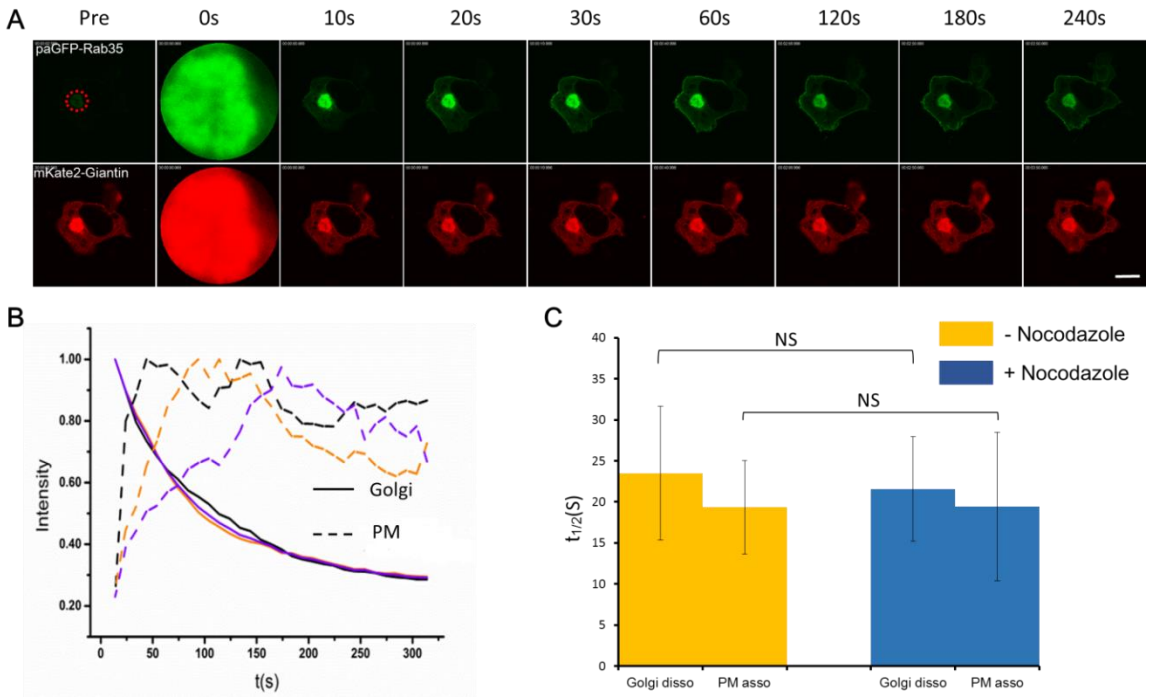

Figure 4-2-8. The trafficking of paGFP-Rab35 from the Golgi apparatus to the PM in the presence of nocodazole. (A) Representative time-lapse sequences of fluorescence distribution of paGFP-Rab35 photoactivated at the Golgi body (upper row, the red circle is active site) and of mKate2-Giantin (lower row) in the presence of 5 μM nocodazole. (B) Quantification of Rab35 dissociation kinetics from the Golgi and association kinetics to the PM. (C) Half-times of fluorescence decay and improve for paGFP-Rab35 with or without 5μM nocodazole treatment. NS, not significant. Scale bar, 10μm.

FRAP (Fluorescence recovery after photobleaching) has been used to characterize the mobility of cellular molecules (Vikstrom et al., 1992), by observing the movement of intracellular materials through photobleaching of the fluorescence. Several images using a low light level are acquired to determine the initial fluorescence, and then a high level of light for a short time inside a region of interest (ROI) is used to bleach the fluorescence in the ROI. The recovery of fluorescence at the ROI after photobleaching is followed by fluorescence microscopy. In this study, we performed the FRAP experiments at the Golgi region to measure the kinetics for trafficking of Rab35 mutant proteins to the Golgi (Table 4-2-1). These data also indicates that Rab35 is highly dynamic in cells.

Although we have confirmed Rab35 trafficking from the Golgi to the PM, it is not clear that whether these Rab35 molecules originated from the PM/cytosol pool or from newly synthesized proteins. Therefore, we can not exclude that the photoactivated paGFP-Rab35 at the Golgi may involve the newly synthesized molecules but is not from the cytosol, the endosome membranes or the PM.

To test our hypothesis, we used the protein synthesis inhibitor cycloheximide (CHX) to inhibit generation of new Rab35 proteins. CHX exerts its effect by interfering with the translocation step during the protein synthesis (movement of two tRNA molecules and the mRNA in relation to the ribosome), thus blocking translational elongation (Schneider-Poetsch et al., 2010). After the treatment of the cells, co-expressing paGFP-Rab35 and mKate2-Giantin with 10μg/ml cycloheximide for 4 hours, FLAP experiments were performed. Under these conditions, significant amount of Rab35 molecules transiently accumnulate at the Golgi followed by a decay with $t_{1/2}$=18.27 seconds, which is similar to that without CHX (Figure 4-2-9E).

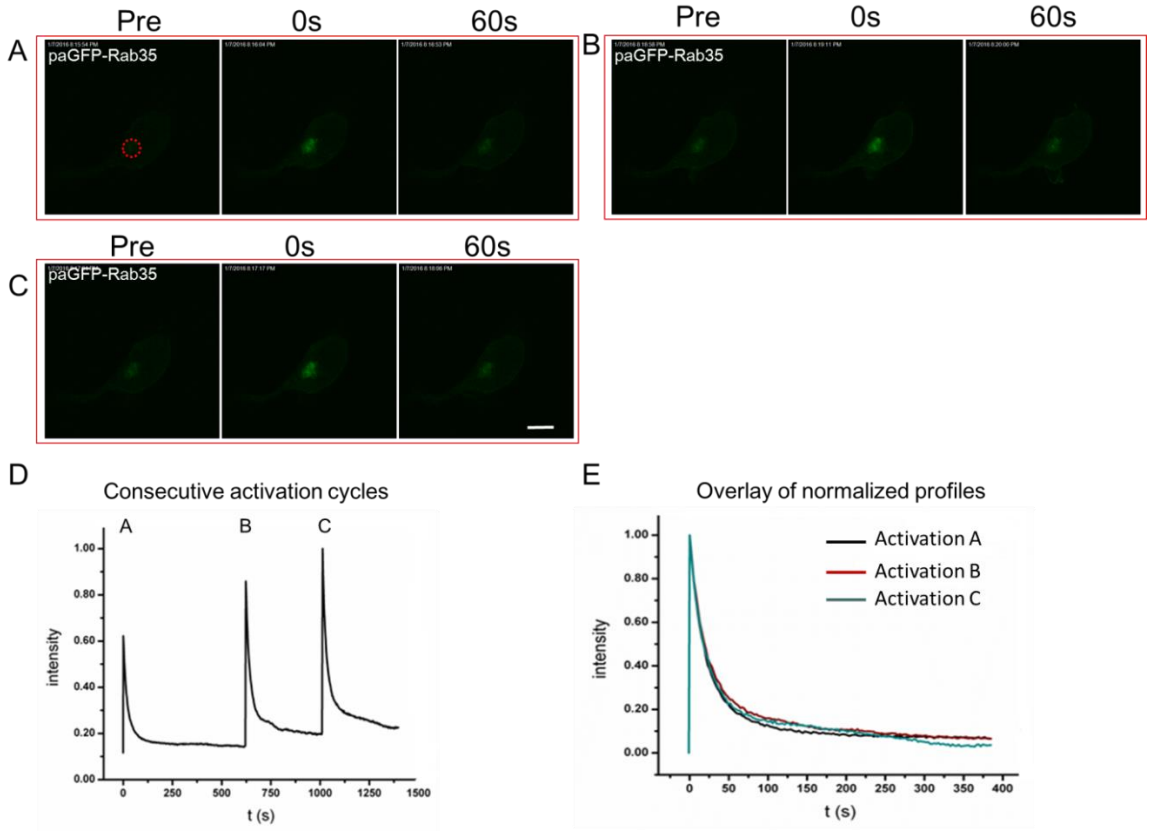

Figure 4-2-9. Activation of paGFP-Rab35 at the Golgi in the presence of cycloheximide. (A, B and C) Time-lapse sequences of fluorescence distribution of paGFP-Rab35 are induced by three times photoactivation at the Golgi in the round A, B and round C (Upper row). (D) Fluorescence curves of consecutive activation cycles in (A), (B), and (C). (E) The overlay of normalized curves in round A, B and C. Scale bar, 10μm.

Moreover, we performed three consecutive activation cycles in the FLAP measurement. All of them display identical $t_{1/2}$s ($t_{1/2}$=17.41±0.8 seconds) (Figure 4-2-9 A-D). These results suggest that Rab35 cycles between the Golgi and the PM.

4.2.3.2 Rab35 trafficks from the PM to the Golgi apparatus in an endocytic pathway

To investigate how Rab35 trafficks from the PM to the Golgi apparatus, the edge of the cell was photoactivated in HeLa cells, which co-express paGFP-Rab35 and mKate2-Giantin proteins. Figure 4-2-10 shows that Rab35 diffuses in the PM due to the lateral diffusion, while trafficking within the cytoplasm. Many Rab35 vesicles were found to accumulate near the Golgi region, indicating that vesicular pathway may be involved in PM-to-Golgi trafficking of Rab35. The half-time of the association to the Golgi region is 157 seconds, which is much longer than the dissociation half-time from Golgi apparatus.

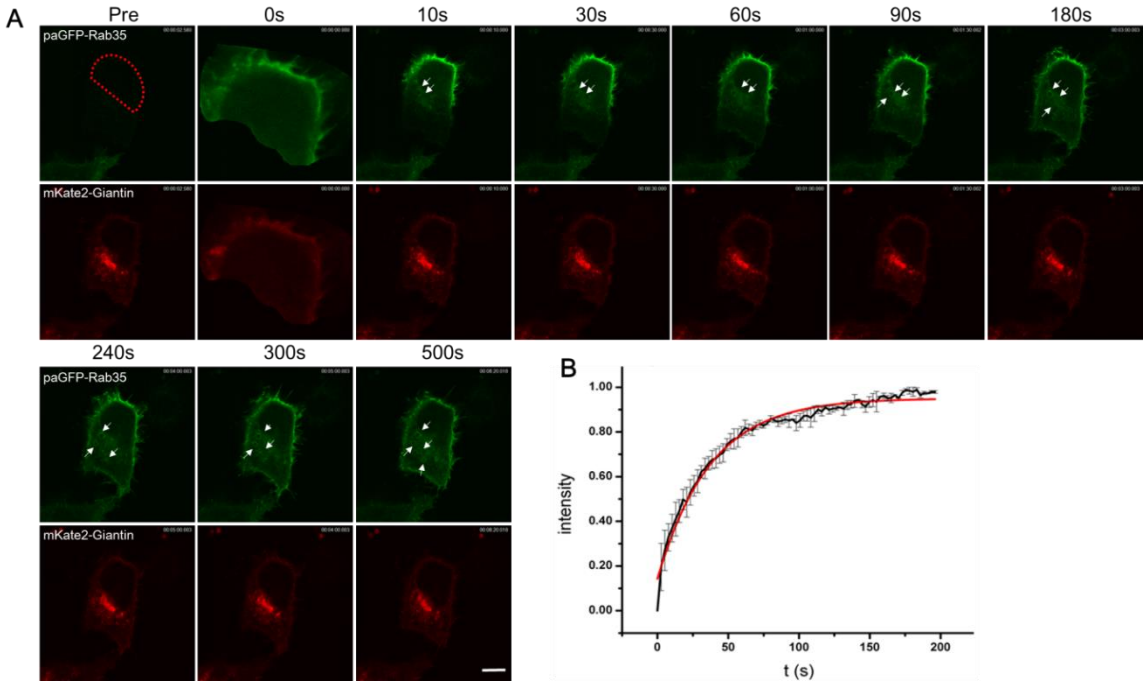

Figure 4-2-10. The trafficking of paGFP-Rab35 after photoactivation at the PM in HeLa cell. (A) Representative time-lapse sequences of fluorescence distribution of paGFP-Rab35 photoactivated At the PM and partial of cytosol (upper row) and of mKate2-Giantin (lower row). The arrows indicate Rab35 vesicles. (B) Quantification of Rab35 association kinetics at Golgi region from the PM and the cytosol. Scale bar, 10μm.

It has been shown before that Rab35 is involved in clathrin-dependent endocytosis (Dutta and Donaldson, 2015; Cauvin et al., 2016). We speculate that Rab35 is involved in the clathrin-dependent endocytosis pathway. Dynamin is a small GTPase involved in clathrin coated vesicles (CCVs) mediated endocytosis in the eukaryotic cell (Henley et al., 1999). The role of Dynamin is responsible for the scission of newly formed CCVs from the PM, the Golgi and the endosomal membranes (Praefcke and McMahon, 2004).

Moreover, dynamin plays a role in many processes including division of organelles, cytokinesis and microbial pathogen resistance (Hinshaw, 2000; Thoms and Erdmann, 2005). There are three dynamin members in human cells. Dynamin1 is mainly expressed in neurons while dynamin2 is expressed in most cell types. Dynamin3 is strongly expressed in the testis, but is also present in heart, brain and lung tissues.

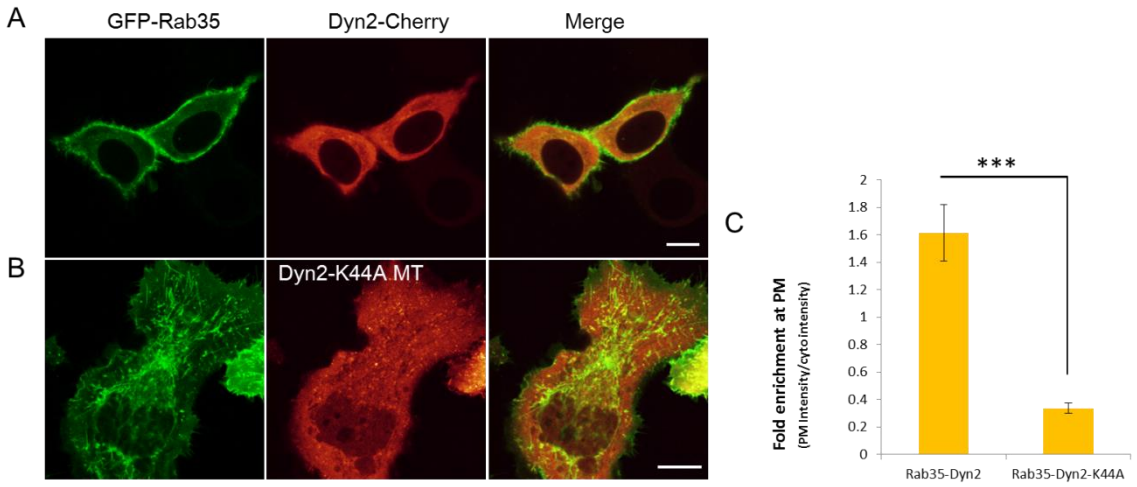

Figure 4-2-11. Rab35 is involved in clathrin coated vesicle (CCV) mediated endocytosis. (A) The subcellular localization of Rab35 with the expression of dynamine2 in HeLa cells. (B) The subcellular localization of Rab35 with the expression of dynamine2K44A mutant in cells. (C) Quantification of GFP-Rab35 enrichment at the PM relative to cytosol GFP-Rab35 intensity in (A and B). Dy2-K44A MT: dynamine2-K44A mutant. ***P < 0.001. Scale bar, 10 μm.

Next, we co-expressed GFP-Rab35 and dynamine2-Cherry in HeLa cells. The localization of Rab35 was not affected (Figure 4-2-11A). However, when Rab35 was co-expressed with dynamin2-K44A (dominant negative mutant), Rab35 loses its enrichment at PM and becomes largely cytosolic (Figure 4-2-11B). In addition, Rab35 tubulation is found which crosses the entire cell.

Altogether above results, we conclude that the Rab35 trafficks from the Golgi to the PM via a non-vesicular transport, while from the PM to the Golgi via an endocytic pathway.

4.2.4 PRA1 is important for plasma membrane localization of Rab35

Next, we sought to understand which protein mediates the non-vesicular pathway of Rab35 trafficking from the Golgi to the PM. GDP-dissociation inhibitor (GDI) is a possible candidate, which recycles prenylated GDP-bound form Rabs between membranes and cytosol (Regazzi et al., 1992; Pylypenko et al., 2006; Wu et al., 2007). PDE6δ is a GDI-like solubilizing factor (GSF) for prenylated Ras proteins (Chandra et al., 2011). However, the PM localization of Rab35 doesn't change in the presence of Deltarasin, a PDE6δ inhibitor, in contrast to that of Ras proteins (Figure4-2-12).

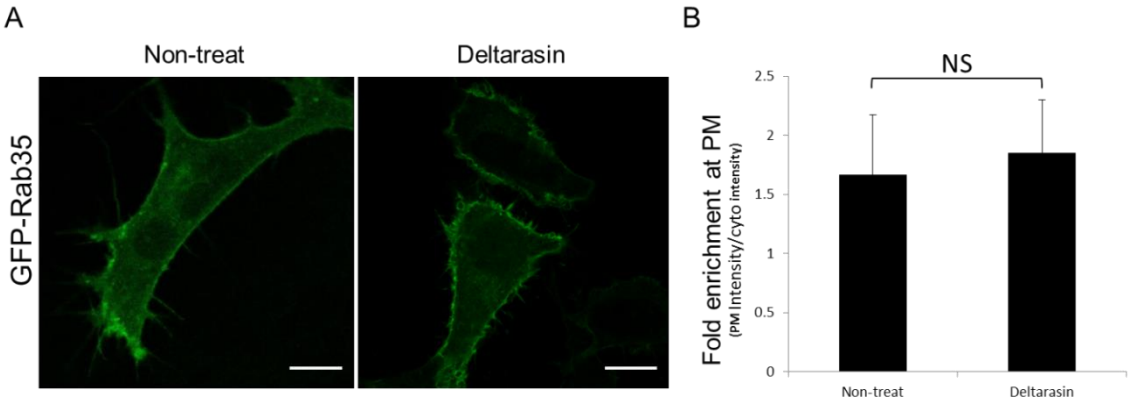

Figure 4-2-12. Subcellular localization of GFP-Rab35 in the presence of Deltarasin. (A) Subcellular localization of GFP-Rab35 without the treatment of Deltarasin. (B) Subcellular localization of GFP-Rab35 in the presence of Deltarasin. (C) Quantification of GFPRab35 enrichment at the PM relative to cytosol GFP-Rab35 intensity in (A and B). NS, not significant. Scale bar, 10 μm.

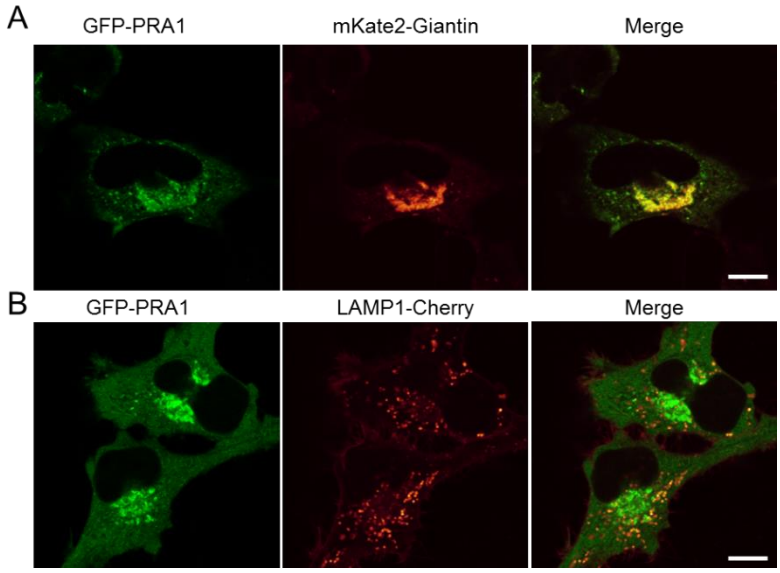

Figure 4-2-13. Subcellular localization of GFP-PRA1. Colocalizations of GFP-PRA1 with the Golgi marker mKate2-Giantin (A) and with the late endosome/lysosome marker LAMP1-Cherry (B).

Prenylated Rab acceptor (PRA1/YIP3) is an integral membrane protein which was proposed as GDI-displacement factor (GDF). It dislodges Rabs from GDI to facilitate GDI-mediates Rab cycles. It was reported to localize at the Golgi and endosomes (Dirac-Svejstrup et al., 1997, Sivars et al., 2003). We found that PRA1 mostly localized on Golgi body while only a few localized on the late endosomal membranes (Figure 4-2-13B).

Biochemistry data showed that PRA1/Yip3 functions on the prenylation of Rabs, especially for endosomal Rab GTPases including Rab9, Rab5 and Rab7. The possible function of GDI involved in the Golgi-to-PM recycling of Rab35 prompt us to investigate the role of PRA1 (GDF) in Rab membrane targeting the function of PRA1 for membrane targeting of Rab proteins. We depleted PRA1 expression by RNA interference (RNAi). We generated PRA1 shRNA constructs and knock-down the endogenous expression of PRA1 (Figure 4-2-14H).

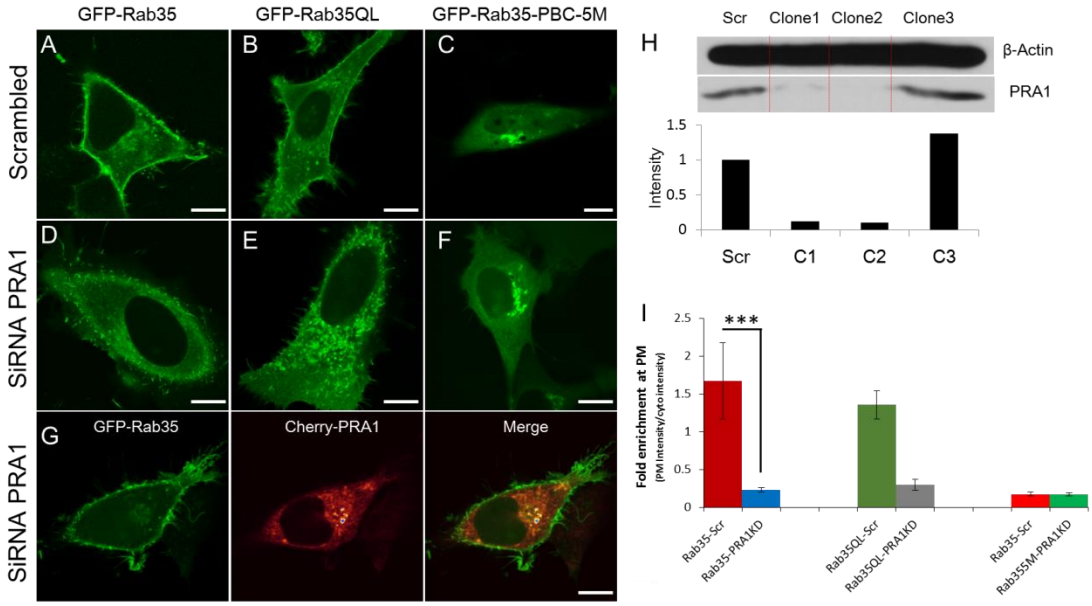

Figure 4-2-14. Subcellular localization of Rab35 in the PRA1 knock-down cells. (A-C) Subcellular localization of GFP-Rab35 wide type (A), GFP-Rab35Q67L mutant (B) and GFP-Rab35-PBC-5M (C) in scrambled shRNA cells. (D-F) Subcellular localization of GFP-Rab35 wide type (D), GFP-Rab35Q67L mutant (E) and GFP-Rab35-PBC-5M (F) in PRA1 knock-down cells. (G) Subcellular localizaition of GFP-Rab35 with the co-expression of Cherry-PRA1 in PRA1 knock-down cells. (H) Knock-down of endogenous PRA1 in HeLa cells, detected by western blot using anti-PRA1 antibody. Scrambled siRNA (scr) cell was used as a control. (I) Quantification of GFP-Rab35 enrichment at the PM relative to the cytosol GFP-Rab35 intensity under these conditions (A-F).***P < 0.001. Scale bar, 10μm.

The PRA1 depletion impairs the PM localization of Rab35 (Figure 4-2-14D) and even the Rab35Q67L dominant active mutant (Figure 4-2-14E). The cytosolic phenotype

of Rab35 wide type can be rescued by co-transfected with mCherry-PRA1, which is resistant to the siRNA (Figure 4-2-14G).

Interestingly, the localization of Rab35-PBC-5M at the Golgi body is not affected by PRA1 knock-down (Figure 4-2-14F). To check the dynamics of Rab35, FRAP (Fluorescence recovery after photobleaching) of Rab35 and its mutant proteins were performed in both the scrambled siRNA and PRA1 knock-down cells (Table 4-2-1). In control cells, the $t_{1/2}$ of Rab35-PBC-5M is 15.7 seconds while it is 16.02 seconds in PRA1 knock-down cells. Therefore, the fact that the PRA1 depletion does not slow down the Rab35-PBC-5M dynamics dramatically may due to its localization at the Golgi but not on endosome. When Rab35 mutant does not undergo the Golgi-PM cycling, its subcellular localization is not regulated by PRA1.

Table 4-2-1. Summary of Rab35and its PBC mutant proteins delivery kinetics in cell.

$t_{1/2}$	FRAP at the Golgi (single exponential fit)	FRAP at the Golgi (PRA1 KD cells)
GFPRab35 WT	ND	14.23s
GFP-Rab35-PBC-1M	ND	21.90
GFP-Rab35-PBC-2M	8.2s	17.54s
GFP-Rab35-PBC-3M	21.5s	13.37s
GFP-Rab35-PBC-4M	18.6s	N.D
GFP-Rab35-PBC-5M	15.7s	16.08s

N.D stands for not done.

These results suggest that PRA1 plays an essential role in the Golgi-PM cycling of Rab35 and hence its PM localization. Therefore, GDI is the key recycling factor involved in the Golgi-to-PM trafficking.

Since PRA1 has been proposed to function as a GDF for sevral endosomal Rab proteins (Dirac-Svejstrup et al., 1997, Sivars et al., 2003), the localization of several Rabs were examined.

We expressed GFP-Rab1, GFP-Rab5 and its dominant active mutant GFP-Rab5Q79L, GFP-Rab7, GFP-Rab8, GFP-Rab9 and GFP-Rab11 proteins in PRA1 knock-down cells. The localization of GFP-Rab1 remains at the Golgi apparatus in PRA1 knock-down cells (Figure 4-2-15A and B). However, the membrane localizations of endosomal Rabs including Rab5, Rab5Q79L, Rab7 and Rab11 are affected dramatically (Figure 4-2-15B). Rab5 and Rab5Q79L vesicles form clusters in the cell. In contrast, Rab7 localizes on enlarged vesicles (Figure 4-2-15B). The localization of Rab11 is very similar to its

S25N dominant negative mutant, which localizes in the perinuclear region (Figure 4-2-15C). However, the localizations of Rab8 and Rab9 are not altered in the PRA1 KD cells. Surprisingly, the depletion of PRA1 does not change the localization of Rab9, which is also an endosomal Rab. Previous result has shown that the membrane association of Rab9 is decreased dramatically in PRA1/YIP3 KD cells (Sivars et al., 2003).

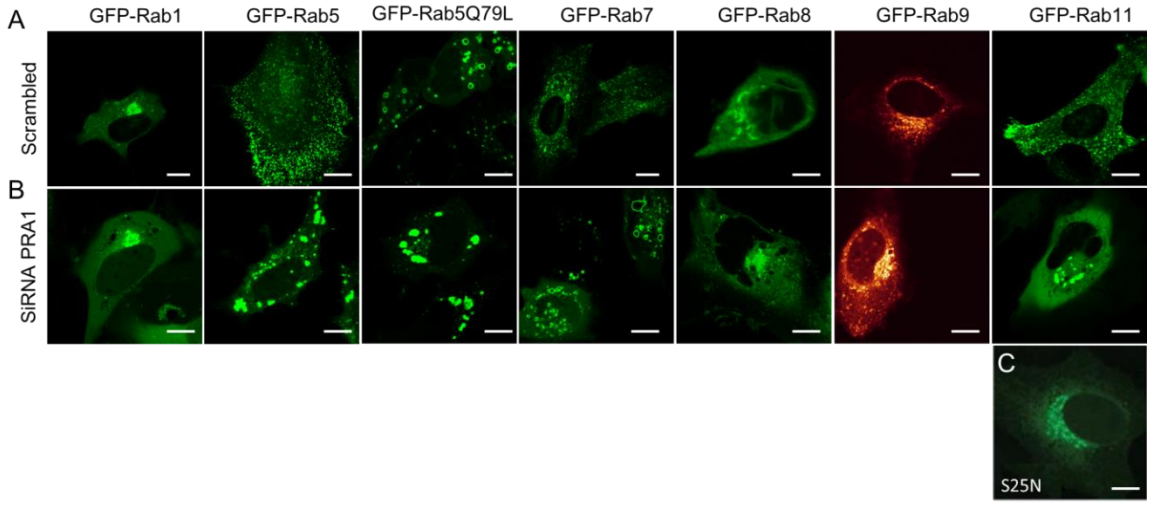

Figure 4-2-15. Rab GTPases subcellular localization in PRA1 knock-down cells. (A)Subcellular localization of GFP-Rab1, GFP-Rab5, GFP-Rab5Q79L, GFP-Rab7, GFP-Rab8 GFP-Rab9 and GFP-Rab11 in scrambled shRNA cells. (B) Subcellular localization of GFP-Rab1, GFP-Rab5, GFP-Rab5Q79L, GFP-Rab7, GFP-Rab8, GFP-Rab9 and GFP-Rab11 in in PRA1 knockdown cells. (C) Subcellular localization of GFP-Rab11S25N. Scale bar, 10 μm.

Altogether, we found that PRA1 is crucial for plasma membrane localization of Rab35. Additionally, PRA1 plays a role in Rab5, Rab7 and Rab11 membrane trafficking.

4.2.5 Nucleotide exchange regulates Rab35 localization at the plasma membrane

Guanine exchange factors (GEFs) mediated the GDP exchange to GTP for the activation of the Rab GTPases. In the GTP-bound form, Rabs recruit downstream effectors to fulfill their functions. Moreover, GEFs serve as the determinant for the membrane targeting of Rabs (Wu et al., 2010; Blümer et al., 2013). Since PRA1 depletion impairs the membrane targeting of Rab35, we asked if Rab35 GEFs affect the correct membrane localization of Rab35. The DENN domain has been found to display Rab GEF activity for Rab35 (Allaire et al., 2010) and DENND1A (connecdenn 1) has been shown to be the major GEF for Rab35 in the endocytic pathway (Marat et al., 2011).

Firstly, the localizations of Rab35S22N and Rab35Q67L were examined in HeLa cells. Less Rab35Q67L (dominant active form) proteins are found on PM and most of them on endosomal membranes compared to that of Rab35 wide type (Figure 4-2-16A). Interestingly, Rab35S22N (dominant negative form) mutant proteins loss their PM localization, and a consideration portion of them are localized on endosomes. These results suggest that the GTPase cycle regulated by GEF and GAP is essential for Rab35 spational cycles and therefore membrane targeting.

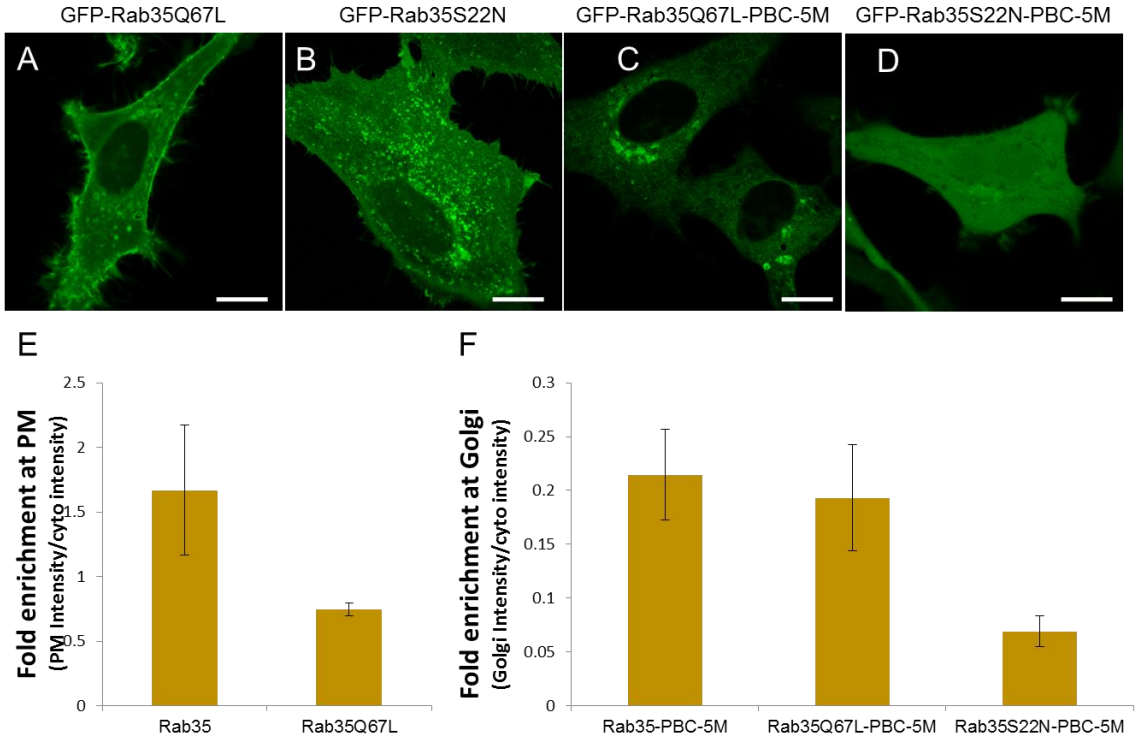

Figure 4-2-16. Subcellular localization of GFP-Rab35 mutant proteins in HeLa cells. (A) The localization of GFP-Rab35Q67L mutant in cell. (B) The localization of GFP-Rab35S22N mutant on endosomes. (C) The localization of GFP-Rab35Q67L-PBC-5M at the Golgi in cell. (D) The localization of GFP-Rab35S22N-PBC-5M in cell. (E) Quantification of GFP-Rab35Q67L enrichment at the PM relative to cytosol. (F) Quantification of GFP-Rab35 enrichment at the Golgi relative to cytosol GFP-Rab35 intensity under these conditions (C, D). Scale bar, 10μm.

Rab35Q67L-PBC-5M and Rab35-PBC-5M mutant protein were found still localize on the Golgi apparatus (Golgi marker did not shown). For Rab35S22N-PBC-5M mutant protein, some of them are still localized at the Golgi although show that they can dissociate from Golgi and become more cytosolic (Figure 4-2-16D) and their localizations at the Golgi were measured (Figure 4-2-16F). The localizations of Rab35

and Rab35-PBC-5M mutant proteins suggest that the membrane targeting of Rab35 is partially contributed by its GEFs.

To examine the precise localization of Rab35S22N mutant proteins, we co-expressed Rab35S22N and EEA1, an early endosome marker or LAMP1, a late endosome/lysosome marker in HeLa cells. Figure 4-2-17 shows most Rab35S22N are localized on early endosome and late endosome/lysosomes. The dominant negative mutant may present intermediate endocytic localization en route to the Golgi. It is known that Rab35 recruits OCRL1 to newborn endosomes, where OCRL1 converts PtdIns(4,5)P_2 to PtdIns(4)P leads to the uncoating of clathrin coated vesicles(CCVs) (Martin, 2001). Rab35S22N mutant impairs the recruitment of OCRL1 to CCVs and causes the accumulation of PtdIns(4,5)P_2 on CCVs, early endosomes and late endosomes. The localization of Rab35S22N protein on endosomal membranes suggests that Rab35 may associate on endosome via the binding between the PBC and PtdIns(4,5)P_2 or other PtdInPs. This electrostatic interaction may enhance the affinity of Rab35S22N with the negative charged lipids on CCPs, early endosomes and late endosomes. Therefore, mutation of the PBC (Rab35S22N-5M) led to more cytosolic localization of the protein (Figure 4-2-16D). These data suggest Rab35 GEFs may be involved in its membrane targeting.

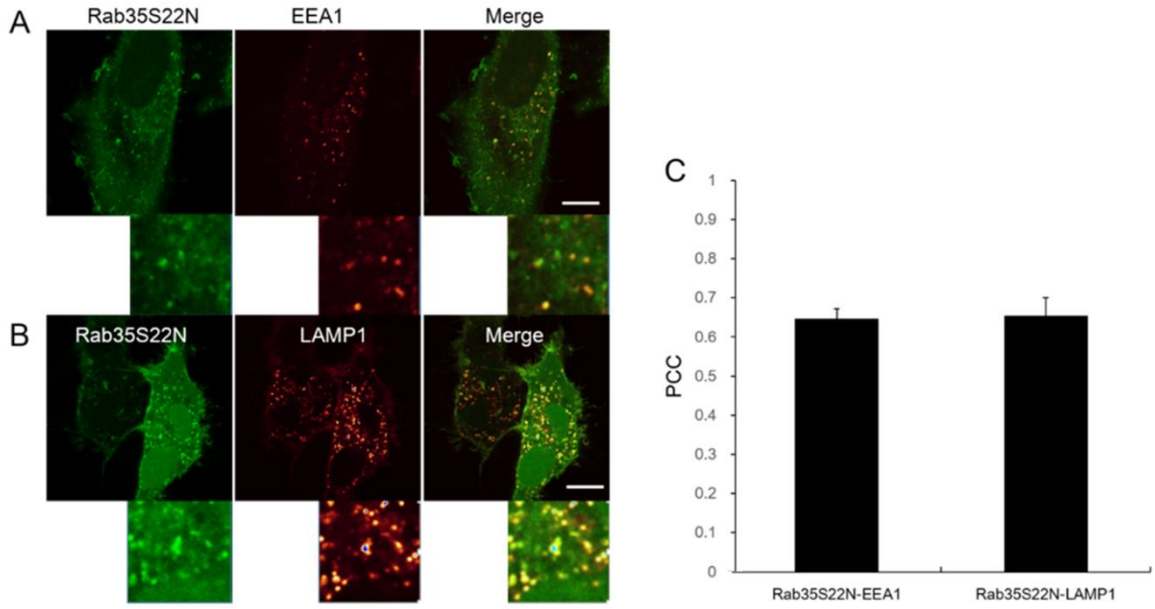

Figure 4-2-17. Subcellular localization of GFP-Rab35S22N mutant in HeLa cells. (A) The colocalizatio of GFP-Rab35S22N with Cherry-EEA1. (B) The colocalizatio of GFP-Rab35S22N with LAMP1-Cherry. (C) Pearson's correlation coefficients (PCC) for colocalization (A and B), respectively. Scale bar, 10μm.

To further identify the function of GEFs for Rab35 membrane targeting, we generated cherry-tagged shRNA constructs to knock down the Rab35 GEF DENND1A in HeLa cells. DENND1A depletion leads to Rab35 being largely cytosolic, suggesting that DENND1A is crucial for Rab35 PM-targeting. By carefully examining the phenotype resulted from DENND1A depletion, we found that the density of Rab35 is higher in the proximity area of PM, which may localize in endsomes (Figure 4-2-18A). This phenotype was also observed in PRA1 depletion cells (Figure 4-2-14D). Interestingly, the depletion of DENND1A did not alter the localization of Rab35-PBC-5M (Figure 4-2-18B), which still localizes at the Golgi apparatus. This result is probably attributed to several reasons. One possible reason is that Rab35-PBC-5M can be actived by another GEF such like DENND1B, DENND1C, Folliculin (FLCN) or an unknown GEF (Allaire et al., 2008; Allaire et al., 2006； Cauvin et al., 2016). Another possibility is that the membrane localization of Rab35-PBC-5M is independent on the GDP or GTP bound form, which means that Rab35-PBC-5M can be recruited by a protein localizing at the Golgi.

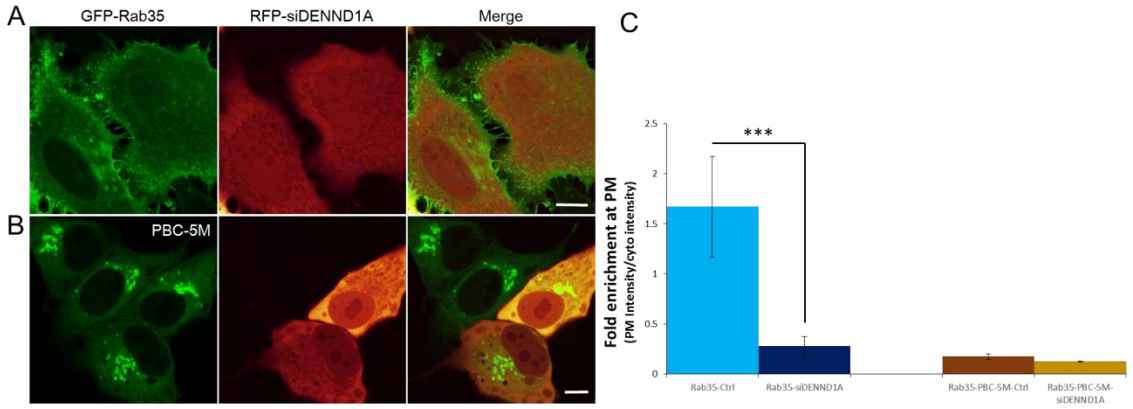

Figure 4-2-18.Subcelluar localization of Rab35 and PBC mutant in DENND1A knock-down HeLa cells. (A) The localization of Rab35 in DENND1A knock-down cells. (B) The localization of Rab35-PBC-5M in DENND1A knock-down cells. (C) Quantification of GFP-Rab35 (A) and GFP-Rab35-PBC-5M enrichment at the PM relative to cytosol intensity. ***P < 0.001. Scale bar, 10μm.

Therefore, the GTPase cycle is essential for the membrane targeting of Rab35 in cells. DENND1A, the Rab35 GEF, plays a crucial role in Rab35 GTPase cycle and thereby Rab35 membrane targeting. It is conceivable that without activation of Rab35 on the endosomes and the endocytic trafficking of Rab35 is disrupted. As a consequence, the cycling between the Golgi and the PM is perturbed. Thus, Rab35 loses its correct membrane targeting in the cell.

4.2.6 OCRL1 is required for Rab35 plasma membrane localization and function

OCRL1, the effector of Rab35, shows important roles in the processes of the cytokinesis and the uncoating of CCVs (Hanono et al., 2006; Cauvin et al., 2016). In addition, OCRL depletion perturbs endocytic recycling and trafficking from endosomes to the TGN (Choudhury et al., 2005; Vicinanza et al., 2011). OCRL1 is a inositol polyphosphate 5-phosphatase(INPP5F), which catalyzes the production of PtdIns(4)P and PtdIns(3,4)P_2 from PtdIns(4,5)P_2 and PtdIns(3,4,5)P_3. An interesting result showed that an OCRL1 pool localizes in the trans-Golgi network (Hanono et al., 2006), where OCRL may play a role in the metabolism of phosphatidylinositides.

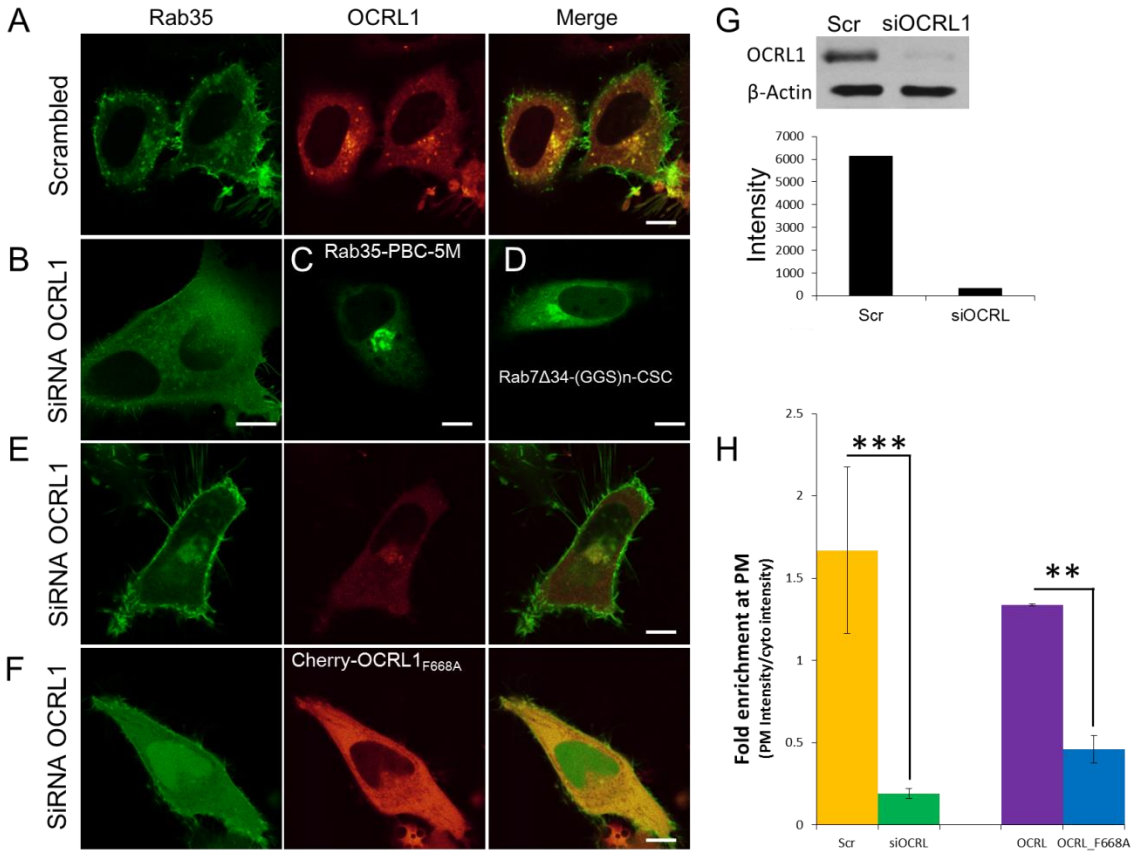

Figure 4-2-19. Subcellular localizaition of Rab35 in OCRL1 knock-down HeLa cells. (A) The colocalization of GFP-Rab35 and mChery-OCRL1 in scrambled shRNA cells. (B) The localization of GFP-Rab35 in OCRL1 knock- down cell. (C) The localization of GFP-Rab35-PBC-5M in OCRL1 knock-down cells. (D) The localization of GFP-Rab7Δ34-(GGS)n-VKL-CSC in OCRL1 knock-down cells. (E) Subcellular localizaition of Rab35 with the co-expression of Cherry-OCRL1 in OCRL1 knock-down cells. (F) Subcellular localizaition of Rab35 with the co-expression of Cherry-OCRL1$_{F668A}$ mutant in OCRL1 knock-down cells. (G) Knockdown of endogenous OCRL1 in HeLa cells, detected by Western blot using

anti-OCRL1 antibody. Scrambled siRNA (scr) cell was used as a control. (H) Quantification of GFP-Rab35 enrichment at the PM relative to cytosol GFP-Rab35 intensity under these conditions (B, E, F). Arrow head: two nucleuses in a binucleate cell. ***P < 0.001; **P < 0.01. Scale bar, 10μm.

To investigate the role of OCRL in Rab35 membrane targeting, OCRL1 depletion was performed by shRNA in HeLa cells. The subcellular localization of Rab35 is largely cytosolic in OCRL knock-down cells (Figure 4-2-19B), while the localization of Rab35-PBC-5M at Golgi apparatus is not altered (Figure 4-2-19C). The cytosolic phenotype of Rab35 in OCRL1 depletion cells can be rescued by the expression of mCherry-OCRL1, which is resistant to siRNA (Figure4-2-19E). Intriguingly, the Lowe syndrome mutant OCRL1-F668A, could not rescue the cytosolic phenotype of Rab35 in OCRL1 knock-down cell (Figure4-2-19F). The crystal structure OCRL1-Rab8a complex revealed that F668 is included in the Rab-binding interface of OCRL1, an IgG-like β-strand structure of the ASPM-SPD-2-Hydin domain. F668A substitution impairs the interaction with Rab8a due to the lower hydrophobicity of alanine compared to phenylalanine (Hou et al., 2011). It is possible that the F668A mutation also disrupts the Rab35 interaction to OCRL1. However, more direct evidences are needed that can be provided by precise methods such as ITC or fluorescence polarization. The results suggest that the OCRL binding is essential for Rab35 membrane targeting.

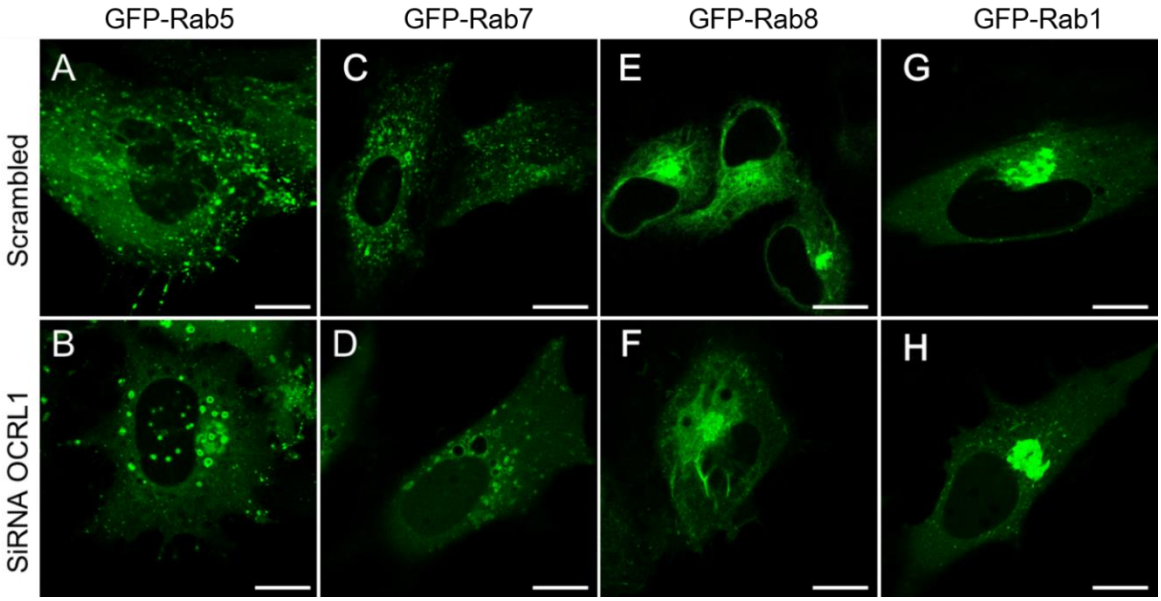

Figure 4-2-20. Subcellular localizations of Rab5, Rab7, Rab8 and Rab1 in OCRL1 knock-down HeLa cells. (A, C, E, G) The localization of GFP-Rab5 (A), GFP-Rab7 (C), GFP-Rab8 (E) and GFP-Rab1 (G) in scrambled siRNA cells. (B, D, F, H) The localization of GFP-Rab5 (B), GFP-Rab7 (D), GFP-Rab8 (F) and GFP-Rab1 (H) in OCRL1 siRNA cells. Scale bar, 10μm.

Previous evidences revealed that OCRL works as an effector of more than ten Rab GTPases including Rab1, Rab5, Rab8, Rab13, Rab35, Rab36, and so on (Fukata et al., 2008). Therefore, we suspect whether the membrane targeting the other Rabs are disturbed which similar with the case of Rab35 in OCRL1 depletion cells. We chose Rab1, Rab5, Rab7 and Rab8 to test the effect of OCRL1 depletion. Figure 4-2-20 clearly shows the enlargement of GFP-Rab5 vesicles (Figure 4-2-20B). Interestingly, although OCRL1 is not an effector of Rab7, the enlarged Rab7 vesicles were observed in OCRL1 knock-down cell (Figure 4-2-20D). Both Rab5 and Rab7 are involved in endocytic pathway, which is now impaired due to the loss-of-function of Rab35 in the absence of OCRL1. Thus, the enlarged Rab7 vesicles may be not induced by OCRL1 depletion directly but the result of endocytic pathway blocking. In contrast, knock-down of OCRL1 does not perturb the membrane targeting of Rab1 and Rab8, though OCRL1 was shown to bind these Rabs (Fukata et al., 2008). The results indicate OCRL1 is involved in endocytic pathway.

Altogether, as an effector of Rab35, OCRL1 depletion leads to the formation of cytosolic of Rab35, which is very similar to the effect of RILP on Rab7 (Li et al., 2014). This is a new evidence of Rab effector playing role in the Rab membrane targeting process. OCRL1 may regulate Rab35 membrane targeting via its 5-phosphatase activity involved in the metabolism of phosphoinositides, which are involved in electrostatic interactions with Rab35. On the other hand, OCRL1 plays an important role in the endocytic trafficking pathway, thereby regulating the Golgi-PM cycling of Rab35.

4.2.7 Conclusion and discussion

In this study, we combined biochemistry, cell biology, molecular biology and confocal microscopy techniques to study the mechanism of Rab35 membrane targeting. The polybasic region is crucial for the PM localization of Rab35 and its divergent functions. The polybasic cluster (PBC) depletion leads to the mistargeting of Rab35 to Golgi. The Golgi apparatus may work as a stop of Rab35 trafficking. Furthermore, the trafficking of Rab35 from Golgi to PM is via a fast non-vesicular pathway and may involve GDI. The trafficking of Rab35 from the PM to the Golgi apparatus is largely mediated by an endocytic pathway.

4.2.7.1 PRA1 affects the membrane localization of Rab35

PRA1 was proposed as a Rab GDF which dislodges the endosomal Rabs from GDI and facilitates the subsequent nucleotide exchange on the membrane (Sivars et al., 2003). The PRA1 depletion disrupts the PM localization of Rab35 and renders Rab35 largely cytosolic. Moreover, the depletion of PRA1 leads to clusters of Rab5 vesicles and enlargement of Rab7 vesicles. These phenomena suggest the important role of PRA1 in endocytic pathway. Although Rab9 was proposed as a model protein to address the GDF functions of PRA1, surprisingly, the membrane localization of Rab9 is not altered obviously in the PRA1 knock-down cells. The localization of Rab35-PBC-5M at the Golgi apparatus means that Rab35-PBC-5M may function similarly to Rab1 and is not invovled in endocytic pathway trafficking. Therefore, the localization and dynamics at the Golgi are not affected by PRA1 depletion.

The aggregation of Rab5 vesicles and the enlargement of Rab7 vesicles suggest that PRA1 pertubes the endocytic pathway.

4.2.7.2 The function of Rab35GEF in the membrane localization of Rab35

Rab35GEF is another regulator for the membrane targeting of Rab35. The depletion of the major GEF for Rab35, DENND1A, renders Rab35 largely cytosolic. This shows that the nucleotide exchange is crucial for Rab35 membrane targeting and function. However, the membrane localization of Rab35-PBC-5M is not affected by the depletion of DENND1A, which indicates that another protein may work as GEF for Rab35-PBC-5M at the Golgi. Rab35 and Rab1a/1b share a high homology in the GTPase domai, whereas

they have different HVDs. Since the most important characteristics of Rab35, the PBC region in the HVD, are eliminated in PBC-5M, Rab35-PBC-5M becomes similar to Rab1, which is localized at the Golgi apparatus. Furthermore, the GDP/GTP exchange of Rab35-PBC-5M is probably also executed by Rab1GEF TRAPPII complex. Some results have shown that TRAPPII is not only the Rab1GEF but also work as a GEF for Rab11 and Rab18 (Thomas and Fromme, 2016; Li et al., 2016). There is one method that can be used to identity whether TRAPP works as a GEF for Rab35-PBC-5M or not in cell. We can knock-down the core subunit of TRAPP complex, such as Trs23. In this way, the GEF function of TRAPP should be impaired.

Additionally, the membrane localization of the dominant negative mutant of Rab35 (Rab35S22N) suggests that Rab35 may be involved in the endocytic pathway, en route to the Golgi apparatus.

4.2.7.3 The Function of the effector OCRL1 in the membrane localization of Rab35

The Rab35 effector, OCRL1, controls the membrane targeting of Rab35. The most important finding of this project is that the depletion of OCRL1 impairs the PM localization of Rab35. OCRL1 depletion also changes the phenotype of Rab5 and Rab7, represented by the enlarged Rab5/Rab7 vesicles in cells. This indicates that OCRL depletion disturbs the whole endocytic pathway. The depletion or mutation of OCRL1 leads to the Lowe syndrome or Dent disease (Charnas and Gahl, 1991, Pirruccello and De Camilli, 2012). However, it still remains elusive how the loss of OCRL1 function results in Lowe syndrome. One of the characteristics of Lowe syndrome is intellectual disability which may be induced by the undifferentiated neurons. Neurite outgrowth is the first step in the processes of neuronal differentiation which leads to synaptic polarization and plasticity. Rab35 controls the neurite outgrowth in response to NGF stimulation in PC12 cells (Chevallier et al., 2009; Kobayashi and Fukuda, 2012; Kobayashi and Fukuda, 2013; Kobayashi et al., 2014; Etoh and Fukuda, 2015). Our results indicate that the depletion or mutation of OCRL1 leads to disruption of Rab35 PM localization, which is probably important for its function in the neurite outgrowth in embryonic and young child stages. This idea can be verified by studying the neurite outgrowth status in OCRL1-depleted SH-SY5Y cells. More direct evidences could be obtained by examination of the

phenotype of Rab35 in the cells from Lowe syndrome patients. If the Rab35 is cytosolic and looks similar to that of in OCRL1 depleted cells, it would indicate that the OCRL1-Rab35 cascade indeed causes the intellectual disability.

The depletion of PBC domain leads to the mislocalization of Rab35 to the Golgi. This suggests that the endocytic pathway could have been disrupted by the absence of the interaction involved in the Rab35 PBC region. We have known that the PM localization of Rab35 could be due to the direct binding to the negatively charged phosphoinositide PtdIns(4,5)P_2 and PtdIns(3,4,5)P_3 (Li et al., 2014; Heo et al., 2006). We also know that, Rab35-GTP recruits OCRL1 on the newly born endosomes to hydrolyze PtdIns(4,5)P_2 and PtdIns(3,4,5)P_3 to PtdIns4P and PtdIns(3,4)P_2, and to induce uncoating of the CCVs (Cauvin et al., 2016). Therefore, Rab35 may bind to the negative charged lipids PtdInPs on the sorting endosomes where it subsequently trafficks to late endosome/lysosome, and then is delivered to the Golgi apparatus.

Phosphoinositides play important roles in defining localized membrane properties and modulates various subcellular biological processes, including cell signaling, protein and membrane trafficking, cytoskeleton organization, and gene expression (Schramp et al., 2012). Recent reports showed that both PtdIns(4,5)P_2 and its primary precursor PtdIns(4)P, have been found at multiple subcellular membrane structures including the Golgi complex (D'Angelo et al., 2008). Indeed, in the trans-Golgi/plasma membrane/endocytic membranes, the tight packing of saturated and negatively charged lipids would favor electrostatic interactions (Leventis and Grinstein 2010; Bigay and Antonny 2012). Moreover, electron microscopy (EM) studies using the pleckstrin homology domain of phospholipase C-δ (PLCδ-PH) as a specific probe (Lemmon and Ferguson, 2000) have revealed that a substantial pool of PtdIns(4,5)P_2 is localized at the nucleus, the Golgi complex, ER, mitochondria, recycling endosomes, and the limiting membrane and intraluminal vesicles of multivesicular endosomes, although the majority of PtdIns(4,5)P_2 is still found at the plasma membrane (Vicinanza et al., 2011; Watt et al., 2002). It's not clear yet whether Rab35 is involved in the phosphoinositides metabolism.

The receptor signaling is dependent on endocytic pathway which starts from PM internalization, and then forms CCPs and CCVs, early endosomes, late endosomes and end at the lysosomes for degradation. A key step during early-to-late endosome

maturation is the formation of intraluminal vesicles (ILVs), which is partially driven by the endosomal sorting complexes required for transport (ESCRT) machinery (Henne et al., 2011; Hurley et al., 2010). Together with endosomal maturation, the ESCRT machinery also controls the intraluminal sorting of many cell-surface receptors, which serves as a mechanism to target receptor cargos for lysosomal degradation (Eden et al., 2009). However, recent evidences also pointed to a another role of endosomal PtdIns(4,5)P_2 in the regulation of ESCRT functions in the endolysosomal sorting of receptor cargos (Tan et al., 2015). Although presented at much lower levels at endosomes compared to at the plasma membrane, PtdIns(4,5)P_2 appears to add an additional layer of control over membrane and/or protein trafficking at endosomes and lysosomes. All above evidences show us a possible role of Rab35 PBC domain in interacting with PtdIns(4,5)P_2.

Altogether, GDF (PRA1), GEF (DENND1A) and the effector (OCRL1) play important but distinct roles during the Rab35 membrane trafficking.

4.2.7.4 The model of Rab35 membrane targeting

Based on previous evidences and our discoveries, I may propose a working model for Rab35 membrane trafficking in cell (Figure 4-2-21). The newly synthesized Rab35 GTPase is first captured by REP1 which presents GDP-bound Rab35 to Rab GGTase for prenylation at the C-terminal dual cysteines. The prenylated Rab35 is carried by GDI in the cytosol, while the PBC domain associates with PtdInsPs (e.g. PtdIns(4,5)P_2). PRA1 dislodges Rab35 from REP/GDI and presents Rab35 to its GEF (DENND1A) for GDP/GTP exchange. The GTP-bound Rab35 recruits its effector OCRL1 to the Golgi apparatus and the endosomes, where OCRL1 hydrolyses PtdIns(4,5)P_2 to PtdIns(4)P. The GDP-bound form of Rab35 is extracted from the Golgi membranes by GDI. The association of Rab35 with PM is dependent on its PBC domain's positive charges, which can bind to the negative charged phosphoinositides at the PM. At the same time the phosphoinositides may work as a scaffold for Rab35 nucleotide exchange, which is catalyzed by GEFs for example DENND1A at the PM.

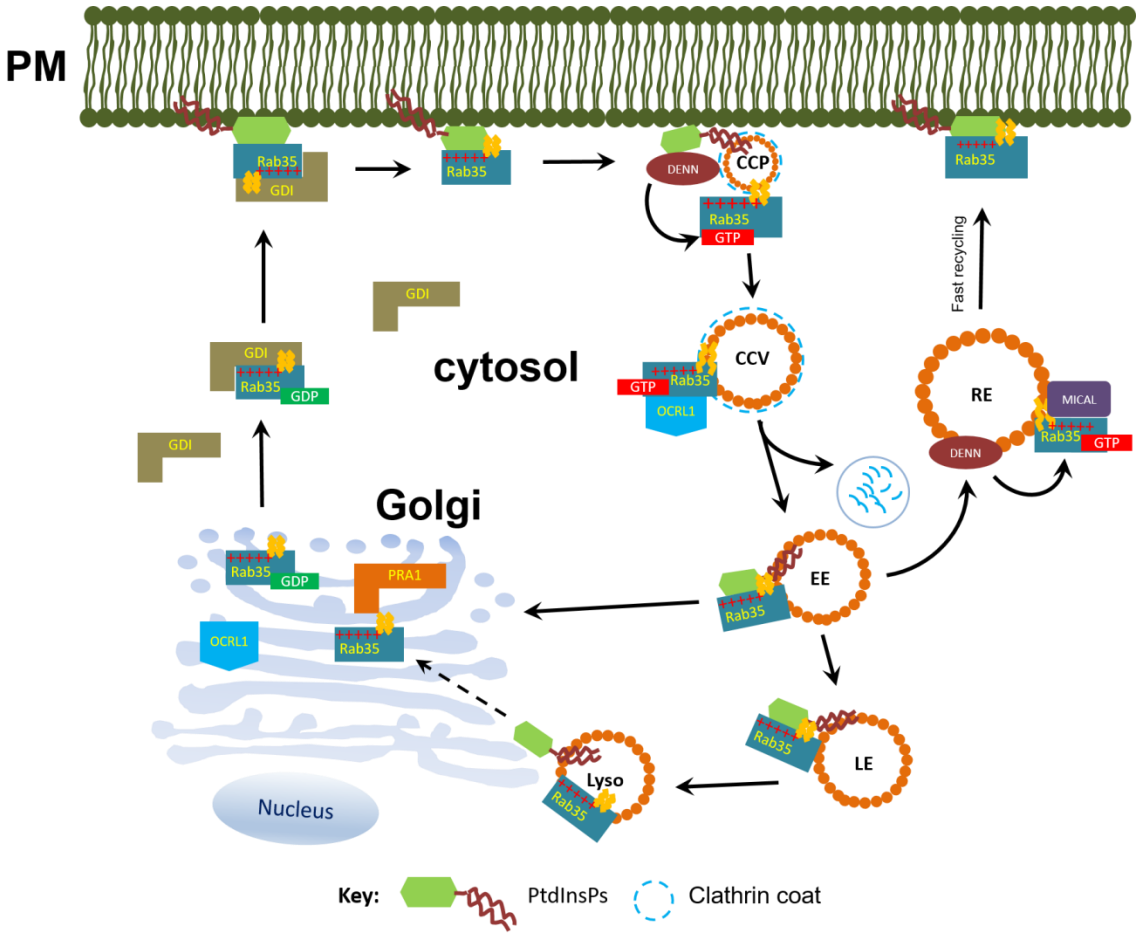

Figure 4-2-21. Model of Rab35 membrane trafficking in cell. CCP, clathrin coat pit; CCV, clathrin coat vesicle; EE, early endosome; LE, late endosome; Lyso, lysosome; RE, recycling endosome.

Once the endocytic events have happened, the formation of CCPs, which contains clathrin coat and AP2, that recruits DENND1A to the CCPs membrane and further fuses into CCVs. The DENN domain of DENND1A contains a lipid-binding module which is sufficient for the stable membrane association with uncoated CCVs (Allaire et al., 2010), where DENND1A recruits Rab35 to CCVs and exchanges the GDP to GTP. The activated GTP-Rab35 recruits its effector OCRL1 to the CCVs to hydrolyze PtdInsPs, which promotes clathrin uncoating. The affinity of PtdInsPs with PBC domain of Rab35 keeps Rab35 on these vesicles such as early endosomes, late endosomes and lysosomes. Finally, Rab35 is routed to the Golgi and enters the next round of trafficking.

Interestingly, the nucleotide exchange of Rab35-PBC-5M mutant may be regulated by another GEF as the TRAPP II complex at the Golgi. The Rab35-PBC-5M could not associate with the PM because of the absence of the positively charged PBC domain. Therefore, Rab35-PBC-5M proteins recycled back to the Golgi apparatus. This

hypothesis can also explain the phenomena that depletions of PRA1, DENND1A and OCRL1 render Rab35 cytosolic but not the Rab35-PBC-5M mutant. However, more work are still needed to further prove the above hypotheses.

5 Appendices

1. ESI-MS spectra of proteins in the project of PEGylated Rab proteins

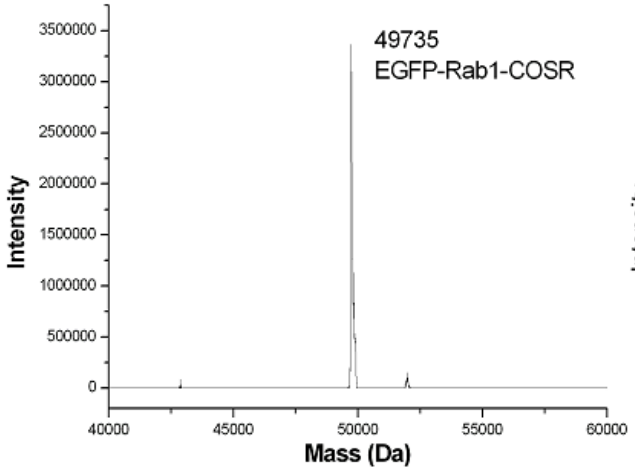

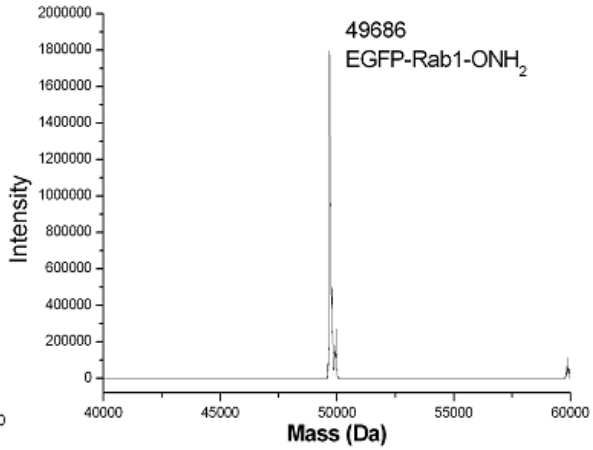

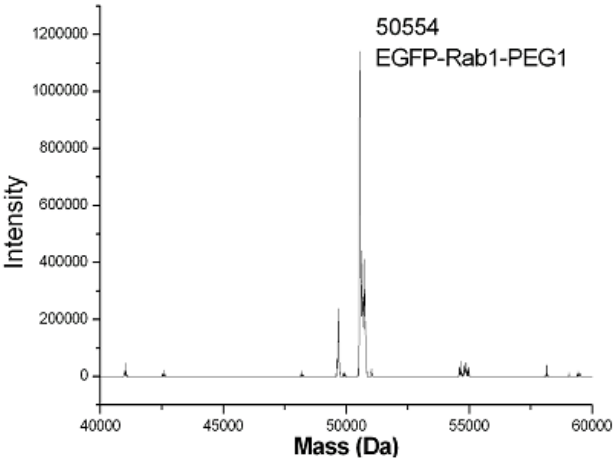

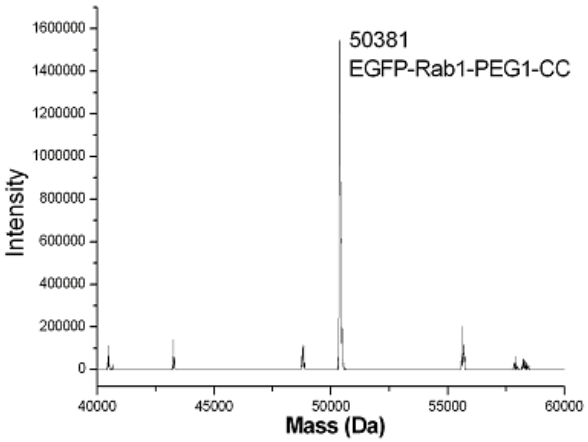

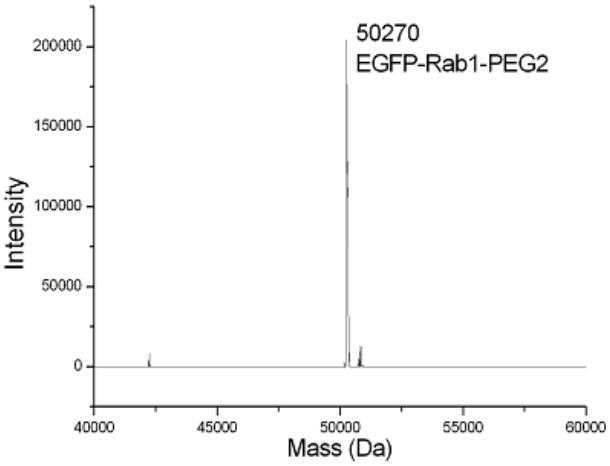

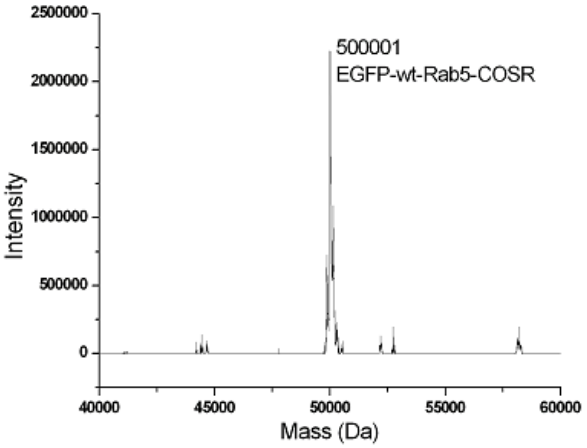

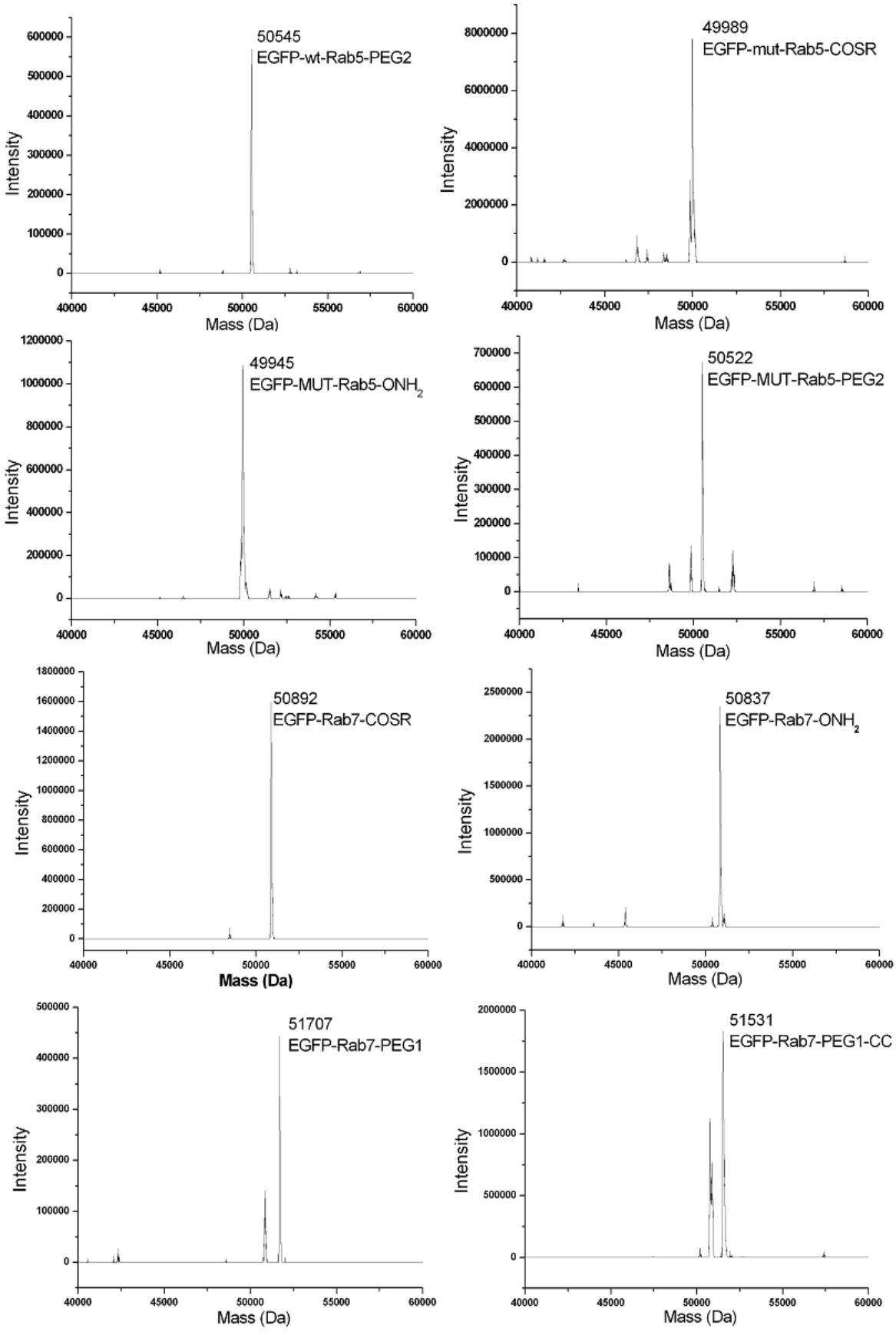
50545
EGFP-wt-Rab5-PEG2
49989
EGFP-mut-Rab5-COSR
49945
EGFP-MUT-Rab5-ONH2
50522
EGFP-MUT-Rab5-PEG2
50892
EGFP-Rab7-COSR
50837
EGFP-Rab7-ONH2
51707
EGFP-Rab7-PEG1
51531
EGFP-Rab7-PEG1-CC
Intensity
Mass (Da)

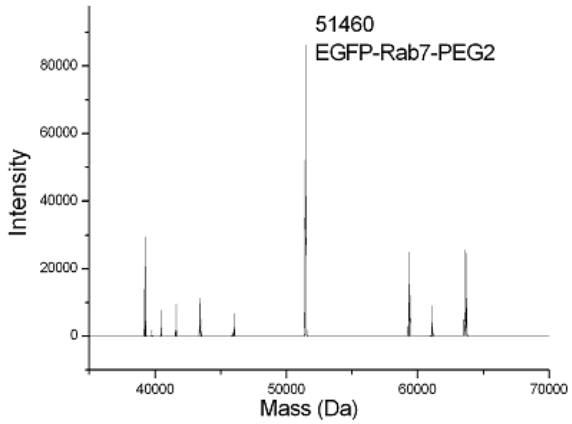
51460
EGFP-Rab7-PEG2
Intensity
Mass (Da)

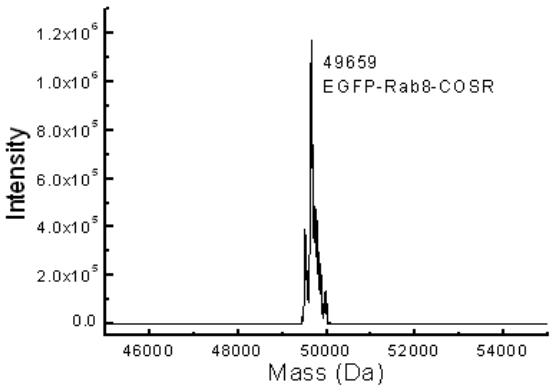
49659
EGFP-Rab8-COSR
Intensity
Mass (Da)

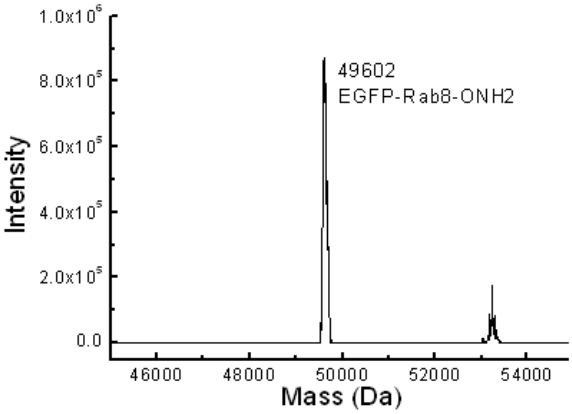
49602
EGFP-Rab8-ONH2
Intensity
Mass (Da)

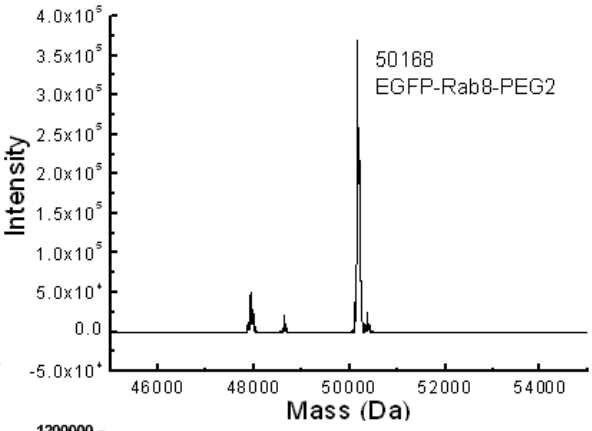
50168
EGFP-Rab8-PEG2
Intensity
Mass (Da)

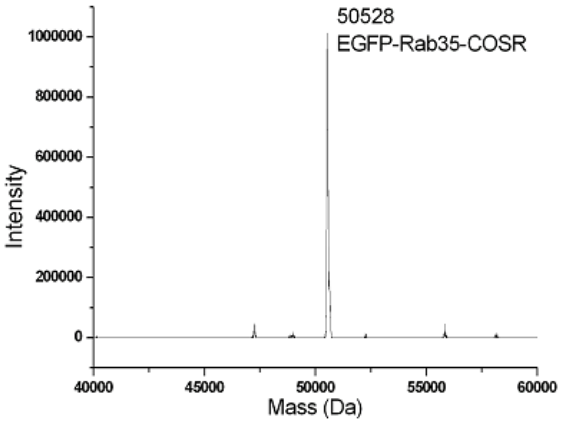
50528
EGFP-Rab35-COSR
Intensity
Mass (Da)

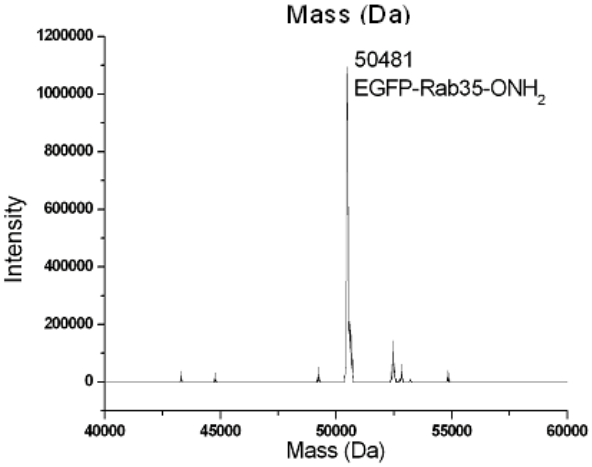
50481
EGFP-Rab35-ONH2
Intensity
Mass (Da)

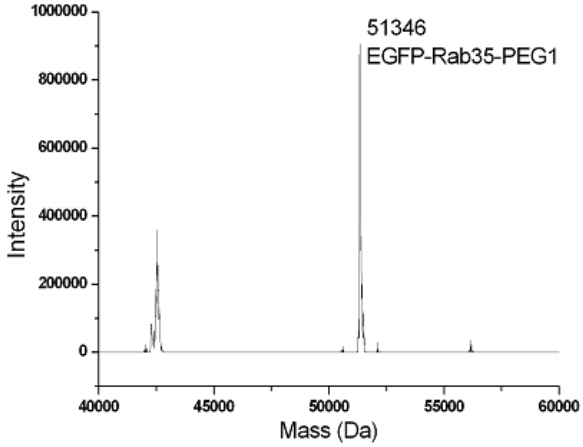
51346
EGFP-Rab35-PEG1
Intensity
Mass (Da)

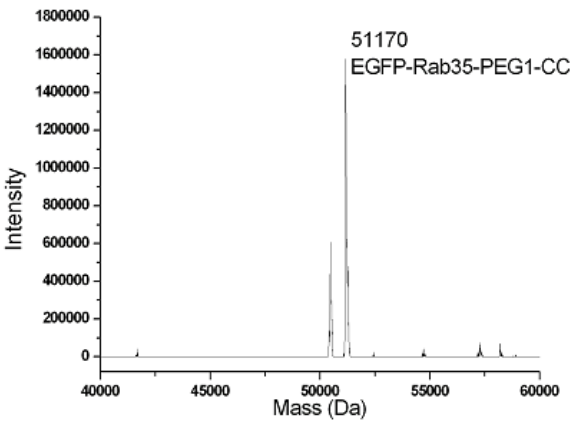
51170
EGFP-Rab35-PEG1-CC
Intensity
Mass (Da)

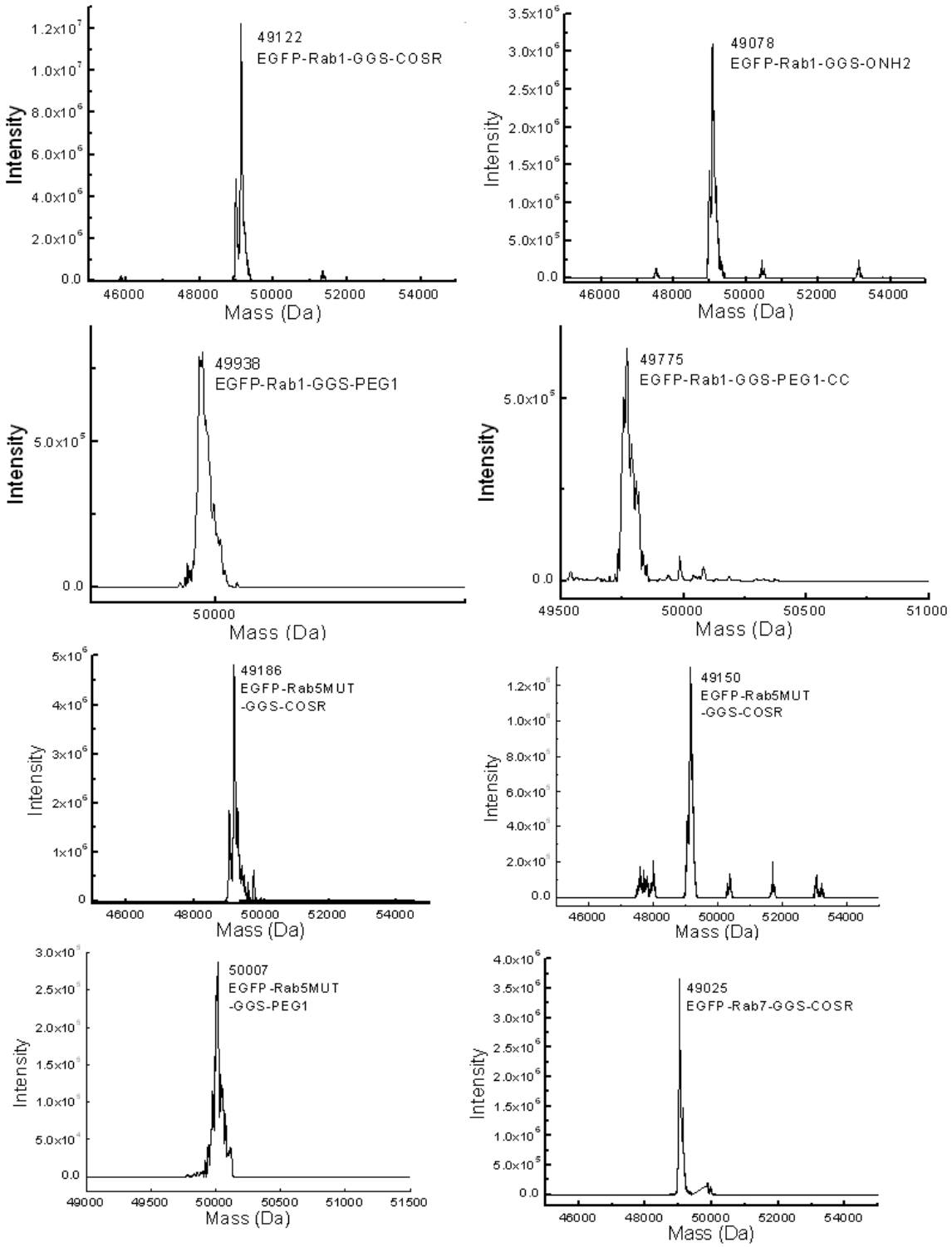
49122
EGFP-Rab1-GGS-COSR
49078
EGFP-Rab1-GGS-ONH2
49938
EGFP-Rab1-GGS-PEG1
49775
EGFP-Rab1-GGS-PEG1-CC
49186
EGFP-Rab5MUT
-GGS-COSR
49150
EGFP-Rab5MUT
-GGS-COSR
50007
EGFP-Rab5MUT
-GGS-PEG1
49025
EGFP-Rab7-GGS-COSR
Intensity
Mass (Da)

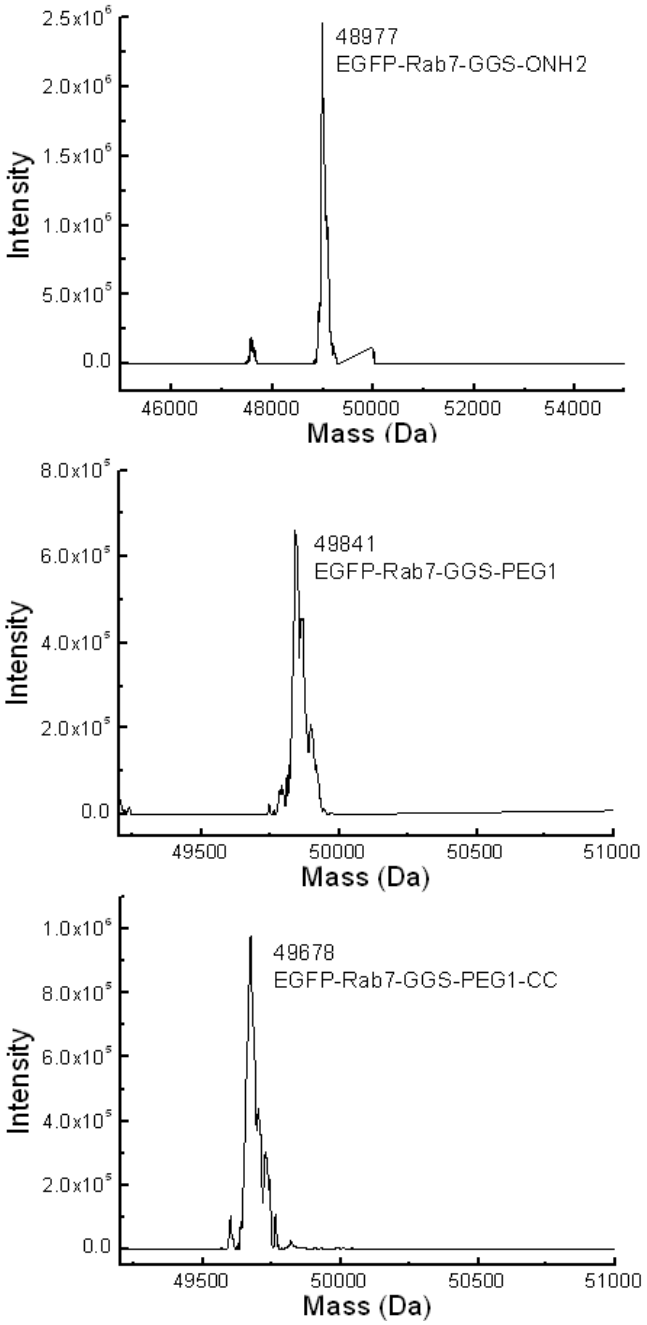
48977
EGFP-Rab7-GGS-ONH2
Intensity
Mass (Da)
49841
EGFP-Rab7-GGS-PEG1
Intensity
Mass (Da)
49678
EGFP-Rab7-GGS-PEG1-CC
Intensity
Mass (Da)

2. Kinetics of PEGylated proteins in cells

2-1. GFP-Rab1Δ31-GGS-PEG-CC

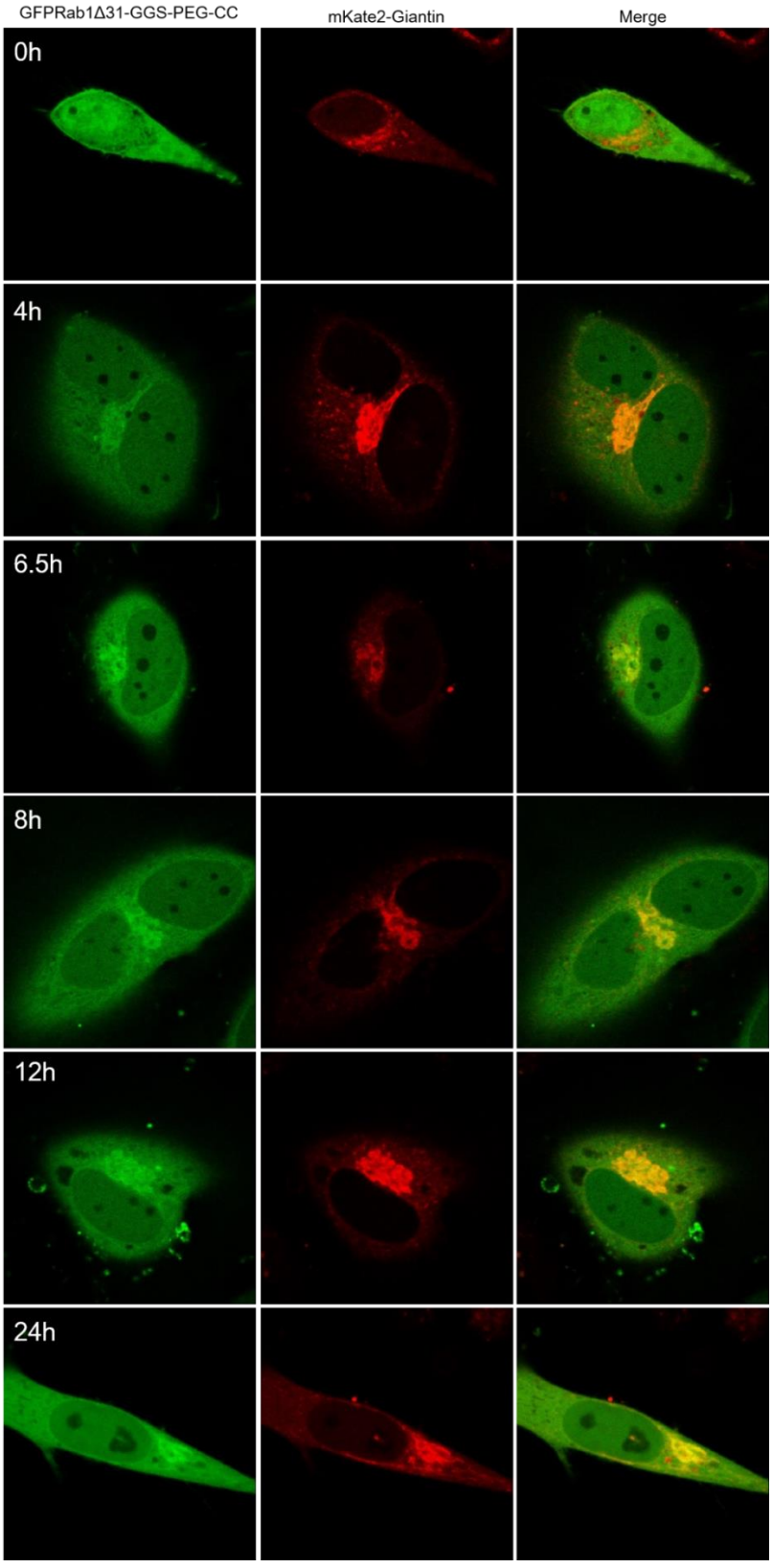

2-2. GFP-Rab5Q79LΔ35-(GGS)n-PEG-CC

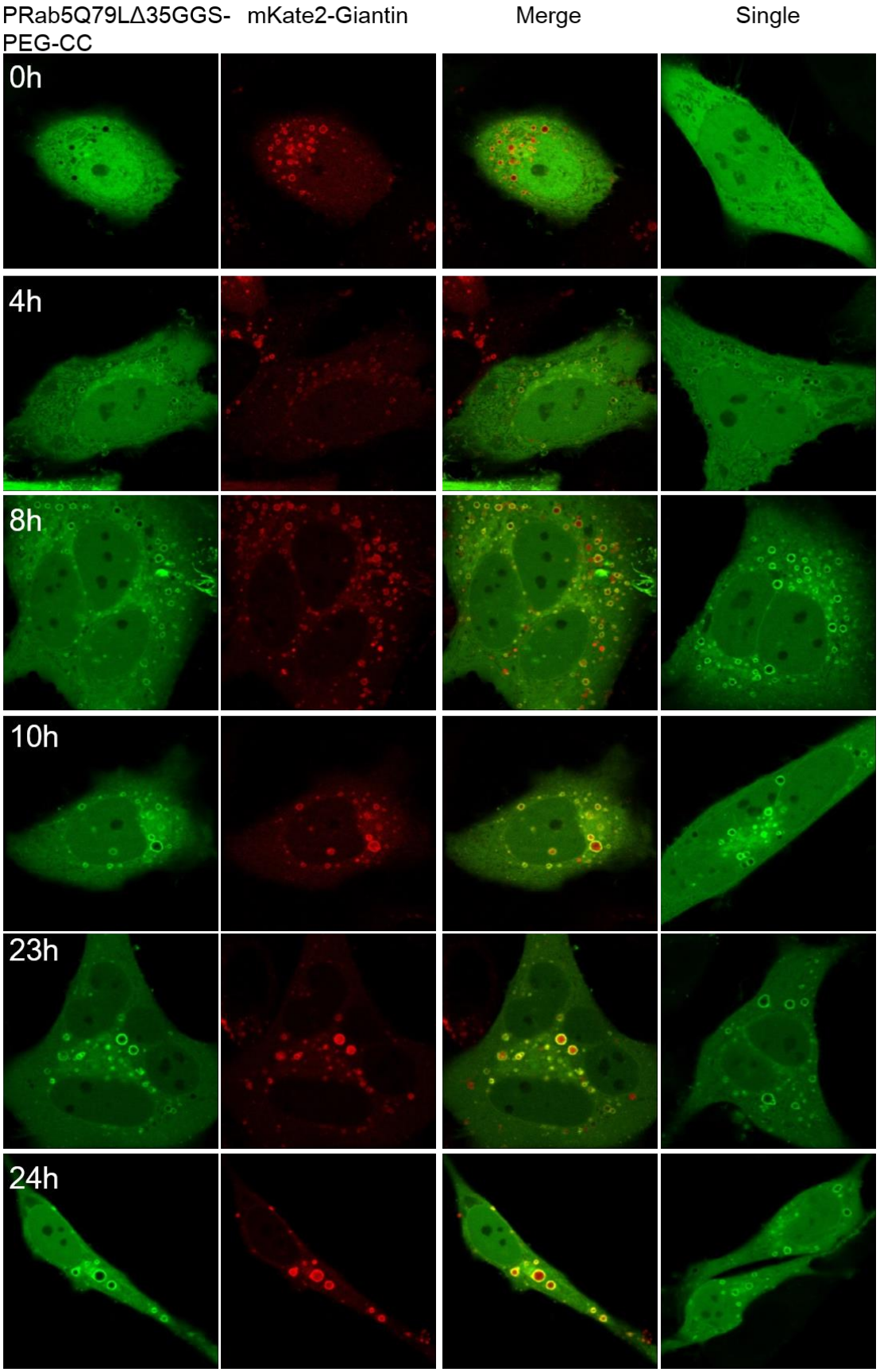

2-3. GFP-Rab7Δ34-(GGS)n-PEG-CC

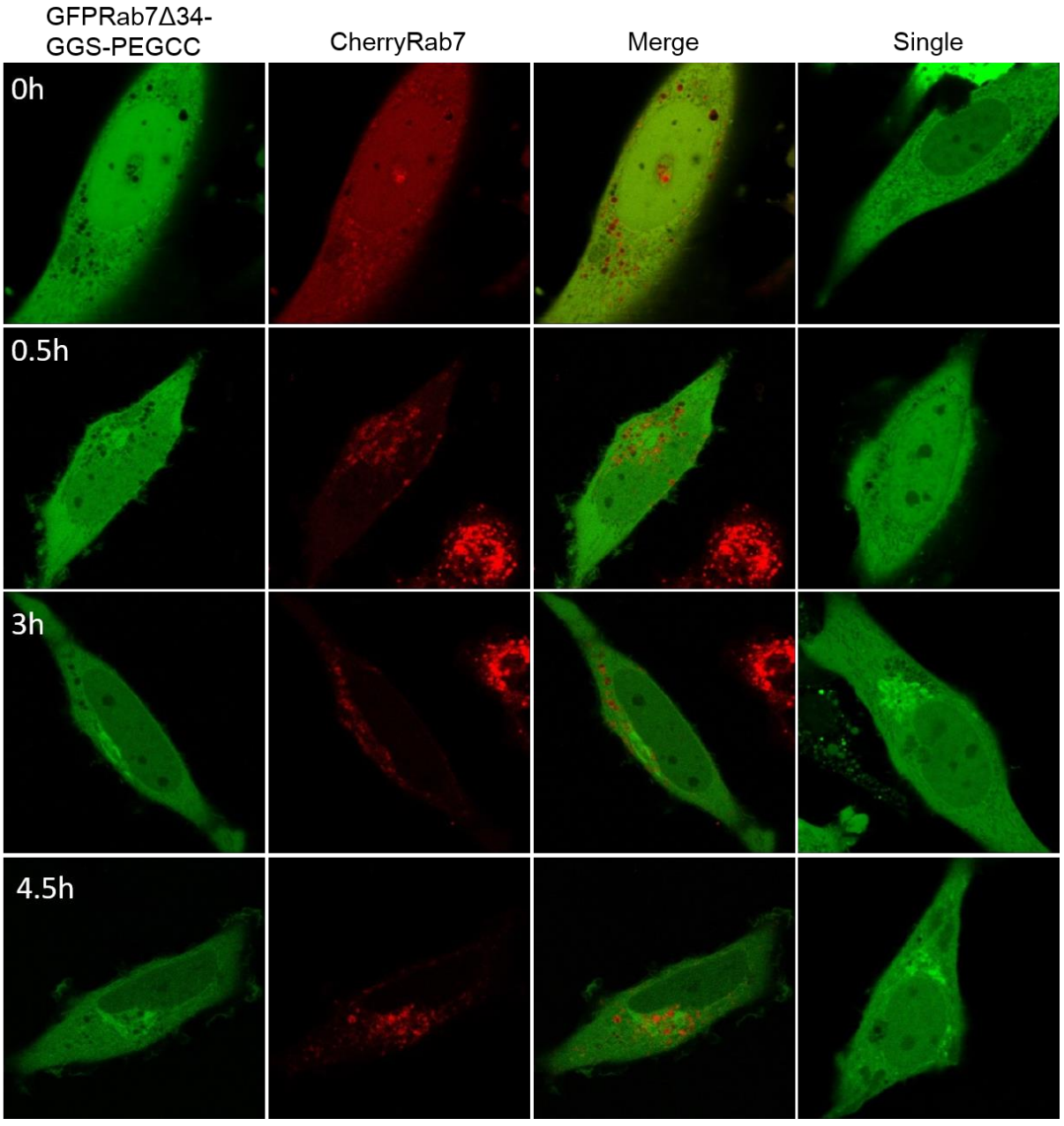

2-3. GFP-Rab7Δ34-(GGS)n-PEG-CC

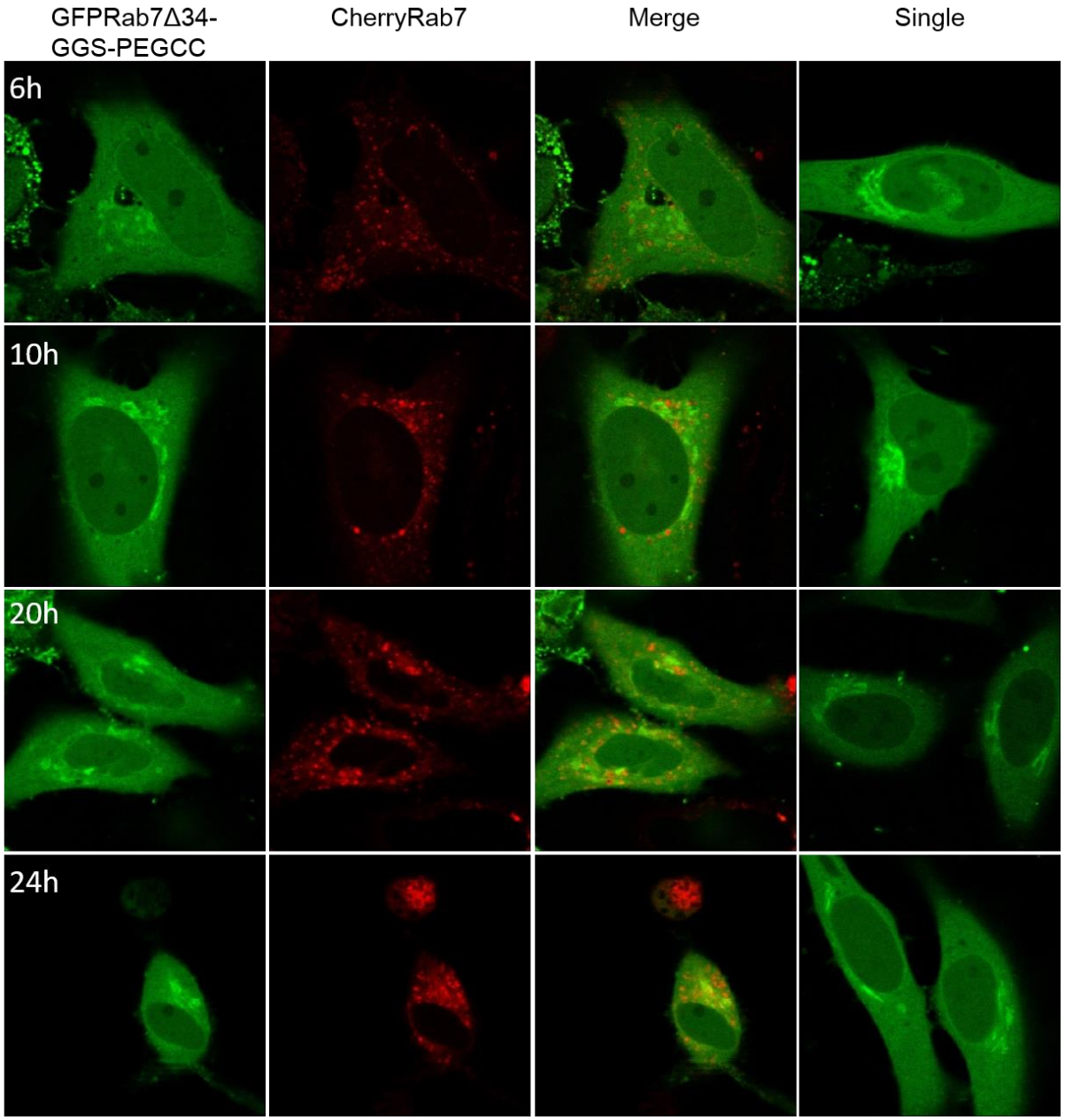

6 References:

Abdul-Ghani M, Gougeon P, Prosser D, Da-Silva L, Ngsee J. (2001). PRA isoforms are targeted to distinct membrane compartments. J Biol Chem 276, 6225–6233.

Ahmadian M, Stege P, Scheffzek K, Wittinghofer A. (1997). Confirmation of the arginine-finger hypothesis for the GAP-stimulated GTP-hydrolysis reaction of Ras. Nat Struct Biol 4, 686-689.

Aivazian D, Serrano R, Pfeffer S. (2006). TIP47 is a key effector for Rab9 localization. J Cell Biol 173,917–926.

Albert S and Gallwitz D. (1999). Two new members of a family of Ypt/Rab GTPase activating proteins. J Biol Chem 274, 33186-33189.

Albert S, Will E, Gallwitz D. (1999). Identification of the catalytic domains and their functionally critical arginine residues of two yeast GTPase-activating proteins specific for Ypt/Rab transport GTPases. EMBO J 18, 5216-5225.

Alexandrov K, Simon I, Iakovenko A, Holz B, Goody R, Scheidig A. (1998). Moderate discrimination of REP-1 between Rab7 x GDP and Rab7 x GTP arises from a difference of an order of magnitude in dissociation rates. FEBS Lett 425, 460-464.

Alexandrov K, Simon I, Yurchenko V, Iakovenko A, Rostkova E, Scheidig A, Goody,R. (1999). Characterization of the ternary complex between Rab7, REP-1 and Rab geranylgeranyl transferase. Eur J Biochem 265, 160-170.

Ali, B.R., Wasmeier, C., Lamoreux, L., Strom, M. and Seabra, M.C. (2004).Multiple regions contribute to membrane targeting of Rab GTPases.J Cell Sci 117, 6401–6412.

Allaire PD, Marat AL, Dall'Armi C, Di Paolo G, McPherson PS, Ritter B. (2010). The Connecdenn DENN domain: a GEF for Rab35 mediating cargo-specific exit from early endosomes. Mol Cell 37:370–382.

Allaire PD, Ritter B, Thomas S, Burman JL, Denisov AY, Legendre-Guillemin V, Harper SQ, Davidson BL, Gehring K, McPherson PS. (2006). Connecdenn, a novel DENN domain-containing protein of neuronal clathrin-coated vesicles functioning in synaptic vesicle endocytosis. J Neurosci 26:13202–13212.

Allaire PD, Seyed Sadr M, Chaineau M, Seyed Sadr E, Konefal S, Fotouhi M, Maret D, Ritter B, Del Maestro RF, McPherson PS. (2013). Interplay between Rab35 and Arf6 controls cargo recycling to coordinate cell adhesion and migration. J Cell Sci 126:722–731.

Anant J, Desnoyers L, Machius M, Demeler B, Hansen J, Westover K, Deisenhofer J, Seabra M. (1998). Mechanism of Rab geranylgeranylation: formation of the catalytic ternary complex. Biochemistry 37, 12559-12568.

Ang A, Fölsch H, Koivisto U, Pypaert M, Mellman I. (2003). The Rab8 GTPase selectively regulates AP-1B-dependent basolateral transport in polarized Madin-Darby canine kidney cells. J Cell Biol 163:339–350.

Ang A, Taguchi T, Francis S, Fölsch H, Murrells L, Pypaert M,Warren G, Mellman I. (2004). Recycling endosomes can serve as intermediates during transport from the Golgi to the plasma

membrane of MDCK cells. J Cell Biol 167, 531–543.

Argenzio E, Margadant C, Leyton-Puig D, Janssen H, Jalink K, Sonnenberg A, Moolenaar WH. (2014). CLIC4 regulates cell adhesion and beta1 integrin trafficking. J Cell Sci 127:5189–5203.

Ayuko Sakane, Kazufumi Honda, and Takuya Sasaki. (2010). Rab13 Regulates Neurite Outgrowth in PC12 Cells through Its Effector Protein, JRAB/MICAL-L2. Mol Cell Biol 30(4):1077-87

Bacon R, Salminen A, Ruohola H, Novick P, Ferro-Novick S. (1989). The GTP-binding protein Ypt1 is required for transport in vitro: the Golgi apparatus is defective in ypt1 mutants. J Cell Biol 109, 1015–1022.

Bahadoran P, Aberdam E, Mantoux F, Busca` R, Bille K, Yalman N, de Saint-Basile G, Casaroli-Marano R, Ortonne J, Ballotti R. (2001). Rab27a: a key to melanosome transport in human melanocytes. J Cell Biol 152: 843–850.

Barlowe C, Orci L, Yeung T, Hosobuchi M, Hamamoto S, Salama N, Rexach MF, Ravazzola M, Amherdt M, Schekman R. (1994). COPII: a membrane coat formed by Sec proteins that drive vesicle budding from the endoplasmic reticulum. Cell 77(6):895-907.

Barr F, Nakamura N, Warren G. (1998). Mapping the interaction between GRASP65 and GM130, components of a protein complex involved in the stacking of Golgi cisternae. EMBO J 17: 3258–3268.

Barr F. (2013). Rab GTPases and membrane identity: causal or inconsequential? J Cell Biol 202, 191–199.

Barrowman J, Bhandari D, Reinisch K, Ferro-Novick S. (2010). TRAPP complexes in membrane traffic: convergence through a common Rab. Nat Rev Mol Cell Biol 11: 759–763.

Barrowman J, Wang W, Zhang Y Ferro-Novick S. (2003). The Yip1p–Yif1p complex is required for the fusion competence of endoplasmic reticulum-derived vesicles. J Biol Chem 278, 19878-19884.

Bayer M, Venkitaraman AR, Wittinghofer A, Bastiaens PI. (2011). The GDI-like solubilizing factor PDEδ sustains the spatial organization and signalling of Ras family proteins. Nat Cell Biol 14(2):148-58.

Ben El Kadhi K, Roubinet C, Solinet S, Emery G, Carréno S. (2011). The inositol 5-phosphatase OCRL controls PI(4,5)P2 homeostasis and is necessary for cytokinesis. Curr Biol 21, 1074–1079.

Benli M, Döring F, Robinson D, Yang X, Gallwitz D. (1996). Two GTPase isoforms, Ypt31p and Ypt32p, are essential for Golgi function in yeast. EMBO J 15: 6460–6475.

Benmerah A, Lamaze C. (2007). Clathrin-coated pits: vive la difference? Traffic 8: 970–982.

Beranger F, Paterson H, Powers S, de Gunzburg J, Hancock JF. (1994). The effector domain of Rab6, plus a highly hydrophobic C terminus, is required for Golgi apparatus localization. Mol Cell Biol 14(1):744–758.

Bergo MO, Leung GK, Ambroziak P, Otto JC, Casey PJ, Gomes AQ, Seabra MC, Young SG.. (2001) Isoprenylcysteine carboxyl methyltransferase deficiency in mice. J Biol Chem

276(8):5841–5845.

Blümer J, Rey J, Dehmelt L, Mazel T, Wu YW, Bastiaens P, Goody RS, Itzen A.(2013). RabGEFs are a major determinant for specific Rab membrane targeting.J Cell Biol 200(3):287-300.

Bock, J.B, Matern, H.T, Peden, A.A, and Scheller, R.H. (2001). A genomic perspective on membrane compartment organization. Nature 409: 839–841.

Bonifacino J, Glick B. (2004).The mechanisms of vesicle budding and fusion. 116:153-166.

Bonifacino J, Lippincott-Schwartz J. (2003). Coat proteins: shaping membrane transport. Nat Rev Mol Cell Biol 4, 409–414.

Bonifacino J, Traub L. (2003). Signals for sorting of transmembrane proteins to endosomes and lysosomes. Annu Rev Biochem 72, 395–447.

Boriack-Sjodin P, Margarit S, Bar-Sagi D, Kuriyan J. (1998). The structural basis of the activation of Ras by Sos. Nature 394, 337–343.

Bos J, Rehmann H, Wittinghofer A. (2007). GEFs and GAPs: Critical Elements in the Control of Small G Proteins. Cell 29, 865-877.

Bourne H, Sanders D, and McCormick F. (1991). The GTPase Superfamily-Conserved Structureand Molecular Mechanism. Nature 349, 117-127.

Bravo-Cordero J, Marrero-Diaz R, Megías D, Genís L, García-Grande A, García M. (2007). MT1-MMP proinvasive activity is regulated by a novel Rab8-dependent exocytic pathway. EMBO J 26, 1499–510.

Bucci, C., Chiariello, M., Lattero, D., Maiorano, M. & Bruni, C. B. (1999). Interaction cloning and characterization of the cDNA encoding the human prenylated Rab acceptor (PRA1). Biochem Biophys Res Commun 258(3):657-62.

Burton J, Roberts D, Montaldi M, Novick P, De Camilli P. (1993). A mammalian guanine nucleotide-releasing protein enhances function of yeast secretory protein Sec4. Nature 361: 464–467.

Cabrera M, Ostrowicz C, Mari M, LaGrassa T, Reggiori F,Ungermann C. (2009). Vps41 phosphorylation and the Rab Ypt7 control the targeting of the HOPS complex to endosome-vacuole fusion sites. Mol Biol Cell 20, 1937–1948.

Cai Y, Chin HF, Lazarova D, Menon S, Fu C, Cai H, Sclafani A, Rodgers DW, De La Cruz EM, Ferro-Novick S, Reinisch KM. (2008). The structural basis for activation of the Rab Ypt1p by the TRAPP membrane-tethering complexes. Cell 133(7):1202-13.

Caldwell K, Caldwell G, Marsischky G, Kolodner R, Labaer J, Rochet J, Bonini N,Lindquist S. (2006). α-synuclein blocks ER-Golgi traffic and Rab1 rescues neuron loss in Parkinson's models. Science 313: 324–328.

Calero, M., Winand, N. J. & Collins, R. N. (2002). Identification of the novel proteins Yip4p and Yip5p as Rab GTPase interacting factors. FEBS Lett 515, 89–98.

Calmels TP, Callebaut I, Leger I, Durand P, Bril A, Mornon JP, Souchet M. (1998). Sequence and

3D structural relationships between mammalian Ras- and Rho-specific GTPase activating proteins (GAPs): the cradle fold. FEBS Lett 426: 205–211.

Carlton J, Bujny M, Rutherford A, Cullen P. (2005). Sorting nexins–unifying trends and new perspectives. Traffic 6: 75–82.

Carney DS, Davies BA, Horazdovsky BF. (2006). Vps9 domain-containing proteins: activators of Rab5 GTPases from yeast to neurons. Trends Cell Biol 16: 27–35.

Carroll KS, Hanna J, Simon I, Krise J, Barbero P, Pfeffer SR. (2001). Role of Rab9 GTPase in facilitating receptor recruitment by TIP47. Science 292(5520):1373–1376.

Casanova J, Wang X, Kumar R, Bhartur S, Navarre J, Woodrum J, Altschuler Y, Ray G, Goldenring J. (1999). Association of Rab25 and Rab11a with the apical recycling system of polarized Madin-Darby canine kidney cells. Mol Biol Cell 10, 47–61.

Casey P, Seabra M. (1996). Protein prenyltransferases. J Biol Chem 271, 5289-5292.

Caswell P, Spence H, Parsons M, White D, Clark K, Cheng K, Mills G, Humphries M, Messent A, Anderson K, McCaffrey M, Ozanne B, Norman J. (2007). Rab25 associates with alpha5beta1 integrin to promote invasive migration in 3D microenvironments. Dev Cell 13, 496–510.

Cauvin C, Rosendale M, Gupta-Rossi N, Rocancourt M, Larraufie P, Salomon R, Perrais D, Echard A. (2016).Rab35 GTPase triggers switch-like recruitment of the Lowe syndrome lipid phosphatase OCRL on newborn endosomes. Curr Biol 26:120–128.

Chandra A, Grecco HE, Pisupati V, Perera D, Cassidy L, Skoulidis F, Ismail SA, Hedberg C, Hanzal-
Charnas LR, Gahl WA. (1991). The oculocerebrorenal syndrome of Lowe. Adv Pediatr 38: 75–107.

Charrasse S, Comunale F, De Rossi S, Echard A, Gauthier-Rouviere C. (2013). Rab35 regulates cadherin-mediated adherens junction formation and myoblast fusion. Mol Biol Cell 24:234–245.

Chavrier, P., J.P. Gorvel, E. Stelzer, K. Simons, J. Gruenberg, and M. Zerial. (1991). Hypervariable C-terminal domain of Rab proteins acts as a targeting signal. Nature 353:769–772.

Chavrier, P., R.G. Parton, H.P. Hauri, K. Simons, and M. Zerial. (1990). Localization of low molecular weight GTP binding proteins to exocytic and endocytic compartments. Cell 62:317–329.

Chen C, Balch W. (2006). The Hsp90 chaperone complex regulates GDI dependent Rab recycling. Mol Biol Cell 17: 3494–3507.

Chen W, Moomaw J, Overton, Kost T, Casey P. (1993). High level expression of mammalian protein farnesyltransferase in a baculovirus system. J Biol Chem 268, 9675-9680.

Cheng K, Lahad J, Kuo W, Lapuk A, Yamada K, Auersperg N,Liu J, Smith-McCune K, Lu K, Fishman D, Gray J, Mills G. (2004). The RAB25 small GTPase determines aggressiveness of ovarian and breast cancers. Nat Med 10, 1251–1256.

Cherfils J, Zeghouf M. (2013). Regulation of small GTPases by GEFs, GAPs, and GDIs. Physiol Rev 93(1):269-309.

Chesneau L, Dambournet D, Machicoane M, Kouranti I, Fukuda M, Goud B, Echard A. (2012). An ARF6/Rab35 GTPase cascade for endocytic recycling and successful cytokinesis. Curr Biol, 22:147-153.

Chevallier J, Koop C, Srivastava A, Petrie RJ, Lamarche-Vane N, Presley JF. (2009). Rab35 regulates neurite outgrowth and cell shape. FEBS Lett 583:1096–1101.

Chia PZ, Gleeson PA. (2014). Membrane tethering. F1000Prime Rep, 6:74.

Chial HJ, Wu R, Ustach CV, McPhail LC, Mobley WC, Chen YQ. (2008). Membrane targeting by APPL1 and APPL2: dynamic scaffolds that oligomerize and bind phosphoinositides.Traffic 9(2):215-29.

Chong S, Mersha FB, Comb DG, Scott ME, Landry D, Vence LM, Perler FB, Benner J, Kucera RB, Hirvonen CA, Pelletier JJ, Paulus H, Xu MQ. (1997). Single-column purification of free recombinant proteins using a self-cleavable affinity tag derived from a protein splicing element. Gene 192, 271-281.

Choudhury R, Diao A, Zhang F, Eisenberg E, Saint-Pol A, Williams C, Konstantakopoulos A, Lucocq J, Johannes L, Rabouille C, Greene LE, Lowe M. (2005). Lowe syndrome protein OCRL1 interacts with clathrin and regulates protein trafficking between endosomes and the trans-Golgi network. Mol Biol Cell 16:3467–3479.

Choudhury R, Noakes CJ, McKenzie E, Kox C, Lowe M. (2009). Differential clathrin binding and subcellular localization of OCRL1 splice isoforms. J Biol Chem 284: 9965–9973.

Christensen EI, Birn H. (2002). Megalin and cubilin: multifunctional endocytic receptors. Nat Rev Mol Cell Biol 3: 256–266.

Christoforidis S, McBride HM, Burgoyne RD, Zerial M. (1999a). The Rab5 effector EEA1 is a core component of endosome docking. Nature 397(6720):621–625.

Christoforidis S, Miaczynska M, Ashman K, Wilm M, Zhao L,Yip S, Waterfield M, Backer J, Zerial M. (1999). Phosphatidylinositol-3-OH kinases are Rab5 effectors. Nat Cell Biol 1: 249–252.

Constantinescu, A. T., Rak, A., Alexandrov, K., Esters, H., Goody, R. S., and Scheidig, A. J. (2002). Rab-subfamily-specific regions of Ypt7p are structurally different from other RabGTPases. Structure 10, 569–579.

Cooper A, Gitler A, Cashikar A, Haynes C, Hill K, Bhullar B,Liu K, Xu K, Strathearn K, Liu F, Cao S,
Cremers, F.P.M., Armstrong, S.A., Seabra, M.C., Brown, M.S., and Goldstein, J.L. (1994). Rep-2, a Rab Escort Protein encoded by the choroideremia-like gene. J Biol Chem 269, 2111-2117.

Cui S , Guerriero CJ, Szalinski CM, Kinlough CL, Hughey RP, Weisz OA. (2010). OCRL1 function in renal epithelial membrane traffic.Am J Physiol Renal Physiol 298(2):F335-45.

Dalfó E, Gómez-Isla T, Rosa J, Nieto Bodelón M, Cuadrado Tejedor M, Barrachina M, Ambrosio S, Ferrer I. (2004). Abnormal alpha-synuclein interactions with Rab proteins in alpha-synuclein A30P transgenic mice. J Neuropathol Exp Neurol 63: 302–313.

Dambournet D, Machicoane M, Chesneau L, Sachse M, Rocancourt M, El Marjou A, Formstecher E, Salomon R, Goud B, Echard A. (2011). Rab35 GTPase and OCRL phosphatase remodel lipids and F-actin for successful cytokinesis. Nat Cell Biol 13:981–988.

Davey JR, Humphrey SJ, Junutula JR, Mishra AK, Lambright DG, James DE, Stockli J. (2012). TBC1D13 is a Rab35 specific gap that plays an important role in GLUT4 trafficking in adipocytes. Traffic13:1429-1441.

De Renzis S, Sönnichsen B, Zerial M. (2002). Divalent Rab effectors regulate the sub-compartmental organization and sorting of early endosomes. Nat Cell Biol 4, 124–133.

Deepa SS, Dong LQ. (2009). APPL1: role in adiponectin signaling and beyond. Am J Physiol Endocrinol Metab, 296(1):E22-36.

Del Toro D, Alberch J, Lázaro-Diéguez F, Martín-Ibáñez R, Xifró X, Egea G, Canals J. (2009). Mutant huntingtin impairs post-Golgi trafficking to lysosomes by delocalizing optineurin/Rab8 complex from the Golgi apparatus. Mol Biol Cell 20: 1478–1492.

Delprato, A., Merithew, E. & Lambright, D. G. (2004). Structure, exchange determinants, and family-wide Rab specificity of the tandem helical bundle and Vps9 domains of Rabex-5. Cell 118, 607–617.

Diao A, Frost L, Morohashi Y, Lowe M. (2008). Coordination of golgin tethering and SNARE assembly: GM130 binds syntaxin 5 in a p115-regulated manner. J Biol Chem. 283(11):6957-67.

Díaz E, Pfeffer S. (1998). TIP47: a cargo selection device for mannose 6-phosphate receptor trafficking. Cell 93: 433–443.

Diekmann Y, Seixas E, Gouw M, Tavares-Cadete F, Seabra MC, Pereira-Leal JB.(2011). Thousands of rab GTPases for the cell biologist.PLoS Comput Biol 2011, 7(10):e1002217.

DiFiglia M, Sapp E, Chase K, Schwarz C, Meloni A, Young C, Martin E, Vonsattel J, Carraway R, Reeves S. (1995). Huntingtin is a cytoplasmic protein associated with vesicles in human and rat brain neurons. Neuron 14: 1075–1081.

Dikshit N, Bist P, Fenlon SN, Pulloor NK, Chua CE, Scidmore MA, Carlyon JA, Tang BL, Chen SL, Sukumaran B. (2015). Intracellular uropathogenic E. coli exploits host Rab35 for iron acquisition and survival within urinary bladder cells. PLoS Pathog 11:e1005083.

Dirac-Svejstrup A, Sumizawa T, Pfeffer S. (1997). Identification of a GDI displacement factor that releases endosomal Rab GTPases from Rab-GDI. EMBO J 16: 465–472.

Dong B, Kakihara K, Otani T, Wada H, Hayashi S. (2013). Rab9 and retromer regulate retrograde trafficking of luminal protein required for epithelial tube length control. Nat Commun 4:1358.

Dressman MA, Olivos-Glander IM, Nussbaum RL, Suchy SF. (2000). Ocrl1, a PtdIns(4,5)P2 5-phosphatase, is localized to the trans-Golgi network of fibroblasts and epithelial cells. J Histochem Cytochem 48: 179–190.

Dutta D, Donaldson JG. (2015). Sorting of undependent cargo proteins depends on Rab35 delivered by clathrin-mediated endocytosis. Traffic 16:994–1009.

Eathiraj S, Pan X, Ritacco C, Lambright DG. (2005). Structural basis of family-wide Rab GTPase recognition by rabenosyn-5. Nature 436(7049):415–419.

Echard A, Hickson GR, Foley E, O'Farrell PH. (2004). Terminal cytokinesis events uncovered after an RNAi screen. Curr Biol 14:1685–1693.

Echard A, Jollivet F, Martinez O, Lacapère J, Rousselet A, Janoueix-Lerosey I, Goud B. (1998). Interaction of a Golgi-associated kinesin-like protein with Rab6. Science 279: 580–585.

Edeling, M. A., Smith, C., and Owen, D. (2006). Life of a clathrin coat: insights from clathrin and AP structures. Nat. Rev. Mol. Cell Biol. *7*, 32-44.

Egami Y, Fukuda M, Araki N. (2011). Rab35 regulates phagosome formation through recruitment of ACAP2 in macrophages during FcgammaR-mediated phagocytosis. J Cell Sci 124: 3557–3567.

Erdmann KS, Mao Y, McCrea HJ, Zoncu R, Lee S, Paradise S, Modregger J, Biemesderfer D, Toomre D, De Camilli P.(2007). A role of the Lowe syndrome protein OCRL in early steps of the endocytic pathway. Dev Cell 13: 377–390.

Etoh K, Fukuda M. (2015). Structure-function analyses of the small GTPase Rab35 and its effector protein Centaurin- eta2/ACAP2 during neurite outgrowth of PC12 cells. J Biol Chem 290:9064–9074.

Evans T, Benner J, Xu M. (1999). The cyclization and polymerization of bacterially expressed proteins using modified self-splicing inteins. J Biol Chem 274, 18359-18363.

Faber P, Barnes G, Srinidhi J, Chen J, Gusella J, MacDonald M. (1998). Huntingtin interacts with a family of WW domain proteins. Hum Mol Genet 7: 1463–1474.

Farnsworth C, Gelb M, Glomset J. (1990). Identification of geranylgeranyl-modified proteins in HeLa cells. Science 247, 320-322.

Farnsworth C, Wolda S, Gelb M, Glomset J. (1989). Human lamin B contains a farnesylated cysteine residue. J Biol. Chem 264, 20422-20429.

Fasshauer D, Bruns D, Shen B, Jahn R, Brunger A. (1997). A structural change occurs upon binding of syntaxin to SNAP-25. J Biol Chem 272, 4582-4590.

Fasshauer D, Sutton R, Brunger, A, Jahn R. (1998). Conserved structural features of the synaptic fusion complex (SNARE proteins reclassified as Q- and R-SNAREs) .Proc Natl Acad Sci 95, 15781–15786.

Faucherre A, Desbois P, Satre V, Lunardi J, Dorseuil O, Gacon G. (2003). Lowe syndrome protein OCRL1 interacts with Rac GTPase in the trans-Golgi network. Hum Mol Genet, 12(19):2449-56.

Forno L. Neuropathology of Parkinson's disease. (1996). J Neuropathol Exp Neurol 55, 259–272.

Fotin A, Cheng Y, Grigorieff N, Walz T, Harrison SC, Kirchhausen T.(2004). Structure of an auxilin-bound clathrin coat and its implications for the mechanism of uncoating.Nature 432(7017):649-53.

Fotin, A., Cheng, Y.F., Sliz, P., Grigorieff, N., Harrison, S. C., Kirchhausen, T., and Walz, T.

(2004b). Molecular model for a complete clathrin lattice from electron cryomicroscopy. Nature 432, 573-579.

Frasa MA, Koessmeier KT, Ahmadian MR, Braga VM. (2012). Illuminating the functional and structural repertoire of human TBC/RABGAPs. Nat Rev Mol Cell Biol 13(2), 67-73.

Frost A, Perera R, Roux A, Spasov K, Destaing O, Egelman E,De Camilli P, Unger V. (2008). Structural basis of membrane invagination by F-BAR domains. Cell 132, 807–817.

Fuchs E, Haas AK, Spooner RA, Yoshimura S, Lord JM, Barr FA. (2007). Specific Rab GTPase-activating proteins define the Shiga toxin and epidermal growth factor uptake pathways. J Cell Biol 177:1133–1143.

Fujimura, K., Tanaka, K., Nakano, A., and Tohe, A. (1994). The saccharomyces-cerevisiae Msi4 gene encodes the yeast counterpart of component-a of Rab geranylgeranyltransferase. J Biol Chem 269, 9205-9212.

Fukuda M. (2011). TBC proteins: GAPs for mammalian small GTPase Rab? Biosci Rep 31:159–168.

Galvez T, Gilleron J, Zerial M, O'Sullivan GA. (2012). SnapShot: mammalian Rab proteins in endocytic trafficking. Cell 151, 234–234.

Gao Y, Balut CM, Bailey MA, Patino-Lopez G, Shaw S, Devor DC. (2010). Recycling of the Ca2+-activated K+ channel, KCa2.3, is dependent upon RME-1, Rab35/EPI64C, and an N-terminal domain.

Gasser T. (2009). Molecular pathogenesis of Parkinson disease: insights from genetic studies. Expert Rev Mol Med 11: e22.

Gavriljuk K, Itzen A, Goody RS, Gerwert K, Kotting C. (2013). Membrane extraction of Rab proteins by GDP dissociation inhibitor characterized using attenuated total reflection infrared spectroscopy. Proc Natl Acad Sci 110:13380–13385.

Patterson GH, Lippincott-Schwartz J. (2002). A photoactivatable GFP for selective photolabeling of proteins and cells. Science 297(5588):1873-7.

Gil J, Rego A. (2008). Mechanisms of neurodegeneration in Huntington's disease. Eur J Neurosci 27: 2803–2820.

Girard M, Allaire PD, McPherson PS, Blondeau F. (2005). Non-stoichiometric relationship between clathrin heavy and light chains revealed by quantitative comparative proteomics of clathrin-coated vesicles from brain and liver. Mol Cell Proteomics 4:1145–1154.

Giridharan SS, Caplan S. (2013). MICAL-family proteins: complex regulators of the actin cytoskeleton. Antioxid Redox Signal 20:2059–2073.

Gitler A, Bevis B, Shorter J, Strathearn K, Hamamichi S, Su L, Caldwell K, Caldwell G, Rochet J, Glomset J A, Gelb M H, Farnsworth C C. (1990). Prenyl proteins in eukaryotic cells: a new type of membrane anchor. Trends Biochem Sci 15, 139-142.

Goedert M. (1998). Neurofibrillary pathology of Alzheimer's disease and other tauopathies. Prog Brain Res 117: 287–306.

Goitre L, Trapani E, Trabalzini L, Retta SF. (2014). The Ras superfamily of small GTPases: the unlocked secrets. Methods Mol Biol 1120:1-18.

Goldenring J, Shen K, Vaughan H, Modlin I. (1993). Identification of a small GTP-binding protein, Rab25, expressed in the gastrointestinal mucosa, kidney, lung. J Biol Chem 268, 18419–18422.

Gomes AQ, Ali BR, Ramalho JS, Godfrey RF, Barral DC, Hume AN, Seabra MC. (2003). Membrane targeting of Rab GTPases is influenced by the prenylation motif. Mol Biol Cell 14(5):1882–1899.

Goody R, Rak A, Alexandrov K. (2005). The structural and mechanistic basis for recycling of Rab proteins between membrane compartments. Cell Mol Life Sci 62: 1657–1670.

Goud B, Salminen A, Walworth N, Novick P. (1988). A GTP-binding protein required for secretion rapidly associates with secretory vesicles and the plasma membrane in yeast. Cell 53: 753–768.

Grant BD, Donaldson JG. Pathways and mechanisms of endocytic recycling. (2009). Nat Rev Mol Cell Biol 10:597–608.

Grieve AG, Daniels RD, Sanchez-Heras E, Hayes MJ, Moss SE, Matter K, Lowe M, Levine TP. (2011). Lowe Syndrome protein OCRL1 supports maturation of polarized epithelial cells. PLoS One 6(8): e24044.

Grigoriev I, Splinter D, Keijzer N, Wulf P, Demmers J, Ohtsuka T, Modesti M, Maly I, Grosveld F, Hoogenraad C, Akhmanova A. (2007). Rab6 regulates transport and targeting of exocytotic carriers. Dev Cell 13: 305–314.

Guignot J, Caron E, Beuzón C, Bucci C, Kagan J, Roy C, Holden D. (2004). Microtubule motors control membrane dynamics of Salmonella-containing vacuoles. J Cell Sci 117: 1033–1045.

Guo W, Roth D, Walch-Solimena C, Novick P. (1999). The exocyst is an effector for Sec4p, targeting secretory vesicles to sites of exocytosis. EMBO J 18: 1071–1080.

Gurkan C, Stagg S, LaPointe P, Balch W. (2006). The COPII cage: unifying principles of vesicle coat assembly. Nat. Rev. Mol Cell Biol *7*, 727-738.

Haas A, Fuchs E, Kopajtich R, Barr F. (2005). A GTPase-activating protein controls Rab5 function in endocytic trafficking. Nat Cell Biol 7, 887–893.

Hales C, Vaerman J, Goldenring J. (2002). Rab11 family interacting protein 2 associates with Myosin Vb and regulates plasma membrane recycling. J Biol Chem 277: 50415–50421.

Hanono A, Garbett D, Reczek D, Chambers DN, Bretscher A. (2006). EPI64 regulates microvillar subdomains and structure. J Cell Biol 175:803–813.

Hanson P, Roth R, Morisaki H, Jahn R, Heuser J. (1997). Structure and conformational changes in NSF and its membrane receptor complexes visualized by quick-freeze/deep-etch electron microscopy. Cell 90, 523–535.

Hanzal-Bayer M, Renault L, Roversi P, Wittinghofer A, Hillig RC. (2002). The complex of Arl2-GTP and PDE delta: from structure to function. EMBO J 21: 2095–2106.

Hanzal-Bayer M, Venkitaraman AR, Wittinghofer A, Bastiaens PI. (2011). The GDI like solubilizing factor PDEdelta sustains the spatial organization and signalling of Ras family proteins. Nat Cell Biol 14(2):148-58.

Harrison R, Brumell J, Khandani A, Bucci C, Scott C, Jiang X, Finlay B, Grinstein S. (2004). Salmonella impairs RILP recruitment to Rab7 during maturation of invasion vacuoles. Mol Biol Cell 15:3146–154.

Hartman H, Hicks K, Fierke C. (2005). Peptide specificity of protein prenyltransferases is determined mainly by reactivity rather than binding affinity. Biochemistry 44, 15314-15324.

Hattula K, Peränen J. (2000). FIP-2, a coiled-coil protein, links Huntingtin to Rab8 and modulates cellular morphogenesis. Curr Biol 10, 1603–1606.

Haubruck H, Prange R, Vorgias C, Gallwitz D. (1989). The Ras-related mouse ypt1 protein can functionally replace the YPT1 gene product in yeast. EMBO J 8(5):1427-32.

Hendrix A, Maynard D, Pauwels P, Braems G, Denys H, Van den Broecke R,Lambert J, Van Belle S, Cocquyt V, Gespach C, Bracke M, Seabra M, Gahl W, De Wever O, Westbroek W. (2010). Effect of the secretory small GTPase Rab27B on breast cancer growth, invasion, and metastasis. J Natl Cancer Inst 102, 866–80.

Henley JR, Cao H, McNiven MA. (1999). Participation of dynamin in the biogenesis of cytoplasmic vesicles. FASEB J.13: S243-7.

Heo WD, Inoue T, Park WS, Kim ML, Park BO, Wandless TJ, Meyer T. (2006). PI(3,4,5)P3 and PI(4,5)P2 lipids target proteins with polybasic clusters to the plasma membrane. Science 314:1458–1461.

Hichri H, Rendu J, Monnier N, Coutton C, Dorseuil O, Poussou RV, Baujat G, Blanchard A, Nobili F, Ranchin B, Remesy M, Salomon R, Satre V, Lunardi J. (2011). From Lowe syndrome to Dent disease: correlations between mutations of the OCRL1 gene and clinical and biochemical phenotypes. Hum Mutat 32(4):379-88.

Hill E, Clarke M, Barr F. (2000). The Rab6-binding kinesin, Rab6-KIFL, is required for cytokinesis. EMBO J 19: 5711–5719.

Ho L, Carmichael J, Swartz J, Wyttenbach A, Rankin J, Rubinsztein D. (2001). The molecular biology of Huntington's disease. Psychol Med 31, 3-14.

Hong W. (2005). SNAREs and traffic. Biochim Biophys Acta 1744, 120-144.

Höning S, Ricotta D, Krauss M, Späte K, Spolaore B, Motley A, Robinson M, Robinson C, Haucke V, Owen D. (2005). Phosphatidylinositol-(4,5)-bisphosphate regulates sorting signal recognition by the clathrin-associated adaptor complex AP2. Mol Cell 18: 519–531.

Horazdovsky B, Davies B, Seaman M, McLaughlin S, Yoon S, Emr S. (1997). A sorting nexin-1 homologue, Vps5p, forms a complex withVps17p and is required for recycling the vacuolar protein-sorting receptor. Mol Biol Cell 8, 1529–1541.

Horiuchi H, Lippe' R, McBride HM, Rubino M, Woodman P, Stenmark H, Rybin V, Wilm M, Ashman K, Mann M, Zerial M. (1997). A novel Rab5 GDP/GTP exchange factor complexed toRabaptin-5 links nucleotide exchange to effector recruitment and function. Cell 90, 1149–1159.

Hou Q, Wu Y, Grabsch H, Zhu Y, Leong S, Ganesan K, Cross D, Tan L, Tao J, Gopalakrishnan V, Tang B, Kon O, Tan P. (2008). Integrative genomics identifies RAB23 as an invasion mediator gene in diffuse-type gastric cancer. Cancer Res 68, 4623–30.

Hsu C, Morohashi Y, Yoshimura S, Manrique-Hoyos N, Jung S, Lauterbach MA, Bakhti M, Gronborg M, Mobius W, Rhee J, Barr FA. (2010). Simons M. Regulation of exosome secretion by Rab35 and its GTPase-activating proteins TBC1D10A-C. J Cell Biol 189:223–232.

Huang B, Hubber A, McDonough JA, Roy CR, Scidmore MA, Carlyon JA. (2010). The Anaplasma phagocytophilum-occupied vacuole selectively recruits Rab-GTPases that are predominantly associated with recycling endosomes. Cell Microbiol 12:1292–1307.

Huber LA, Pimplikar S, Parton RG, Virta H, Zerial M, Simons K. (1993). Rab8, a small GTPase involved in vesicular traffic between the TGN and the basolateral plasma membrane. J Cell Biol 123, 35-45.

Hume A, Collinson L, Rapak A, Gomes A, Hopkins C, Seabra M. (2001). Rab27a regulates the peripheral distribution of melanosomes in melanocytes. J Cell Biol 152, 795–808.

Hutagalung AH, Novick P. (2011). Role of Rab GTPases in membrane traffic and cell physiology. Physiol Rev 91,119–149.

Hutt D, Da-Silva L, Chang L, Prosser D, Ngsee J. (2000). PRA1 inhibits the extraction of membranebound Rab GTPase by GDI1. J Biol Chem 275, 18511–18519.

Ibáñez P, Bonnet A, Débarges B, Lohmann E, Tison F, Pollak P, Agid Y, Dürr A, Brice A. (2004). Causal relation between alphasynuclein gene duplication and familial Parkinson's disease. Lancet 364, 1169–1171.

Ignatev A, Kravchenko S, Rak A, Goody R, Pylypenko O. (2008). A structural model of the GDP dissociation inhibitor rab membrane extraction mechanism. J Biol Chem 283, 18377–18384.

Ioannou MS, Girard M, McPherson PS. (2016). Rab13 Traffics on Vesicles Independent of Prenylation. J Biol Chem 291(20):10726-35.

Ismail SA, Chen YX, Rusinova A, Chandra A, Bierbaum M, Gremer L, Triola G, Waldmann H, Bastiaens PI, Wittinghofer A. (2011). Arl2-GTP and Arl3-GTP regulate a GDIlike transport system for farnesylated cargo. Nat Chem Biol 7,942-9.

Itzen A, Pylypenko O, Goody RS, Alexandrov K, Rak A. (2006). Nucleotide exchange via local protein unfolding: structure of Rab8 in complex with MSS4. EMBO J 25, 1445–1455.
J Biol Chem 285:17938–17953.

Jackson A, Flett A, Smythe C, Hufton L, Wettey F, Smythe E. (2003). Clathrin promotes incorporation of cargo into coated pits by activation activation of the AP2 adaptor micro2 kinase. J Cell Biol 163, 231–236.

Jahn R. and Scheller R.H. (2006). SNAREs--engines for membrane fusion. Nat. Rev. Mol. Cell Biol. *7*,631-643.

Janoueix-Lerosey I, Jollivet F, Camonis J, Marche PN, Goud B. (1995). Two-hybrid system screen with the small GTP-binding protein Rab6. Identification of a novel mouse GDP dissociation inhibitor isoform and two other potential partners of Rab6. J Biol Chem 270:14801–

14808.

Jedd G, Mulholland J, Segev N. (1997). Two new Ypt GTPases are required for exit from the yeast trans-Golgi compartment. J Cell Biol 137: 563–580.

Jedd G, Richardson C, Litt R, Segev N. (1995). The Ypt1 GTPase is essential for the first two steps of the yeast secretory pathway. J Cell Biol 131: 583–590.

Jenkins D, Seelow D, Jehee F, Perlyn C, Alonso L, Bueno D,Donnai D, Josifova D, Josifiova D, Mathijssen I, Morton J, Orstavik K, Sweeney E, Wall S, Marsh J, Nurnberg P, Passos-Bueno M, Wilkie A. (2007). RAB23 mutations in Carpenter syndrome imply an unexpected role for hedgehog signaling in cranial-suture development and obesity. Am J Hum Genet 80, 1162-170.

Jin Y, Sultana A, Gandhi P, Franklin E, Hamamoto S, Khan AR, Munson M, Schekman R,Weisman LS. (2011). Myosin V transports secretory vesicles via a Rab GTPase cascade and interaction with the exocyst complex. Dev Cell 21, 1156–1170.

Joberty G, Tavitian A, Zahraoui A. (1993). Isoprenylation of Rab proteins possessing a C-terminal CaaX motif. FEBS Lett 330(3):323-8.

Johansson M, Rocha N, Zwart W, Jordens I, Janssen L, Kuijl C, Olkkonen V, Neefjes J. (2007). Activation of endosomal dynein motors by stepwise assembly of Rab7-RILP-p150Glued, ORP1L, the receptor betalll spectrin. J Cell Biol 176, 459–471.

John Colicelli. (2004). Human RAS Superfamily Proteins and Related GTPases. Sci STKE 2004 (250):RE13.

Jordens I, Fernandez-Borja M, Marsman M, Dusseljee S, Janssen L, Calafat J, Janssen H, Wubbolts R, Neefjes J. (2001). The Rab7 effector protein RILP controls lysosomal transport by inducing the recruitment of dynein-dynactin motors. Curr Biol 11: 1680–1685.

Jordens I, Marsman M, Kuijl C, and Neefjes J. (2005). Rab proteins, connecting transport and vesicle fusion. Traffic *6*, 1070-1077.

Juan S. Bonifacino, Benjamin S. Glick. (2004). The Mechanisms of Vesicle Budding and Fusion. Cell 116,153–166.

Kanno E, Ishibashi K, Kobayashi H, Matsui T, Ohbayashi N, Fukuda M. (2010). Comprehensive screening for novel rab-binding proteins by GST pull-down assay using 60 different mammalian Rabs. Traffic 11:491–507.

Karki S, Holzbaur E. (1995). Affinity chromatography demonstrates a direct binding between cytoplasmic dynein and the dynactin complex. J Biol Chem 270, 28806–28811.

Khosravifar R, Clark G J,Abe K, Cox A D, McLain T,Lutz R J, Sinensky M, and Der C J. (1992). Ras (CXXX) and Rab (CC/CXC) prenylation signal sequences are unique and functionally distinct. J Biol Chem 267, 24363-24368.

Khosravifar R, Lutz R J, Cox A D, Conroy L, Bourne J R, Sinensky M, Balch W E, Buss J E, Der C J. (1991). Isoprenoid modification of Rab proteins terminating in CC or CXC motifs. Proc Natl Acad Sci 88, 6264-6268.

Kinchen JM, Ravichandran KS. (2010). Identification of two evolutionarily conserved genes regulating processing of engulfed apoptotic cells. Nature 464(7289):778–782.

Klinkert K, Echard A. (2016). Rab35 GTPase: a central regulator of phosphoinositides and F-actin in endocytic recycling and beyond. Traffic 17(10):1063-77.

Klopper T, Kienle N, Fasshauer D, Munro S. (2012). Untangling the evolution of Rab G proteins: implications of a comprehensive genomic analysis. BMC Biol 10: 71.

Kobayashi H, Etoh K, Fukuda M. (2014). Rab35 is translocated from Arf6-positive perinuclear recycling endosomes to neurite tips during neurite outgrowth. Small GTPases 5:e29290.

Kobayashi H, Etoh K, Ohbayashi N, Fukuda M. (2014). Rab35 promotes the recruitment of Rab8, Rab13 and Rab36 to recycling endosomes through MICAL-L1 during neurite outgrowth. Biol Open 3:803–814.

Kobayashi H, Fukuda M. (2012). Rab35 regulates Arf6 activity through centaurin-beta2 (ACAP2) during neurite outgrowth. J Cell Sci 125:2235–2243.

Kobayashi H, Fukuda M. (2013). Rab35 establishes the EHD1-association site by coordinating two distinct effectors during neurite outgrowth. J Cell Sci 126, 2424–2435.

Kouranti I, Sachse M, Arouche N, Goud B, Echard A. (2006). Rab35 regulates an endocytic recycling pathway essential for the terminal steps of cytokinesis. Curr Biol 16:1719–1725.

Kulasekaran G, Nossova N, Marat AL, Lund I, Cremer C, Ioannou MS, McPherson PS. (2015). Phosphorylation-dependent regulation of connecdenn/DENND1 guanine nucleotide exchange factors. J Biol Chem 290, 17999–18008.

Lafer EM. (2002). Clathrin–protein interactions. Traffic 3,513–520

Langemeyer L, Nunes Bastos R, Cai Y, Itzen A, Reinisch KM, Barr FA. (2014). Diversity and plasticity in Rab GTPase nucleotide release mechanism has consequences for Rab activation and inactivation. Elife 3:e01623.

Lee M, Mishra A, Lambright D. (2009). Structural mechanisms for regulation of membrane traffic by Rab GTPases. Traffic 10, 1377–1389.

Li C, Luo X, Zhao S, Siu GK, Liang Y, Chan HC, Satoh A, Yu SS. (2016). COPI-TRAPPII activates Rab18 and regulates its lipid droplet association. EMBO J, pii: e201694866.

Li F, Yi L, Zhao L, Itzen A, Goody RS, Wu YW. (2014). The role of the hypervariable C-terminal domain in Rab GTPases membrane targeting. Proc Natl Acad Sci 18; 111(7):2572-7.

Li G, Stahl PD. (1993). Post-translational processing and membrane association of the two early endosome-associated rab GTP-binding proteins (rab4 and rab5). Arch Biochem Biophys 304(2), 471–478.

Li X, Sapp E, Chase K, Comer-Tierney L, Masso N, Alexander J, Reeves P, Kegel K, Valencia A, Esteves M, Aronin N, Difiglia M. (2009). Disruption of Rab11 activity in a knock-in mouse model of Huntington's disease. Neurobiol Dis 36, 374–383.

Li X, Sapp E, Valencia A, Kegel K, Qin Z, Alexander J, Masso N, Reeves P, Ritch J, Zeitlin S, Aronin N, Difiglia M. (2008). A function of huntingtin in guanine nucleotide exchange on Rab11.

Neuroreport 19, 1643–1647.

Li X, Standley C,Sapp E, Valencia A, Qin Z, Kegel K, Yoder J,Comer-Tierney L, Esteves M, Chase K, Alexander J, Masso N,Sobin L, Bellve K, Tuft R, Lifshitz L, Fogarty K, Aronin N,DiFiglia M. (2009). Mutant huntingtin impairs vesicle formation from recycling endosomes by interfering with Rab11 activity. Mol Cell Biol 29, 6106–6116.

Li Y, Wandinger-Ness A, Goldenring J, Cover T. (2004). Clustering and redistribution of late endocytic compartments in response to Helicobacter icobacter pylori vacuolating toxin. Mol Biol Cell 15, 1946–1959.

Lian J, Stone S, Jiang Y, Lyons P, Ferro-Novick S. (1994). Ypt1p implicated in v-SNARE activation. Nature 372, 698–701.

Lin DC, Quevedo C, Brewer NE, Bell A, Testa JR, Grimes ML, Miller FD, Kaplan DR. (2006). APPL1 associates with TrkA and GIPC1 and is required for nerve growth factor-mediated signal transduction. Mol Cell Biol 26(23):8928-41.

Lin T, Orrison BM, Leahey AM, Suchy SF, Bernard DJ, Lewis RA, Nussbaum RL. (1997). Spectrum of mutations in the OCRL1 gene in the Lowe oculocerebrorenal syndrome. Am J Hum Genet 60, 1384-1388.

Lin X, Yang T, Wang S, Wang Z, Yun Y, Sun L, Zhou Y, Xu X, Akazawa C, Hong W, Wang T. (2014). RILP interacts with HOPS complex via VPS41 subunit to regulate endocytic trafficking. Sci Rep 4, 7282.

Lin J, Liang Z, Zhang Z, Li G. (2001). Membrane topography and topogenesis of prenylated Rab acceptor (PRA1). J Biol Chem 276(45), 41733-41.

Lin, R.C and Scheller, R.H. (1997). Structural organization of the synaptic exocytosis core complex. Neuron 19, 1087–1094.

Lipatova Z, Tokarev AA, Jin Y, Mulholland J, Weisman LS, Segev N. (2008). Direct interaction between a myosin V motor and the Rab GTPases Ypt31/32 is required for polarized secretion. Mol Biol Cell 19(10):4177-4187.

Lippincott-Schwartz J. (1998). Cytoskeletal proteins and Golgi dynamics. Curr Opin Cell Biol 10(1):52–59.

Losev E, Reinke C, Jellen J, Strongin D, Bevis B, Glick B. (2006). Golgi maturation visualized in living yeast. Nature 441, 1002–1006.

Lowe M. (2005). Structure and function of the Lowe syndrome protein OCRL1. Traffic 6, 711–719.

Luo M, Gong C, Chen C, Hu H, Huang P, Zheng M, Yao Y, Wei S, Wulf G,Lieberman J, Zhou X, Song E, Lu K. (2015). The Rab2A GTPase promotes breast cancer stem cells and tumorigenesis via Erk signaling activation. Cell Rep 11, 111–24.

Lynch-Day M, Bhandari D, Menon S, Huang J, Cai H, Bartholomew C, Brumell J, Ferro-Novick S, Klionsky D. (2010). Trs85 directs a Ypt1 GEF, TRAPPIII, to the phagophore to promote autophagy. Proc Natl Acad Sci 107, 7811–7816.

Machner M, Isberg R. (2006). Targeting of host Rab GTPase function by the intravacuolar pathogen Legionella pneumophila. Dev Cell 11, 47–56.

Machner M, Isberg R. (2007). A bifunctional bacterial protein links GDI displacement to Rab1 activation. Science 318, 974–977.

Machner, M.P. and Isberg, R.R. (2006). Targeting of host Rab GTPase function by the intravacuolar pathogen Legionella pneumophila. Dev Cell 11, 47–56.

Mao X, Kikani CK, Riojas RA, Langlais P, Wang L, Ramos FJ, Fang Q, Christ-Roberts CY, Hong JY, Kim RY, Liu F, Dong LQ. (2006). APPL1 binds to adiponectin receptors and mediates adiponectin signalling and function. Nat Cell Biol, 8(5), 516-23.

Mao Y, Balkin DM, Zoncu R, Erdmann KS, Tomasini L, Hu F, Jin MM, Hodsdon ME, De Camilli P. (2009). A PH domain within OCRL bridges clathrin-mediated membrane trafficking to phosphoinositide metabolism. EMBO J 28(13), 1831-42.

Marat AL, Dokainish H, McPherson PS. (2011). DENN domain proteins: regulators of Rab GTPases. J Biol Chem 286:13791–13800.

Marat AL, Dokainish H, McPherson PS. (2011). DENN domain proteins: regulators of Rab GTPases. J Biol Chem 286: 13791–13800.

Marat AL, McPherson PS. (2010). The connecdenn family, Rab35 guanine nucleotide exchange factors interfacing with the clathrin machinery. J Biol Chem 285:10627–10637.

Markgraf DF, Peplowska K, Ungermann C. (2007). Rab cascades and tethering factors in the endomembrane system. FEBS Lett 581(11):2125-30.

Martincic I, Peralta M, Ngsee J. (1997). Isolation and characterization of a dual prenylated Rab and VAMP2 receptor. J Biol Chem 272, 26991–26998.

Martinez O, Schmidt A, Salaméro J, Hoflack B, Roa M, Goud B. (1994). The small GTP-binding protein rab6 functions in intra-Golgi transport. J Cell Biol 127, 1575–1588.

Marzesco AM, Galli T, Louvard D, Zahraoui A. (1998). The rod cGMP phosphodiesterase delta subunit dissociates the small GTPase Rab13 from membranes. J Biol Chem 273, 22340–22345.

Matanis T, Akhmanova A, Wulf P, Del Nery E, Weide T, Stepanova T, Galjart N, Grosveld F, Goud B, De Zeeuw C, Barnekow A, Hoogenraad C. (2002). Bicaudal-D regulates COPI-independent Golgi-ER transport by recruiting the dynein-dynactin motor complex. Nat Cell Biol 4, 986–992.

Matesic L, Yip R, Reuss A, Swing D, O'Sullivan T, Fletcher C, Copeland N, Jenkins N. (2001). Mutations in Mlph, encoding a member of the Rab effector family, cause the melanosome transport defects observed in leaden mice. Proc Natl Acad Sci 98: 10238–10243.

Matsuura-Tokita K, Takeuchi M, Ichihara A, Mikuriya K, NakanoA. (2006). Live imaging of yeast Golgi cisternal maturation. Nature 441, 1007–1010.

May A, Misura K, Whiteheart S, Weis W. (1999). Crystal structure of the amino-terminal domain of N-ethylmaleimide-sensitive fusion protein. Nat Cell Biol 1, 175–182.

Mayer A, Wickner W, Haas A. (1996). Sec18p (NSF)-driven release of Sec17p (alpha-SNAP) can precede docking and fusion of yeast vacuoles. Cell 85, 83–94.

McBride HM, Rybin V, Murphy C, Giner A, Teasdale R, Zerial M. (1999). Oligomeric complexes link Rab5 effectors with NSF and drive membrane fusion via interactions between EEA1 and syntaxin 13. Cell 98, 377-386.

McCaffery J, Barlowe C, Lindquist S. (2008). The Parkinson's disease protein alpha-synuclein disrupts cellular Rab homeostasis. Proc Natl Acad Sci 105, 145–150.

McCaffrey M, Ozanne B, Norman J. (2007). Rab25 associates with alpha5beta1 integrin to promote invasive migration in 3D microenvironments. Dev Cell 13, 496–510.

McGrail M, Gepner J, Silvanovich A, Ludmann S, Serr M,Hays T. (1995). Regulation of cytoplasmic dynein function in vivo by the Drosophila Glued complex. J Cell Biol 131, 411–425.

Medkova M, France Y, Coleman J, Novick P. (2006). The rab exchange factor Sec2p reversibly associates with the exocyst. Mol Biol Cell 17, 2757–2769.

Memon A. (2004). The role of ADP-ribosylation factor and SARI in vesicular trafficking in plants. Biochimica Biophysica Acta 1664, 9-30.

Menon S, Cai H, Lu H, Dong G, Cai Y, Reinisch K, Ferro-Novick S. (2006). mBET3 is required for the organization of the TRAPP complexes. Biochem Biophys Res Commun 350: 669–677.

Miaczynska M, Christoforidis S, Giner A, Shevchenko A, Uttenweiler-Joseph S, Habermann B, Wilm M, Parton RG, Zerial M. (2004). APPL proteins link Rab5 to nuclear signal transduction via an endosomal compartment.Cell 116(3):445-56.

Mierzwa B, Gerlich DW. (2014). Cytokinetic abscission: molecular mechanisms and temporal control. Dev Cell 31:525–538.

Mills I, Jones A, Clague M. (1998). Involvement of the endosomal autoantigen EEA1 in homotypic fusion of early endosomes. Curr Biol 8, 881–884.

Miserey-Lenkei S, Waharte F, Boulet A, Cuif MH, Tenza D, El Marjou A, Raposo G, Salamero J, Heliot L, Goud B, Monier S. (2007). Rab6- interacting protein 1 links Rab6 and Rab11 function. Traffic 8:1385–1403.

Miyamoto Y, Yamamori N, Torii T, Tanoue A, Yamauchi J. (2014). Rab35, acting through ACAP2 switching off Arf6, negatively regulates oligodendrocyte differentiation and myelination. Mol Biol Cell 25:1532–1542.

Mizuno-Yamasaki E, Medkova M, Coleman J Novick P. (2010). Phosphatidylinositol 4-phosphate controls both membrane recruitment and a regulatory switch of the Rab GEF Sec2p. Dev Cell 18, 828–840.

Montagnac G, de Forges H, Smythe E, Gueudry C, Romao M, Salamero J, Chavrier P. (2011). Decoupling of activation and effector binding underlies ARF6 priming of fast endocytic recycling. Curr Biol 21, 574–579.

Moomaw J, Casey P. (1992). Mammalian protein geranylgeranyltransferase. Subunit composition and metal requirements. J Biol Chem 267, 17438-17443.

Morimoto S , Nishimura N, Terai T, Manabe S, Yamamoto Y, Shinahara W, Miyake H, Tashiro S, Shimada M, Sasaki T. (2005). Rab13 mediates the continuous endocytic recycling of occludin to the cell surface. J Biol Chem 280 (3), 2220–2228.

Mosesson Y, Mills G, Yarden Y. (2008). Derailed endocytosis: an emerging feature of cancer. Nat Rev Cancer 8, 835–850.

Mossessova E, Gulbis JM, Goldberg J. (1998). Structure of the guanine nucleotide exchange factor Sec7 domain of human arno and analysis of the interaction with ARF GTPase. Cell 92: 415–423.

Moyer B, Allan B, Balch W. (2001). Rab1 interaction with a GM130 effector complex regulates COPII vesicle cis-Golgi tethering. Traffic 2, 268–276.

Müller M, Peters H, Blümer J, Blankenfeldt W, Goody R, Itzen A. (2010). The Legionella effector protein DrrA AMPylates the membrane traffic regulator Rab1b. Science 329, 946–949.

Murata T, Delprato A, Ingmundson A, Toomre D, Lambright D, Roy C. (2006). The Legionella pneumophila effector protein DrrA is a Rab1 guanine nucleotide-exchange factor. Nat Cell Biol 8, 971–977.

Murray JT, Panaretou C, Stenmark H, Miaczynska M, Backer JM. (2002). Role of Rab5 in the recruitment of hVps34/p150 to the early endosome. Traffic 3, 416–427.

Nahorski MS, Seabra L, Straatman-Iwanowska A, Wingenfeld A, Reiman A, Lu X, Klomp JA, Teh BT, Hatzfeld M, Gissen P, Maher ER. (2012). Folliculin interacts with p0071 (plakophilin-4) and deficiency is associated with disordered RhoA signaling, epithelial polarization and cytokinesis. Hum Mol Genet 21:5268–5279.

Nancy V, Callebaut I, El Marjou A, de Gunzburg J. (2002). The delta subunit of retinal rod cGMP phosphodiesterase regulates the membrane association of Ras and Rap GTPases.J Biol Chem 277: 15076–15084.

Nava Segev. (2001). Ypt and Rab GTPases: insight into functions through novel interactions. Curr Opin Cell Biol 13, 500-11.

Nickerson ML, Warren MB, Toro JR, Matrosova V, Glenn G, Turner ML, Duray P, Merino M, Choyke P, Pavlovich CP, Sharma N, Walther M, Munroe D, Hill R, Maher E, Greenberg C, Lerman MI, Linehan WM, Zbar B, Schmidt LS. (2002). Mutations in a novel gene lead to kidney tumors, lung wall defects, and benign tumors of the hair follicle in patients with the Birt-Hogg-Dubé syndrome. Cancer Cell 2(2):157-64.

Nielsen E, Christoforidis S, Uttenweiler-Joseph S, Miaczynska M, Dewitte F, Wilm M, Hoflack B, Zerial M. (2000). Rabenosyn-5, a novel Rab5 effector, is complexed with hVPS45 and recruited to endosomes through a FYVE finger domain. J Cell Biol 151, 601–612.

Noakes CJ, Lee G, Lowe M. (2011). The PH domain proteins IPIP27A and B link OCRL1 to receptor recycling in the endocytic pathway. Mol Biol Cell 22(5):606-23.

Nokes RL, Fields IC, Collins RN, Fölsch H. (2008). Rab13 regulates membrane trafficking between TGN and recycling endosomes in polarized epithelial cells. J Cell Biol 182(5):845-53.

Nookala RK, Langemeyer L, Pacitto A, Ochoa-Montano B, Donaldson JC, Blaszczyk BK, Chirgadze DY, Barr FA, Bazan JF, Blundell TL. (2012). Crystal structure of folliculin reveals a hidDENN function in genetically inherited renal cancer. Open Biol 2:120071.

Norden AG, Lapsley M, Igarashi T, Kelleher CL, Lee PJ, Matsuyama T, Scheinman SJ, Shiraga H, Sundin DP, Thakker RV, Unwin RJ, Verroust P, Moestrup SK. (2002). Urinary megalin deficiency implicates abnormal tubular endocytic function in Fanconi syndrome. J Am Soc Nephrol 13: 125–133.

Nordmann M, Cabrera M, Perz A, Bröcker C, Ostrowicz C, Engelbrecht-Vandré S, Ungermann C. (2010). The Mon1-Ccz1 complex is the GEF of the late endosomal Rab7 homolog Ypt7. Curr Biol 20(18):1654-9.

Noren CJ, Wang J, Perler FB. (2000). Dissecting the chemistry of protein splicing and its applications. Angew Chem Int Ed Engl **39**,450–66.

Novick P, Field C, Schekman R. (1980). Identification of 23 complementation groups required for post-translational events in the yeast secretory pathway. Cell 21, 205-15.

Novick P. (2016). Regulation of membrane traffic by Rab GEF and GAP cascades. Small GTPases 7(4):252-256.

Nuoffer C, Wu SK, Dascher C, Balch WE. (1997). Mss4 does not function as an exchange factor for Rab in endoplasmic reticulum to Golgi transport. Mol Biol Cell 8, 1305–1316.

Ortiz D, Medkova M, Walch-Solimena C, Novick P. (2002). Ypt32 recruits the Sec4p guanine nucleotide exchange factor, Sec2p, to secretory vesicles: evidence for a Rab cascade in yeast. J Cell Biol 157: 1005–1015.

Owen D, Collins B, Evans P. (2004). Adaptors for clathrin coats: structure and function. Annu Rev Cell Dev Biol 20: 153–191.

Pan X, Eathiraj S, Munson M, Lambright D. (2006). TBC-domain GAPs for Rab GTPases accelerate GTP hydrolysis by a dual-finger mechanism. Nature 442, 303–306.

Pasqualato S, Senic-Matuglia F, Renault L, Goud B, Salamero J, Cherfils J. (2004). The Structural GDP/GTP Cycle of Rab11 Reveals a Novel Interface Involved in the Dynamics of Recycling Endosomes. J Biol Chem 279, 11480–11488.

Patino-Lopez G, Dong X, Ben-Aissa K, Bernot KM, Itoh T, Fukuda M, Kruhlak MJ, Samelson LE, Shaw S. (2008). Rab35 and its GAP EPI64C in T cells regulate receptor recycling and immunological synapse formation. J Biol Chem 283, 18323–18330.

Pedersen H, Hölder S, Sutherlin D, Schwitter U, King D, Schultz P. (1998). A method for directed evolution and functional cloning of enzymes. Proc Natl Acad Sci 95, 10523-10528.

Pereira-Leal, J.B., and Seabra, M.C. (2000). The mammalian Rab family of small GTPases: definition of family and subfamily sequence motifs suggests a mechanism for functional specificity in the Ras superfamily. J Mol Biol 301, 1077–1087.

Pfeffer SR. (2012). Rab GTPase localization and Rab cascades in Golgi transport. Biochem Soc Trans 40(6), 1373-1377.

Pfeffer SR. (2013b). Rab GTPase regulation of membrane identity. Curr Opin Cell Biol 25(4), 414–419.

Pind S, Nuoffer C, McCaffery J, Plutner H, Davidson H, Farquhar M, Balch W. (1994). Rab1 and Ca^{2+} are required for the fusion of carrier vesicles mediating endoplasmic reticulum to Golgi transport. J Cell Biol 125, 239–252.

Pirruccello M, Swan LE, Folta-Stogniew E, De Camilli P. (2011). Recognition of the F&H motif by the Lowe syndrome protein OCRL. Nat Struct Mol Biol 18(7), 789-95.

Poteryaev D, Datta S, Ackema K, Zerial M, Spang A. (2010). Identification of the switch in early-to-late endosome transition. Cell 141(3), 497–508.

Praefcke GJ, McMahon HT. (2004). The dynamin superfamily: universal membrane tubulation and fission molecules? Nat Rev Mol Cell Biol 5(2):133-47.

Puthenveedu MA, Bachert C, Puri S, Lanni F, Linstedt AD. (2006). GM130 and GRASP65-dependent lateral cisternal fusion allows uniform Golgi-enzyme distribution. Nat Cell Biol 8(3):238-48.

Pylypenko O, Rak A, Durek T, Kushnir S, Dursina B, Thomae N, Constantinescu A, Brunsveld L, Watzke A, Waldmann H, Goody R, Alexandrov K. (2006). Structure of doubly prenylated Ypt1:GDI complex and the mechanism of GDI-mediated Rab recycling. EMBO J 25: 13–23.

Pylypenko O, Rak A, Reents R, Niculae A, Sidorovitch V, Cioaca MD, Bessolitsyna E, Thomä NH, Waldmann H, Schlichting I, Goody RS, Alexandrov K. (2003). Structure of Rab escort protein-1 in complex with Rab geranylgeranyltransferase. Mol Cell 11(2), 483–494.

Radhakrishna H, Donaldson JG. (1997). ADP-ribosylation factor 6 regulates a novel plasma membrane recycling pathway. J Cell Biol 139:49–61.

Rahajeng J, Giridharan SS, Cai B, Naslavsky N, Caplan S. (2012). MICAL-L1 is a tubular endosomal membrane hub that connects Rab35 and Arf6 with Rab8a. Traffic13:82–93.

Rak A, Fedorov R, Alexandrov K, Albert S, Goody R, Gallwitz D, Scheidig A. (2000). Crystal structure of the GAP domain of Gyp1p: first insights into interaction with Ypt/Rab proteins. EMBO J 19: 5105–5113.

Rak A, Pylypenko O, Durek T, Watzke A, Kushnir S, Brunsveld L, Waldmann H, Goody R, Alexandrov K. (2003). Structure of Rab GDP-dissociation inhibitor in complex with prenylated YPT1 GTPase. Science 302, 646–650.

Rak A, Pylypenko O, Niculae A, Pyatkov K, Goody RS, Alexandrov K. (2004). Structure of the Rab7:REP-1 complex: Insights into the mechanism of Rab prenylation and choroideremia disease. Cell 117(6):749–760.

Raman N, Weir E, Müller S. (2010). The Mon1-Ccz1 complex is the GEF of the late endosomal Rab7 homolog Ypt7. Curr Biol 20(18):1654–1659.

Renault L, Guibert B, Cherfils J. (2003). Structural snapshots of the mechanism and inhibition of

a guanine nucleotide exchange factor. Nature 426: 525–530.

Rice, LM and Brunger, AT. (1999). Crystal structure of the vesicular transport protein Sec17. Mol Cell 4: 85–95.

Richardson P, Zon L. (1995). Molecular cloning of a cDNA with a novel domain present in the tre-2 oncogene and the yeast cell cycle regulators BUB2 and cdc16. Oncogene 11, 1139–1148.

Rieder S, Emr S. (1997). A novel RING finger protein complex essential for a late step in protein transport to the yeast vacuole. Mol Biol Cell 8, 2307–2327.

Rink J, Ghigo E, Kalaidzidis Y, Zerial M. (2005). Rab conversion as a mechanism of progression from early to late endosomes. Cell 122, 735–749.

Rink J, Ghigo E, Kalaidzidis Y, Zerial M. (2005). Rab Conversion as a Mechanism of Progression from Early to Late Endosomes. Cell 122:735–749.

Ritter B, Denisov AY, Philie J, Allaire PD, Legendre-Guillemin V, Zylbergold P, Gehring K, McPherson PS. (2007). The NECAP PHear domain increases clathrin accessory protein binding potential. EMBO J 26:4066–4077.

Rivera-Molina F, Novick P. (2009). A Rab GAP cascade defines the boundary between two Rab GTPases on the secretory pathway. Proc Natl Acad Sci 106, 14408–14413.

Rojas R, van Vlijmen T, Mardones G, Prabhu Y, Rojas A, Mohammed S, Heck A, Raposo G, van der Sluijs P, Bonifacino J. (2008). Regulation of retromer recruitment to endosomes by sequential action of Rab5 and Rab7. J Cell Biol 183, 513–526.

Roskoski R, and Ritchie P. (1998). Role of the carboxyterminal residue in peptide binding to protein farnesyltransferase and protein geranylgeranyltransferase. Arch. Biochem. Biophys 356, 167-176.

Rossi G, Kolstad K, Stone S, Palluault F, Ferro-Novick S. (1995). BET3 encodes a novel hydrophilic protein that acts in conjunction with yeast SNAREs. Mol Biol Cell 6, 1769–1780.

Rothman, J.E. (1994). Mechanisms of intracellular protein transport. Nature 372, 55–63.

Sacher M, Jiang Y, Barrowman J, Scarpa A, Burston J, Zhang L, Schieltz D, Yates Abeliovich H Jr, Ferro-Novick S. (1998). TRAPP, a highly conserved novel complex on the cis-Golgi that mediates vesicle docking and fusion. EMBO J 17, 2494–2503.

Sahlender D, Roberts R, Arden S, Spudich G, Taylor M, Luzio J, Kendrick-Jones J, Buss F. (2005). Optineurin links myosin VI to the Golgi complex and is involved in Golgi organization and exocytosis. J Cell Biol 169, 285–295.

Salminen A, Novick P. (1987). A ras-like protein is required for a post-Golgi event in yeast secretion. Cell 49: 527–538.

Salminen A, Novick P. (1989). The Sec15 protein responds to the function of the GTP binding protein, Sec4, to control vesicular traffic in yeast. J Cell Biol 109, 1023–1036.

Sanford J, Pan Y, Wessling-Resnick M. (1993). Prenylation of Rab5 is dependent on guanine nucleotide binding. J Biol Chem 268, 23773-23776.

Sapperstein S, Walter D, Grosvenor A, Heuser J, Waters M. (1995). p115 is a general vesicular transport factor related to the yeast endoplasmic reticulum to Golgi transport factor Uso1p. Proc Natl Acad Sci 92, 522–526.

Sato M, Sato K, Liou W, Pant S, Harada A, Grant BD. (2008). Regulation of endocytic recycling by C. elegans Rab35 and its regulator RME-4, a coated-pit protein. EMBO J27:1183–1196.

Schmick M, Vartak N, Papke B, Kovacevic M, Truxius DC, Rossmannek L, Bastiaens PI. (2014). KRas localizes to the plasma membrane by spatial cycles of solubilization, trapping and vesicular transport. Cell 157(2):459-71.

Schneider-Poetsch T, Ju J, Eyler DE, Dang Y, Bhat S, Merrick WC, Green R, Shen B, Liu JO. (2010). Inhibition of eukaryotic translation elongation by cycloheximide and lactimidomycin. Nat Chem Biol 6(3): 209-217.

Schoebe, S., Oesterlin, L.K., Blankenfeldt, W., Goody, R.S. and Itzen, A. (2009). RabGDI displacement by DrrA from Legionella is a consequence of its guanine nucleotide exchange activity. Mol. Cell 36, 1060–1072.

Seabra M, Brown M, Goldstein J. (1993). Retinal degeneration in choroideremia: deficiency of rab eranylgeranyl transferase. Science 259: 377–381.

Seabra M, Brown M, Slaughter C, Sudhof T, GoldsteinJ. (1992a). Purification of component A of Rab geranylgeranyl transferase: possible identity with the choroideremia gene product. Cell 70, 1049-1057.

Seabra M, Ho Y, Anant J. (1995). Deficient geranylgeranylation of Ram/Rab27 in choroideremia. J Biol Chem 270: 24420–24427.

Seabra M. (1996b). Nucleotide dependence of Rab geranylgeranylation. Rab escort protein interacts preferentially with GDP-bound Rab. J Bio Chem 271, 14398-14404.

Seals D, Eitzen G, Margolis N, Wickner W, Price A. (2000). A Ypt/Rab effector complex containing the Sec1 homolog Vps33p is required for homotypic vacuole fusion. Proc Natl Acad Sci 97, 9402–9407.

Seaman M, McCaffery J, Emr S. (1998). A membrane coat complex essential for endosome-to-Golgi retrograde transport in yeast. J Cell Biol 142, 665–681.

Sebti S. (2005). Protein farnesylation: implications for normal physiology, malignant transformation, and cancer therapy. Cancer Cell 7, 297-300.

Segev N. (1991). Mediation of the attachment or fusion step in vesicular transport by the GTP-binding Ypt1 protein. Science 252, 1553–1556.

Shah M, Baterina OY Jr, Taupin V, Farquhar MG. (2013). ARH directs megalin to the endocytic recycling compartment to regulate its proteolysis and gene expression. J Cell Biol 202:113–127.

Shao,Y. and Paulus,H. (1997). Protein splicing: estimation of the rate of O-N and S-N acyl rearrangements, the last step of the splicing process. J Pept Res *50*, 193-198.

Shen F, Seabra M. (1996). Mechanism of digeranylgeranylation of Rab proteins. Formation of a complex between monogeranylgeranyl-Rab and Rab escort protein. J Bio Chem 271, 3692-3698.

Shim J, Lee SM, Lee MS, Yoon J, Kweon HS, Kim YJ. (2010). Rab35 mediates transport of Cdc42 and Rac1 to the plasma membrane during phagocytosis. Mol Cell Biol 30:1421–1433.

Shin H, Hayashi M, Christoforidis S, Lacas-Gervais S, Hoepfner S, Wenk M, Modregger J, Uttenweiler-Joseph S, Wilm M, Nystuen A, Frankel W, Solimena M, De Camilli P, Zerial M. (2005). An enzymatic cascade of Rab5 effectors regulates phosphoinositide turnover in the endocytic pathway. J Cell Biol 170, 607–618.

Shirane M, Nakayama K. (2006). Protrudin induces neurite formation by directional membrane trafficking. Science 314, 818–821.

Short B, Haas A, Barr F. (2005). Golgins and GTPases, giving identity and structure to the Golgi apparatus. Biochim Biophys Acta 1744, 383–395.

Simonsen A, Gaullier J, D'Arrigo A, Stenmark H. (1999). The Rab5 effector EEA1 interacts directly with syntaxin-6. J Biol Chem 274, 28857–28860.

Simonsen A, Lippé R, Christoforidis S, Gaullier J, Brech A, Callaghan J, Toh B, Murphy C, Zerial M, Stenmark H. (1998). EEA1 links PI(3)K function to Rab5 regulation of endosome fusion. Nature 394, 494–498.

Singleton A, Farrer M, Johnson J, Singleton A, Hague S, Kachergus J, Hulihan M, Peuralinna T, Dutra A, Nussbaum R,Lincoln S, Crawley A, Hanson M, Maraganore D, Adler C, Cookson M, Muenter M, Baptista M, Miller D, Blancato J, Hardy J, Gwinn-Hardy K. (2003). α-Synuclein locus triplication causes Parkinson's disease. Science 302: 841.

Sivars U, Aivazian D, Pfeffer S. (2003). Yip3 catalyses the dissociation of endosomal Rab–GDI complexes. Nature 425, 856–859.

Smeland TE, Seabra MC, Goldstein JL, Brown MS. (1994). Geranylgeranylated Rab proteins terminating in Cys-Ala-Cys, but not Cys-Cys, are carboxyl-methylated by bovine brain membranes in vitro. Proc Natl Acad Sci 91(22):10712–10716.

Snyder J, Worthylake D, Rossman K, Betts L, Pruitt W, Siderovski D, Der C,Sondek J. (2002). Structural basis for the selective activation of Rho GTPases by Dbl exchange factors. Nature Struct Biol 9, 468–475.

Söllner T, Whiteheart S, Brunner M, Erdjument-Bromage H, Geromanos S, Tempst P, Rothman J. (1993). SNAP receptors implicated in vesicle targeting and fusion.Nature 362,318–324.

Sorkin A. (2004). Cargo recognition during clathrin-mediated endocytosis: a team effort. Curr Opin Cell Biol 16, 392–399.

Spillantini M, Crowther R, Jakes R, Hasegawa M, Goedert M. (1998). α-Synuclein in filamentous inclusions of Lewy bodies from Parkinson's disease and dementia with Lewy bodies. Proc Natl Acad Sci 95, 6469–6473.

Spillantini M, Goedert M. (2000). The alpha-synucleinopathies: Parkinson's disease, dementia with Lewy bodies, and multiple system atrophy. Ann NY Acad Sci 920: 16–27.

Stein M, Pilli M, Bernauer S, Habermann B, Zerial M, Wade R. (2012). The interaction properties of the human Rab GTPase family-comparative analysis reveals determinants of molecular binding selectivity. PLoS One 7, e34870.

Stenmark H, Valencia A, Martinez O, Ullrich O, Goud B, Zerial M. (1994). Distinct structural elements of Rab5 define its functional specificity. EMBO J 13, 575-583.

Stenmark, H, Vitale G, Ullrich O, Zerial M. (1995). Rabaptin-5 is a direct effector of the small GTPase Rab5 in endocytic membrane fusion. Cell 83, 423–432.

Strom M, Hume A, Tarafder A, Barkagianni E, Seabra M. (2002). A family of Rab27-binding proteins. Melanophilin links Rab27a and myosin Vα function in melanosome transport. J Biol Chem 277:25423–25430.

Strom M, Vollmer P, Tan TJ, Gallwitz D. (1993). A yeast GTPase-activating protein that interacts specifically with a member of the Ypt/Rab family. Nature 361, 736–739.

Su T, Cariappa R, Stanley K. (1999). N-glycans are not a universal signal for apical sorting of secretory proteins. FEBS Lett 453: 391–394.

Suchy SF, Nussbaum RL. (2002). The deficiency of PIP2 5-phosphatase in Lowe syndrome affects actin polymerization. Am J Hum Genet, 71: 1420-1427.

Suchy SF, Olivos-Glander IM, Nussbaum RL. (1995). Lowe syndrome, a deficiency of phosphatidylinositol 4,5-bisphosphate 5-phosphatase in the Golgi apparatus. Hum Mol Genet 4: 2245–2250.

Suh H, Lee D, Lee K, Ku B, Choi S, Woo J, Kim Y, Oh B. (2010). Structural insights into the dual nucleotide exchange and GDI displacement activity of SidM/DrrA. EMBO J 29, 496–504.

Sun Y, Bilan PJ, Liu Z, Klip A. (2010). Rab8A and Rab13 are activated by insulin and regulate GLUT4 translocation in muscle cells.Proc Natl Acad Sci 107(46):19909-14.

Sun Y, Jaldin-Fincati J, Liu Z, Bilan PJ, Klip A. (2016). A complex of Rab13 with MICAL-L2 and α-actinin-4 is essential for insulin-dependent GLUT4 exocytosis. Mol Biol Cell 27(1):75-89.

Sutton R, Fasshauer D, Jahn R, Brunger A. (1998). Crystal structure of a SNARE complex involved in synaptic exocytosis at 2.4 Å resolution. Nature 395, 347–353.

Swan LE, Tomasini L, Pirruccello M, Lunardi J, De Camilli P. (2010). Two closely related endocytic proteins that share a common OCRL-binding motif with APPL1. Proc Natl Acad Sci 107(8):3511-6.

Swanson K and Hohl R. (2006). Anti-cancer therapy: targeting the mevalonate pathway. Curr Cancer Drug Targets 6, 15-37.

Sztul E and Lupashin V. (2006). Role of tethering factors in secretory membrane traffic. Am J Physiol Cell Physiol 290, C11- 26.

Tan X, Sun Y, Thapa N, Liao Y, Hedman AC, Anderson RA. (2015). LAPTM4B is a PtdIns(4,5)P_2 effector that regulates EGFR signaling, lysosomal sorting, and degradation. EMBO J, 34(4):475-90.

Tang B, Ng E. (2009). Rabs and cancer cell motility. Cell Motil Cytoskeleton 66,365–70.

Tarafder A, Wasmeier C, Figueiredo A, Booth A, Orihara A, Ramalho J, Hume A, SeabraM. (2011). Rab27a targeting to melanosomes requires nucleotide exchange but not effector binding. Traffic 12, 1056–1066.

Terebiznik M, Vazquez C, Torbicki K, Banks D, Wang T, Hong W, Blanke S, Colombo M, Jones N. (2006). Helicobacter pylori VacAtoxin promotes bacterial intracellular survival in gastric epithelial cells. Infect Immun 74, 6599–6614.

Thoma N, Iakovenko A, Kalinin A, Waldmann Hm, Goody R, Alexandrov K. (2001). Allosteric regulation of substrate binding and product release in geranylgeranyltransferase type II. Biochemistry 40, 268-274.

Thoma N, Niculae A, Goody R, Alexandrov K. (2001). Double prenylation by RabGGTase can proceed without dissociation of the mono-prenylated intermediate. J Biol Chem 276, 48631-48636.

Thomas C, Fricke I, Scrima A, Berken A, Wittinghofer A. (2007). Structural evidence for a common intermediate in small G protein-GEF reactions. Mol Cell 25, 141–149.

Thoms S, Erdmann R. (2005). Dynamin-related proteins and Pex11 proteins in peroxisome division and proliferation. FEBS J 272 (20), 5169–81.

Tobias H, Nickias K, Dirk F, Sean M. (2012). Untangling the evolution of Rab G proteins: implications of a comprehensive genomic analysis. BMC Bio 10, 71.

Touchot N, Chardin P, Tavitian A. (1987). Four additional members of the ras gene superfamily isolated by an oligonucleotide strategy: Molecular cloning of YPT-related cDNAs from a rat brain library.Proc Natl Acad Sci 84, 8210–8214.

Uejima T, Ihara K, Goh T, Ito E, Sunada M, Ueda T, Nakano A, Wakatsuki S. (2010). GDP-bound and nucleotide-free intermediates of the guanine nucleotide exchange in theRab5-Vps9 system. J Biol Chem 285, 36689–36697.

Ullrich O, Reinsch S, Urbé S, Zerial M, Parton R. (1996). Rab11 regulates recycling through the pericentriolar recycling endosome. J Cell Biol 135, 913–924.

Ungewickell A, Ward ME, Ungewickell E, Majerus PW. (2004). The inositol polyphosphate 5-phosphatase Ocrl associates with endosomes that are partially coated with clathrin. Proc Natl Acad Sci 101, 13501–13506.

Utskarpen A, Slagsvold H, Iversen T, Wälchli S, Sandvig K. (2006). Transport of ricin from endosomes to the Golgi apparatus is regulated by Rab6A and Rab6A. Traffic 7, 663–672.

Valencia A, Chardin P, Wittinghofer A, Sander C. (1991). The Ras protein family – evolutionary

tree and role of conserved amino-acids. Biochem 30, 4637-4648.

Van Gele M, Dynoodt P, Lambert J. (2009). Griscelli syndrome: a model system to study vesicular trafficking. Pigment Cell Melanoma Res 22: 268–282.

Vaughan K, Vallee R. (1995). Cytoplasmic dynein binds dynactin through a direct interaction between the intermediate chains and p150Glued. J Cell Biol 131, 1507–1516.

Velier J, Kim M, Schwarz C, Kim T, Sapp E, Chase K, Aronin N, DiFiglia M. (1998). Wild-type and mutant huntingtins function in vesicle trafficking in the secretory and endocytic pathways. Exp Neurol 152, 34–40.

Vetter IR, Wittinghofer A. (2001). The guanine nucleotide-binding switch in three dimensions. Science 294, 1299–1304.

Vicinanza M, Di Campli A, Polishchuk E, Santoro M, Di Tullio G, Godi A, Levtchenko E, De Leo MG, Polishchuk R, Sandoval L, Marzolo M, De Matteis MA.(2011). OCRL controls trafficking through early endosomes via PtdIns4,5P(2)-dependent regulation of endosomal actin. EMBO J 30:4970–4985.

Walseng E, Bakke O, Roche PA. (2008). Major histocompatibility complex class II-peptide complexes internalize using a clathrin- and dynamin-independent endocytosis pathway. J Biol Chem 283:14717–14727.

Wang HH, Cui Q, Zhang T, Wang ZB, Ouyang YC, Shen W, Ma JY, Schatten H, Sun QY. (2016). Rab3A, Rab27A, and Rab35 regulate different events during mouse oocyte meiotic maturation and activation. Histochem Cell Biol 145:647–657.

Wang X, Kumar R, Navarre J, Casanova J, Goldenring J. (2000). Regulation of vesicle trafficking in Madin-Darby canine kidney cells by Rab11a and Rab25. J Biol Chem 275, 29138–29146.

Wang Y, Wang J, Sun H, Martinez M, Sun Y, Macia E, Kirchhausen T, Albanesi J, Roth M, Yin H. (2003). Phosphatidylinositol 4 phosphate regulates targeting of clathrin adaptor AP-1 complexes to the Golgi. Cell 114, 299-310.

Watanabe, T., Ito, Y., Yamada, T., Hashimoto, M., Sekine, S. and Tanaka, H. (1994). The role of the C-terminal domain and type III domains of chitinase A1 from Bacillus circulans WL-12 in chitin degradation. J Bacteriol 176, 4465-4472.

Waterman-Storer C, Karki S, Holzbaur E. (1995). The p150 Glued component of the dynactin complex binds to both microtubules and the actin-related protein centractin (Arp-1). Proc Natl Acad Sci USA 92, 1634-1638.

Wennerberg K, Rossman K, Der C. (2005). The Ras superfamily at a glance. J Cell Sci 118, 843-846.

Wheeler D, Zoncu R, Root D, Sabatini D, Sawyers C. (2015). Identification of an oncogenic RAB protein. Science 350, 211-7.

White J, Johannes L, Mallard F, Girod A, Grill S, Reinsch S,Keller P, Tzschaschel B, Echard A, Goud B, Stelzer E.(1999). Rab6 coordinates a novel Golgi to ER retrograde transport pathway in live cells. J Cell Biol 147, 743-760.

Wickner W, Schekman R. (2008). Membrane fusion. Nat Struct Mol Biol 15:658-664.

Wixler V, Wixler L, Altenfeld A, Ludwig S, Goody R, Itzen A. (2011). Identification and characterisation of novel Mss4-binding Rab GTPases. Biol Chem 392, 239–248.

Wu M, Wang T, Loh E, Hong W, Song H. (2005). Structural basis for recruitment of RILP by small GTPase Rab7. EMBO J 24(8):1491–1501.

Wu X, Bradley M, Cai Y, Kummel D, De La Cruz E, Barr F, Reinisch K. (2011). Insights regarding guanine nucleotide exchange from the structure of a DENN-domain protein complexed with its Rab GTPase substrate. Proc Natl Acad Sci USA 108, 18672-77.

Wu X, Rao K, Bowers M, Copeland N, Jenkins N, Hammer J.(2001). Rab27a enables myosin Va-dependent melanosome capture by recruiting the myosin to the organelle. J Cell Sci 114, 1091–1100.

Wu X, Rao K, Zhang H, Wang F, Sellers J, Matesic L, Copeland N, Jenkins N, Hammer J.(2002). Identification of an organelle receptor for myosin-Va. Nat Cell Biol 4, 271–278.

Wu Y, Oesterlin L, Tan K, Waldmann H, Alexandrov K Goody R. (2010). Membrane targeting mechanism of Rab GTPases elucidated by semisynthetic protein probes. Nat Chem Biol 6, 534–540.

Wu Y, Tan K, Waldmann H, Goody R, Alexandrov K. (2007). Interaction analysis of prenylated Rab GTPase with Rab escort protein and GDP dissociation inhibitor explains the need for both regulators. Proc Natl Acad Sci USA 104(30):12294–12299.

Wu YW, Goody RS, Abagyan R, Alexandrov K. (2009). Structure of the disordered C terminus of Rab7 GTPase induced by binding to the Rab geranylgeranyl transferase catalytic complex reveals the mechanism of Rab prenylation. J Biol Chem 284(19): 13185–13192.

Wu YW, Waldmann H, Reents R, Ebetino FH, Goody RS, Alexandrov K. (2006). A protein fluorescence amplifier: Continuous fluorometric assay for rab geranylgeranyltransferase. ChemBioChem 7(12):1859–1861.

Yamamura R, Nishimura N, Nakatsuji H, Arase S, Sasaki T. (2008). The interaction of JRAB/MICAL-L2 with Rab8 and Rab13 coordinates the assembly of tight junctions and adherens junctions. Mol Biol Cell 19(3):971-83.

Yamasaki A, Menon S, Yu S, Barrowman J, Meerloo T, Oorschot V, Klumperman J, Satoh A, Ferro-Novick S. (2009). mTrs130 is a component of a mammalian TRAPPII complex, a Rab1 GEF that binds to COPI coated vesicles. Mol Biol Cell 20, 4205–4215.

Yang J, Liu W, Lu X, Fu Y, Li L, Luo Y. (2015). High expression of small GTPase Rab3D promotes cancer progression and metastasis. Oncotarget 6, 11125–38.

Yang J, Zhang Z, Roe SM, Marshall CJ, Barford D. (2009). Activation of Rho GTPases by DOCK exchange factors is mediated by a nucleotide sensor. Science 325, 1398–1402.

Yang X, Li X, Zhang Y, Rodriguez-Rodriguez L, Xiang M, Wang H,Zheng X. (2016). Rab1 in cell signaling, cancer and other diseases. Oncogene 35 (44), 5699-5704.

Yokoyama K, Goodwin G W, Ghomashchi F, Glomset J, Gelb M. (1991). A protein geranylgeranyltransferase from bovine brain: implications for protein prenylation specificity. Proc

Natl Acad Sci 88, 5302-5306.

Yoon S, Shin S, Mercurio A. (2005). Hypoxia stimulates carcinoma invasion by stabilizing microtubules and promoting the Rab11 trafficking of the alpha6beta4 integrin. Cancer Res 65, 2761–9.

Yoon SO, Shin S, Mercurio AM. (2005). Hypoxia stimulates carcinoma invasion by stabilizing microtubules and promoting the Rab11 trafficking of the α6β4 integrin. Cancer Res, 65(7):2761–9.

Young J, Stauber T, del Nery E, Vernos I, Pepperkok R, Nilsson T. (2005). Regulation of microtubule-dependent recycling at the trans-Golgi network by Rab6A and Rab6A. Mol Biol Cell 16, 162–177.

Yu R, Jahn R, Brunger A. (1999). NSF N-terminal domain crystal structure (models of NSF function). Mol Cell 4, 97-107.

Yu S, Satoh A, Pypaert M, Mullen K, Hay J, Ferro-Novick S. (2006). mBet3p is required for homotypic COPII vesicle tethering in mammalian cells. J Cell Biol 174: 359–368.

Zeigerer A, Gilleron J, Bogorad RL, Marsico G, Nonaka H, Seifert S, Epstein-Barash H, Kuchimanchi S, Peng CG, Ruda VM, Del Conte-Zerial P, Hengstler JG, Kalaidzidis Y,Koteliansky V, Zerial M . (2012). Rab5 is necessary for the biogenesis of the endolysosomal system in vivo. Nature 485, 465–470.

Zerial M, McBride H. (2001). Rab proteins as membrane organizers. Nat Rev Mol Cell Biol 2(2):107-17.

Zhang D, Iyer LM, He F, Aravind L. (2012). Discovery of novel DENN proteins: implications for the evolution of eukaryotic intracellular membrane structures and human disease. Front Genet 3:283.

Zhang X, Hartz PA, Philip E, Racusen LC, Majerus PW. (1998). Cell lines from kidney proximal tubules of a patient with Lowe syndrome lack OCRL inositol polyphosphate 5-phosphatase and accumulate phosphatidylinositol 4,5-bisphosphate. J Biol Chem 273: 1574–1582.

Zhang X, Jefferson AB, Auethavekiat V, Majerus PW. (1995). The protein deficient in Lowe syndrome is a phosphatidylinositol-4,5-bisphosphate 5-phosphatase. Proc Natl Acad Sci USA 92: 4853–4856.

Zhu AX, Zhao Y, Flier JS. (1994). Molecular cloning of two small GTP-binding proteins from human skeletal muscle. Biochem Biophys Res Commun 205:1875–1882.

Zhu G, Zhai P, Liu J, Terzyan S, Li G, Zhang X. (2004). Structural basis of Rab5-Rabaptin5 interaction in endocytosis. Nat Struct Mol Biol 11, 975–983.

Zhu H, Liang Z, Li G. (2009). Rabex-5 is a Rab22 effector and mediates a Rab22-Rab5 signaling cascade in endocytosis. Mol Biol Cell 20(22):4720–4729.

Zoncu R, Perera R, Sebastian R, Nakatsu F, Chen H, Balla T,Ayala G, Toomre D, De Camilli P. (2007). Loss of endocytic clathrincoated pits upon acute depletion of phosphatidylinositol 4,5-bisphosphate. Proc Natl Acad Sci 104, 3793–3798.

Zoncu R, Perera RM, Balkin DM, Pirruccello M, Toomre D, De Camilli P. (2009). A phosphoinositide switch controls the maturation and signaling properties of APPL endosomes. Cell 136(6):1110-21.

Eidesstattliche Versicherung (Affidavit)

Fu Li
Name, Vorname
(Surname, first name)

155084
Matrikel-Nr.
(Enrollment bunmer)

Belehrung:

Wer vorsätzlich gegen eine die Täuschung über Prüfungsleistungen betreffende Regelung einer Hochschulprüfungsordnung verstößt, handelt ordnungswidrig. Die Ordnungswidrigkeit kann mit einer Geldbuße von bis zu 50.000,00 € geahndet werden. Zuständige Verwaltungsbehörde für die Verfolgung und Ahndung von Ordnungswidrigkeiten ist der Kanzler/die Kanzlerin der Technischen Universität Dortmund. Im Falle eines mehrfachen oder sonstigen schwerwiegenden Täuschungsversuches kann der Prüfling zudem exmatrikuliert werden, §63 Abs. 5 Hochschulgesetz NRW.

Die Abgabe einer falschen Versicherung an Eides statt ist strafbar.

Wer vorsätzlich eine falsche Versicherung an Eides statt abgibt, kann mit einer Freiheitsstrafe bis zu drei Jahren oder mit Geldstrafe bestraft werden, § 156 StGB. Die fahrlässige Abgabe einer falschen Versicherung an Eides statt kann mit einer Freiheitsstrafe bis zu einem Jahr oder Geldstrafe bestraft werden, § 161 StGB.

Official notification:

Any person who intentionally breaches any regulation of university examination regulations relating to deception in examination performance is acting improperly. This offence can be punished with a fine of up to EUR 50,000.00. The competent administrative authority for the pursuit and prosecution of offences of this type is the chancellor of the TU Dortmund University. In the case of multiple or other serious attempts at deception, the candidate can also be unenrolled, Section 63, paragraph 5 of the Universities Act of North Rhine-Westphalia.

The submission of a false affidavit is punishable.

Any person who intentionally submits a false affidavit can be punished with a prison sentence of up to three years or a fine, Section 156 of the Criminal Code. The negligent submission of a false affidavit can be punished with a prison sentence of up to one year or a fine, Section 161 of the Criminal Code.

I have taken note of the above official notification.

_____
Ort, Datum
(Place, date)

_____
Unterschrift
(Signature)

Titel der Dissertation:
(Title of the thesis):

_____

_____

Ich versichere hiermit an Eides statt, dass ich die vorliegende Dissertation mit dem Titel selbstständig und ohne unzulässige fremde Hilfe angefertigt habe. Ich habe keine anderen als die angegebenen Quellen und Hilfsmittel benutzt sowie wörtliche und sinngemäße Zitate kenntlich gemacht. Die Arbeit hat in gegenwärtiger oder in einer anderen Fassung weder der TU Dortmund noch einer anderen Hochschule im Zusammenhang mit einer staatlichen oder akademischen Prüfung vorgelegen.

I hereby swear that I have completed the present dissertation independently and without inadmissible external support. I have not used any sources or tools other than those indicated and have identified literal and analogous quotations. The thesis in its current version or another version has not been presented to the TU Dortmund University or another university in connection with a state or academic examination.

_____
Ort, Datum
(Place, date)

_____
Unterschrift
(Signature)

Acknowledgements

After more than five years study at Max Planck Institute, the completion of my dissertation and subsequent Ph.D. has been a long journey. I would like to thank all people during my PhD training time.

First of all, I am deeply grateful to my research supervisor Dr. Yaowen Wu for giving me an opportunity of working in his lab. I could never have come this far without his patient help and support. He's been motivating, encouraging, and enlightening. Dr. Wu is not only a mentor, but a friend. I have learned so much from him: how to think about science, as importantly, how to communicate the results. I also thank him for the critical reading and revision of my draft thesis.

I want to express my gratitude to Prof. Dr. Roger Goody, our previous director and the first examiner of my PhD thesis. He is always extremely generous with his time, knowledge to support and help me. I am grateful for his gentle encouragement all the time. In addition, I would like to express my gratefulness to Prof. Dr. Philippe Bastiaens, the second examiner of my PhD thesis. I thank him for his constructive suggestions which light my ideas throughout my studying time.

Next, I want to express my thanks to the past and present members of the Wu Lab. I am glad that I have met my lovely colleagues not only for cooperation, but for the help, motivation, inspiration, and an excellent research environment in our group! I would like to especially give my sincere thanks to the former members of our lab, Drs. Long Yi and Wei Liu for the corporation of several projects, helpful discussions and continuous encouragement. I want to thank Stephanie Voß for her nice microscopy techniques and scientific discussion of the ongoing project. Big thanks to Drs. Xi Chen, Supansa Pantoom, Lei Zhao, Aimin Yang, Georgios Konstantinidis and Laura Klewer, Simone Brand for scientific and non-scientific discussion. I am not only learned scientific knowledge, but also got a lot of fun from all of you. I love you all. I want to say a special thanks to Dr. Xi Chen for my thesis proof reading.

Thirdly, I also acknowledge members from Goody group, especially Nathalie Bleimling, for her constructive suggestions to solve my problem during my study and providing many useful plasmids. In addition, I would like thank to Drs. Matthias Müller

and Emerich Mihai Gazdag for their scientific discussion and warmly encouragements. Special thanks go to Dr. Ola Sabet and Dr. Malte Schmick for their helpful suggestion for my study. I have to say many thanks to Dr. Sven Muller, for his kind support and help in microscope using.

My sincere gratitude gave to Christa Hornemann for her kind support and help in official and life matters.

Last, but certainly not least, I must acknowledge with tremendous and deep thanks my family especially my parents, who have always encouraged me to study. Thank you for sharing with my frustrations and happiness. Without you, I could not be here to complete my PhD thesis from a small village.

Publications

"Chemical labeling of intracellular proteins via affinity conjugation and strain-promoted cycloadditions in live cells."
Chen X, **Li F**, Wu YW.
***Chem Commun* (Camb).** 2015, 51(92):16537-40.

"Locking GTPases covalently in their functional states."
Wiegandt D, Vieweg S, Hofmann F, Koch D, **Li F**, Wu YW, Itzen A, Müller MP, Goody RS.
***Nat Commun*.** 2015, 6:7773.

"A bioorthogonal small-molecule-switch system for controlling protein function in live cells."
Liu P*, Calderon A*, Konstantinidis G*, Hou J*, Voss S, Chen X, **Li F**, Banerjee S, Hoffmann JE, Theiss C, Dehmelt L, Wu YW.
Angew Chem Int Ed Engl. 2014, 53(38):10049-55. (*equal contribution)

"A rapid and fluorogenic TMP-AcBOPDIPY probe for covalent labeling of proteins in live cells."
Liu W*, **Li F***, Chen X*, Hou J*, Yi L, Wu YW.
***J Am Chem Soc*.** 2014, 136(12):4468-71. (*equal contribution)

"The role of the hypervariable C-terminal domain in Rab GTPases membrane targeting."
Li F, Yi L, Zhao L, Itzen A, Goody RS, Wu YW.
***Proc Natl Acad Sci U S A*.** 2014, 111(7):2572-7.